THESIS, SUBMITTED FOR THE DEGREE OF DOCTOR OF PHILOSOPHY

IN THE UNIVERSITY OF OXFORD.

METAMORPHIC STUDIES IN THE SCOTTISH HIGHLANDS

by

ANDREW JAMES BAKER

of LINACRE COLLEGE

and THE DEPARTMENT OF EARTH SCIENCES,

UNIVERSITY OF OXFORD

VOLUME 2 FIGURES AND TABLES

LIST OF TABLES

LIST OF FIGURES

TABLE 1.1

Structural chronologies in the Dalradian.

Area	Chronology	Reference
Buchan-Banff	D1 Boyndie Syncline D3 monoclinal folding only strongly developed in west.	Treagus and Roberts (1981), c.f. Johnson (1962) and Fettes (1971).
W of Portsoy	D1 D2 deformation associated with area around Portsoy. D3.	Treagus and Roberts (1981), c.f. Johnson (1962).
Glens Clova & Esk	D1 D2 folds with NW-SE axes. D3 folds with NE-SW axes.	Harte and Johnson (1969).
Central Highlands (Pitlochry)	D1 Tay Nappe D2 NW sliding NW of steep belt, SE shear of Tay Nappe D3 NW sliding (N of Tay Nappe inversion). D4 Highland Border Downband	Bradbury et al. (1979).
Central Highlands (Schichallion & Braemar)	D1 Tay Nappe D2 NW sliding NW of Tay Nappe inversion D3 later more upright folds (D2=D2+D3 of Bradbury et al. according to J. Treagus, pers. comm.)	J. Treagus, pers. comm.

TABLE 1.2

Relationship of porphyroblast growth to local phases of deformation.

Area	Phases	Structural Age	Reference
Buchan area	andalusite, staurolite and cordierite	D1–D3 interval	Treagus and Roberts (1981)
W of Portsoy	andalusite	pre to early D2	
	garnet, staurolite and kyanite	synchronous with D2	Treagus and Roberts (1981)
Glens Clova & Esk	kyanite, staurolite and garnet	D2–D3 interval	Harte and Johnson (1969).
	sillimanite	post D3	
Central Hghds.	staurolite, garnet and chloritoid	syn D2	J. Treagus, pers. comm.
	kyanite	post D2	
Central Hghds.	migmatisation kyanite	D2–D3 pre and post D3	Bradbury (1979)

TABLE 1.3

ESTIMATES OF PRESSURE AND TEMPERATURE

AREA	ESTIMATES	BASIS	REFERENCE
Spean Bridge	5.5kb, 535 °C	Reactions in calcsilicates.	Richardson and Powell (1976)
Aureole of Huntly-Portsoy Gabbro	4-6kb at 800 °C	Cordierite Thermobarometry	Ashworth and Chinner (1978)
Glens Ey and Tilt, Schichallion	12kb at 600 °C	Garnet biotite thermometry and $3An \rightarrow Gr + 2Ky + Qtz$	Wells and Richardson (1979)
Glen Avon	8kb at 600 °C		
Southern Moines	8-10kb at about 600 °C	Garnet amphibole thermometry and reactions involving amphiboles	Wells (1979)
Eastern Dalradian	2 to 6kb	Alsilicate phase diagram and a number of continuous dehydration reactions	Harte and Hudson (1979)

TABLE 1.4

AGES OF IGNEOUS ROCKS

NAME OF INTRUSION	AGE	BASIS	REFERENCE
Ben Vuirich Granite	514±7	U-Pb Zircon	Pankhurst and Pidgeon (1976)
Connemara Gabbros	510±10	U-Pb Zircon	Pidgeon (1969)
Newer Gabbros	489±19	Rb-Sr WR	Pankhurst (1970)
Dunfallandy Hill Granite	481±15	Rb-Sr WR	Pankhurst and Pidgeon (1976)
Ox Mountains Granodiorite	477±6	Rb-Sr WR	
Strichen Granite	475±5	Concordant Monazite	Pidgeon and Aftalion (1978)
Insch Pegmatite		Rb-Sr Mu-Fspar	Bell (1968)
Longmanhill Granite	470±49	Rb-Sr WR	Pankhurst (1974)
Oughterard Granite	460±7		
Buchan Tourmaline Pegmatites	463±6	Rb-Sr Mu-WR	vanBreemen and Boyd (1972)
Auchedly Granite Pegmatites	462±10	K-Ar Mu	Pankhurst (1970)
Portsoy Pegmatite	458±11	Rb-Sr Mu-Fspar	Bell (1968)
Glen Dessary Syenite	456±5	U-Pb Zircon	vanBreemen et al. (1979a)
Kennethmont Granite	453±4	Rb-Sr WR	Pankhurst (1974)
Glen Kyllachy Granite	445±5	Rb-Sr Mu-WR	vanBreemen and Piasecki (1983)
Aberchirder Granite	444±9	Rb-Sr WR	Pankhurst (1974)

NAME OF INTRUSION	AGE	BASIS	REFERENCE
Various Moine Pegmatites	442 to 436	Rb-Sr	vanBreemen et al. (1974), vanBreemen et al. (1979a)
Strathspey Complex	436±8		
Loch Laggan Complex	439±7	Rb-Sr	Clayburn (1981)
Corrieyairack Red Granite	434±9	Min.-WR	
Strontian Tonalite	435±10		Pidgeon and Aftalion (1978)
Loch Borrolan Complex	430±4	U-Pb	vanBreemen et al. (1979b)
Late voluminous calc-alkali Granites	415 to 399	Various	References in Pankhurst and Sutherland (1982)

TABLE 1.5

REGIONAL CONSTRAINTS ON THE TIMING OF METAMORPHISM

AREA	AGE	BASIS AND REFERENCE
Connemara	510±10	Synmetamorphic Connemara Gabbros, Pidgeon (1969)
Ox Mountains	477±6	Ox Mountains Granodiorite post retrogression, Yardley et al. (1979). cf. Pankhurst et al. (1976).
Highland Border	489±10	K-Ar whole rock age on muscovite rich slate, Harper (1967).
	484	Arenig Highland Border Complex was metamorphosed with Dalradian, Henderson and Robertson (1982) & Ikin and Harmon (1984), cf. Curry et al. (1982).
Central Perthshire	514-480	Ben Vuirich Granite and Dunfallandy Hill Granite broadly synmetamorphic, Pankhurst and Pidgeon (1976), Bradbury et al. (1976), Bradbury (1979).
Glen Esk sillimanite zone	515±7	Rb-Sr age on muscovite, Dempster (1984)
Buchan Zones	489±19	Newer Gabbros intruded while area was still very hot, Pankhurst (1970), Fettes (1970).
Southern Moines	486±9	Rb-Sr whole rock date, Lambert et al. (1982).
Northern Moines	455±4	Synmetamorphic Glen Dessary Syenite, vanBreemen et al. (1979a).
	467±20	Rb-Sr whole rock date, Brewer et al. (1979).

TABLE 1.6

REGIONAL CONSTRAINTS ON THE AGE OF DEFORMATION

AREA	STRUCTURE	AGE	BASIS AND REFERENCE
Highland Border	Local D2 and Highland Border Downbend	484	Arenig Highland Border Complex is deformed by Grampian D2, Harris et al. (1972), Henderson and Robertson (1982), cf. Curry et al. (1982).
Central Perthshire	Local D2 and D3: NW directed sliding	510 to 480	Structural relations of granites, Bradbury et al. (1976; 1979).
South Sill. Zone	Tay Nappe Formation	515	Tay Nappe formation must predate the muscovite cooling date reported by Dempster (1984).
Buchan Zones	Local D1/D3 interval	489±19	Newer Gabbros date D1/D3 interval, Fettes (1970), Pankhurst (1970).
	Shear Zones from to	489±19 475±5	Structural relationships of shear zones with Newer Gabbros and post metamorphic Granites, Kneller and Ashcroft (1984).
	Local D3	475±5	Strichen Granite postdates deformation, Pidgeon and Aftalion (1978).
Southern Moines	Late phases of deformation	445±4	Structural relationships of Glen Kyllachy Granite, vanBreemen and Piasecki (1983).
Northern Moines	Swordly Slide	450	reference in vanBreemen and Piasecki (1983).
	Moine Thrust	430±4 to 420	late movement on thrust bracketed by these dates, vanBreemen et al. (1979b), Beckinsale and Obradovich (1973).

TABLE 2.1

Maximum assemblages in metasedimentary rocks from various parts of the Dalradian.

Assemblages are in metapelite lithologies unless otherwise indicated.

GLEN AVON

Kyanite-staurolite-garnet-biotite+chlorite (apparently retrogressive)-plagioclase-ilmenite-rutile+sulphides. (One example contains paragonite-quartz.)

Muscovite-Calcite-Quartz (Limestones).

Zoisite-biotite-muscovite-calcite-quartz-opaques.

Garnet-Zoisite-biotite-muscovite-quartz-ilmenite-rutile

Garnet-zoisite-biotite-chlorite-quartz-opaques(+late calcite).

Garnet-biotite-chlorite-tremolite-plagioclase-calcite-quartz-opaques. (in calcareous rock)

AILNACK GORGE

Garnet-muscovite-biotite-chlorite-plagioclase-quartz-opaques

Biotite-calcite-plagioclase-calcite.

Garnet-kyanite-biotite-plagioclase-quartz(+retrogressive muscovite and margarite)

Garnet-biotite-muscovite-calcite-quartz-rutile-opaques (+retrogressive chlorite

Garnet-zoisite-biotite-chlorite-quartz-opaques.

BANFF COAST TO WEST OF PORTSOY (Peacock et al. (1968) and this study).

Garnet-zoisite-biotite-calcite-plagioclase-quartz-opaques

Kyanite-staurolite-muscovite-biotite-plagioclase-quartz-opaques.

Garnet-staurolite-biotite-muscovite-plagioclase-quartz-opaques

Tremolite-biotite-calcite quartz (calcschists)

Tremolite-biotite-zoisite-quartz-plagioclase-calcite (calcschists)
Garnet-tremolite-biotite-quartz-opaques (calcschists to east of Portsoy

Gabbro)

GLEN EY

Kyanite-garnet-biotite-muscovite-plagioclase-quartz-rutile-ilmenite & retrogressive chlorite

Garnet-chlorite-biotite-quartz-plagioclase-opaques-margarite-kyanite

BLACKWATER (to immediate northwest of Morven Cabrach Newer Gabbro

Andalusite-staurolite-garnet-biotite-muscovite-quartz-plagioclase-opaques

Garnet-amphibole-epidote-biotite-calcite-quartz-sphene-opaques (metagreywacke ?)

GLEN SHEE

Garnet-staurolite-biotite-muscovite-paragonite-plagioclase-opaques (to immediate west of the Duchray Hill Gneiss)

Garnet-biotite-muscovite-chlorite-plagioclase-quartz-opaques-rutile (Glen Shee)

Biotite-muscovite-chlorite-calcite-plagioclase-quartz-opaques

CENTRAL HIGHLANDS (SCHICHALLION AREA)

Kyanite-staurolite-garnet-biotite-muscovite-plagioclase-quartz-ilmenite-rutile

Garnet-zoisite-hornblende-kyanite-biotite-plagioclase-quartz-opaques (Wells and Richardson,1979) (marl?)

GLEN CLOVA/ DUCHRAY HILL GNEISS

Garnet-kyanite-biotite-muscovite-quartz-plagioclase-ilmenite-opaques (staurolite is present at the lower grades, but appears to be absent or retrogressive at the higher grades, muscovite is absent from some areas of the Duchray Hill Gneiss, rutile is present in some rocks, but generally not)

Garnet-hornblende-biotite-plagioclase-quartz-opaques (marl?)

GLEN MUICK

Garnet-sillimanite-K feldspar-biotite-plagioclase-quartz-ilmenite-rutile (muscovite and other retrogressive phases present in most rocks, Kfeldspar is absent from most assemblages)

Garnet-cummingtonite-plagioclase-biotite-quartz-opaques (marl?)

GLEN GIRNOCK

Kyanite-staurolite-garnet-biotite-muscovite-quartz-opaques (rare and minor fibrolite)

GLEN MARK

Garnet-biotite-muscovite-plagioclase-fibrolite-quartz-opaques

Hornblende-plagioclase-quartz-rutile-sphene (metasedimentary amphibolite)

TABLE 2.2

Staurolite compositions

Rock	Fe/Mg	Fe+Mg+Mn		Al		Si	
		24	23	24	23	24	23
1	4.92	2.17	2.08	9.17	8.78	3.98	3.81
21	2.14	1.57	1.50	9.22	8.83	4.21	4.03
238	4.42	1.97	1.89	8.99	8.62	4.19	4.02
258	4.85	1.95	1.81	9.17	8.79	4.08	3.91
41A	3.84	1.84	1.76	9.29	8.90	4.05	3.88
37F	4.12	1.65	1.58	9.21	8.83	4.20	4.03
117B	5.00	1.88	1.80	9.18	8.80	4.08	3.91
621A	5.28	1.86	1.78	9.26	8.87	4.05	3.90
634B	2.75	2.04	1.96	8.96	8.59	4.14	3.97
635B	5.48	2.07	1.98	9.29	8.90	3.94	3.78
GD289	21.10	1.77	1.70	9.34	8.95	4.03	3.86
648A	6.15	1.87	1.79	9.29	8.90	4.00	3.83
135B	4.36	1.94	1.86	8.72	8.36	3.87	3.71
W17	3.89	1.83	1.75	9.21	8.83	4.04	3.87
CF2	5.59	1.74	1.86	9.26	8.87	3.98	3.81
733	5.30	1.89	1.81	9.17	8.79	4.11	3.94
				AVERAGE		4.06	3.89

AVERAGE Al/Si=2.26

TABLE 2.3

Assemblages in Metabasic rocks

GLEN MUICK

Garnet-clinopyroxene-hornblende-plagioclase-quartz-ilmenite-sphene

CROMAR

Hornblende-plagioclase-clinopyroxene-quartz-ilmenite

MARYCULTER

Garnet-hornblende-plagioclase-quartz-opaques

GLENS MARK & ESK

Garnet-hornblende-plagioclase-quartz-sphene-opaques±epidote

GLEN CLOVA

Garnet-zoisite-hornblende-plagioclase-quartz-sphene-opaques

Garnet-hornblende-gedrite-chlorite-biotite-plagioclase-quartz-opaques

DUCHRAY HILL GNEISS

Garnet-hornblende-plagioclase-quartz-sphene-opaques

(clinopyroxene occurs with the above in the northern part of the Duchray Hill Gneiss)

Garnet-hornblende-zoisite-plagioclase-quartz-sphene-opaques

KYANITE ZONE-SCHICHALLION AREA

Garnet-hornblende-plagioclase-quartz-opaques-sphene with scapolite, biotite, zoisite or epidote and often late chlorite or calcite.

GLEN GIRNOCK

Various garnet and clinopyroxene absent assemblages generally: hornblende-plagioclase-quartz-opaques, sometimes also with epidote and occasionally with cummingtonite.

;

TABLE 3.1

Stratigraphy of the Glen Muick area.

(a) after Read (1928a)

Deeside		Central Highlands	Tarfside
Glen Tanar Quartzite & Micaschist	–	Pitlochry Schist	
Deeside Limestone	–	Loch Tay Limestone	
Queens Hill Quartzite & Micaschist	–	Ben Lui Schist	

(b) after Harte (1979)

		Pitlochry Schist	–	Glen Effock Schist
Glen Tanar Quartzite & Micaschist Deeside Limestone	–	Loch Tay Limestone Ben Lui Schist	–	Tarfside Group
Queens Hill Quartzite & Micaschist				

(see figure 3.1)

TABLE 5.1

Data for the dolomite-calcite solvus ($Ca_2(CO_3)_2$ and $CaMg(CO_3)_2$ as components.

T (°C)	$X_{Dol,Cc}$	$X_{Cc,Dol}$	A_1/RT	A_2/RT	a_{Dol}	a_{Cc}
400	0.04	0.02	3.73	0.30	0.98	0.99
500	0.07	0.03	3.32	0.37	0.97	0.98
600	0.13	0.04	2.90	0.57	0.97	0.97
700	0.22	0.05	2.52	1.00	0.96	0.96
800	0.38	0.06	1.82	1.12	0.96	0.95

TABLE 5.2

THERMODYNAMIC DATA FOR PHASES

Phase	Entropy 298K, JK	Ref.	Volume 1bar,298 cm	Ref.
Quartz	41.46	R	22.688	R
Kyanite	82.30	RH	44.09	R
Andalusite	91.38	RH	51.53	R
Sillimanite	95.77	RH	49.90	R
Anorthite	201.79	R,T	100.79	R
High Sanidine	232.88	R	109.05	R
Diopside	143.09	R	66.09	R
Enstatite	66.03	K	31.47	H
Pyrope	266.27	HN	113.27	R
Grossular	260.12	HN	125.30	R
Tremolite	548.90	R	27.292	R
Muscovite	287.89	R,T	140.71	R
Talc	260.83	R	136.25	R
Calcite	91.71	R	36.934	R
Wollastonite	81.69	R	39.93	R
Steam	188.83	R	-	
Carbon Dioxide	213.79	R	-	
Phlogopite	318.40	T	149.91	R
Corundum	50.92	R	25.575	R
Forsterite	95.19	R	43.79	R
Dolomite	155.18	R	64.34	R
Zoisite	295.85	P	135.9	H
Mg Spinel	80.63	R	39.71	R
14A MgClinochlore	465.26	R	207.11	H

R Robie et al. (1978), RH Robie and Hemingway (1984),
T Text, K Krupka et al. (1979), HN Haselton and Newton (1980),
P Perkins et al. (1980), H Helgeson et al. (1978).

TABLE 5.3

HEAT CAPACITY DATA FOR PHASES IN $KCMASHCO_2$

$$c_p = a + bT + cT^{2} + dT^{-\frac{1}{2}} + eT^{-2}$$

Phase	a	b	c x 10^{6}	d x 10^{-3}	e x 10^{-7}
∝Quartz	44.603	0.037754	-	-	-0.10018
β Quartz	-58.928	0.010031	-	-	-
Kyanite	303.9	-0.01339	-	-2.9043	-0.0895200
Andalusite	290.4	-0.01052	-	-2.6278	-0.1109000
Sillimanite	226.1	0.01407	-	-1.376	-0.2440000
Anorthite	516.83	-0.092492	41.883	-4.5885	-0.1408500
High Sanidine	693.37	-0.1717	49.188	-8.3054	0.3462200
Diopside	191.82	0.083079	-21.718	-	-0.4279500
Enstatite	350.68	-0.14725	58.264	-4.2957	0.1678900
Pyrope	544.97	0.02068	-	-2.27463	-0.8329926
Grossular	516.35	0.03218	-	-1.4031	-0.9942021
Tremolite	6131.0	-4.189	1756.8	-85.656	5.1385000
Muscovite	917.67	-0.08111	-	-10.348	0.2834100
Talc	534.3	0.037416	-	-2.1532	-0.8805200
Calcite	99.715	0.02692	-	-	-0.2157600
Wollastonite	200.8	-0.0259	7.435	-1.826	-0.0157900
Steam	7.368	0.027468	-4.8117	0.36174	-0.0223160
Carbon Dioxide	87.820	-0.0026442	-	-0.99886	0.0706410
Phlogopite	955.94	-0.08560	-	-10.522	0.3345450
Corundum	157.36	0.00071899	-	-0.98804	-0.1896900
Forsterite	227.98	0.0034139	-	-1.7446	-0.0893970
Dolomite	547.88	-0.16759	77.076	-6.5479	0.2840000
Zoisite	697.52	0.013263	-	-5.3179	-0.3794100
Mg Spinel	222.91	0.0061267	-	-1.5512	-0.1685700
Clinochlore	1221.8	-0.05059	-4.8117	-10.9615	-0.2398110

References: Robie et al. (1978) except,
zoisite and talc (Holland, 1981a)
enstatite (Krupka et al. , 1979)
pyrope and grossular (Haselton and Newton,1980)
kyanite, andalusite and sillimanite
(Robie and Hemingway,1984)
chlinochlore and phlogopite
(see text)

TABLE 5.4

Heat capacity and entropy estimates for phlogopite and 14A Mg Clinochlore (calculated following Helgeson et al. (1978).

Reference reactions

Phlogopite

Phlogopite + Al_2O_3 = Mu + 3MgO

Mg Clinochlore

Mg Clinochlore + $0.5K_2O$ = Phlog + $2Mg(OH)_2$ + 0.5Co + H_2O

Additional heat capacity data

MgO (Periclase) $c_p = 65.211-1.2699\times10^{-3}T-0.38724\times10^{3}-0.046185\times10^{7}T^{-2}$

$S_{298} = 26.94$

$Mg(OH)_2$ (Brucite) $c_p = 102.22 +0.015107T-2617200T^{-2}$

$S_{298} = 63.18$

K_2O $c_p = 49.265+0.046059T+614.47T^{-\frac{1}{2}}-1324900T^{-2}$

$S_{298} = 94.14$

Estimated entropies and heat capacities

Phlogopite

$S_{298}=318.40JK^{-1}$

$c_p=955.94-0.08560T-10.522\times10^{3}T^{-\frac{1}{2}}+0.334545T^{-2}\times10^{7}$

14A Mg Clinochlore

$S_{298}=465.26JK^{-1}$

$c_p=1221.8-0.05059T-4.8117\times10^{-6}T^{2}-10.9615\times10^{3}T^{-\frac{1}{2}}-0.239811T^{-2}\times10^{7}$

TABLE 5.5

Compressibilities and Expansivities

Phase	Compressibility $Jbar^{-2} \times 10^{-6}$ /cm^3	Expansivity $Jbar^{-1} K^{-1} \times 10^{-5}$ /cm^3
Diopside	12.22	3.43
Enstatite	12.22	4.22
Forsterite	17.32	3.31
Pyrope	10.75	1.97
Grossular	9.79	2.26
Mg Spinel	11.51	2.05
Kyanite	11.46	2.09
Sillimanite	8.45	3.35
Plagioclase	6.19	4.60
Corundum	10.92	1.55
Quartz	25.10	10.46
Wollastonite	9.65	5.00

Data from Clark (1966), Brace et al. (1969) and Hazen and Finger (1978).

TABLE 5.6

Experimentally determined reactions in $KCMASHCO_2$

	REACTION	LINEAR COMBINATION
A	$3En + Co \rightarrow Py$	
B	$Mu \rightarrow Ksp + Co + H_2O$	
C	$5Phl + 6Cc + 24Qtz \rightarrow 3Tr + 5Ksp + 6CO_2 + 2H_2O$	
D	$Dol + 2Qtz \rightarrow Di + 2CO_2$	
E	$5Dol + 8Qtz + H_2O \rightarrow Tr + 3Cc + 7CO_2$	
F	$Tr \rightarrow 2Di + 3En + Qtz + H_2O$	
G	$Fo + Tc \rightarrow 5En + H_2O$	
H	$Mu + Qtz \rightarrow Ksp + And + H_2O$	
	$Mu + Qtz \rightarrow Ksp + Sill + H_2O$	
	$Mu + Qtz \rightarrow Ksp + Ky + H_2O$	
I	$2Zo + Mu + 2Qtz \rightarrow 4An + Ksp + 2H_2O$	
J	$Mu + Cc + 2Qtz \rightarrow Ksp + An + H_2O + CO_2$	
K	$4Zo + Qtz \rightarrow Gr + 5An + 2H_2O$	
L	$Cc + Qtz \rightarrow Woll + CO_2$	
M	$Tc \rightarrow 3En + Qtz + H_2O$	
N	$3Dol + Ksp + H_2O \rightarrow Phl + 3Cc + 3CO_2$	$0.6E-0.2C$
O	$3Dol + 4Qtz + H_2O \rightarrow Tc + 3Cc + 3CO_2$	$F+E-2D-M$
P	$Di + 3Dol \rightarrow 2Fo + 4Cc + 2CO_2$	$\frac{1}{3}(6M-6G+4F+4E-11D)$
Q	$Cc + Qtz + Ky \rightarrow An + CO_2$	$J-H$
	$Cc + Qtz + And \rightarrow An + CO_2$	$J-H$
R	$3En + Sill \rightarrow Pyr + Qtz$	$A + B - H$
S	$An + 4En \rightarrow Pyr + Di + Qtz$	$1/6(6A+6B-6J+10D-2E-2F)$
T	$Ky + 2Zo + Qtz \rightarrow 4An + H_2O$	$H-I$
U	$2Zo + CO_2 \rightarrow Cc + 3An + H_2O$	$I-J$
V	$3An \rightarrow Gross + 2Ky + Qtz$	$K-2I+2H$
W	$2Cc + An + Qtz \rightarrow Gr + 2CO_2$	$K-2I+2J$
X	$An + 2Wo \rightarrow Gr + Qtz$	$K-2I+2J-2L$
Y	$Cc + An + Woll \rightarrow Gr + CO_2$	$K-2I+2J-L$
Z	$Tr + 3Cc + 2Qtz \rightarrow 5Di + 3CO_2 + 2H_2O$	$5D-E$
AA	$5Tc + 6Cc + 4Qtz \rightarrow 3Tr + 6CO_2 + 2H_2O$	$2E-5(2D-F+M)$
AB	$2Dol + Tc + 4Qtz \rightarrow Tr + 4CO_2$	$2D-F+M$

TABLE 5.6 (Ctd.)

	REACTION	LINEAR COMBINATION
AC	$Tr + 11Dol \longrightarrow 8Fo + 13Cc + 9CO_2 + H_2O$	4/3(6M-6G+4F+4E-8D)-E
AD	$6Zo \longrightarrow 6Am + 2Gr + Co + 3H_2O$	8+2I+2K
AE	$3An + 3Cc \longrightarrow 2Gr + Co + 3CO_2$	8-2I+2K+3J
AF	$Mu + 3Dol + 2Qtz \longrightarrow Phl + An + 2Cc + 4CO_2$	0.6E-0.2C+J
AG	$Tr + 3Cc \longrightarrow 4Di + Dol + CO_2 + H_2O$	E-4D

An Anorthite
And Andalusite
Cc Calcite
Co Corundum
Di Diopside
Dol Dolomite
En Enstatite
Fo Forsterite
Gross Grossular
Ksp High Sanidine
Ky Kyanite
Mu Muscovite
Phl Phlogopite
Pyr Pyrope
Qtz Quartz
Sill Sillimanite
Tc Talc
Tr Tremolite
Woll Wollastonite
Zo Zoisite

TABLE 5.7

Estimated enthalpies and entropies for reactions in $KCMASHCO_2$

REACTION	ΔH^r_{298}, kJ	ΔS^r_{298}, JK^{-1}	ΔV^r_{298}, $Jbar^{-1}$
A	24.8	17.26	-0.672
B	108.4	184.74	-0.609
C	633.0	1334.2	-15.166
D	159.8	332.57	-4.363
E	471.0	1024.15	-11.940
F	117.0	165.66	-2.364
G	101.0	162.96	-2.269
H (And)	103.2	183.74	-0.282
H (Sill)	107.3	188.13	-0.445
I	231.5	455.19	+5.432
J	188.0	374.77	-1.318
K	223.5	421.87	+6.926
L	91.5	162.31	-1.969
M	109.0	167.55	-1.915
N	156.0	347.65	-4.316
O	159.4	357.12	-3.672
P	214.0	376.17	-2.379
Q (And)	84.8	191.03	-1.036
Q (Ky)	88.9	200.11	-0.292
R	25.9	13.87	-0.835
S	15.5	-15.09	-2.462
T	132.4	280.53	+6.458
U	43.5	80.42	+6.750
V	-41.3	-139.19	-6.620
W	136.5	261.03	-7.205
X	-46.5	-63.59	-3.266
Y	45.0	98.72	-5.235
Z	327.0	638.70	-9.865
AA	606.0	1285.85	-17.485
AB	311.6	667.03	-8.276
AC	1024.5	1810.81	-15.020
AD	323.9	573.29	+6.552
AE	193.4	332.03	-13.700
AF	344.0	722.42	-5.454
AG	166.2	306.13	-5.502

TABLE 5.8

Chlorite and Spinel Reactions: Thermodynamic data

REACTION	LINEAR COMBINATION
AH: 3Chl + 5Mu → 5Phl + 8Ky + Qtz + 12H_2O	
AI: 4En + Sp → Pyr + Fo	
AJ: 3Chl + 14Qtz → 3Ky + 5Tc + 7H_2O	AH−5H(Ky)+5O−5N
AK: 3Chl + 10Cc + 21Qtz → 3Tr + 2Zo + 8H_2O + 10CO_2	AH+AC−I+4Q(Ky)−4H(Ky)
AL: Chl → Fo + 2En + Sp + 4H_2O	$\frac{1}{3}$(AH−3AI+11M−5H(Ky)+5O −5N+3R(Ky)−6G)

REACTION	ΔH^r_{298}, kJ	ΔS^r_{298}, JK^{-1}	ΔV^r_{298}, $Jbar^{-1}$
AH	877.5	1722.59	−19.992
AI	28.6	16.71	−0.853
AJ	399.0	896.64	−12.544
AK	1238.0	2703.40	−37.656
AL	336.2	603.34	−6.067

TABLE 5.9

Estimated heats of formation from the oxides at 298K compared with calorimetric values. Heats of formation returned to 298K using heat capacity data of Robie et al. (1978). Errors quoted are those at the temperature of measurement, not at 298K.

TABLE 5.9

Heats of formation from the oxides at 298K.

PHASE	CALCULATED $H_{f,298}^{oxides}$, kJ	CALORIMETRIC $H_{f,298}^{oxides}$, kJ
Diopside	-143.3	-141.9±1.7 (A), -141.7 (G)
Enstatite ($MgSiO_3$)	-35.0	-35.56±0.63 (I)
Tremolite	-508.9	-506±15 (C)
Pyrope	-78.6	-79.5±1.6 (D)
Dolomite	-303.1	-300.9±1.1 (B)
Talc	-214.0	-182.8±1.42 (E)
Forsterite	-61.8	-60.8±1.1 (D), -56.7 (F), [(M) -63.26±1.05 (I), -63.77±0.63]
Calcite	-178.2	-178.8±1.0 (B)
Wollastonite	-86.7	-86.93+1.5 (A), -88.7 (H)
Kyanite	-7.7	-6.92±1.2 (J)
Sillimanite	0.5	0.78±0.7 (J)
Andalusite	-3.6	-3.19±1.2 (K)
Anorthite	-97.0	-95.1±1.3 (A), -98.95 (L)
Grossular	-316.9	-316.5±2.8 (A)
Muscovite	-263.67	-263.67±2.53 (N)
K feldspar (High Sanidine)	-156.87	-
Zoisite	-256.35	-
Phlogopite	-373.87	-
14A MgClinochlore	-500.7	-
Mg Spinel (ordered)	-29.0	-

REFERENCES

A Charlu et al. (1978)

B Robie et al. (1978)

C Weeks (1956)

D Charlu et al. (1975)

E Barany (1963)

F Robie et al. (1984)

G Navrotsky and Coons (1976)

H Kelley (1962)

I Torgeson and Sahama (1948) (clinoenstatite value)

J Anderson and Kleppa (1969) & Charlu et al. (1975)

K Anderson et al. (1977) & D

L Newton et al. (1980)

M Shearer and Kleppa (1973)

N Barany (1964)

TABLE 5.10

Estimated enthalpies of reaction for various reactions in KCMASH.

Reaction	ΔH^r_{298}, kJ	ΔS^r_{298}, JK^{-1}	ΔV^r_{298}, $Jbar^{-1}$
Phlog+3Qtz→Ksp+3Enst+H_2O (PHLOG)	112.4	177.02	-1.45
Phlog+Sill+2Qtz→Ksp+Pyr+H_2O (PHLOG*)	138.3	190.89	-2.287
3An+6En→2Pyr+Gross+3Qtz (OPX)	26.9	-84.51	-7.129
3An+3Di→Pyr+2Gross+3Qtz (CPX)	9.3	-123.75	-6.871
Phlog+qtz+2Sill→Pyr+Mu (PHL)	31.0	2.76	-1.84
Phlog+Qtz+2Ky→Pyr+Mu (PHL)	47.4	29.7	-0.68
3An+Phlog→Pyr+Gross+Mu (MGMICA)	6.1	-109.50	-7.30
REACTIONS WITH DISORDERED PHLOGOPITE			
Phlog + 3Qtz → Ksp + 3En + H_2O (PHLOG)	108	158.35	-1.45
Phlog+Sill+2Qtz → Ksp +Pyr+H_2O (PHLOG*)	133.9	172.22	-2.287
Phlog+Qtz+2Sill → Pyr+Mu	26.6	-15.91	-1.84
Phlog+Qtz+2Ky → Pyr+Mu (PHL)	43.0	11.03	-0.69
3An+Phlog → Pyr+Gross+Mu (MGMICA)	1.7	-128.17	-7.30

TABLE 5.11

Temperature estimates by PHL compared with gt-bi temperatures.

Rock	lnK	P(kb)	Garnet biotite T s		PHL T s	
			H&S (°C),	G&S (°C)	Ord.(°C)	Dis (°C)
ZZ	-4.97	7	546	475	303	424
41A	-4.53	7	560	510	334	477
W35	-3.82	7	625	570	393	583
135B	-4.23	7	608	586	353	518
129A	-3.90	7	673	580	386	570
141A	-3.99	7	627	586	378	555
155	-3.73	7	660	634	401	599
180	-3.87	8	604	530	377	558
637D	-3.97	6	610	570	391	574
648A	-4.12	6	690	668	378	550
W03	-4.53	10	590	562	303	434
W04	-4.68	10	531	520	292	416
W17	-4.58	10	590	567	299	428
645	-4.68	5	607	600	343	486

H&S : Hodges and Spear (1982) calibration of garnet biotite thermometer.

G&S : Ganguly and Saxena (1984) calibration of the garnet biotite thermometer.

Ord. : Thermodynamic data for ordered phlogopite.

Dis. : Thermodynamic data for disordered phlogopite.

TABLE 6.1

Thermodynamic expressions for selected geobarometers in CMAS. etc.

REACTION	ΔH^r_{970K}, kJ	ΔS^r_{970}, JK^{-1}	$\Delta V^r_{1,298}$, $Jbar^{-1}$
GRAIL	-3.95	-24.3	-1.84
ALSIL (Ky)	-36.9	-133.49	-6.61
ALSIL (Sill)	-21.84	-108.15	-5.44
MGMICA (ordered phl)	8.2	-104.8	-7.3
OPX	22.0	-89.51	-7.13
CPX	15.47	-112.52	-6.87
GRIP	-9.91	-52.25	-3.04
MGMICA (disordered phlogopite)	3.7	-123.46	-7.3

TABLE 6.2

Thermodynamic data for various phases.

A Text

B Ganguly (1972)

C Metz et al. (1983)

D Helgeson et al. (1978)

E Haselton and Westrum (1980)

F Robie et al. (1978)

G Powell and Evans (1983)

H entropy from ref. reaction

3Mgcelad + Ann → 3Fecelad + Phlog

PHASE	$S_{298}(calK^{-1})$	$V_{1,298}(cm^3)$	SOURCE
Fe Staurolite	117.16	223.38	A,B
Almandine	81.3	115.28	C,D
Quartz	9.88	22.688	D
Muscovite	68.80	140.71	D
Annite	95.20	154.32	D
Kyanite	20.00	44.09	D
Andalusite	22.20	51.53	D
Grossular	60.87	125.30	D
Anorthite	49.1	100.79	D
Pyrope	63.64	113.27	E,F
Phlogopite	76.1	149.66	D
Steam	45.10	-	D
MgCeladonite	73.14	138.00	G
FeCeladonite	79.51	138.00	H

TABLE 6.3

LOCATION	GRID REF.	SPEC. NO.	AFM Ass.	GARNET COMPOSITION ALM	PYR	GRO	SPES	BI Fe/Mg	T(°C)
W of Portsoy	NJ538674	620	GT BI	84	7	7	2	1.87	566
W of Portsoy	NJ437665	627	GT BI	75	2	13	9	5.52	573
W of Portsoy	NJ549673	117	ST GT BI	74	14	6	7	.85	570
Portsoy	NJ583664	289	ST GT BI	82	8	5	4	1.63	564
Cowhythe Gneiss	NJ602668	632	-	74	10	3	14	1.69	683
*Buchan staur. zone	NJ611498	43945	AND ST GT BI	70	9	5	16	1.31	572
*Buchan staur. zone	NJ633564	43940	ST GT BI	70	7	4	18	1.33	498
Glen Avon	NJ178086	27	KY ST GT BI	68	15	14	3	.61	551
Glen Avon	NJ178086	37	KY ST GT BI	70	15	12	3	.58	520
Glen Avon	NJ174088	41	KY ST GT BI	73	13	14	-	.78	560
Glen Avon	NJ182060	ZZ	KY GT BI	64	17	14	5	.50	546
Glen Avon	NJ165101	W35	KY ST GT BI	74	17	8	2	.82	625
Ailnack Gorge	NJ145149	60	GT BI	73	8	19	-	.96	510
Glenbuchat	NJ335196	1	ST GT BI	75	10	5	11	1.19	564
Blackwater	NJ362304	949	GT BI	84	7	3	7	2.19	600
Glen Livet	NJ214226	21	ST GT BI	75	13	11	-	.80	550
Glen Ey	NO087867	179	KY GT BI	63	19	18	1	.64	674
Glen Ey	NO087867	180	KY GT BI	68	18	11	2	.63	604
Glen Ey	NO087872	GE4	KY GT BI	67	15	14	3	.78	626
Glen Clunie	NO148864	3	KY GT BI	75	17	7	1	.95	678
Glen Clunie	NO142872	216	KY GT BI	73	18	7	2	.84	664
Schichallion	NN662592	W03	KY GT BI	79	14	6	2	.96	590
Schichallion	NN735562	W04	KY GT BI	85	12	2	1	1.05	531
Schichallion	NN659585	W17	KY ST GT BI	72	11	15	3	1.00	590
Glen Tilt	NN928737	W12	GT BI	68	12	19	1	1.08	635
Glen Tilt	NN937736	W14	GT BI	73	11	16	-	1.13	630
W of Duchray H.G.	NO181724	731	GT BI	67	15	5	14	.90	640
W of Duchray H.G.	NO178762	733	ST GT BI	77	14	8	1	.81	552
W of Duchray H.G.	NO156803	918	GT BI	65	12	20	1	.83	542
Duchray H.G.	NO185685	637A	KY GT BI	78	14	5	2	1.13	648
Duchray H.G.	NO185685	637B	GT BI	76	14	6	4	1.22	690
Duchray H.G.	NO185685	637D	GT BI	78	14	5	2	1.03	610
Duchray Hill G.	NO190713	638	GT BI	73	15	5	6	1.11	694
Glen Clova	NO315745	129	KY ST GT BI	80	14	4	4	1.25	673
Glen Clova	NO324746	135	KY ST GT BI	78	13	6	4	1.08	608
Glen Clova	NO324746	141	KY GT BI	80	12	7	2	1.25	627
Glen Clova	NO315776	155	KY GT BI	80	14	5	2	1.20	660
Glen Esk	NO413796	645	GT BI	74	11	6	8	1.21	607
Glen Esk	NO387803	647	GT BI	79	12	6	3	1.42	676
Glen Esk	NO440785	648	SIL ST GT BI	81	11	6	2	1.65	690
Glen Girnock	NO324927	535	ST GT BI	77	12	9	2	1.37	682
S of Glen Muick	NO324834	315	-	76	12	9	4	1.61	754
S of Glen Muick	NO367853	956	GT BI	72	13	6	9	1.58	800
Cromar	NJ483014	595	-	76	16	4	5	1.38	799
Cromar	NJ477008	919	-	74	20	4	2	1.00	762
Glen Muick	NO387920	430	-	66	27	5	2	.71	798
Glen Muick	NO382909	7	-	67	28	5	1	.70	807

TABLE 6.4

Comparison of different garnet biotite thermometers.

Rock	Ferry & Spear T (°C)	Hodges & Spear T (°C)	Ganguly & Saxena T (°C)
620	538	566	575
627	521	573	622
117	548	570	542
289	544	564	571
632	671	683	710
43945	562	572	600
43940	493	498	534
27	496	551	491
37	476	520	469
41	505	560	510
ZZ	493	546	475
W35	599	625	570
60	436	510	475
1	543	564	570
949	584	600	640
21	505	550	485
179	608	674	580
180	559	604	530
GE4	574	626	570
3	648	678	606
216	634	664	590
W03	565	590	562
W04	523	531	520
W17	532	590	567
W12	603	635	636
W14	566	630	595
731	627	640	615
733	521	552	504
918	527	542	536
637A	626	648	596
637B	665	690	652

TABLE 6.4 (ctd.)

Rock	Ferry and Spear T (°C)	Hodges and Spear T (°C)	Ganguly and Sax. T (°C)
637D	593	610	570
638	671	694	653
129	655	673	580
135	584	608	586
141	598	627	612
155	645	660	634
645	583	607	600
647	649	676	655
648	664	690	668
535	645	683	657
315	718	754	744
956	786	800	780
595	782	799	758
919	763	762	675
430	798	798	670
7	803	807	650

TABLE 6.5

Garnet amphibole exchange thermometer temperatures.

LOCATION	GRID REF.	SPEC. NO.	T(°C)
Schichallion	NN723658	747	639
Schichallion	NN670590	752	566
Glen Brerachan	NN985617	GB2	600
Glen Clova	NO333737	727	607
Glen Clova	NO333722	730	667
Duchray H.G.	NO247714	735	658
Duchray H.G.	NO253738	801	690
Duchray H.G.	NO234775	807	778
Duchray H.G.	NO234772	809	713
S of Glen Muick	NO389834	816	697
S of Glen Muick	NO362855	866	655
Glen Muick	NO382909	3	750
Glen Muick	NO382909	4	735
Glen Muick	NO378893	355	750
Glen Muick	NO329899	858	791

TABLE 6.6

Estimated metamorphic conditions using the Ellis and Green gt-cpx exchange thermometer and the reaction CPX (NP: Netwon and Perkins and TXT: see text).

LOCATION	GRID REF.	SPEC. NO.	X(AN) PLAG	GARNET COMPOSITION				CPX COMP.		T(°C)	P(kb)	
				ALM	PYR	GROS	SPES	Fe/Mg	a(DI)		NP	TXT
Duchray Hill G.	NO234775	807	46	52	11	32	5	.50	.55	717	8.3	7.4
Duchray Hill G	NO234772	809	35	55	10	30	5	.69	.54	742	8.5	7.5
W G. Muick	NO329889	858	38	56	13	28	3	.75	.50	819	9.9	8.8
E G. Muick	NO378893	355	41	60	13	26	2	.71	.51	766	8.4	7.4
Cairn Leuchan	NO382909	4	38	61	14	24	2	.84	.48	815	9.3	8.2
Cairn Leuchan	NO382909	3	39	60	13	25	2	.80	.48	792	8.8	7.7

TABLE 6.7

Estimated temperatures from two feldspar thermometry

Rock	Albite in K feldspar	Anorthite in Plagioclase	T (°C) Stormer	T (°C) P & P	T (°C) P & B
919	11	31	750	540	626
430	13	30	800	570	775
CL2	14	34	785	600	726

P & P : Powell and Powell (1977)

P & B : Brown and Parsons (1981)

TABLE 6.8

Pressures estimated using the reaction ALSIL.

Rock	Location	T (°C)	X_{An}	P(kb)
37	Glen Avon	520	22	7.7
41	Glen Avon	560	31	7.8
ZZ	Glen Avon	546	30	7.8
W35	Glen Avon	625	26	7.6
GE4	Glen Ey	635	36	8.7
W03	Schichallion	590	10	9.8
W17	Schichallion	590	20	10.3
637A	Duchray Hill	650	25	6.2
135B	Glen Clova	610	25	6.9
141A	Glen Clova	630	31	6.0
129A	Glen Clova	670	20	6.1
155	Glen Clova	660	26	6.4
595	Cromar	800	35	8.8
919	Cromar	800	31	7.2
430	Glen Muick	800	30	9.1
7	Glen Muick	800	33	8.8

TABLE 6.9

Pressures estimated using the reaction GRAIL

LOCATION	SPEC. NO.	T (°C)	X(Ilm.)	P(kb)
Glen Avon	W35	625	.97	6.5
Glen Ey	180	604	-	> 5.2
Schichallion	W03	590	.96	7.8
Schichallion	W17	590	.92	7.5
Duchray H.G.	637	648	.98	< 7.5
Glen Clova	135	608	.96	7.8
Glen Clova	155	660	.95	< 8.5
Glen Esk	648	690	.98	< 8.0
Glen Muick	430	802	-	> 4.7
Cromar	919	705	.88	< 10.5

TABLE 6.10

Pressures calculated from the reaction GRIP.

Rock	Location	X_{An}	lnK	T (°C)	P (kb)
135B	Glen Clova	26	-2.2	640	6.8
129A	Glen Clova	18	-2.17	640	< 7.1
141A	Glen Clova	26	-2.13	640	< 7.1
155	Glen Clova	26	-2.19	640	< 7.0
W03	Central Hghds.	10	-0.90	565	9.1
W17	Central Hghds.	20	-1.18	570	8.6
41A	Glen Avon	31	-1.92	510	7.3
ZZ	Glen Avon	29	-2.10	510	6.9
180	Glen Ey	32	-2.20	530	> 5.7
637D	Duchray H. G.	25	-2.63	600	< 5.5
648	Glen Esk		-2.34	670	< 7.0
645B	Glen Esk	26	-2.41	600	< 6.0
647A	Glen Esk	30	-2.38	660	< 6.8
430A	Glen Muick	30	-2.72	800	> 7.2
919B	Cromar	31	-2.85	800	< 6.9
956	Glen Mark	30	-2.48	780	< 7.7

TABLE 6.11

Pressures estimated from the geobarometer Celad.

Rock	lnK	T (°C)	P(Kb)
ZZ	6.09	500	7.5
W04	8.38	520	5.5
CF2	6.62	500	6.5
60A	7.26	500	6.0
41A	7.70	530	6.0
949C	7.96	620	7.5
731	3.99	620	11.5
W17	7.70	580	7.0
90A	5.24	500	8.0
W35	6.95	600	8.0

TABLE 6.12

Pressures calculated from the reaction MGMICA (disordered phlogopite).

Rock	Location	lnK	T (C)	P (kb)
41A	Glen Avon	-7.4	510	7.1
ZZ	Glen Avon	-7.6	480	6.7
W35	Glen Avon	-7.8	570	7.2
637B	Duchray H. G.	-8.1	650	7.2
637D	Duchray H. G.	-9.0	570	6.1
638F	Duchray H. G.	-8.8	650	6.8
648A	Glen Esk	-9.0	670	6.8
645B	Glen Esk	-9.2	600	6.1
647A	Glen Esk	-9.0	655	6.7
155	Glen Clova	-8.6	640	7.0
129	Glen Clova	-8.1	640	7.5
135B	Glen Clova	-6.5	580	8.6
141A	Glen Clova	-8.0	640	7.6
180B	Glen Ey	-7.2	530	7.5
W17	Central Hghds.	-5.6	570	9.4
W12	Central Hghds	-4.5	630	11.1
W03	Central Hghds	-6.5	560	8.4
731	W of D. H. G.	-9.5	620	5.9
956	Glen Mark	-8.2	780	8.4
955	Glen Mark	-8.8	780	7.7
GB2	Glen Brerachan	-7.9	600	7.4
632C	Cowhythe Gneiss	-10.6	680	5.0

TABLE 6.13

Relative pressures estimated from the reaction FEMICA

Rock	Location	lnK	T (°C)	P(kb)
41	Glen Avon	-1.8	510	7.5
ZZ	Glen Avon	-2.3	480	6.8
W35	Glen Avon	-2.7	570	7.7
637B	Duchray H.G.	-3.8	650	7.3
637D	Duchray H.G.	-4.1	570	6.0
638F	Duchray H.G.	-4.5	650	6.6
648A	Glen Esk	-4.7	670	6.3
645B	Glen Esk	-4.3	600	5.8
647A	Glen Esk	-4.6	655	6.3
155	Glen Clova	-4.2	640	6.5
129	Glen Clova	-4.0	640	6.8
135B	Glen Clova	-3.8	580	6.3
141A	Glen Clova	-3.2	640	7.1
180	Glen Ey	-2.2	530	7.7
W17	Central Hghds.	0	570	9.7
W12	Central Hghds.	-0.6	630	9.9
W03	Central Hghds.	-0.20	560	9.5
731	W of D. H. G.	-4.8	620	5.6
956	Glen Mark	-4.5	780	8.3
955	Glen Mark	-4.9	780	7.6
GB2	Glen Brerachan	-2.4	600	7.8
632C	Cowhythe Gneiss	-6.3	680	4.7

TABLE 6.14

Estimated relative pressures from the reactions MGTSCH and FETSCH.

Rock	Location	T (°C)	MGTSCH		FETSCH	
			lnK	P(kb)	lnK	P(kb)
41	Glen Avon	510	-4.5	7.1	0.14	7.0
ZZ	Glen Avon	480	-5.3	6.1	-1.85	5.0
W35	Glen Avon	570	-6.0	7.6	-1.85	7.4
637B	Duchray H. G.	650	-8.7	6.7	-3.8	7.5
637D	Duchray H. G.	570	-8.9	5.0	-3.9	5.4
638F	Duchray H. G.	650	-9.3	6.3	-4.7	6.8
648A	Glen Esk	670	-10.3	5.3	-4.5	6.8
645B	Glen Esk	600	-8.1	5.5	-4.7	4.7
647A	Glen Esk	655	-8.2	6.8	-5.2	5.8
155	Glen Clova	640	-7.9	6.7	-4.9	5.7
129A	Glen Clova	640	-7.7	7.1	-3.7	6.9
135B	Glen Clova	580	-8.6	5.1	-4.7	4.7
141	Glen Clova	640	-8.0	5.9	-2.6	6.7
180	Glen Ey	530	-8.3	5.2	-4.7	4.4
W17	Central Hghds	570	0.01	11.1	5.1	11.5
W12	Central Hghds	630	-2.4	10.5	3.8	11.8
W03	Central Hghds	560	0.28	11.3	5.3	11.6
731	W of D. H. G.	620	-11.8	3.2	-5.4	4.9
956	Glen Mark	780	-6.1	11.2	-5.7	8.3
955	Glen Mark	780	-8.4	7.9	-6.7	6.0
G82	Glen Brerachan	600	-5.1	6.8	-0.33	6.9
632C	Cowhythe Gneiss	680	-11.9	3.8	-6.8	4.6

TABLE 6.15

Comparison of pressures estimated by different methods

AREA	MGMICA	FEMICA	MGTSCH	FETSCH	CELAD	GRAIL	GRIP	CPX	ALSIL	AVERAGE
Glen Avon	7.1	7.3	7.9	7.2	7.5	6.5	7.1	-	7.7	7.3
Glen Ey	7.5	7.7	5.7	5.1	-	5.2	5.7	-	8.7	7.0
Central Hghds.	9.6	9.7	11.5	12.3	6.0	7.7	8.9	-	10.1	9.5
AB731	5.9	5.6	3.9	5.6	-	-	-	-	-	5.3
D. H. G.	6.7	6.6	6.5	7.3	-	7.5	5.5	7.4	6.2	6.8
Glen Clova	7.7	6.7	6.7	6.7	-	7.8	6.8	-	6.4	7.0
Glen Esk	6.5	6.1	6.4	6.5	-	8.0	6.0	-	-	6.4
Glen Mark	8.0	7.5	9.8	7.9	-	-	7.7	-	-	8.3
Muick/Cromar	-	-	-	-	-	-	-	8.8	9.0	8.5
Cowhythe G.	5.0	4.7	4.3	5.3	-	-	-	-	-	4.8

TABLE 6.16

X_{H_2O} estimated from the reaction ST2

Rock	Location	T(°C)	lnK	P	X_{H_2O}
41A	Glen Avon	560	-1.34	7	0.3
37F	Glen Avon	520	-1.96	7	0.15
278	Glen Avon	550	-1.53	7	0.25
648A	Glen Esk	690	-0.82	6	1.00
135B	Glen Clova	610	-0.73	6	0.50
W17	Central Highlands	590	-1.57	10	0.50

TABLE 6.17

X_{H_2O} estimated from the reaction PARAG

Rock	Location	T (°C)	X_{Na}, Parag.	X_{Alb}	X_{H_2O}
37F	Glen Avon	520	0.33	0.78	0.3
41A	Glen Avon	560	0.31	0.69	0.5
ZZ	Glen Avon	540	0.13	0.65	0.2
W35	Glen Avon	630	0.17	0.73	0.8
180B	Glen Ey	600	0.13	0.69	0.3
W03	Central Highlands	590	0.39	0.90	0.5
W04	Central H.	530	0.27	0.80	0.3
W17	Central H.	590	0.24	0.80	0.4
637D	D. H. G.	650	0.12	0.75	0.7
135B	Glen Clova	610	0.15	0.74	0.5
141A	Glen Clova	630	0.12	0.68	0.6
155	Glen Clova	660	0.14	0.74	0.8
129A	Glen Clova	670	0.13	0.75	0.8

TABLE 6.18

X_{H_2O} estimated from the reaction CHL.

Rock	Location	lnK	T (°C)	X_{H_2O}
41A	Glen Avon	-3.1	560	0.6
W35	Glen Avon	-1.26	625	>0.1
W04	Central Highlands	-4.28	530	0.4
W17	Central Highlands	-3.4	590	0.7
949C (And)	Andalusite Zone	-2.1	600	>0.1
731	W of D. H. G.	-2.3	640	>0.1
60A	Ailnack	-2.6	510	>0.4
90A	Ailnack	-1.5	510	>0.3

TABLE 6.19

Mu + Qtz → Sill + Kspar + H_2O

Rock	lnK	X_{H_2O}
956	1.41	0.3
955	1.37	0.3

Phlog + Sill + 2Qtz → Ksp + Pyr + H_2O

Rock	lnK	X_{H_2O}
430A	-1.15	0.13
CL2	-1.26	0.16
9198	-2.05	0.3

TABLE 8.1 (a)

Compositional Data used for the calulation of P-T paths

129A (Glen Clova)

Garnet composition Rim - $Alm_{80}Gross_{07}Spess_{02}Py_{12}$

Core - $Alm_{77}Gross_{08}Spess_{02}Py_{13}$

Biotite - $Annite_{560}MnBiotite_{001}Phlogopite_{440}$

Plagioclase Core - $Anorthite_{18}$

Rim - $Anorthite_{28}$

155 (Glen Clova)

Garnet composition Rim - $Alm_{79}Gross_{07}Spess_{02}Py_{12}$

Core - $Alm_{77}Gross_{08}Spess_{02}Py_{13}$

Biotite - $Annite_{559}MnBiotite_{001}Phlogopite_{440}$

Plagioclase Core - $Anorthite_{31}$

Rim -?

TABLE 8.1 (b)

Compositional data used for the calulation of P-T paths

155 (Glen Clova)

Garnet composition Rim - $Alm_{813}Gross_{043}Spess_{023}Py_{137}$

Core - $Alm_{800}Gross_{047}Spess_{023}Py_{140}$

Biotite - $Annite_{559}MnBiotite_{001}Phlogopite_{440}$

Plagioclase Core - $Anorthite_{25}$

Rim -$Anorthite_{31}$

637D (Duchray Hill Gneiss)

Garnet composition Rim - $Alm_{78}Gross_{06}Spess_{02}Py_{14}$

Core - $Alm_{76}Gross_{08}Spess_{01}Py_{15}$

Biotite - $Annite_{520}MnBiotite_{001}Phlogopite_{479}$

Plagioclase Core - $Anorthite_{23}$

Rim - $Anorthite_{26}$

TABLE 8.2

Calculation of reactions involving pyrope, sillimanite, cordierite, enstatite and quartz in MAS.

DATA

Phase	H^{oxides}_{970}, kJ	S_{1000}, JK^{-1}	$V_{1,298}$, cm^3
MgCordierite	-66.4	1131.56*	233.20
Enstatite ($MgSiO_3$)	-35.23	195.64	31.32
Sillimanite	-1.88	295.06	49.90
Pyrope	-84.93	777.81	113.20
Quartz	-	115.56	22.688

Thermodynamic data for reactions in the anhydrous system

Reaction	H^r_{970}, kJ	S^r_{970}, JK^{-1}	V $Jbar^{-1}$
Cd $\rightarrow$ 2En + 2Sill + Qtz	-7.8	-34.6	-4.78
3En + Sill $\rightarrow$ Pyr + Qtz	22.25	11.4	-0.84
3Cd $\rightarrow$ 2Pyr + 4Sill + 5Qtz	21.8	-81.04	-16.01
4En + Cd $\rightarrow$ 2Pyr + 3Qtz	37.3	-11.76	-6.56

TABLE 8.3

Contact metamorphic conditions in the Glen Muick area

Rock	Reaction	Conditions (kb)
GM3az (Newer Diorite aureole)	4En + MgCd → 2Py + 3Qtz	0.6 (dry)
		4.2 (wet, constant f_{H_2O})
	MGOPX	0.8
	FEOPX	2.0
	FECD	<4.4
	3FeCd → 2Alm + 5Sill + 2Qtz	<3.4 (wet)
	andalusite → sillimanite	<4.0
	Gt-Opx Fe-Mg exchange	710°C
	Al in opx with gt	750°C
	gt-bi thermometry (F&S)	780-950°C (centres)
		680-750°C (edges)
	gt-cd thermometry	750°C (centres)
683	An + Woll → Gr + Qtz & nearby andalusite → sillimanite	<3.4
IN1	FECD	2.25
	MGCD*	1.6

TABLE 8.4

Estimates of contact metamorphic pressures from the Dalradian and Moine

Intrusion	Age	Pressure	Regional Pressure
Glen Etive	399+5(A)	1.5kb (B)	5.5 (C)
Lochnagar	415+5 (D)	2.0kb	8.0
Foyers	403+9 (A)	4.0kb (E)	?
Strontian	435+10 (F)	4.0kb (G)	?
Newer Granite, Glen Tilt	400 ?	* 4.0-5.0kb (H)	10.0

(* probably circa 3kb)

REFERENCES

A Clayburn (1982)
B Droop and Treloar (1981)
C Richardson and Powell (1976)
D Halliday et al. (1979)
E Tyler and Ashworth (1983)
F Pidgeon and Aftalion (1978)
G Ashworth and Tyler (1983)
H Wells and Richardson (1979)

TABLE 8.5

Newer Gabbro contact metamorphic pressures and temperatures

Haddo House Aureole

606A

Reaction	Implied conditions
FEOPX	3.4
MGOPX	2.5
MgCd + 4En → 2Pyr + Qtz	0.2 (dry)
	3.8 (wet with constant γ_{MgCd})
Gt Opx Fe-Mg exchange	630°C
Al in Opx coexisting with garnet	750°C
Gt-Cd thermometry	700-750°C
Gt-Bi thermometry	670-800°C

Comparison with data from Droop and Charnley (1984) for Huntly and Belhelvie aureoles (estimates for both aureoles by ALSIL and Cd Gt + Sill + Qtz are 4.5-5kb).

CB1 (Huntly)	FEOPX	4.0
	MGOPX	4.5
	MgCd + 4En → 2Pyr + Qtz	1.0 (dry)
		4.7 (wet, assuming constant γ_{MgCd})
HM5 (Belhelvie)	FEOPX	4.3
	MGOPX	2.6
	MgCd + 4En → 2Pyr + Qtz	0 (dry)
		3.5 (wet, assuming constant γ_{MgCd})

TABLE 9.1 (a)

AB1078

	Clinopyroxene	Plagioclase (Symplectite)	Plagioclase (Corona)	Garnet
Wt%				
Na	0.46	8.76	4.57	0.08
Mg	12.95	0.02	-	1.78
Al	1.55	22.34	29.38	20.87
Si	51.82	63.79	52.57	37.95
K	0.02	0.21	0.11	0.03
Ca	23.39	4.34	12.09	13.73
Ti	0.15	-	0.02	0.21
Mn	0.07	-	-	3.31
Fe	8.39	0.30	0.22	21.91
TOTAL	98.82	99.76	98.96	99.92
Mole%				
Na	0.03	0.75	0.41	0.01
Mg	0.73	-	-	0.21
Al	0.07	1.17	1.59	1.94
Si	1.96	2.82	2.41	3.00
K	-	0.01	0.01	-
Ca	0.95	0.21	0.59	1.16
Ti	-	-	-	0.01
Mn	-	-	-	0.22
Fe	0.27	-	0.01	1.45
TOTAL	4.01	4.98	5.01	8.02

TABLE 9.1 (b)

AB105A

	Clinopyroxene	Plagioclase (symplectite)	Plagioclase (garnet corona)	Garnet
Wt%				
Na	0.38	6.96	4.64	0.04
Mg	12.83	0.02	0.02	2.19
Al	0.89	26.09	29.55	21.74
Si	52.15	58.29	53.17	38.17
K	0.06	0.16	0.17	0.06
Ca	23.82	7.85	12.23	14.18
Ti	0.08	-	0.02	0.13
Mn	0.11	0.01	0.01	2.92
Fe	8.65	0.35	0.19	21.55
TOTAL	98.97	99.73	100.00	100.98
Mole %	6(O)	8(O)	8(O)	12(O)
Na	0.03	0.61	0.41	-
Mg	0.72	-	-	0.25
Al	0.04	1.38	1.58	2.00
Si	1.97	2.62	2.41	2.97
K	-	0.01	0.01	-
Ca	0.96	0.38	0.59	1.18
Ti	-	-	-	0.01
Mn	-	-	-	0.19
Fe	0.27	0.01	-	1.40
TOTAL	4.02	5.00	5.01	8.02

105A

Hornblende Analyses

	Symplectite	Garnet Corona	Large amphibole
Wt %			
Na	1.05	1.86	1.67
Mg	12.79	8.99	10.21
Al	7.53	12.65	12.23
Si	47.32	41.59	44.20
K	0.16	0.43	0.33
Ca	11.96	11.73	12.06
Ti	0.62	1.18	1.06
Mn	0.16	0.20	0.18
Fe	14.03	16.41	15.37
TOTAL	95.62	95.04	97.31
Mole %			
Na	0.30	0.55	0.48
Mg	2.85	2.07	2.26
Al	1.33	2.30	2.15
Si	7.08	6.41	6.58
K	0.03	0.09	0.06
Ca	1.91	1.93	1.92
Ti	0.07	0.14	0.12
Mn	0.02	0.03	0.02
Fe	1.75	2.11	1.91
TOTAL	15.35	15.62	15.50

TABLE 9.1 (c)

Reintegrated pyroxene compositions from defocussed beam analyses. 105A (Corrected for variable ZAF factors).

	Oxide wt. %	Molecular 6(O)
Na	2.38	0.17
Mg	8.31	0.43
Al	9.32	0.38
Si	55.92	2.00
K	0.10	-
Ca	17.52	0.67
Ti	0.07	-
Mn	0.13	-
Fe	6.76	0.22
TOTAL	100.51	3.87

(Based on 15 defocussed beam analyses).

TABLE 10·1

CHRONOLOGY OF EVENTS IN THE EASTERN DALRADIAN

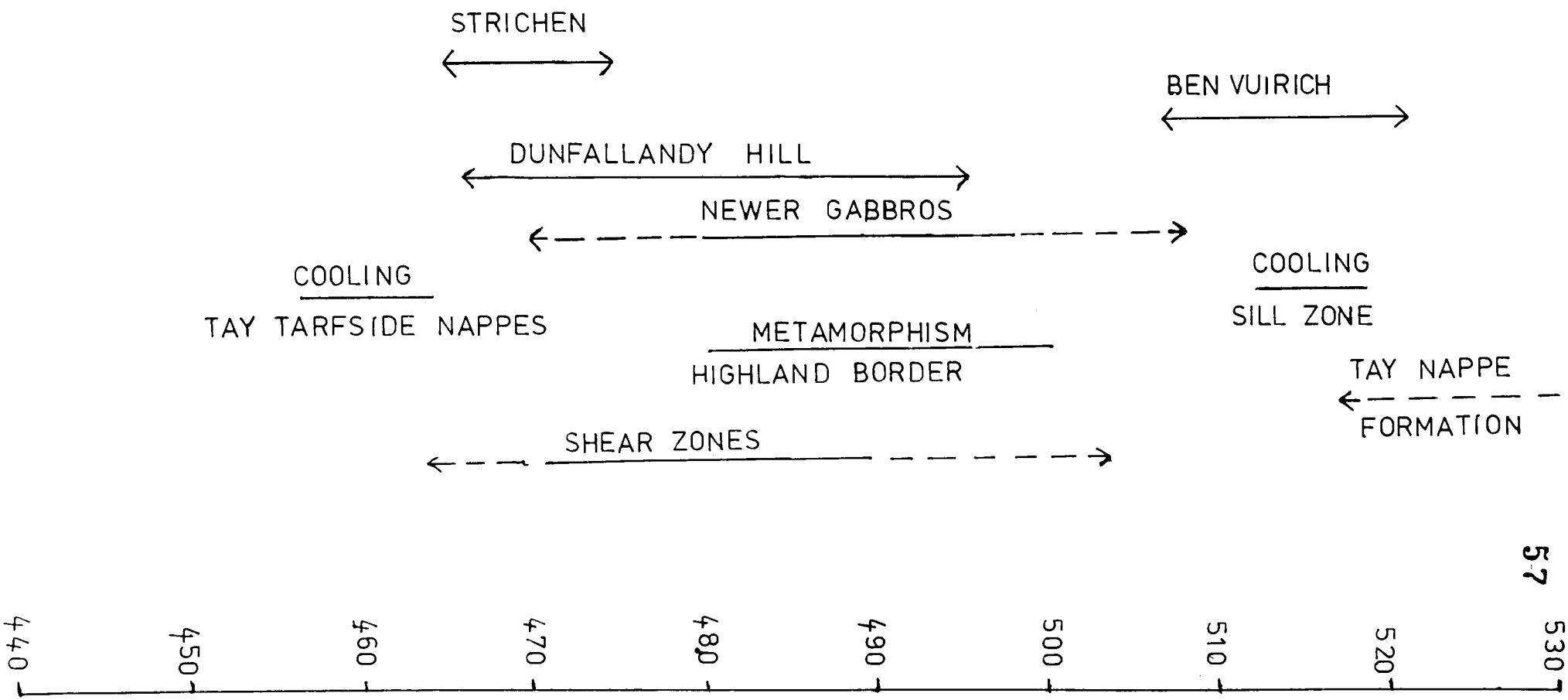

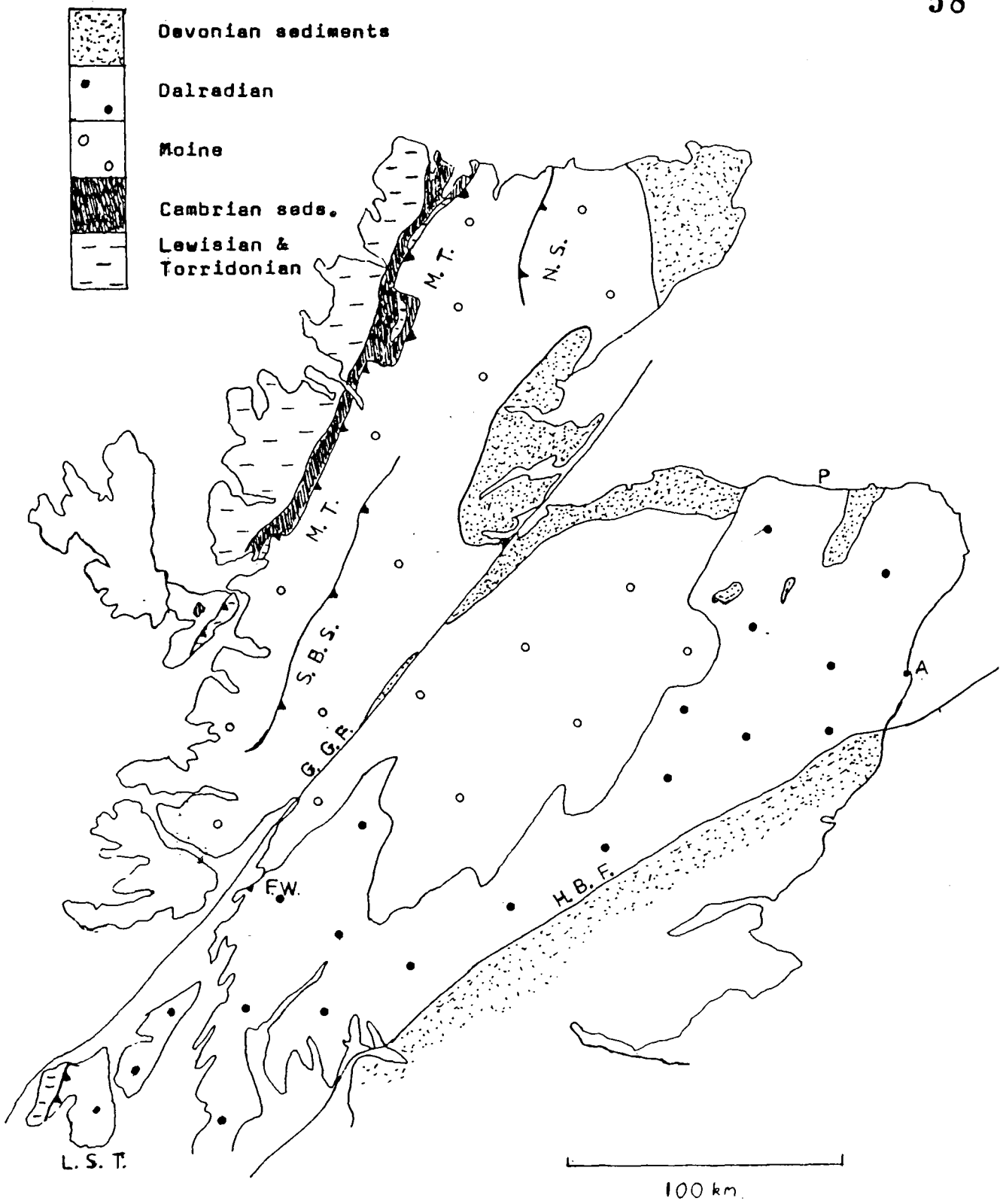

FIGURE 1.1

Geological sketch map of northern Scotland.

M.T. Moine Thrust
N.S. Naver Slide
S.B.S. Sgurr Beag Slide
G.G.F. Great Glen Fault
H.B.F. Highland Boundary Fault
L.S.T. Loch Skerrols Thrust
A Aberdeen
F.W. Fort William
P Portsoy

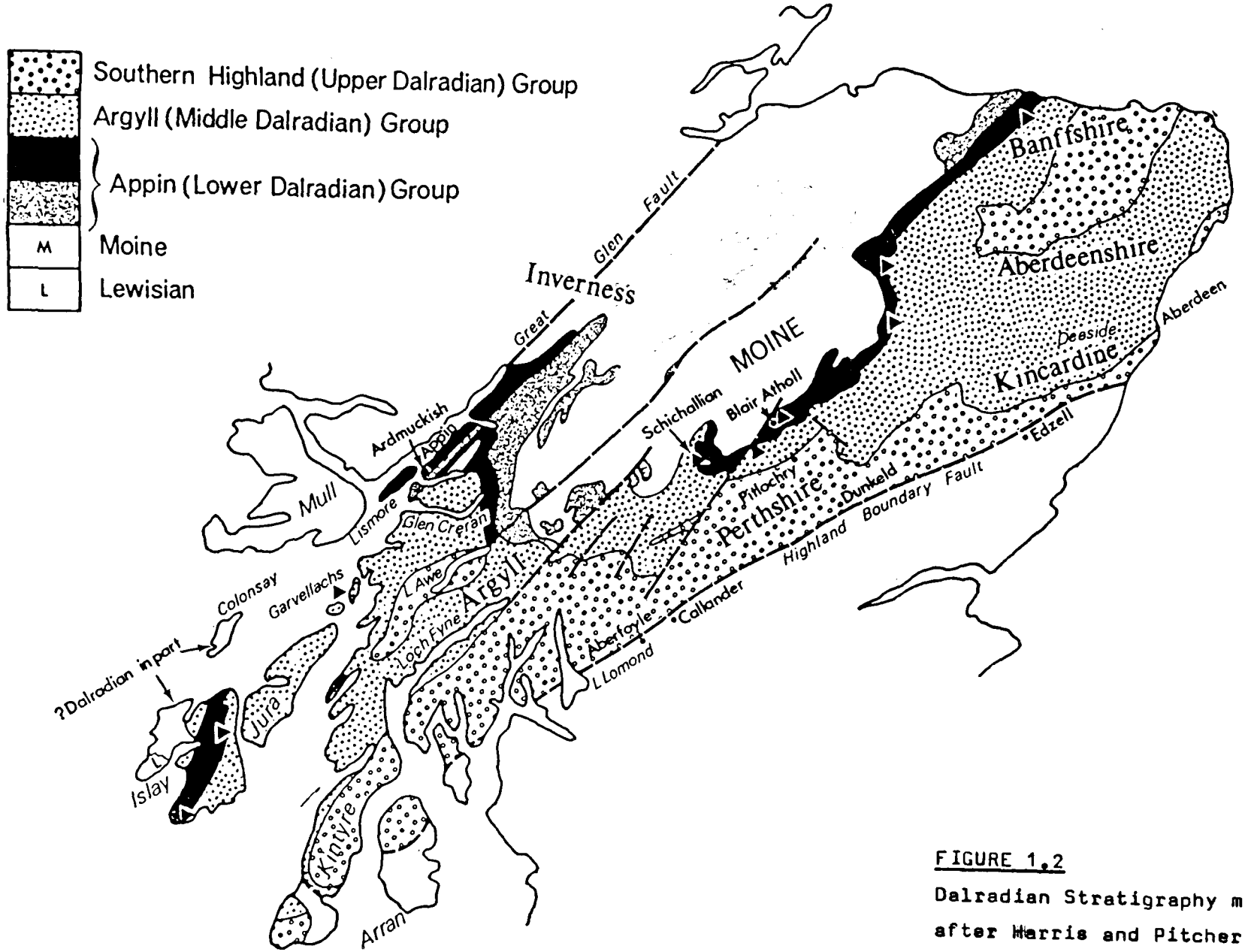

FIGURE 1.2

Dalradian Stratigraphy modified after Harris and Pitcher (1975).

FIGURE 1.2b

Dalradian stratigraphy of Ireland, from Harris and Pitcher (1975).

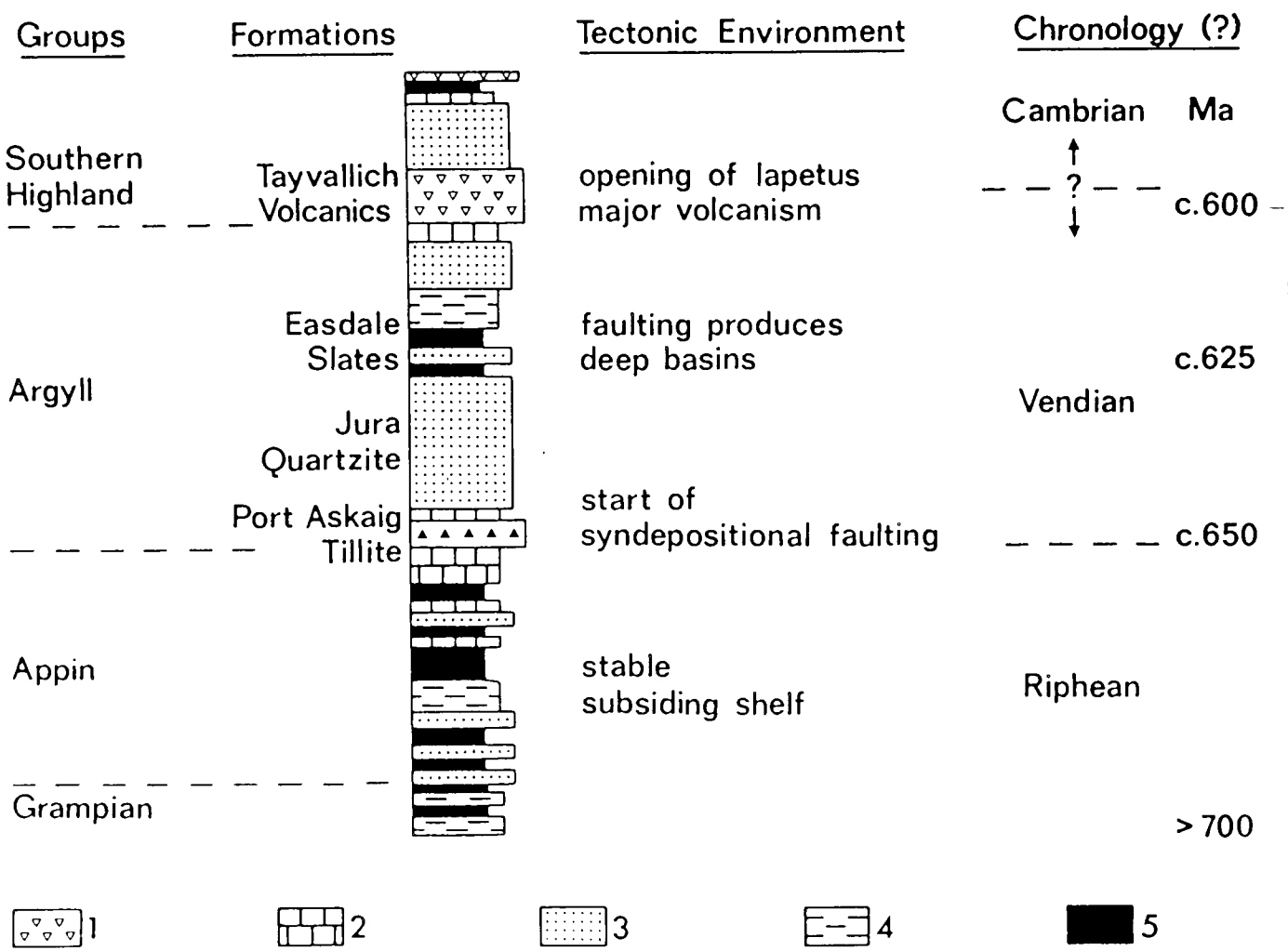

FIGURE 1.3

Summary of Dalradian stratigraphy and basin evolution from Anderton (1982).

1 lavas and tuffs
2 limestones and dolomites
3 sands
4 silts
5 muds

FIGURE 1.4

A: Structural geology of the Dalradian and Moine.

MT : Moine Thrust

G.G.F. : Great Glen Fault

T : Tarfside Nappe

B.A. proposed Banff Nappe

H.B.F. Highland Boundary Fault

Dotted area is inverted lower limb of the Tay Nappe. Parallel lines are the Tummel Steep Belt.

B: Cross section is along the line GH. Geology is after Coward (1983a), Brewer et al. (1983) , Bradbury et al. (1979) and other sources in the literature.

Key as above except IBS : Iltay Boundary Slide.

Dotted area is Dalradian.

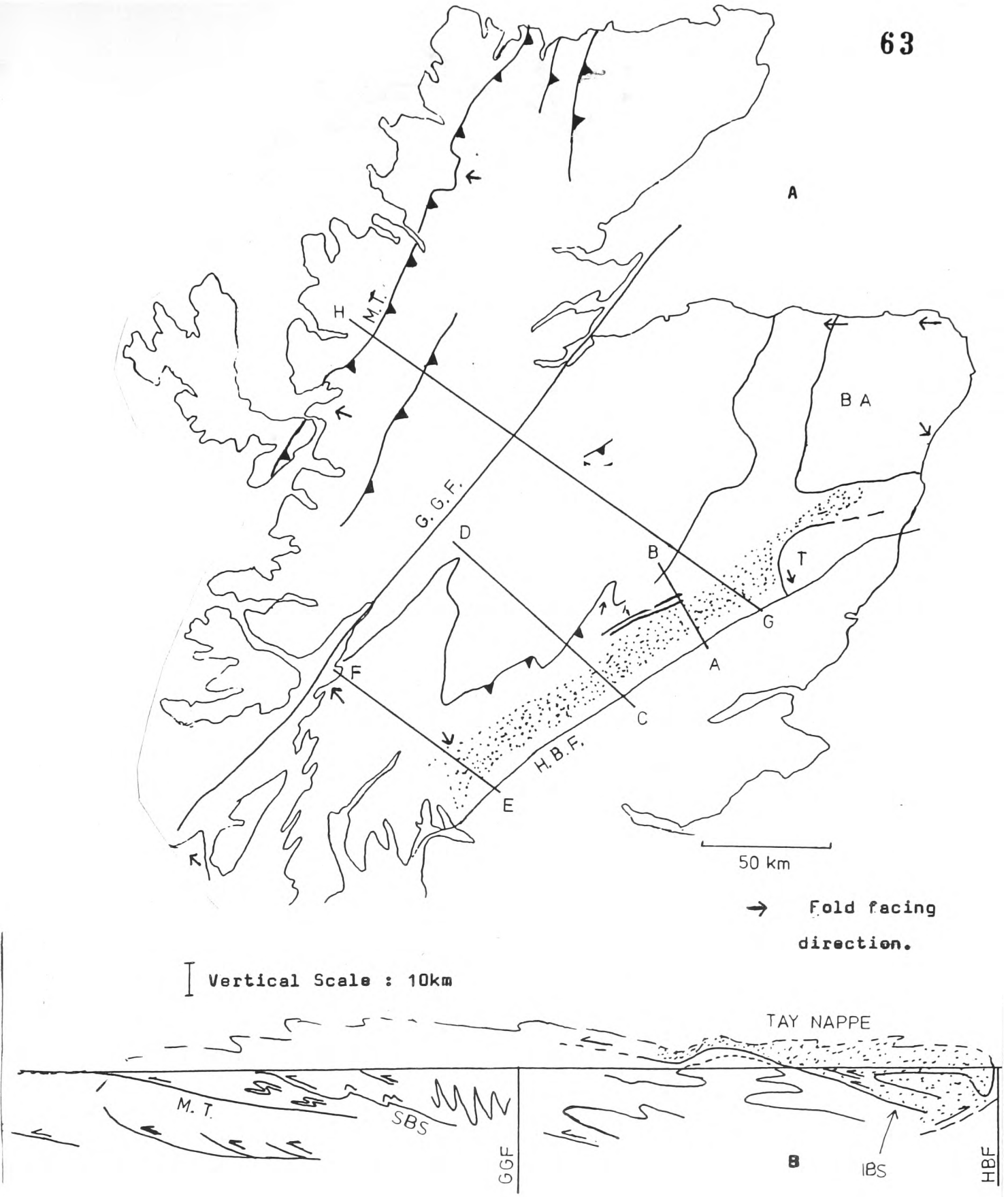
A
H
M.T.
G.G.F.
D
B
T
G
A
F
C
H.B.F.
E
B A
50 km
→ Fold facing direction.
Vertical Scale : 10km
TAY NAPPE
M.T.
SBS
GGF
B
IBS
HBF

FIGURE 1.4

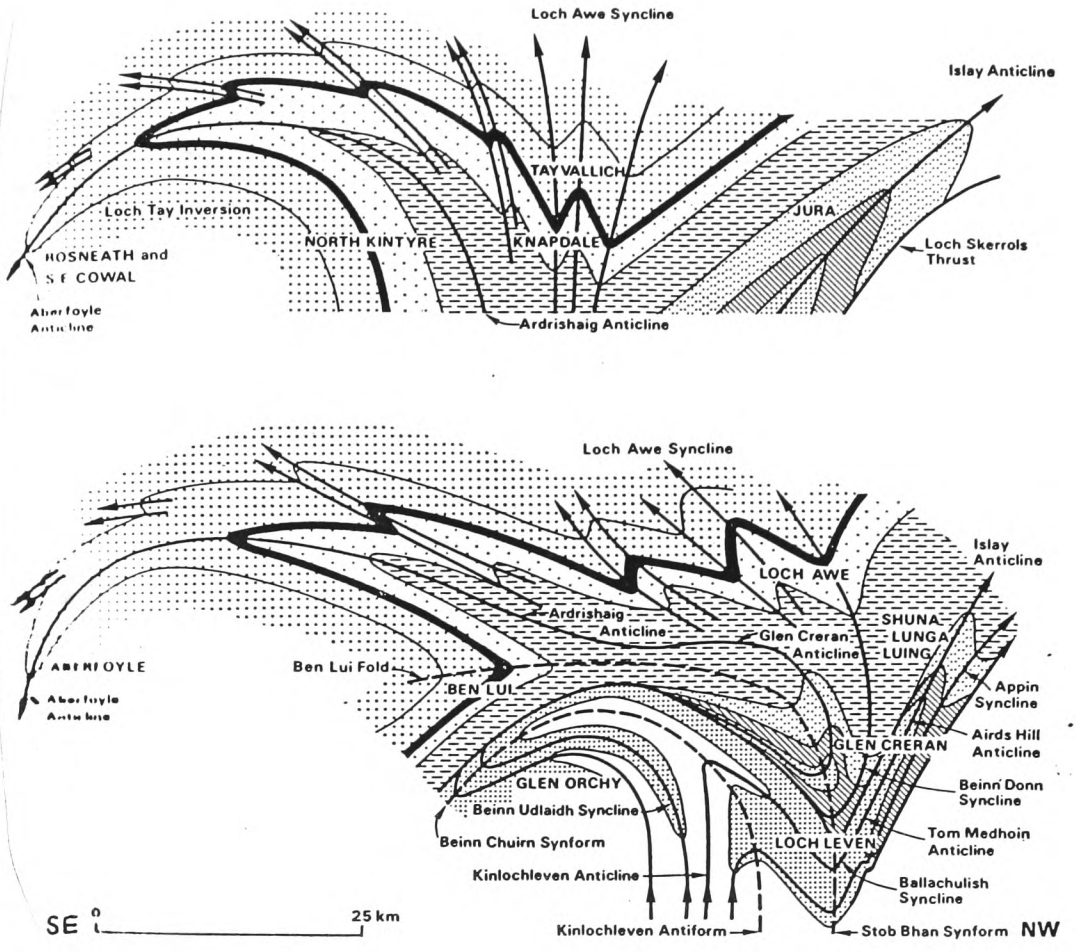

FIGURE 1.5a

Sketch cross section along the line E-F, from Roberts and Treagus (1977).

FIGURE 1.5b

Sketch section along the line A-B in figure 1.4, from Bradbury et al. (1979)

A: Southern Highland Group, B: Argyll Group,

C::Appin Group, D: Grampian Group (Moine).

1: Highland Boundary Fault, 2: Highland Border Steep Belt

3: Dunkeld Downbend, 4: Loch Tay Inversion

5: Tummel Steep Belt, 6: Slides in Blair Atholl Belt

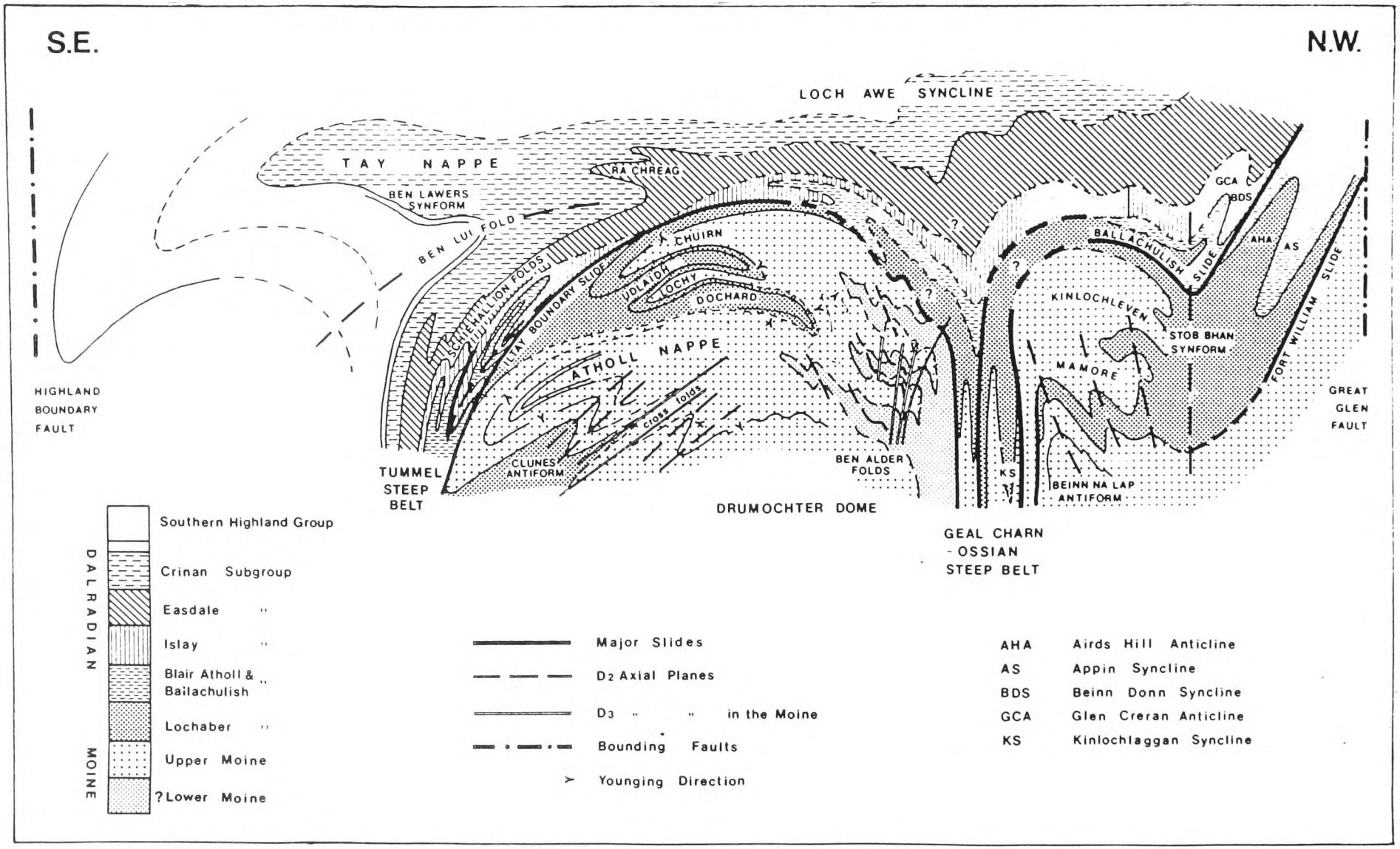

FIGURE 1.6 : Sketch cross section along the line C-D from Thomas (1979).

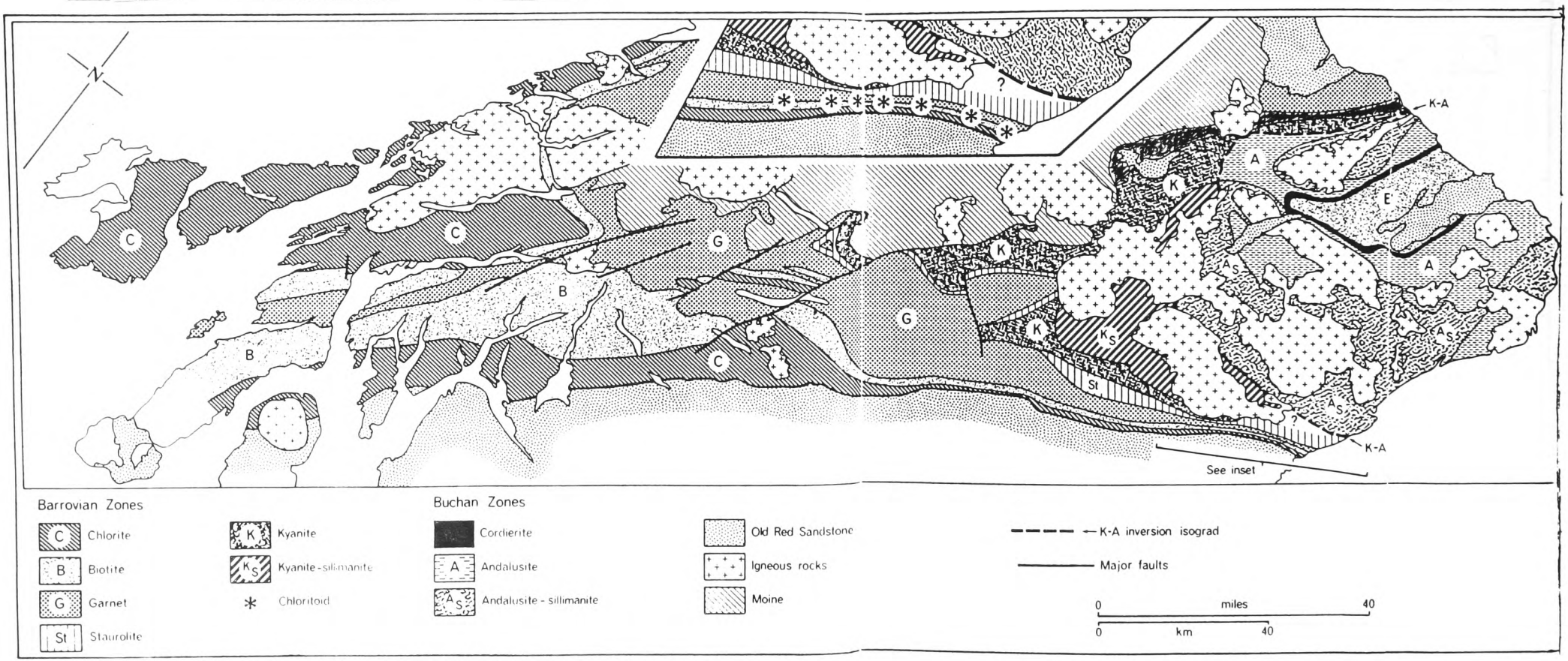

FIGURE 1.7

Mineral Zones in the Dalradian, modified after Atherton (1977).

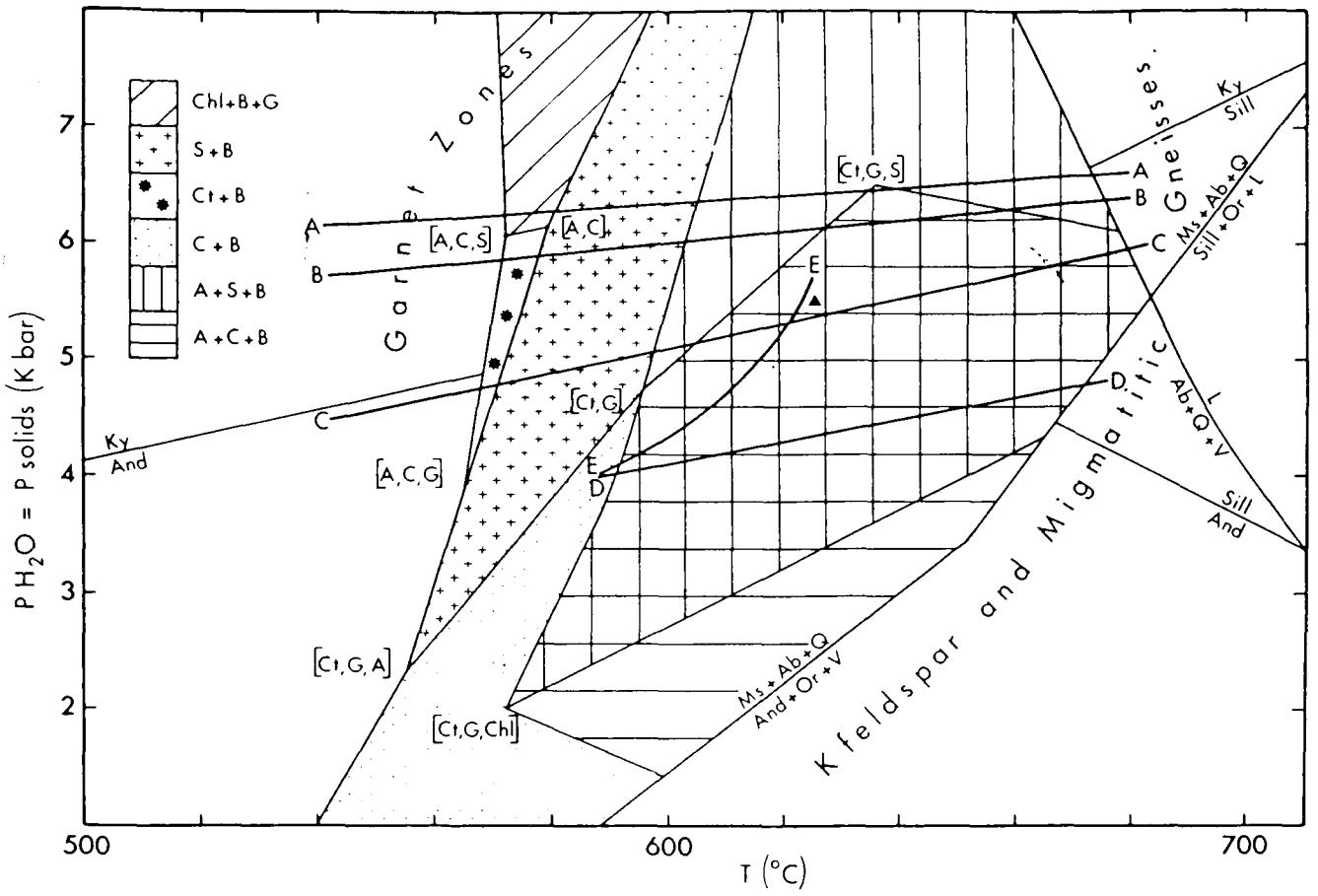

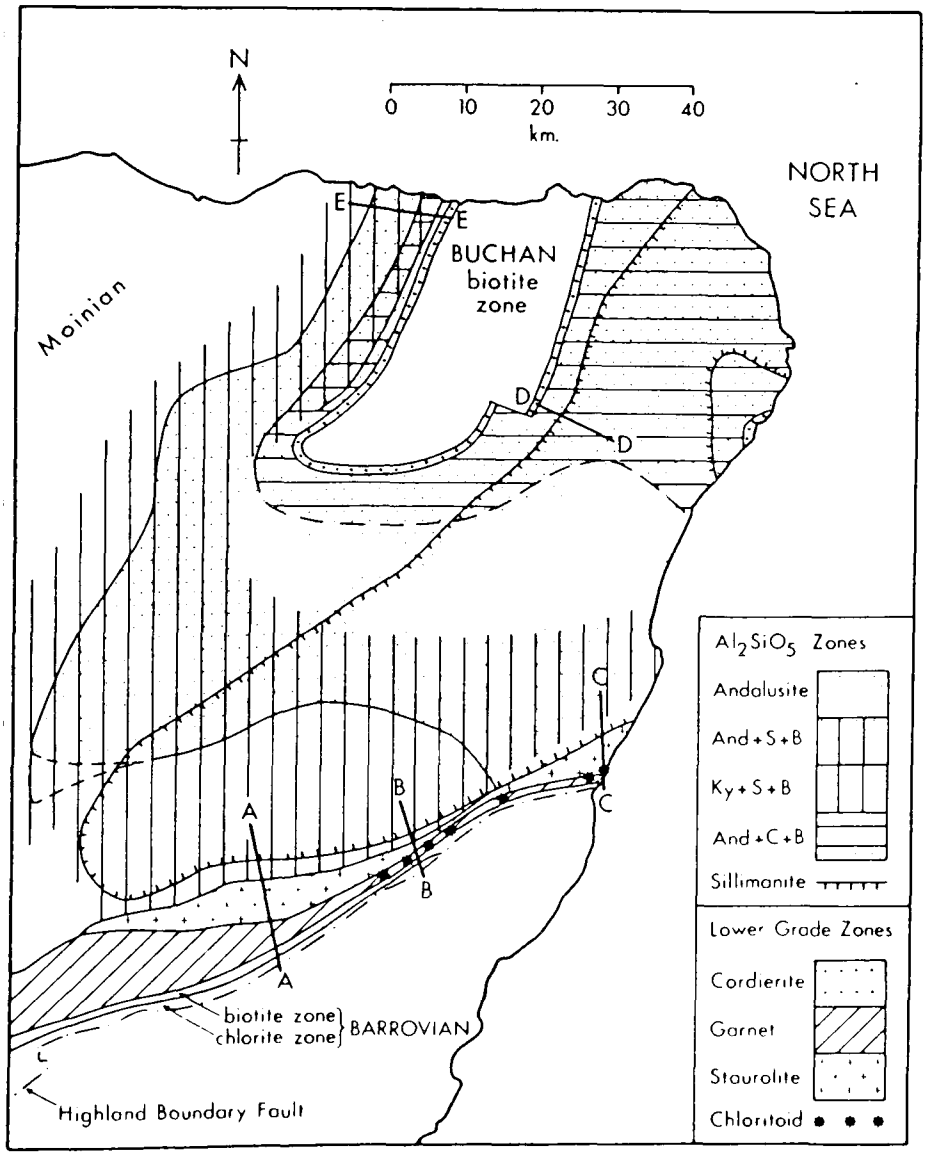

FIGURE 1.8
Facies series in Dalradian metapelites, from Harte and Hudson (1979).

FIGURE 1.9

Comparison between the P-T syntheses of Wells and Richardson (1979) and Harte and Hudson (1979). The kyanite-andalusite isograd is after Chinner and Heseltine (1979), ticked line is the outer limit of sillimanite. Circles show locations of the thermochemical estimates of Wells and Richardson. Dotted line is the 620 C isotherm and dot dash lines are isobars from Harte and Hudson (1979).

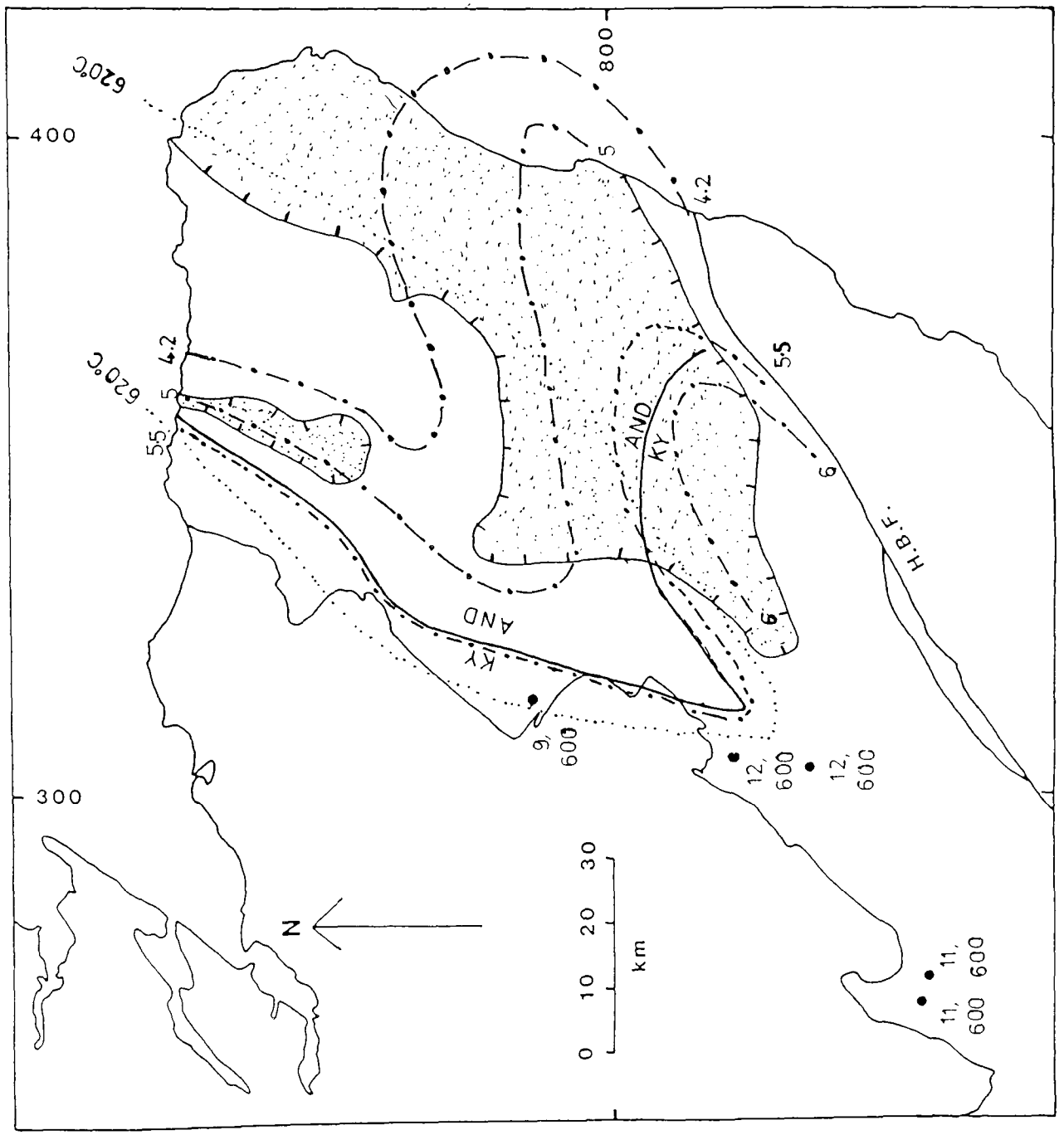

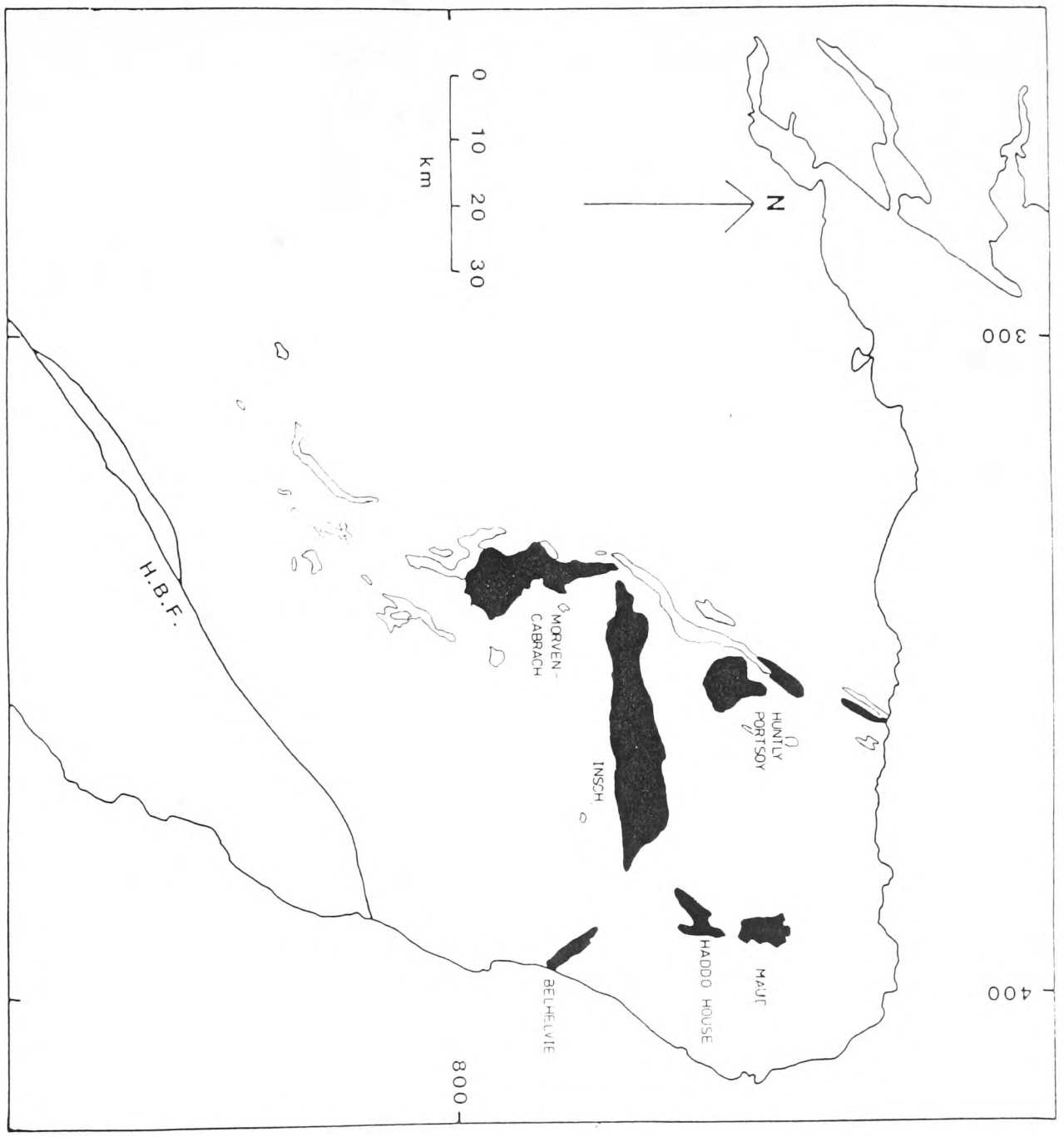

FIGURE 1.10

Basic Intrusions in the Dalradian.

Unshaded : Older Gabbros, Shaded : Newer Gabbros

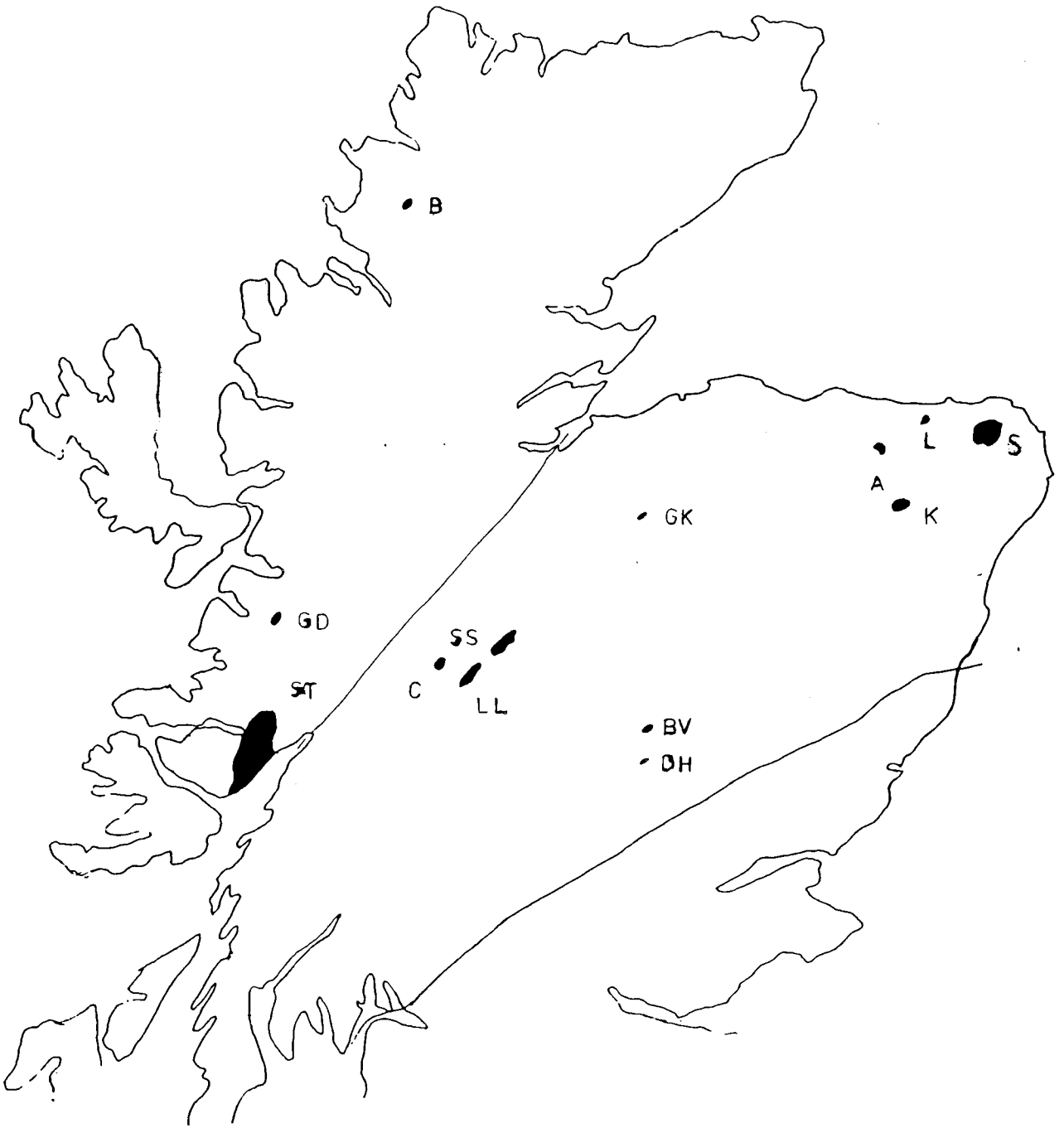

FIGURE 1.11

Dated crustally derived granites. A: Aberchirder, B: Loch Borrolan Complex, BV: Ben Vuirich, C: Corrieyairack Red Granite, DH: Dunfallandy Hill, GD: Glen Dessary Syenite, GK: Glen Kyllachy, K: Kennethmont, LL: Loch Laggan, L: Longmanhill, S: Strichen, SS: Strathspey, ST: Strontian.

FIGURE 1.12

Newer Granites in the Dalradian and Moine intruded at circa 400Ma.

E-Etive, L-Lochnagar, C-Cairngorm, K-Kincardine, F-Foyers.

FIGURE 1.13

Location of age constraints detailed in tables 1.5 and 1.6.

HBC Highland Border Complex.
DF Dunfallandy Hill Granite
BV Ben Vuirich Granite
H K-Ar whole rock date of Harper (1967)
D Rb-Sr muscovite date of Dempster (1984)
NG Newer Gabbros
S Strichen Granite
GK Glen Kyllachy Granite
L Rb-Sr whole rock date of Lambert et al. (1982)
BR Rb-Sr whole rock date of Brewer et al. (1979)
GD Glen Dessary Syenite
SW Swordly Slide
LB Loch Borrolan Complex (constraints on Moine Thrust movement).

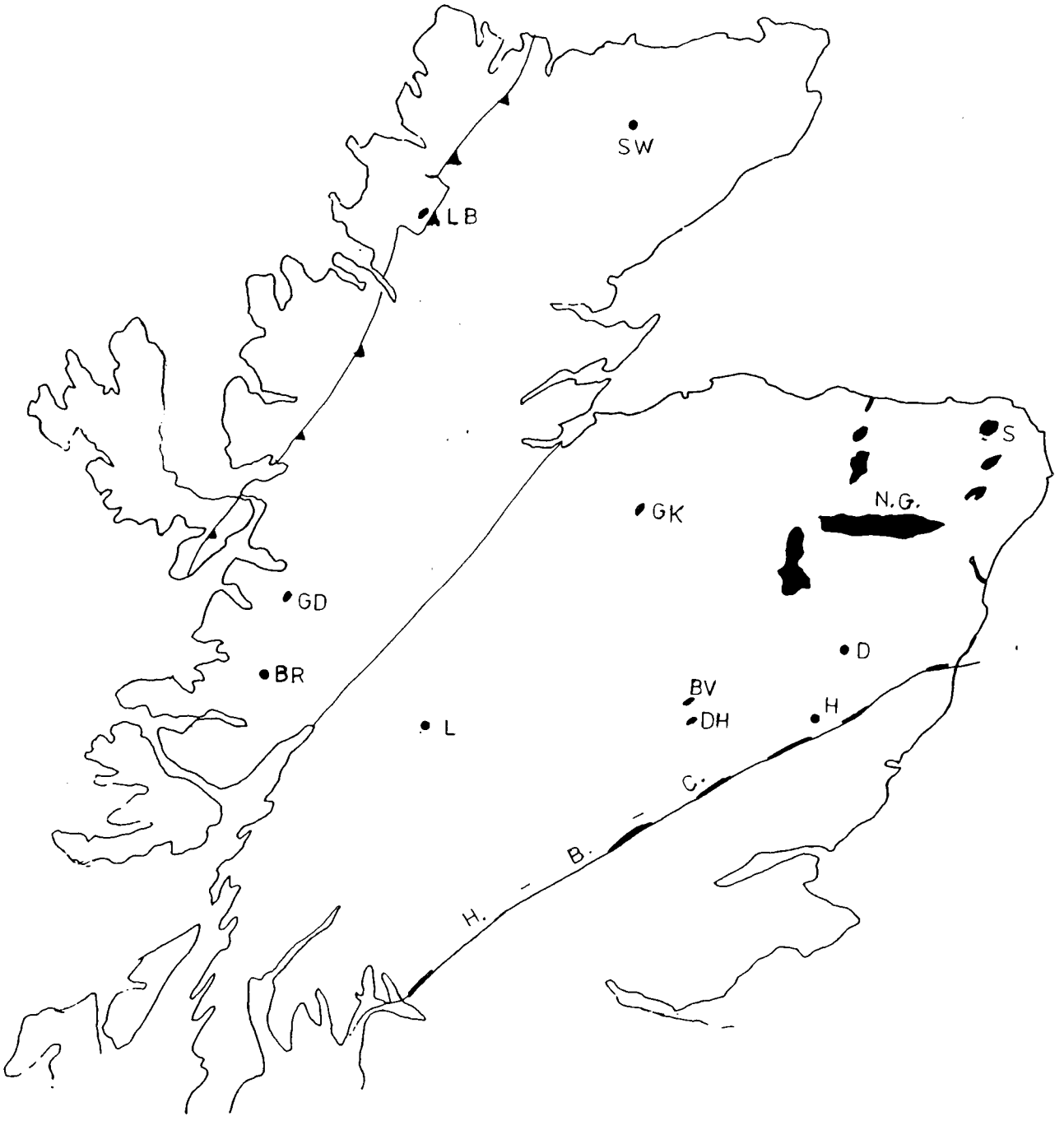

FIGURE 1.13

FIGURE 2.1

Stability of some assemblages in the Dalradian.

■ paragonite+quartz

✳ chloritoid+quartz (Chinner,1967, Atherton and +biotite Smith, 1979)

o garnet+chlorite (shown within the kyanite zone)

● chlorite+calcite+quartz

□ muscovite+calcite+quartz & muscovite+zoisite+quartz

P Portsoy

A Aberdeen

S Schichallion and the Central Highlands

E Glen Ey

DG Duchray Hill Gneiss

GC Glen Clova

GE Glen Esk

GA Glen Avon

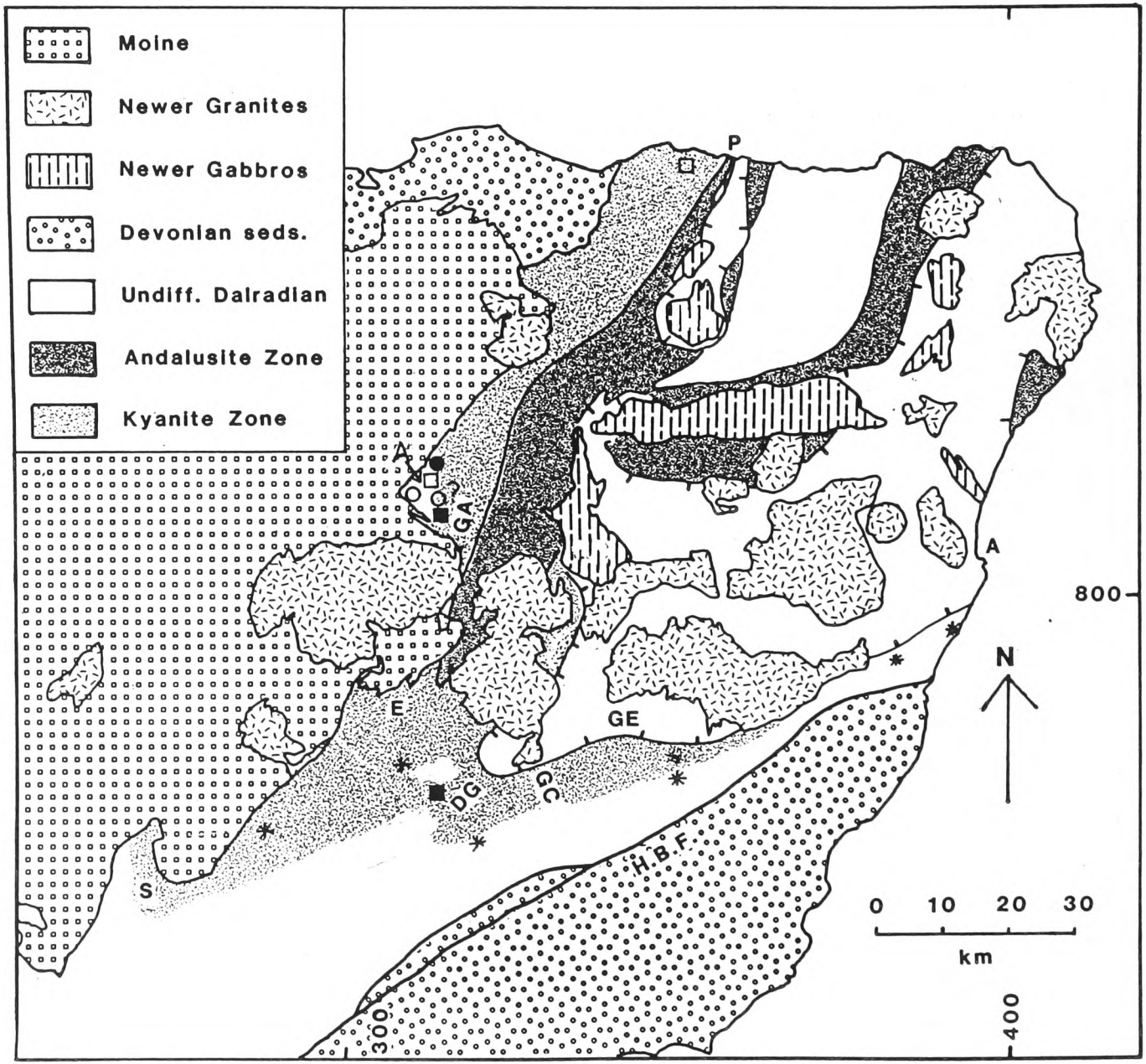
Moine
Newer Granites
Newer Gabbros
Devonian seds.
Undiff. Dalradian
Andalusite Zone
Kyanite Zone
P
A
GA
GE
E
DG
GC
S
H.B.F.
N
800
400
300
0 10 20 30
km

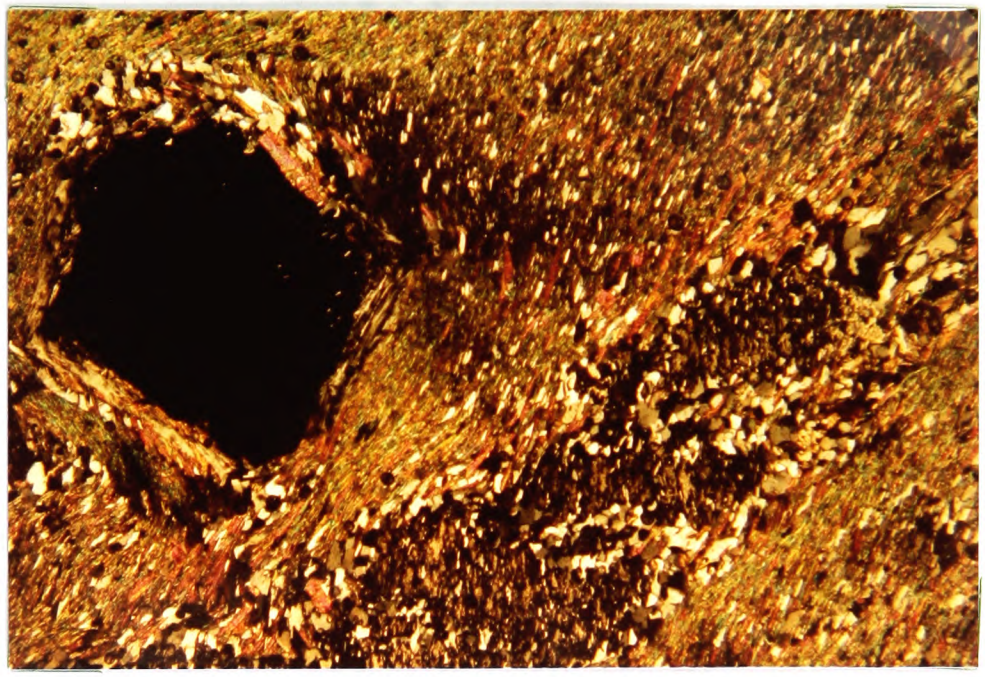

FIGURE 2.2(a)

37F (x50) Schist, Glen Avon.

Garnet and kyanite porphyroblasts.

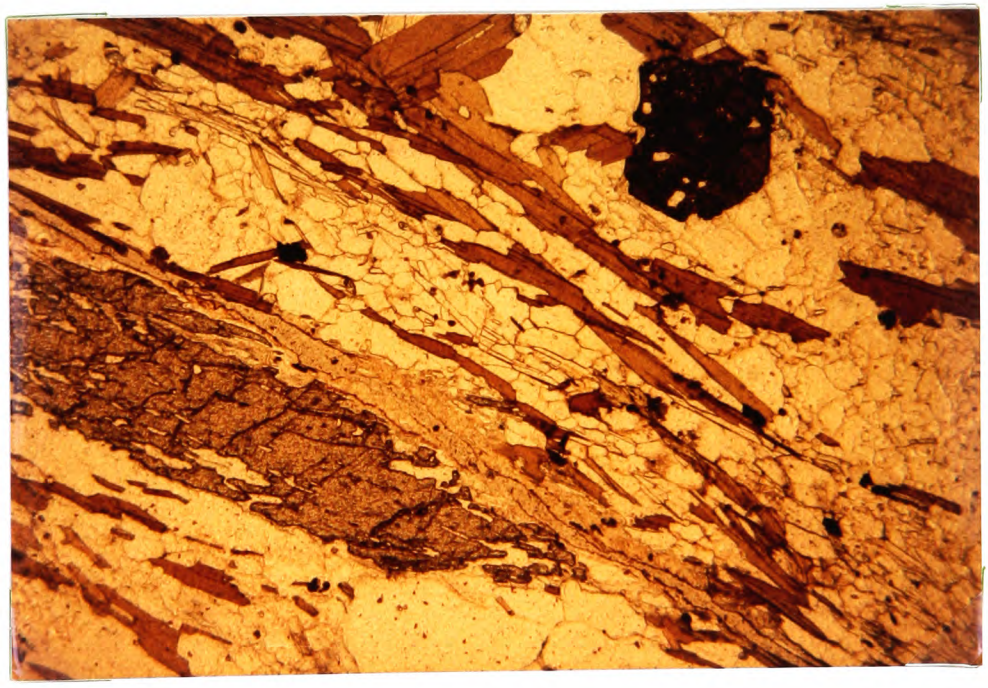

FIGURE 2.2(b)

W03 (x50). Garnet-kyanite schist,

Schichallion.

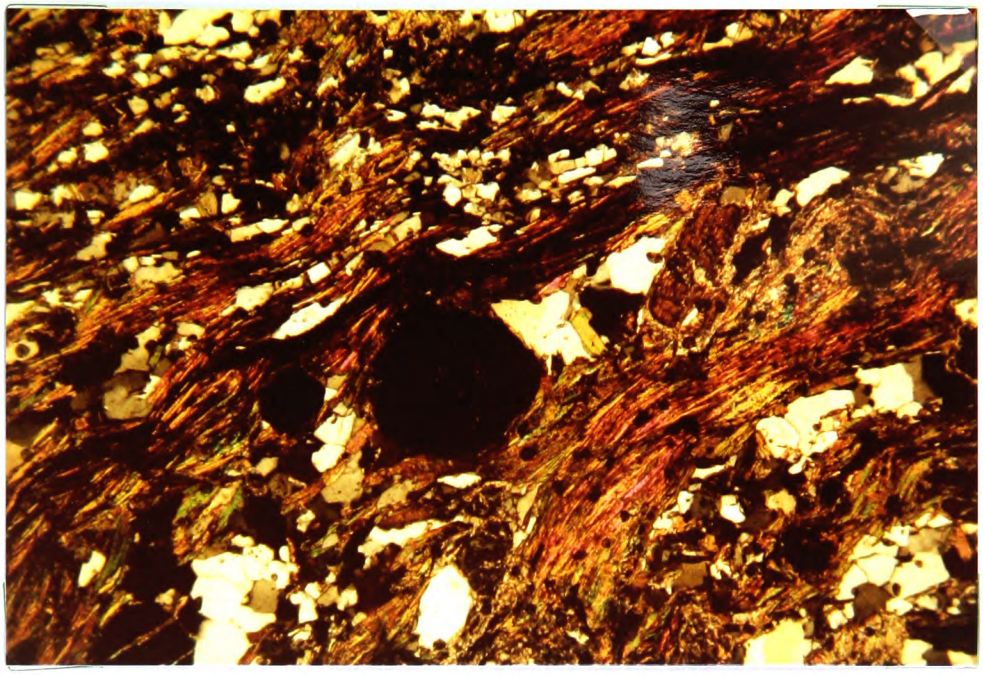

FIGURE 2.3 (a)

GE5 (x50) Garnet-kyanite shist, Glen Ey.

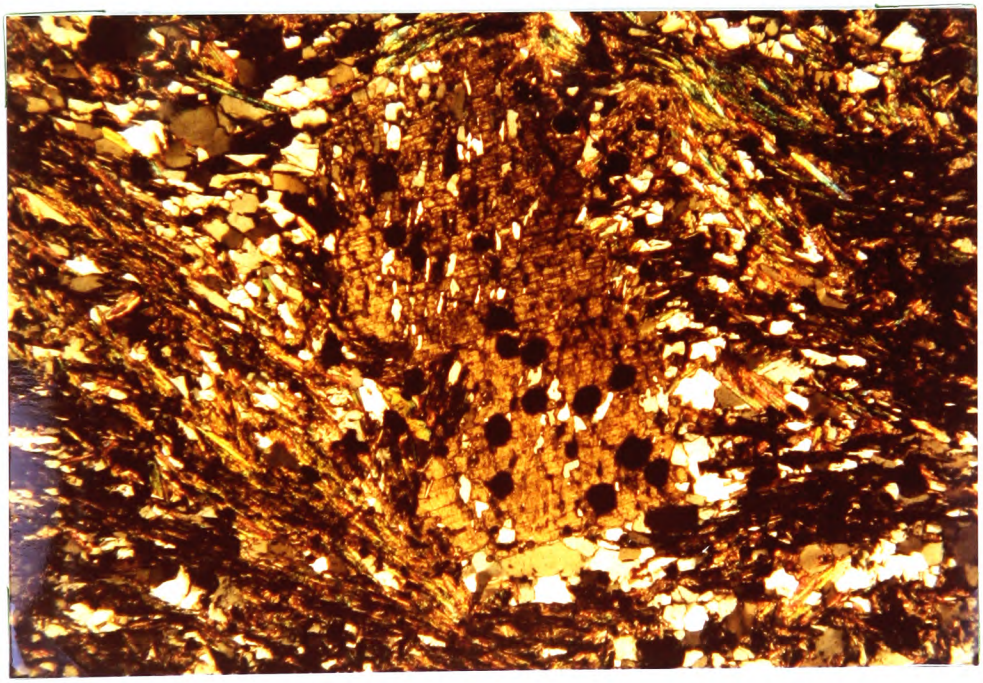

FIGURE 2.3 (b)

(x50). Kyanite porphyroblast overgrowing small garnets, Glen Ey.

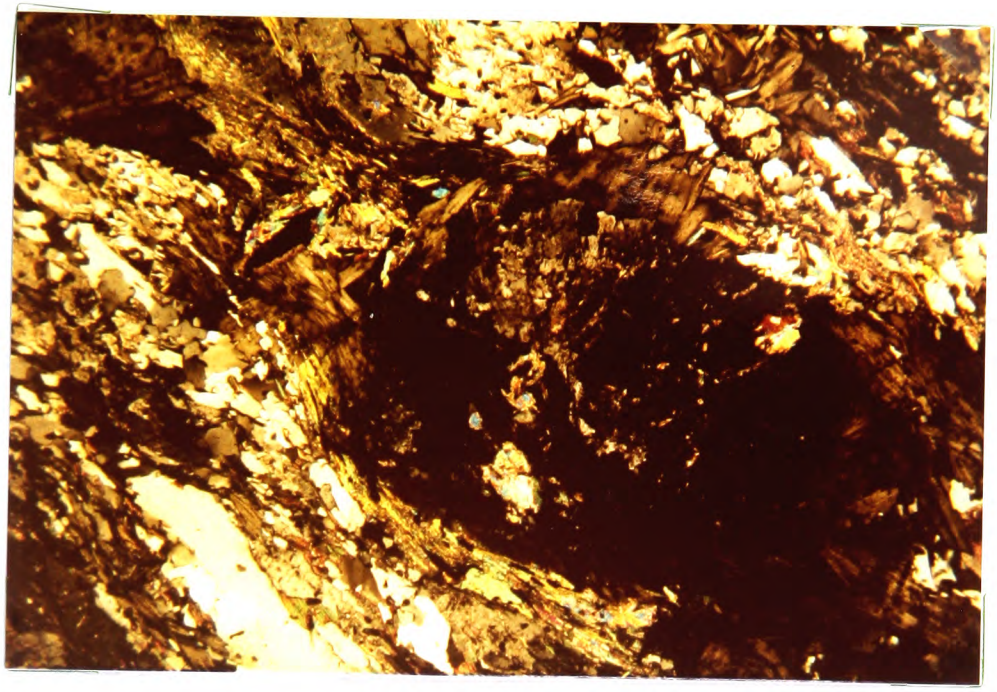

FIGURE 2.4 (a)

41A (x50) Chlorite replacing garnet

Glen Avon.

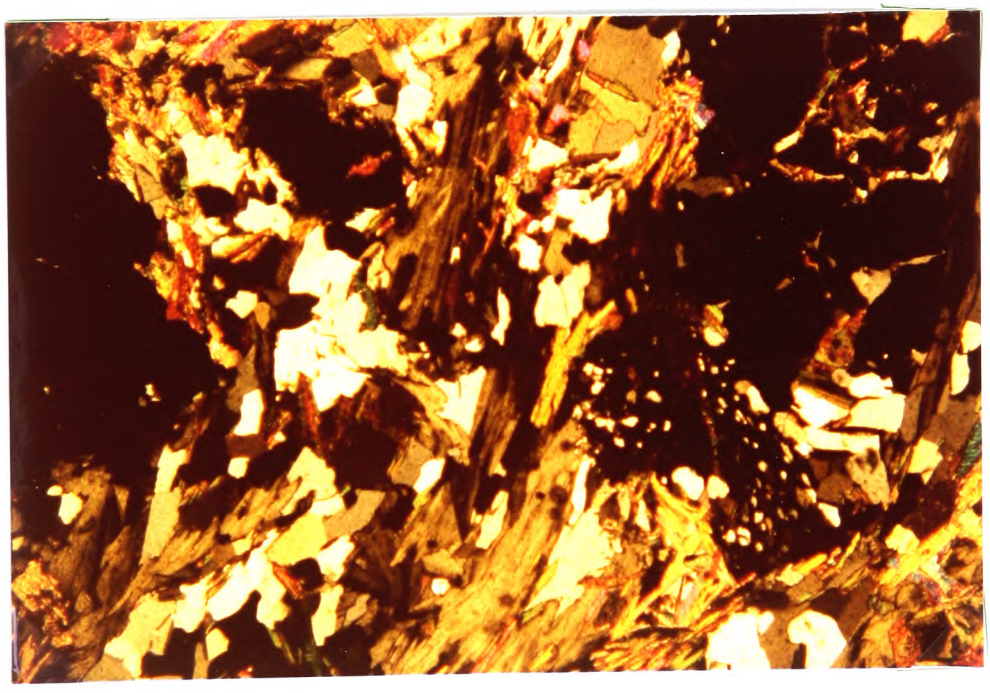

FIGURE 2.4 (b)

W35 (x50). Chlorite forming a well defined

schistosity. Glen Avon.

FIGURE 2.5

(x50). Muscovite-chlorite schistosity.

Garnet occurs elsewhere. Ailnack Gorge.

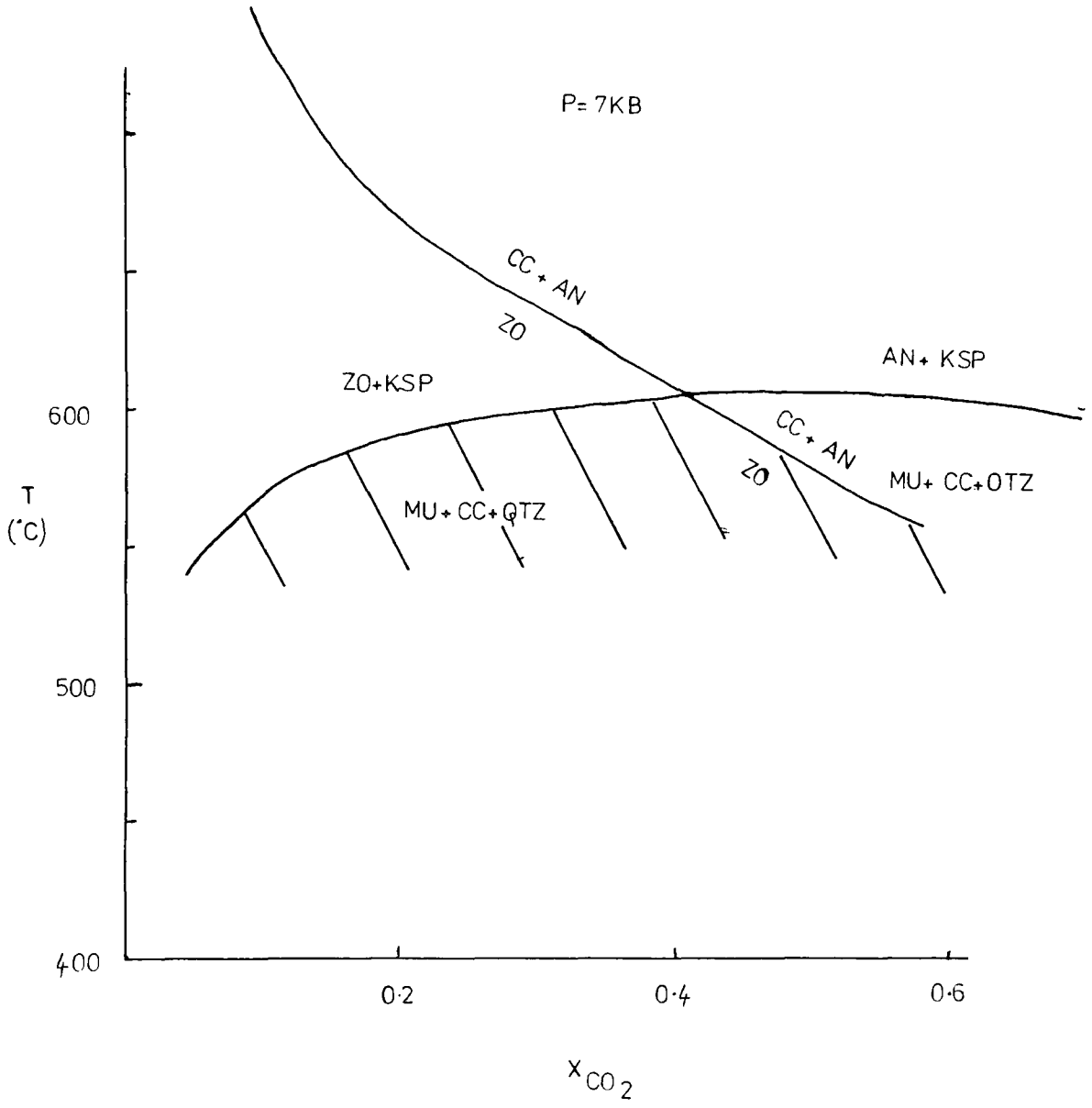

FIGURE 2.6

Stability of the assemblage muscovite-zoisite -calcite-quartz at 7kb. Pure phases, based on data of chapter 5

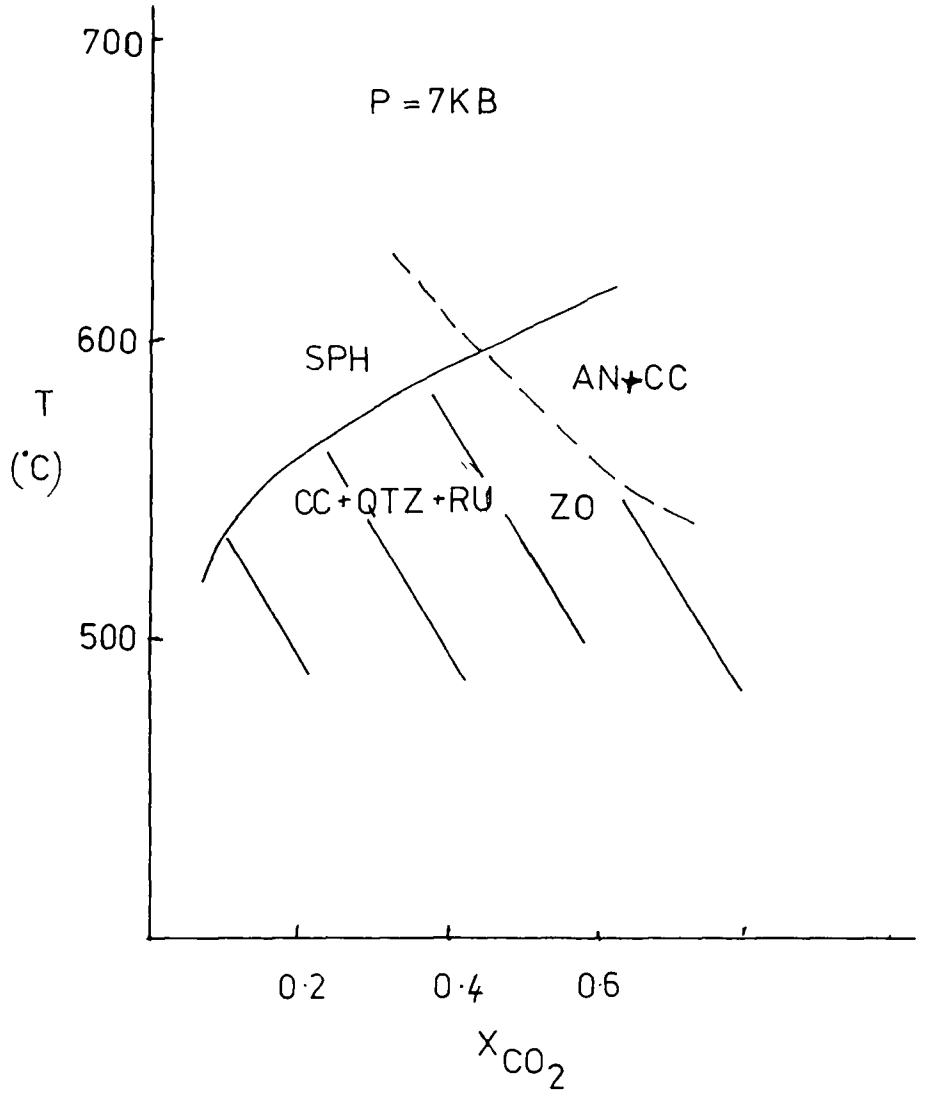

FIGURE 2.7

Stability of the assemblage zoisite-calcite-rutile -quartz at 7kb. Data of chapter 5, Robie et al. (1978) and Jacobs and Kerrick (1981).

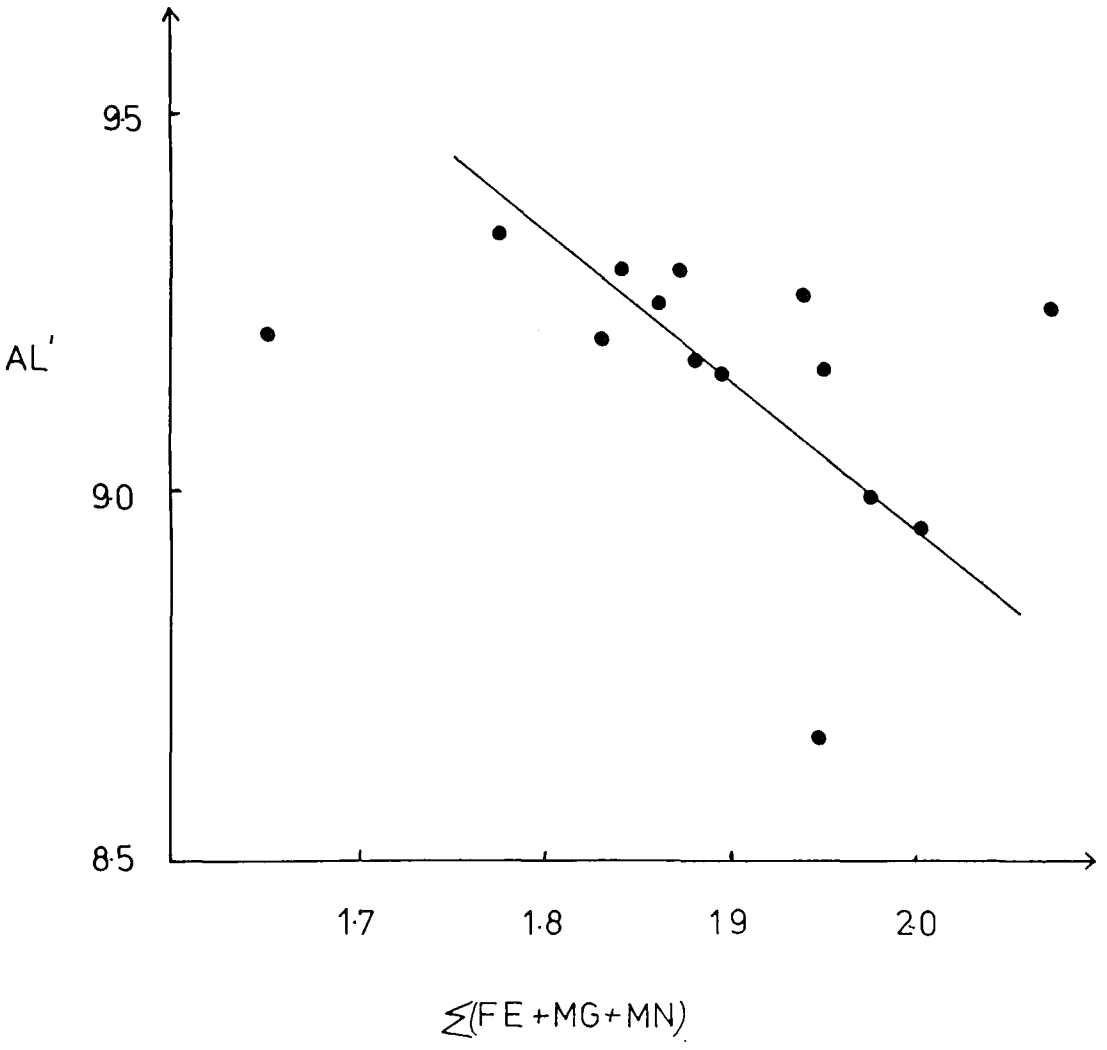

FIGURE 2.8

Staurolite compositions in Dalradian rocks

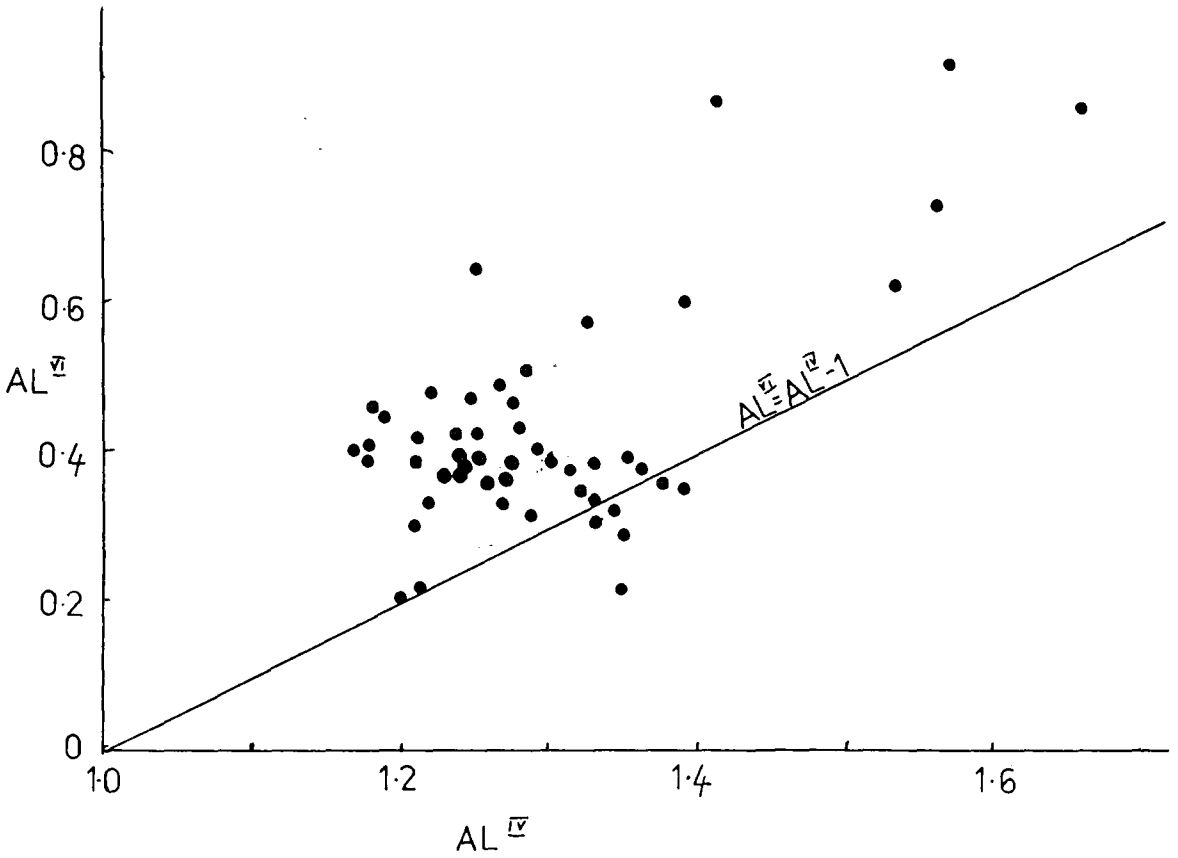

FIGURE 2.9

Aluminium contents of biotites.

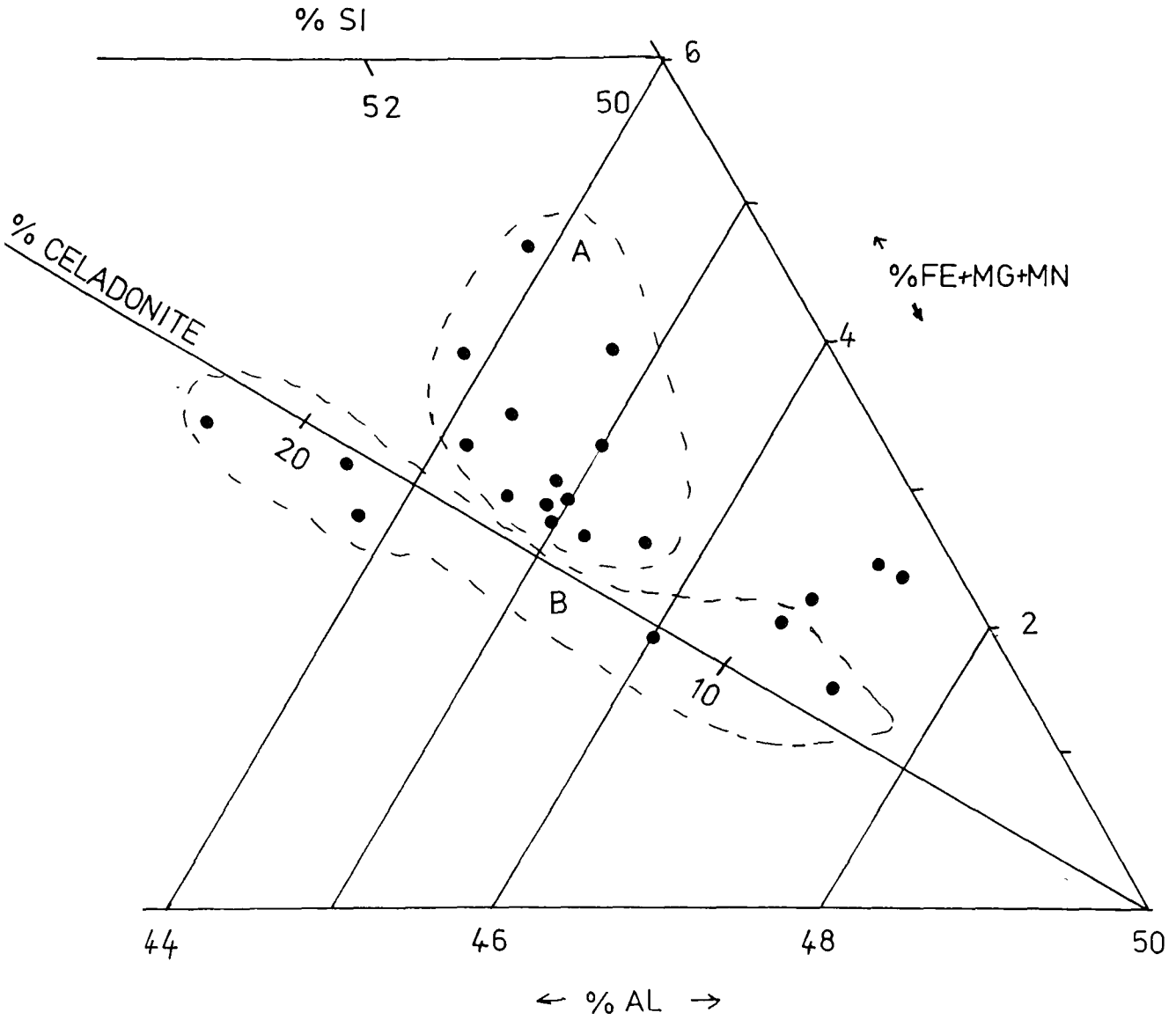

FIGURE 2.10

Muscovite compositions, plotted in part of the Al-Si-(Mg+Fe+Mn) triangle.

A Central Highlands and Glen Avon

B High kyanite zone : Glen Esk, Glen Clova and the Duchray Hill Gneiss

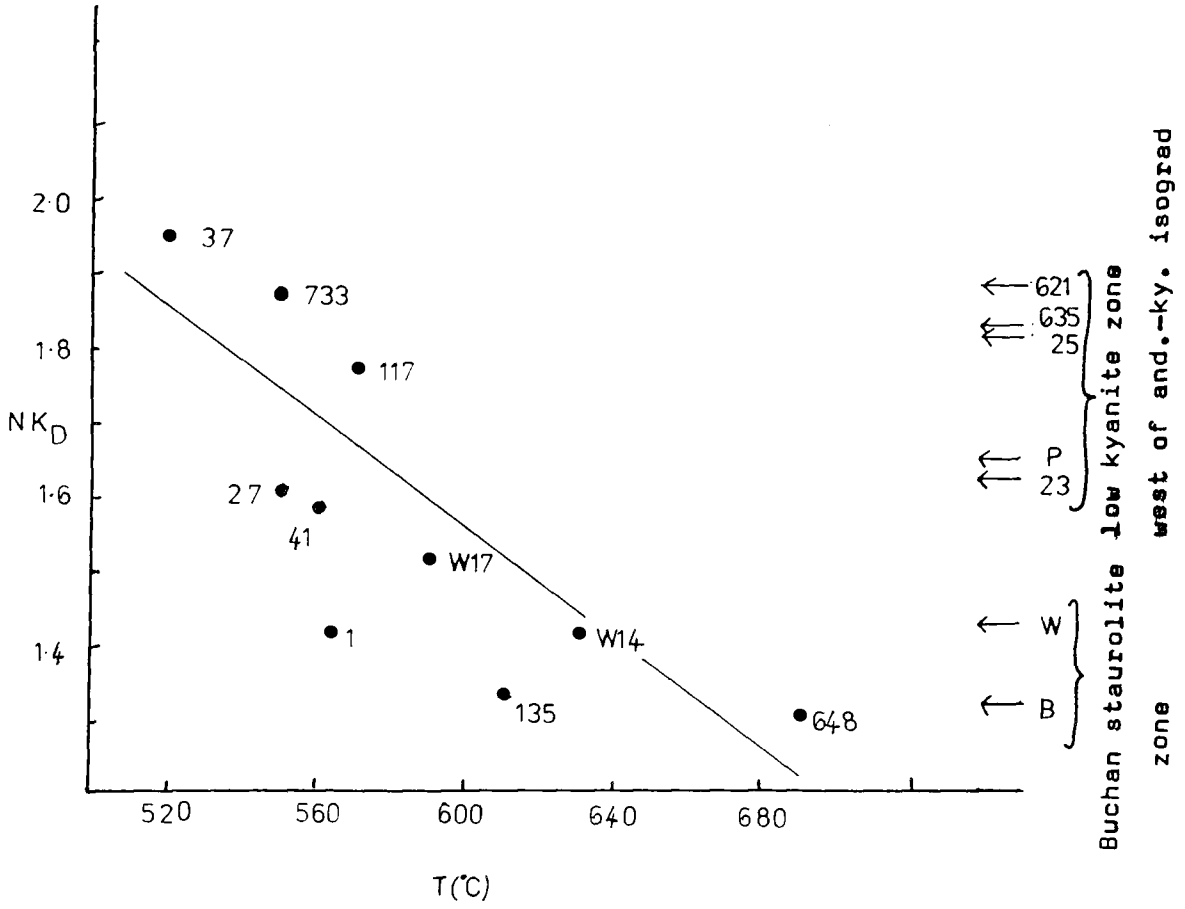

FIGURE 2.11

Staurolite-biotite lnKs plotted against Hodges and Spear garnet biotite temperatures. Arrows indicate ln Ks for garnet absent assemblages.

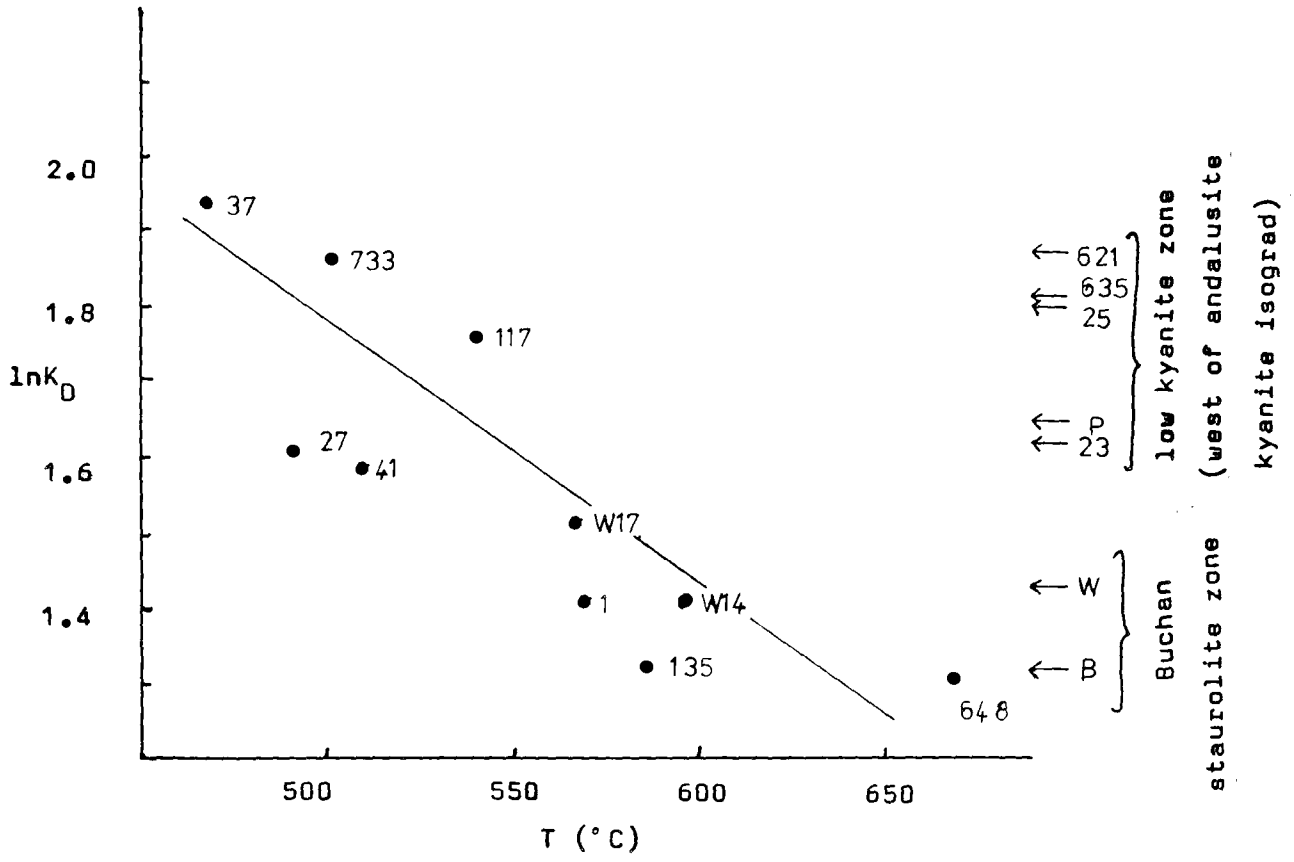

FIGURE 2.12

Staurolite-biotite lnKs plotted against Ganguly and Saxena garnet and biotite temperatures. Arrows indicate garnet absent assemblages.

FIGURE 2.13

Data for staurolite biotite Fe-Mg exchange from the literature

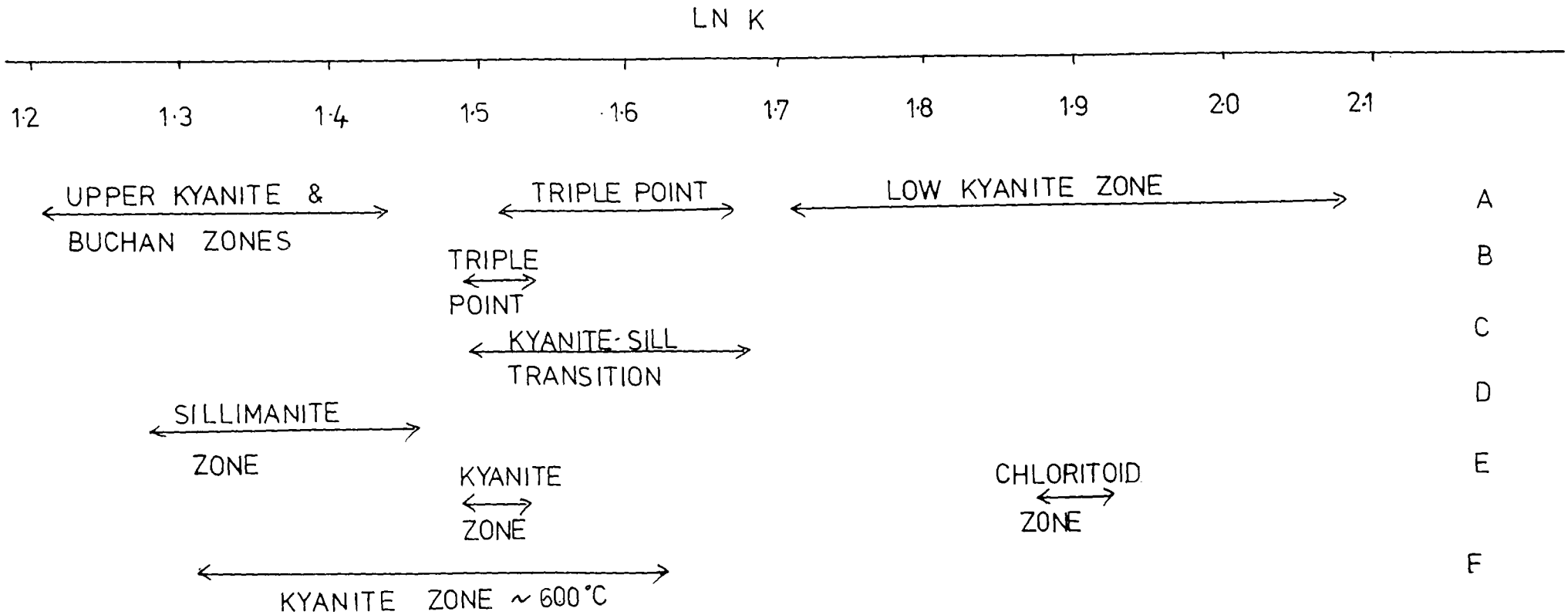

A This study

B Truchas Peaks (Grambling, 1982)

C Penfold Creek (Fletcher and Greenwood, 1979)

D Connemara (Yardley et al., 1980)

E Eastern Alps (Droop, 1983)

F Mohr and Newton (1983)

FIGURE 2.14

Amphibole compositions

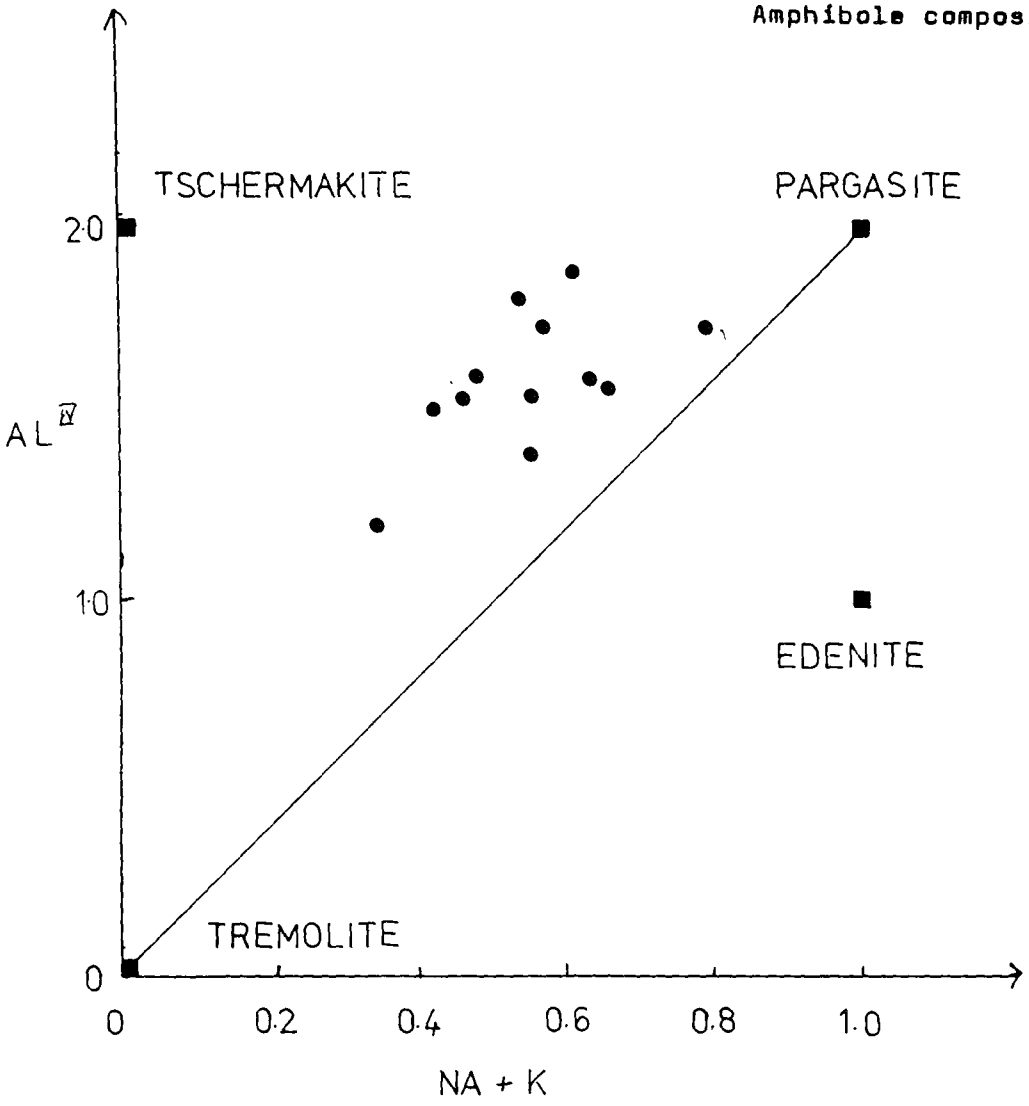

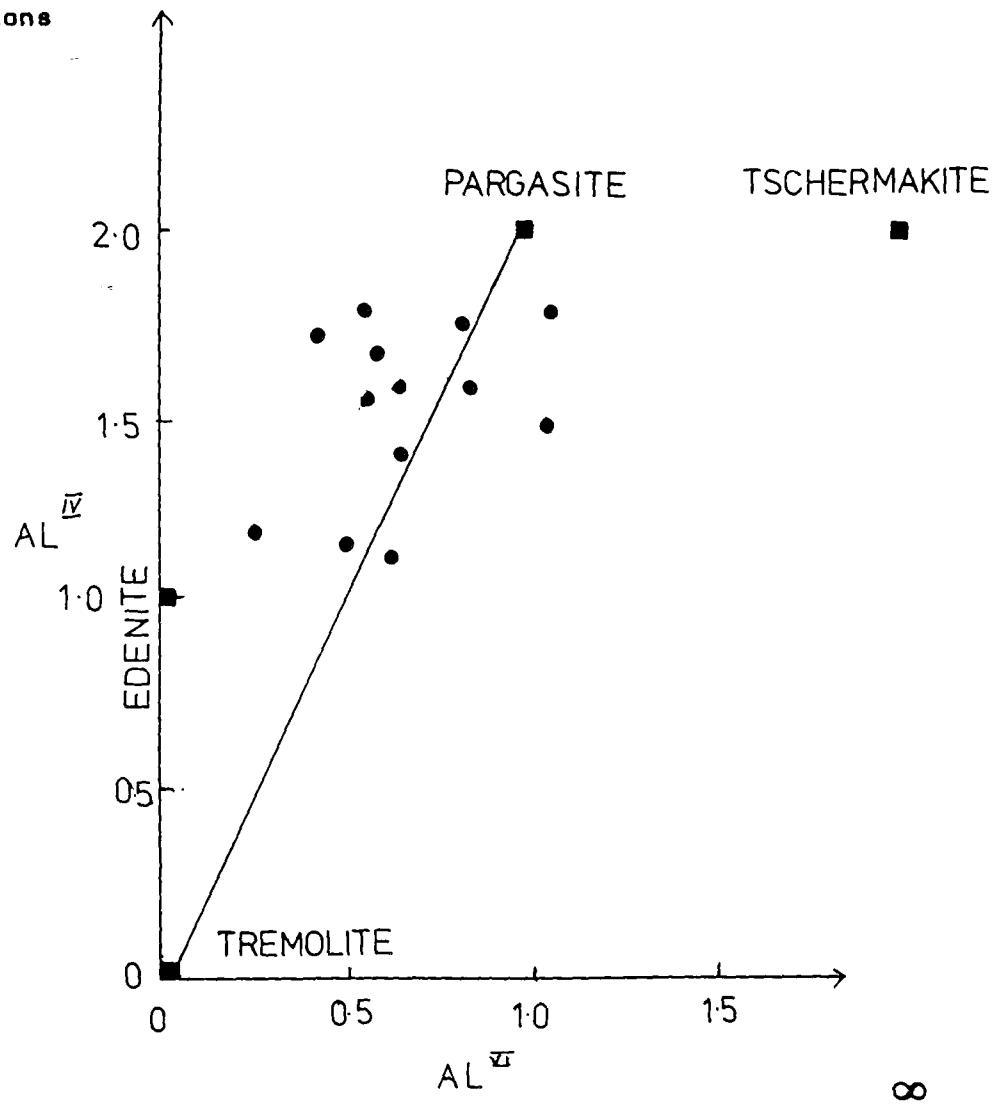

FIGURE 2.15

Plots illustrating progressive reaction between plagioclase and hornblende.
A: Ca/Na in plagioclase and on the M4 site in the hornblende.
B: Albite in plagioclase against Na on the amphibole A site.
Temperature contours from garnet biotite thermometer temperature estimates from the areas concerned.

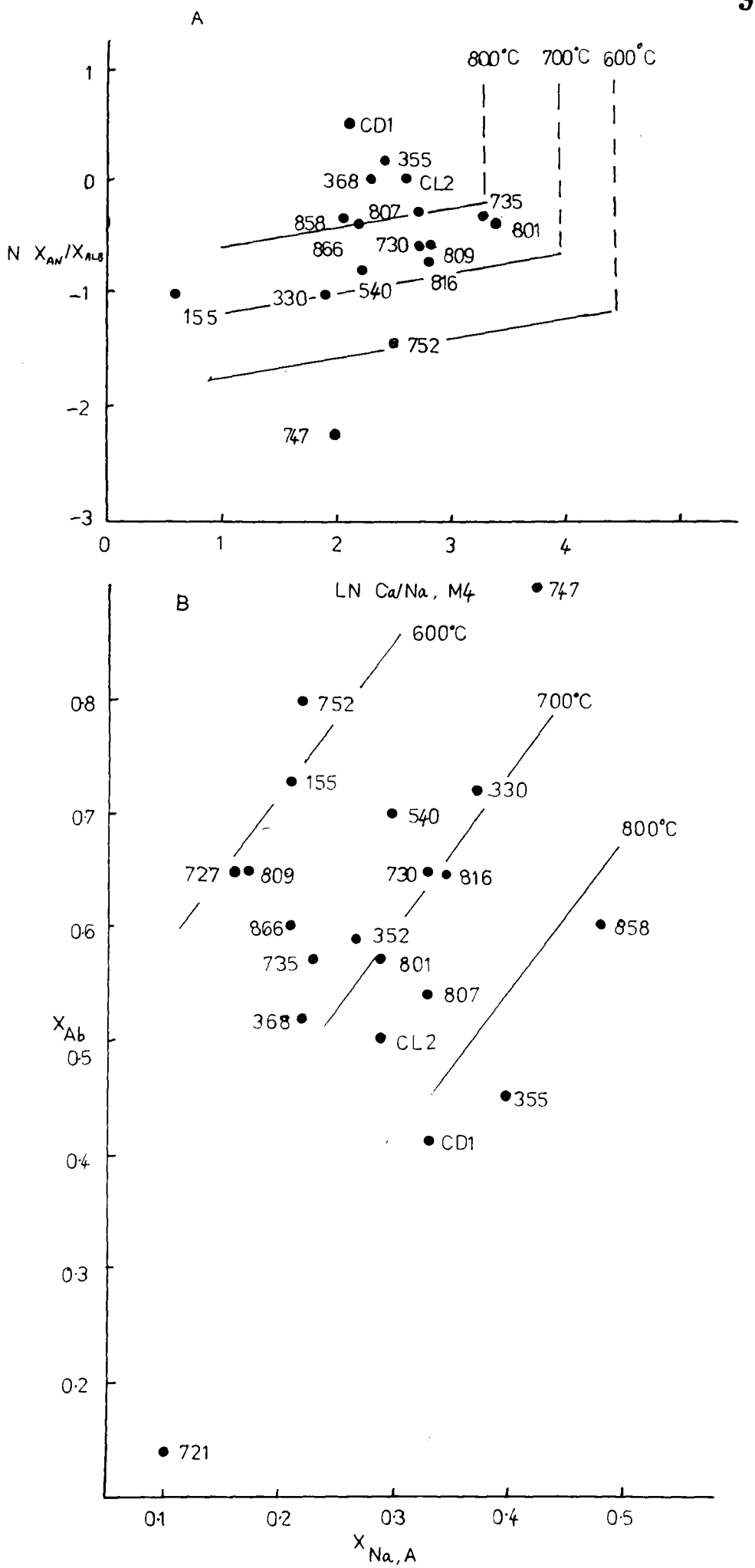
A
800°C
700°C
600°C
CD1
355
368
CL2
735
858
807
801
866
730
809
816
330
540
155
752
747
N X_{AN}/X_{ALB}
LN Ca/Na, M4
B
600°C
752
700°C
155
330
540
800°C
727
809
730
816
858
866
352
735
801
807
368
CL2
355
CD1
721
X_{Ab}
$X_{Na,A}$

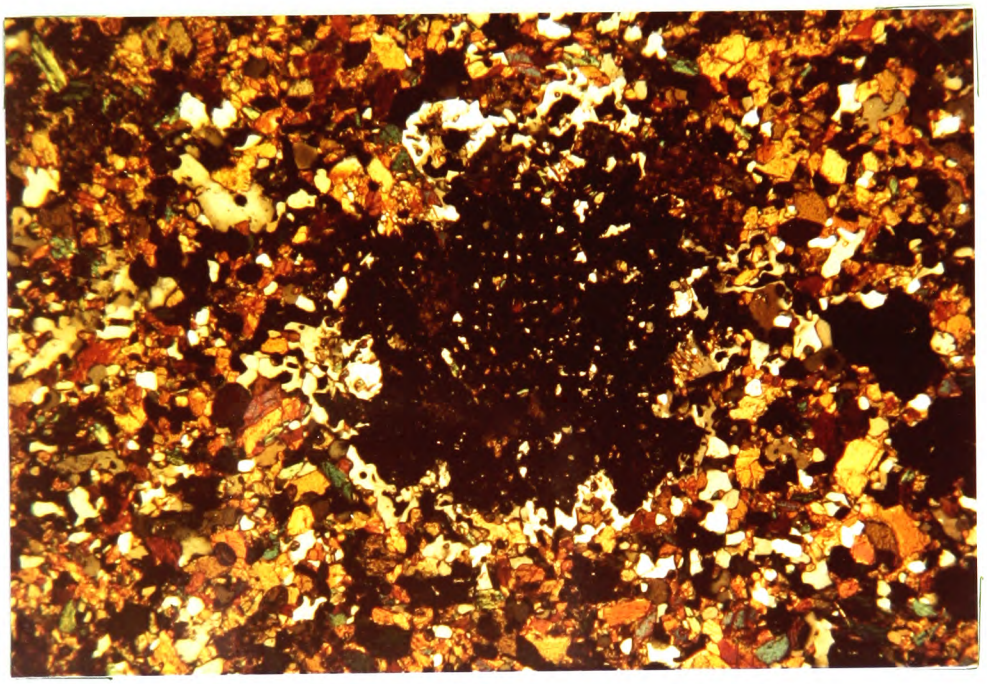

FIGURE 2.16

747B (x50). Garnet amphibolite, Schichallion area. Irregular garnets, surrounded by coronas of plagioclase.

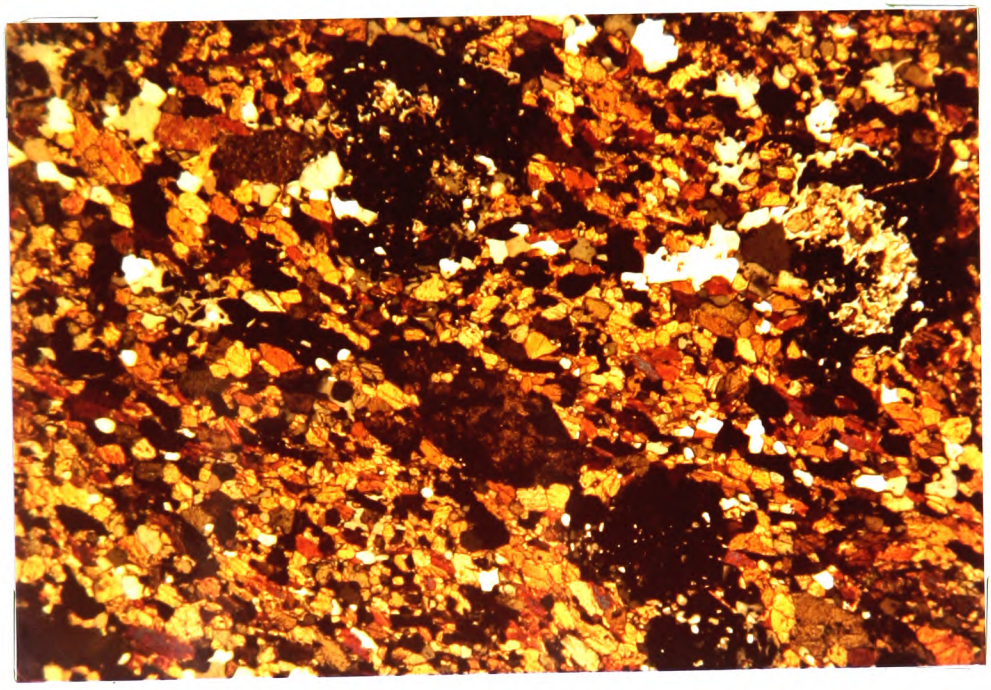

FIGURE 2.17

747A (x50). Garnet amphibolite, Schichallion area. Irregular garnets with centres replaced by calcite and plagioclase.

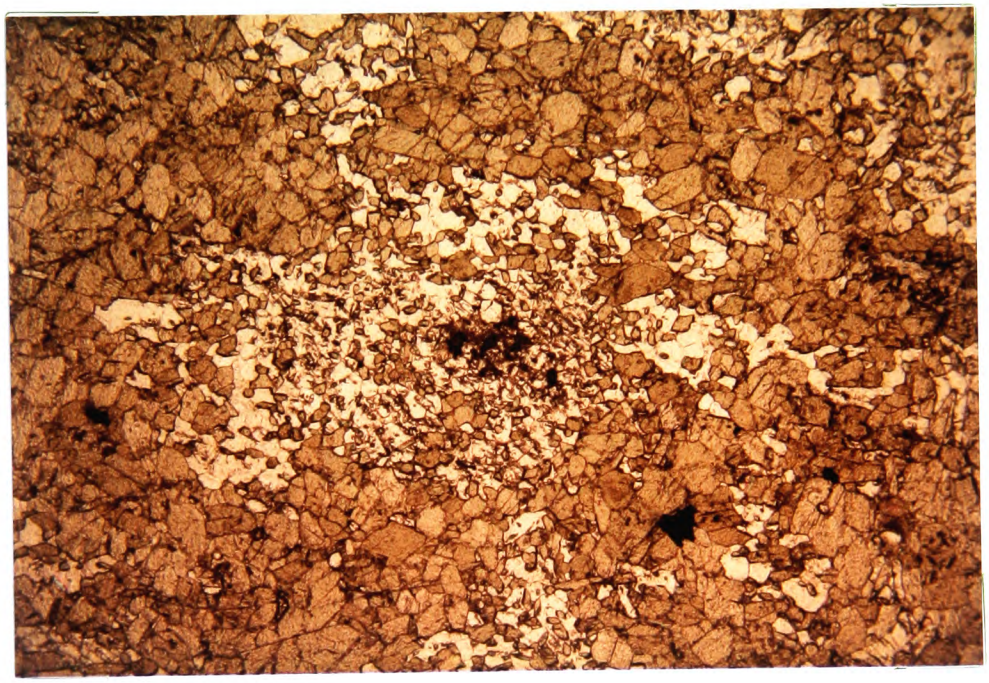

FIGURE 2.18

747A (x50). Garnet amphibolite, Glen Esk

Resorbed garnet (relict still visible), replaced by plagioclase and minor hornblende.

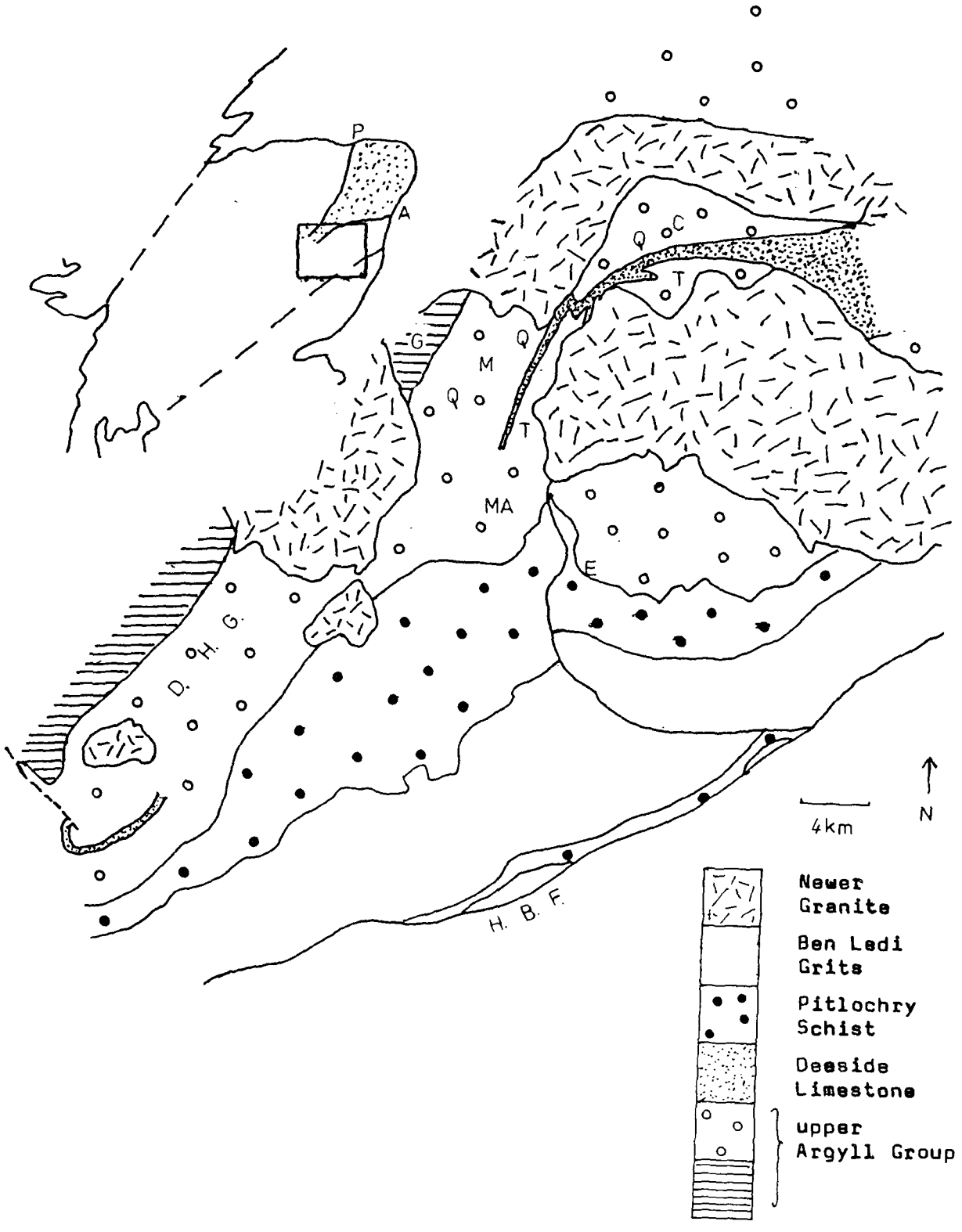

FIGURE 3.1

Sketch map of parts of the southeast Dalradian.

P : Portsoy, A : Aberdeen, D.H.G. : Duchray Hill Gneiss, G : Glen Girnock, M : Glen Muick, MA : Glen Mark, C : Cromar, E : Glen Esk, H.B.F. : Highland Border Fault. Q : Queens Hill Group, T : Glen Tanar Group.

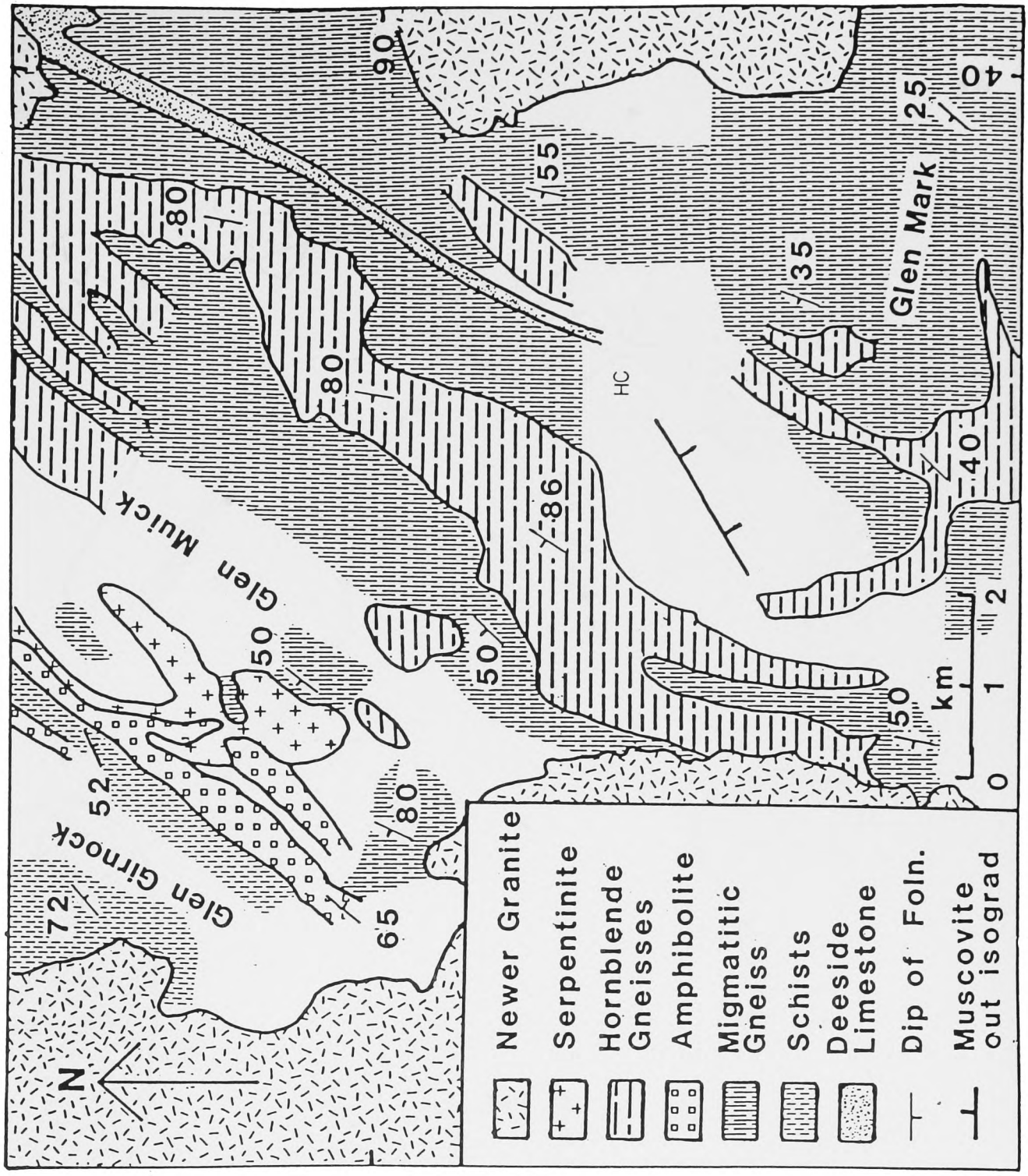

FIGURE 3.2

Geological sketch map of the Glen Muick area.

HC : Hare Cairn

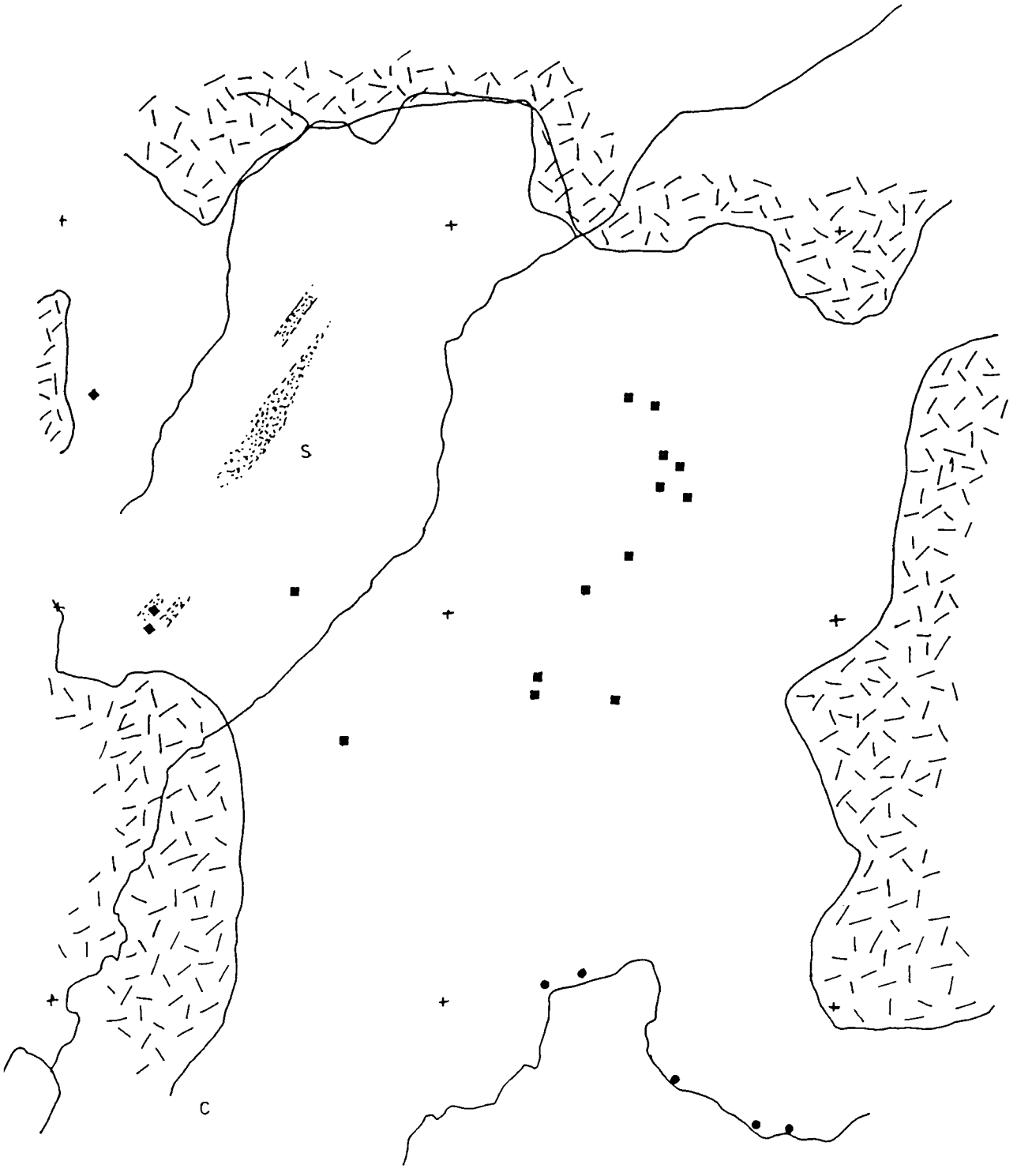

FIGURE 3.3

Metabasite assemblages in the Glen Muick area. Squares-garnet-clinopyroxene assemblages, circles-garnet-assemblages, diamonds-two amphibole assemblages, S-serpentinite, stipple lower grade garnet-clinopyroxene absent assemblages.

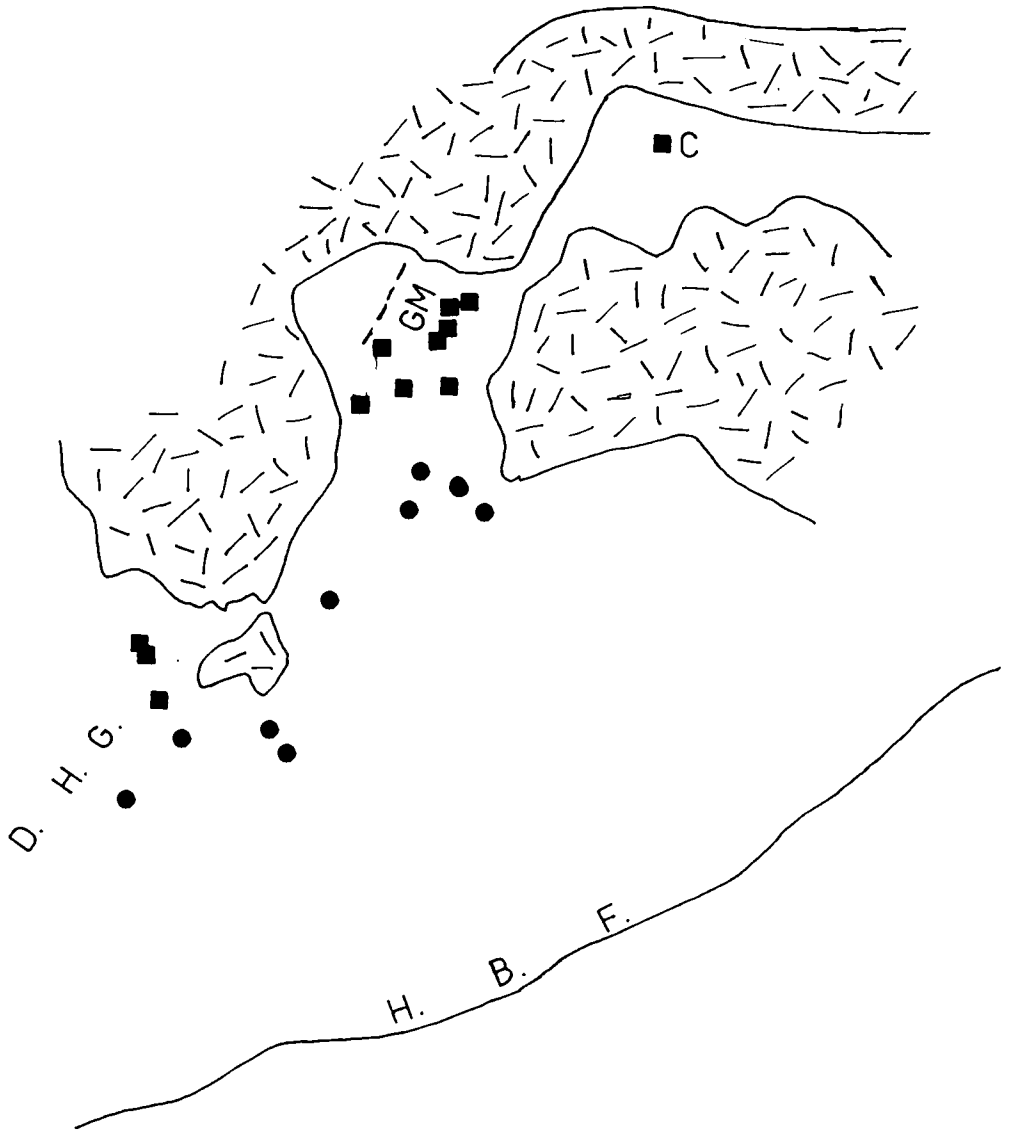

FIGURE 3.4

Garnet-clinopyroxene assemblages in the Glen Muick area (squares), clinopyroxene absent (circles). C is a garnet absent clinopyroxene assemblage.

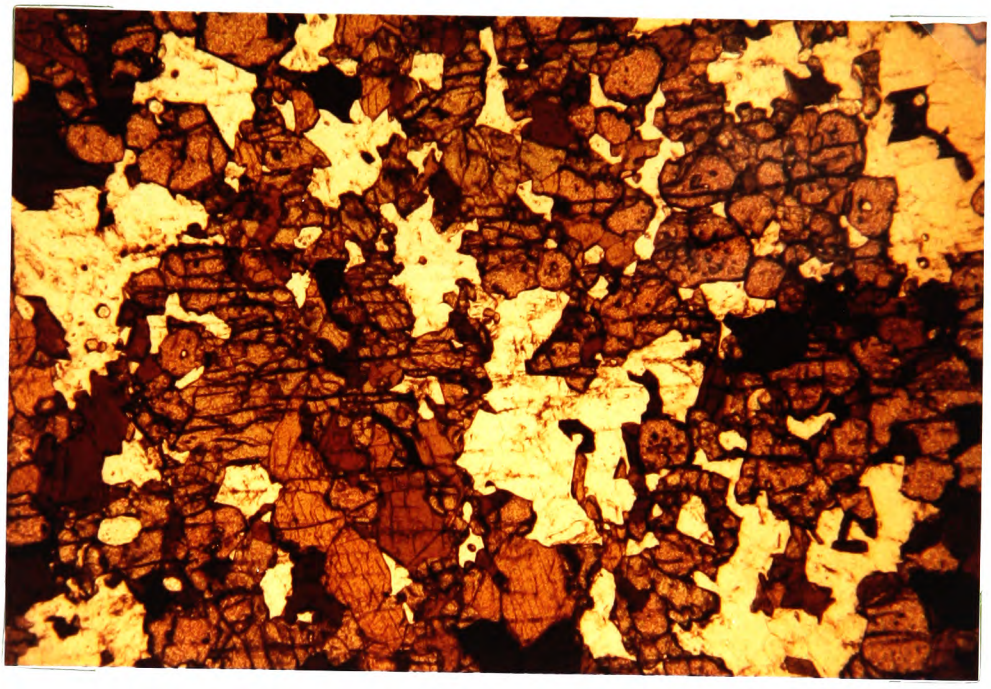

FIGURE 3.5 (a)

CL2 (x50) Garnet-clinopyroxene amphibolite, Glen Muick.

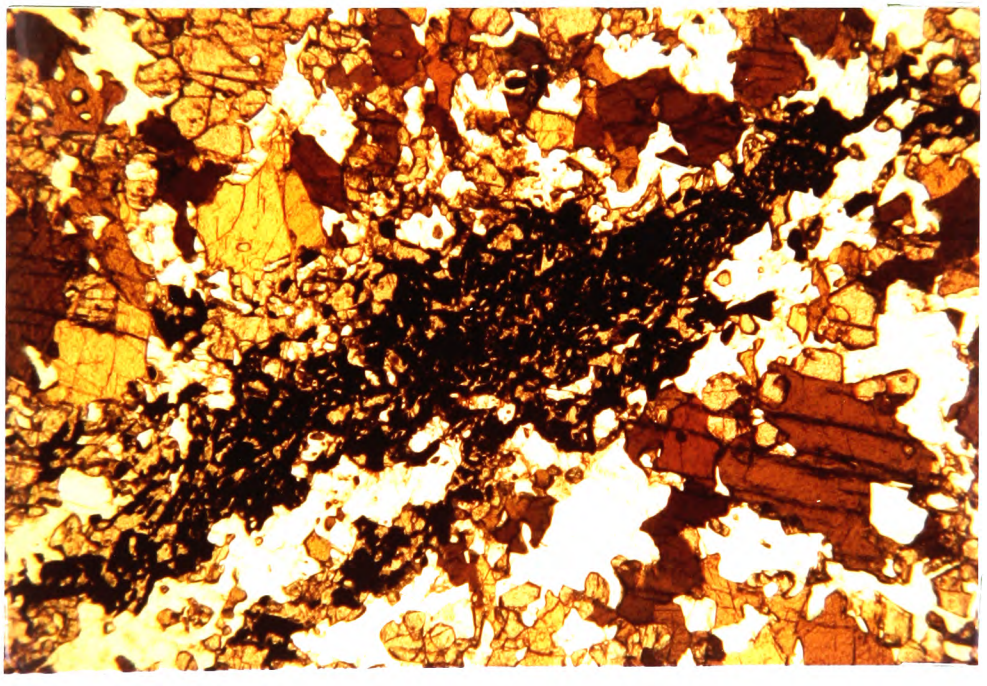

FIGURE 3.5 (b)

CL2 (x50) Intergrowth of clinopyroxene and ilmenite in Glen Muick amphibolite.

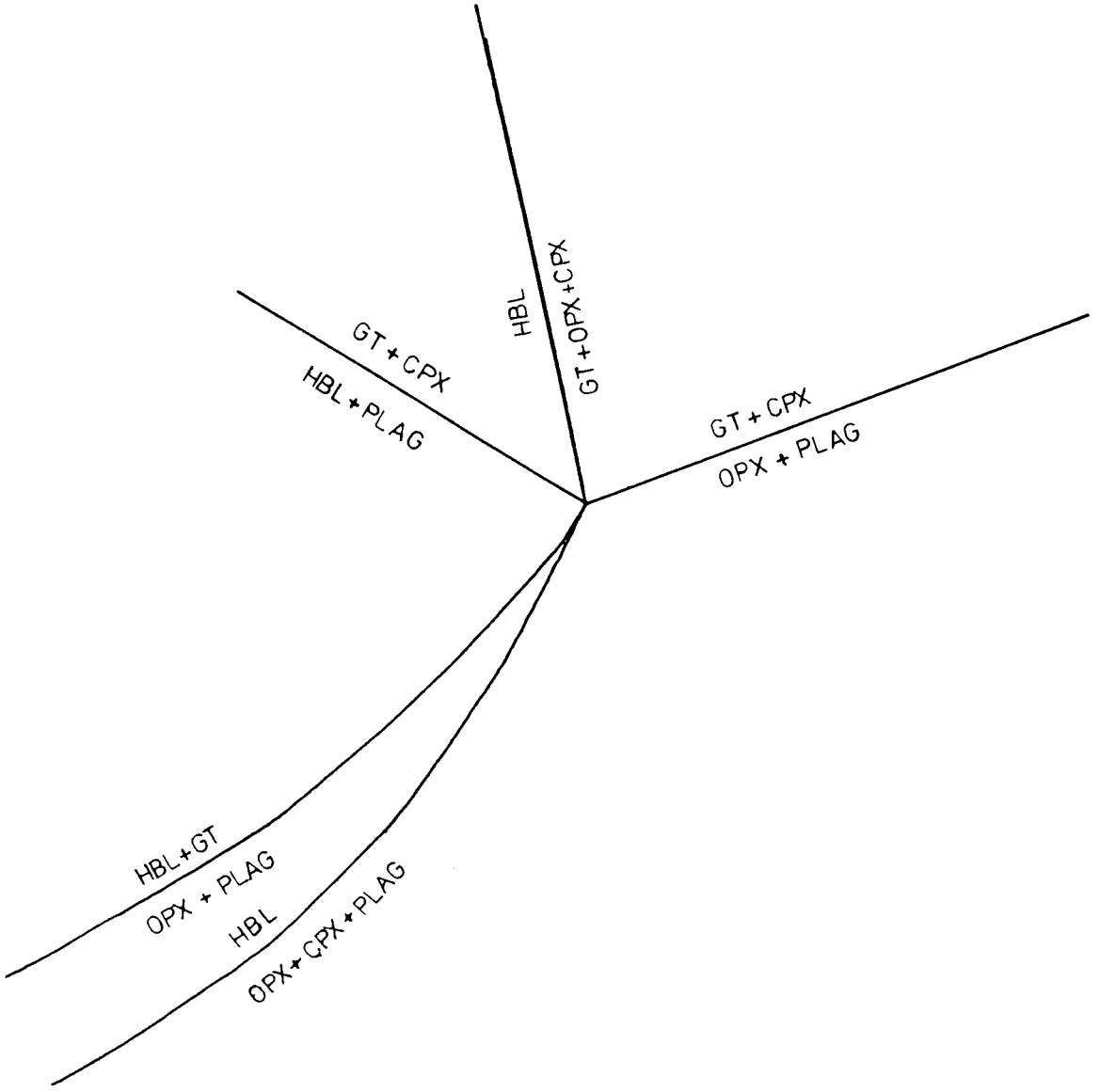

FIGURE 3.6

Schreinemakers analysis of the phases garnet, clinopyroxene, orthopyroxene, hornblende and plagioclase in the system CFASH, projection from quartz and water, following Wells (1979).

FIGURE 3.7

Retrogressed amphibolite gneiss, E. Glen Muick (GR NO347889)

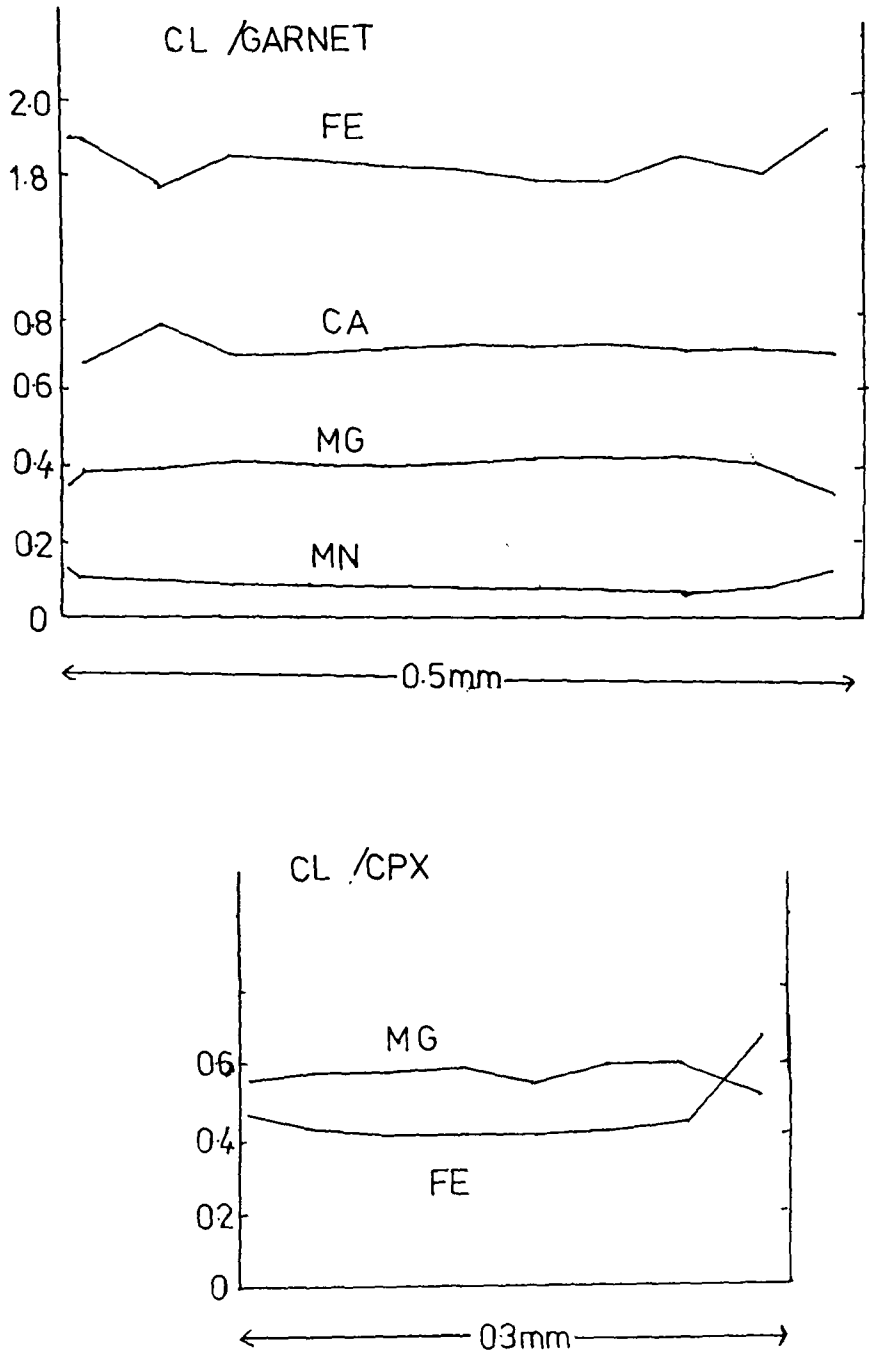

FIGURE 3.8

Zoning profiles of garnet and clinopyroxene from a Glen Muick metabasite

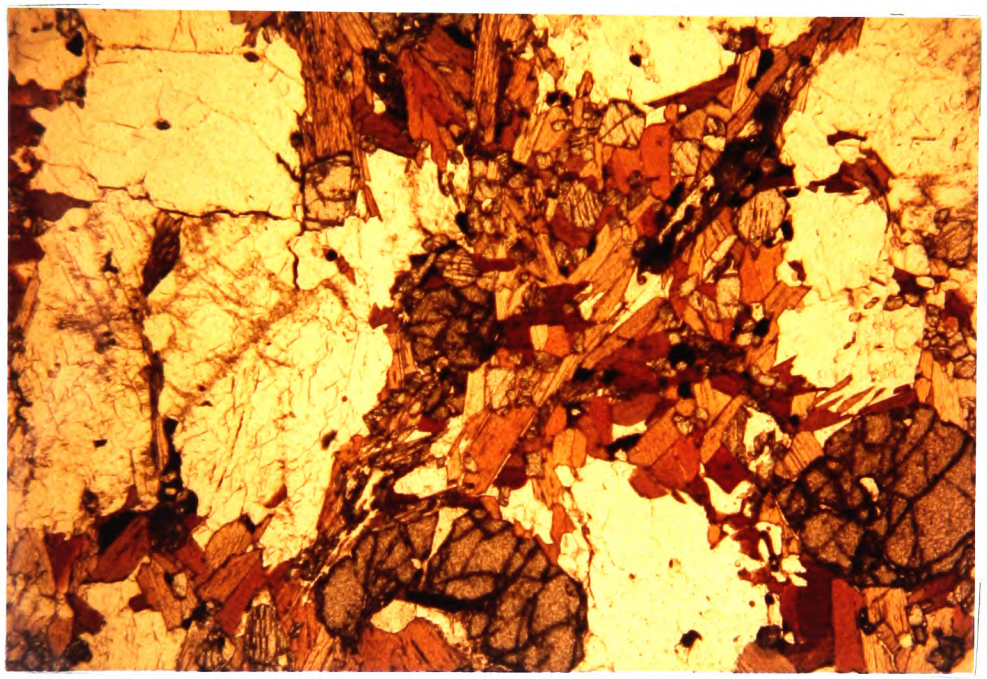

FIGURE 3.9

430A (x50) Garnet-sillimanite-K feldspar

Gneiss, Glen Muick.

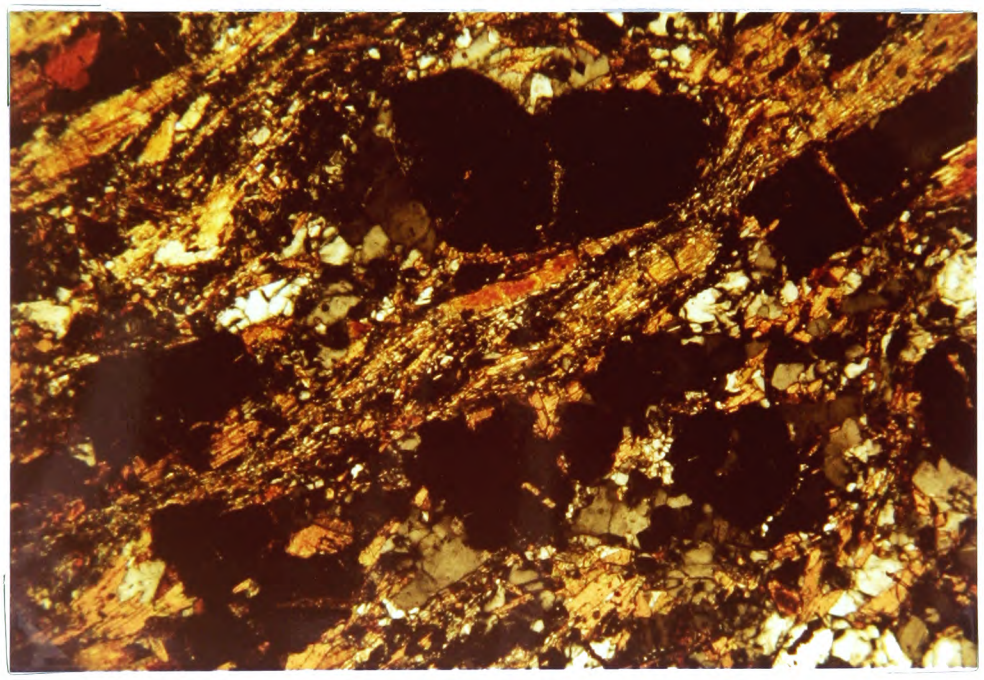

FIGURE 3.10

CL4 (x50) Deformed garnet-sillimanite-K feldspar Gneiss, Glen Muick.

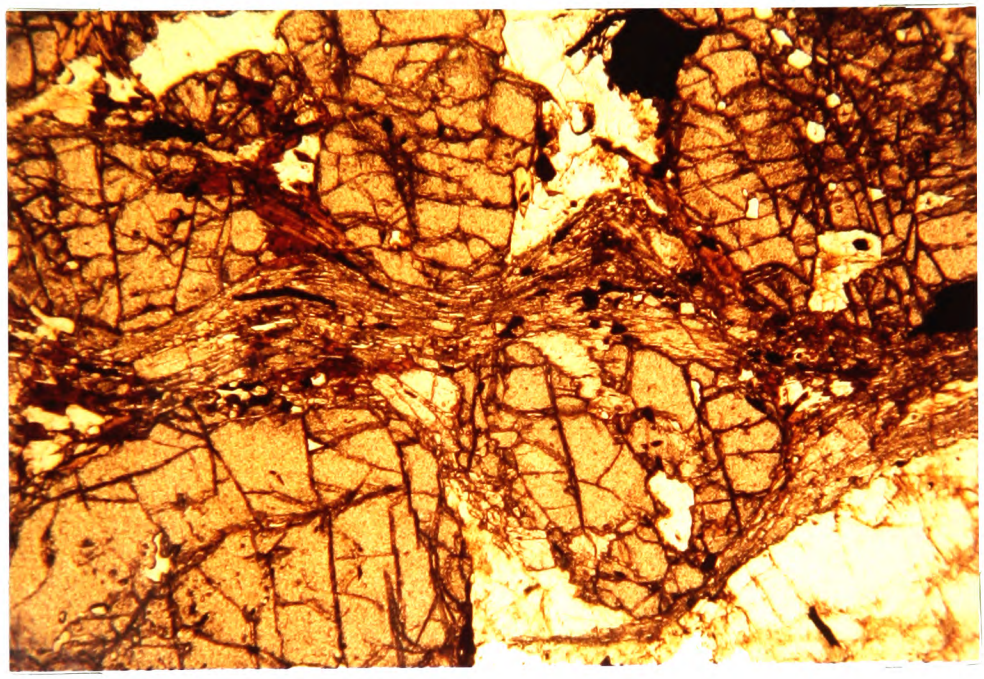

FIGURE 3.11

(x50). Deformed sillimanite gneiss with sillimanite aggregates wrapped around kyanite, Cairn Leuchan.

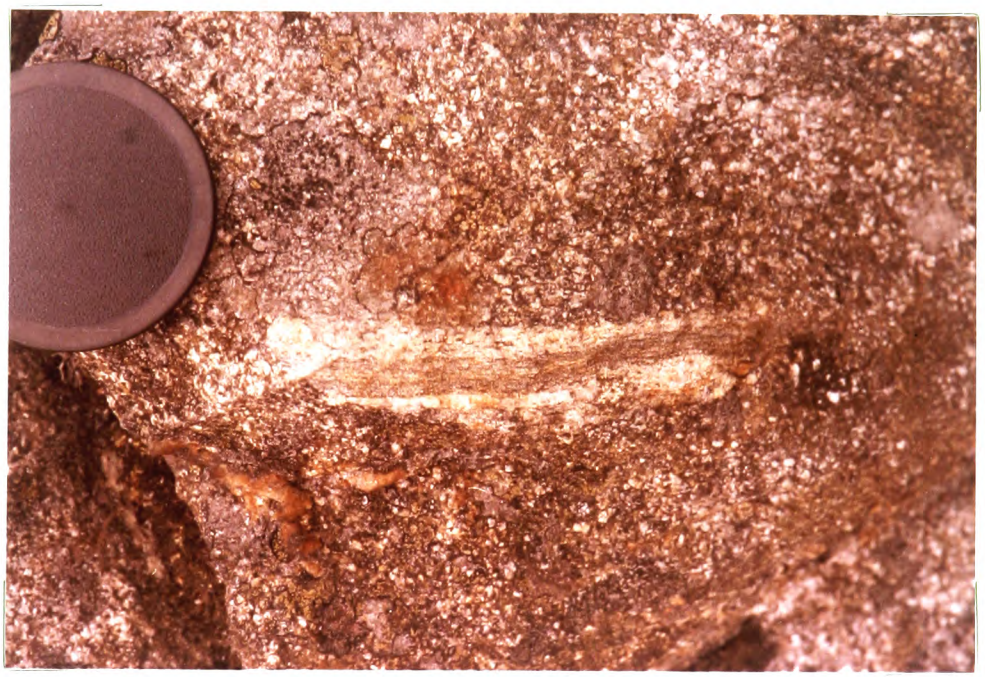

FIGURE 3.12

Schlieren in pelitic migmatite (oligoclase porphyroblast gneiss), Scar Hill, Cromar

FIGURE 3.13

Metapelite assemblages in the Glen Muick area. Circles-sillimanite-Kfeldspar assemblages, squares-peak metamorphic muscovite, diamonds-andalusite, C-cordierite, K-kyanite and * staurolite bearing schists.

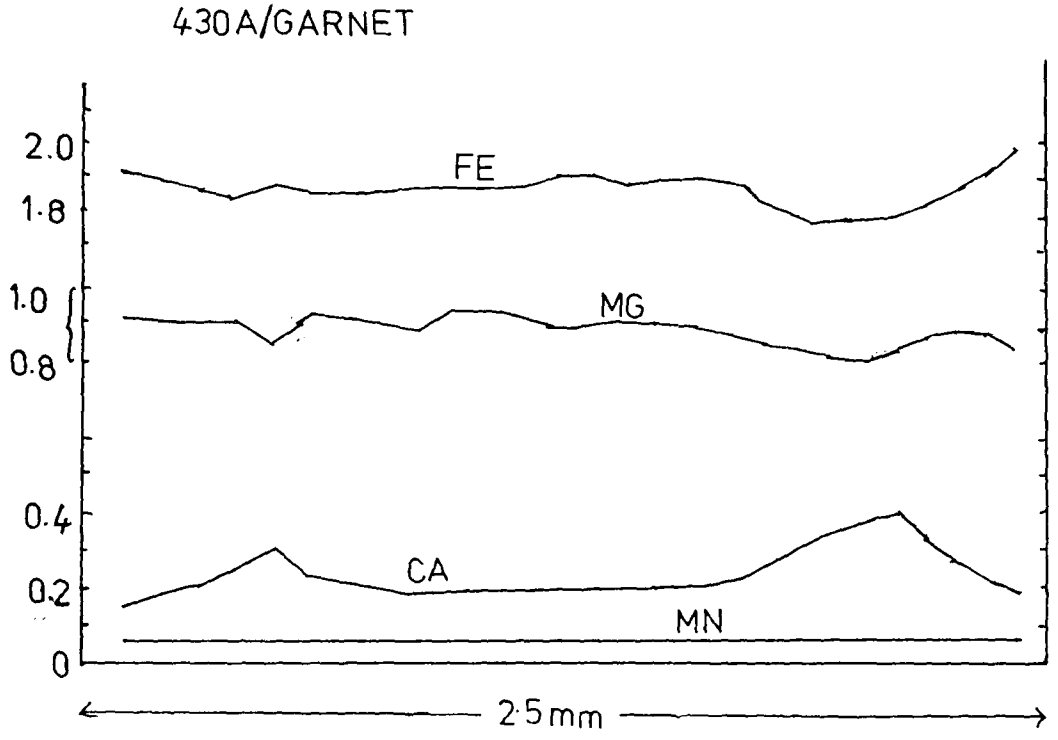

FIGURE 3.14

Zoning profile from a Glen Muick sillimanite-K feldspar gneiss

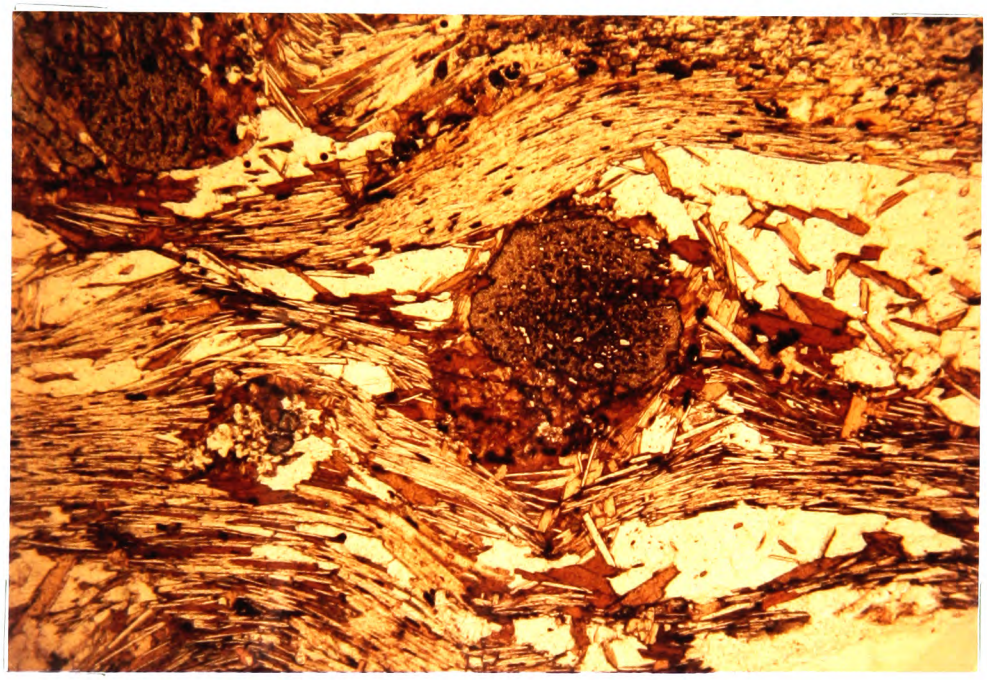

FIGURE 3.15

468A (x50) Garnet-muscovite-biotite schist,

Glen Girnock.

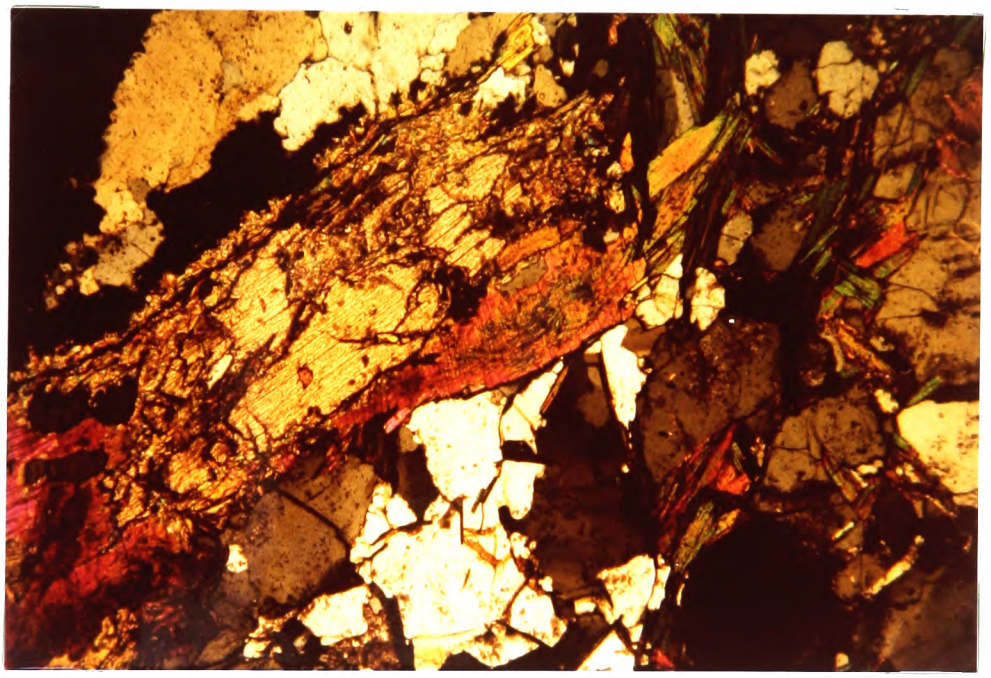

FIGURE 3.16

468A (x50) Kyanite in schist, Glen Girnock.

Note shreds of fibrolite in muscovite.

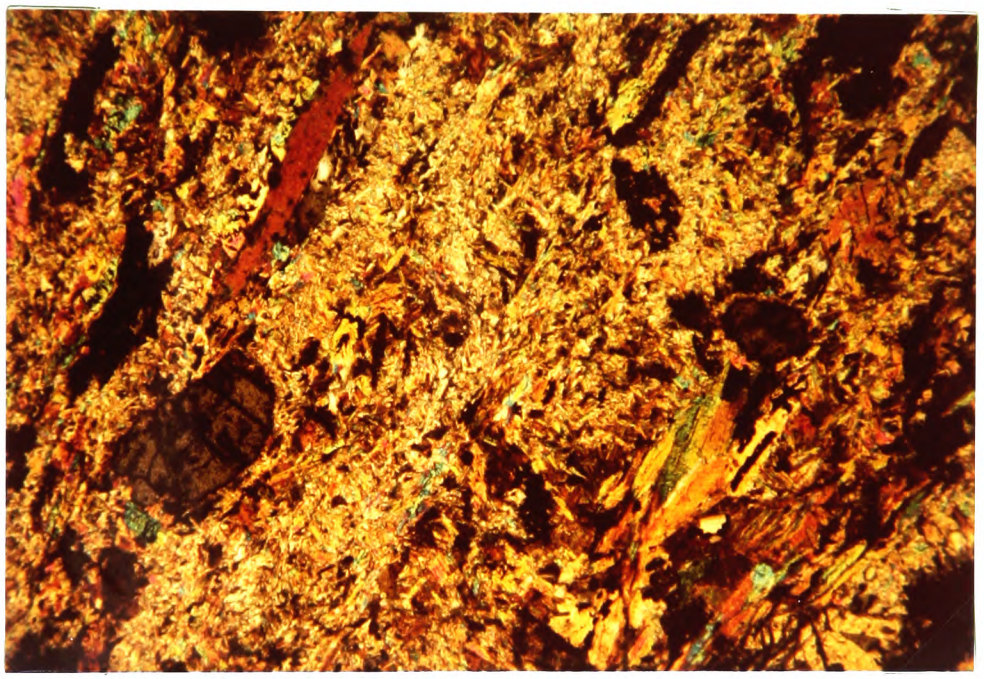

FIGURE 3.17

CF3 (x50) Retrogressed migmatite, Craig Ferrar Cromar. Chlorite (black), porphyroblastic micas and staurolite.

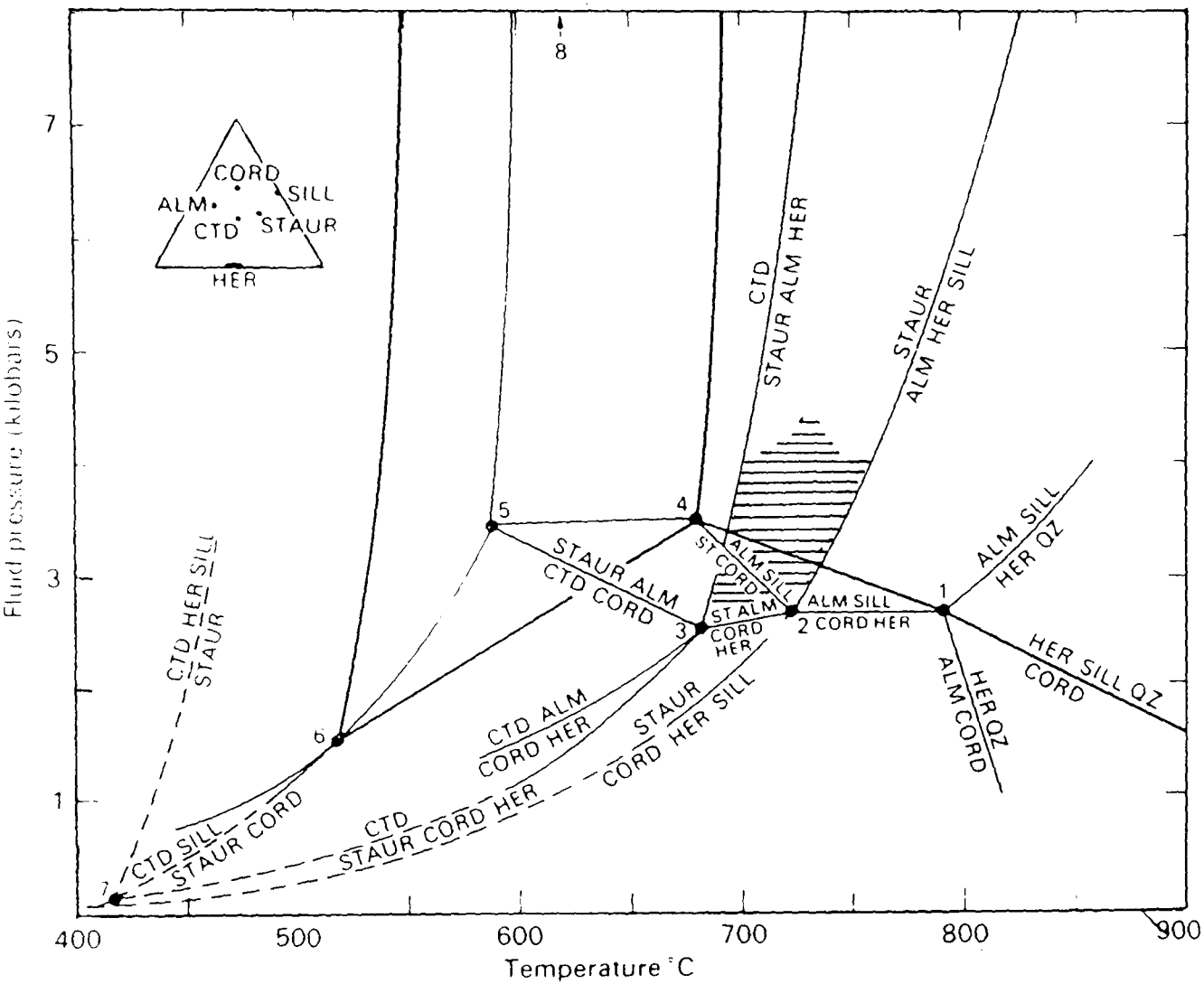

FIGURE 3.18

Approximate stability of staurolite-almandine-hercynite assemblages. (Stability shown in the pure KFMASH system, from Richardson (1968)).

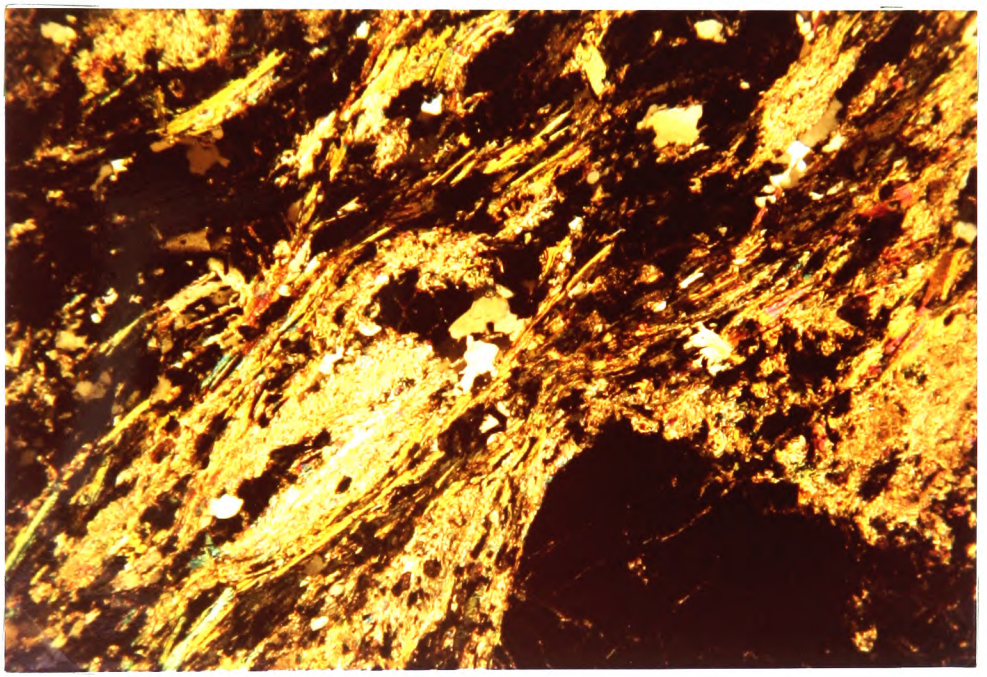

FIGURE 3.19

(x50) Retrogressed rock, Hare Cairn. Muscovite and chlorite lie within the foliation.

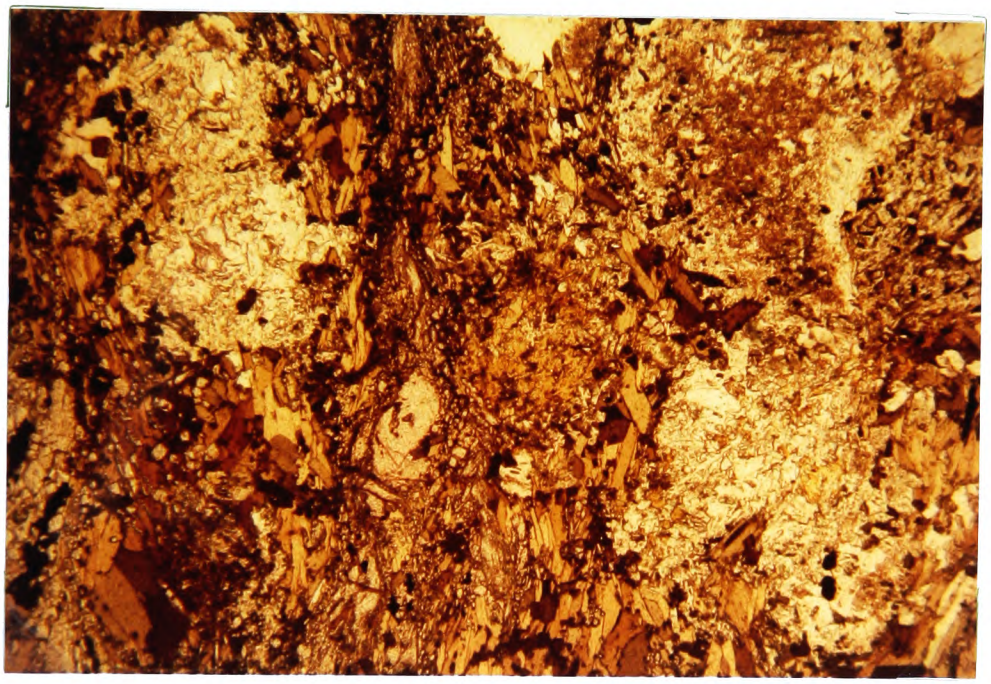

FIGURE 3.20

(x50) Sillimanite gneiss affected by contact metamorphism. Garnets replaced by cordierite. N of Cairn Leuchan.

FIGURE 3.21

Mineral zones in the Glen Muick area. Lower grade zones from Barrow (1893).

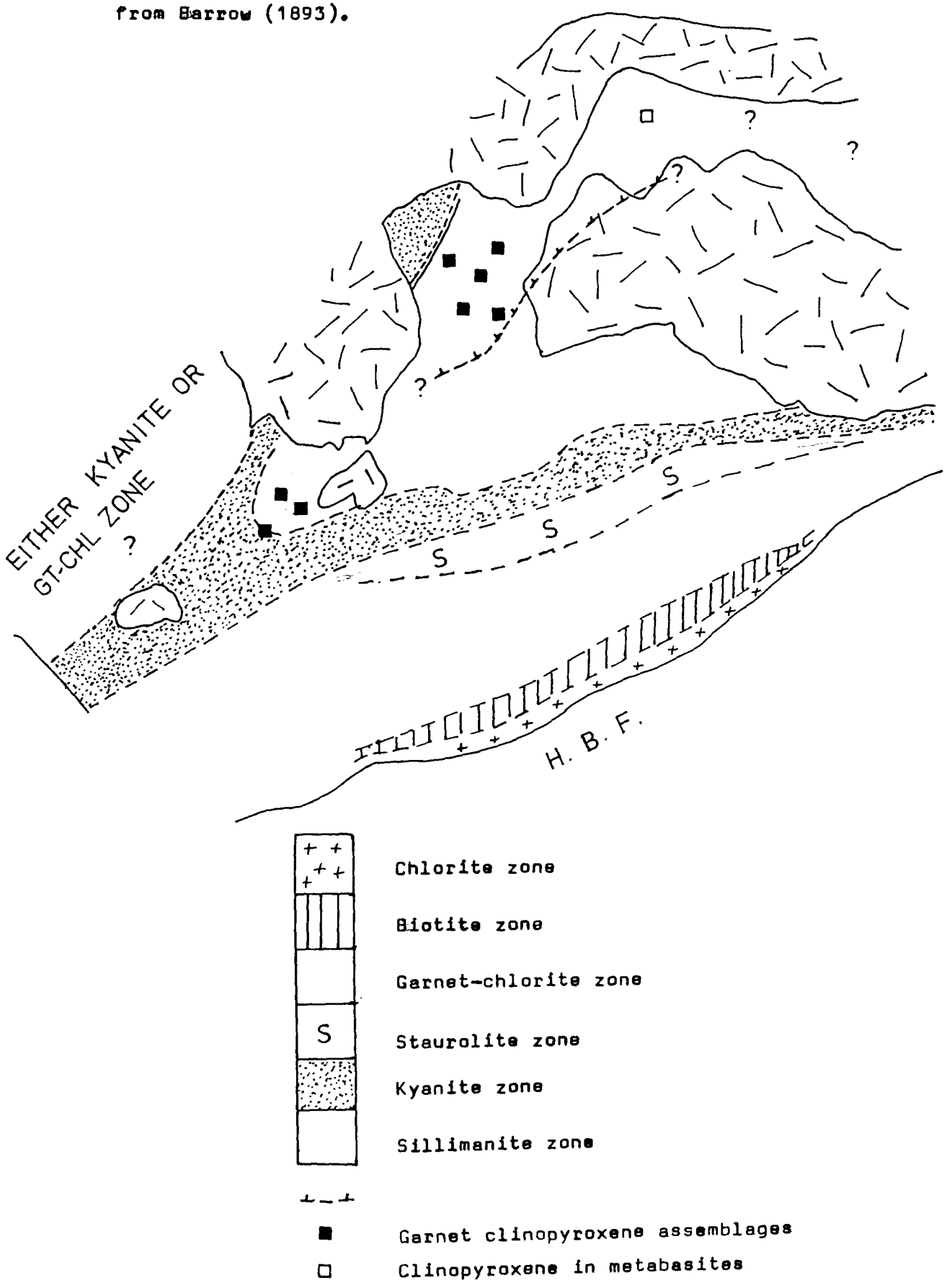

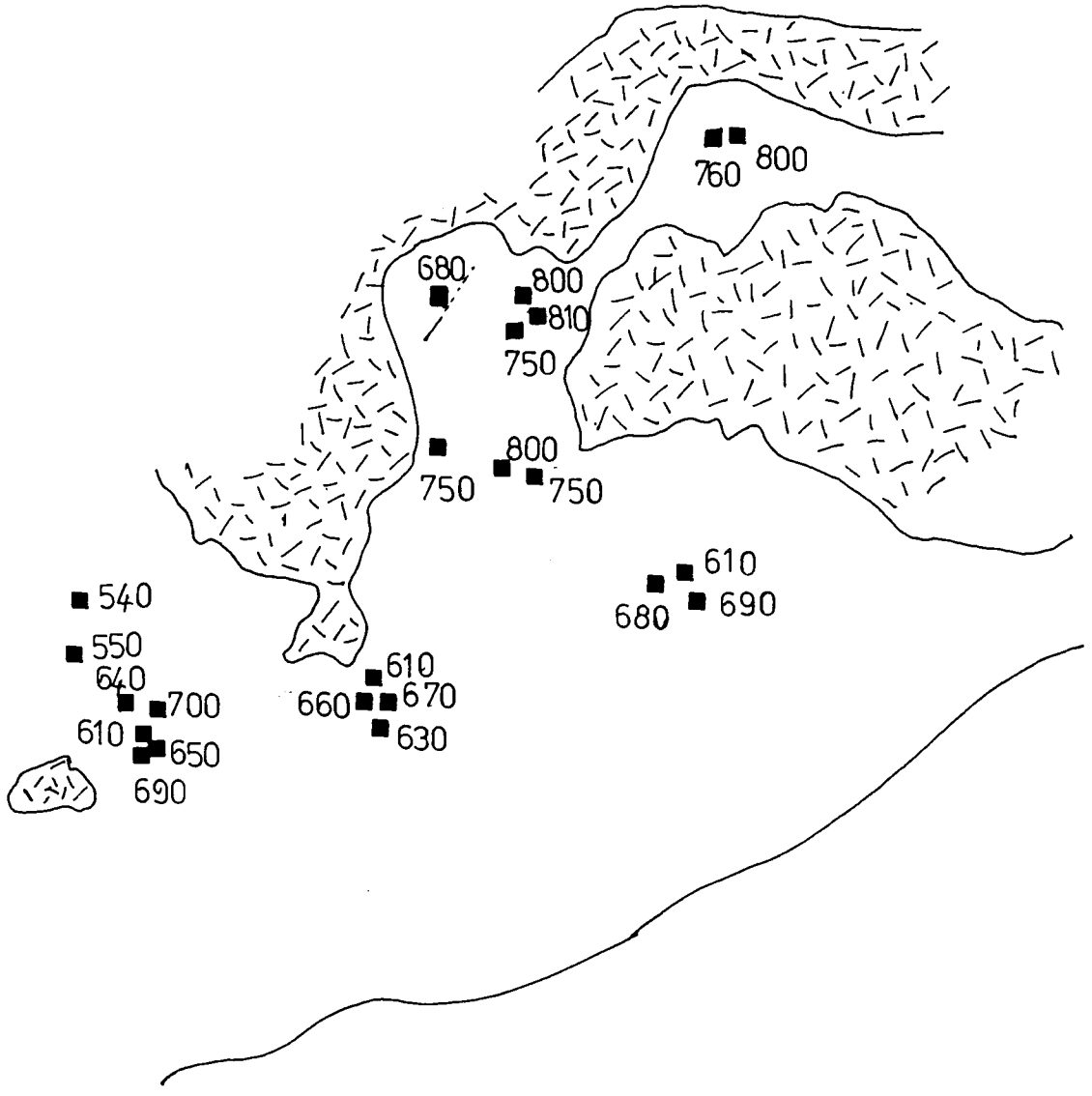

FIGURE 3.22

Garnet biotite temperatures in the Glen Muick area.
(Hodges and Spear model for garnet).

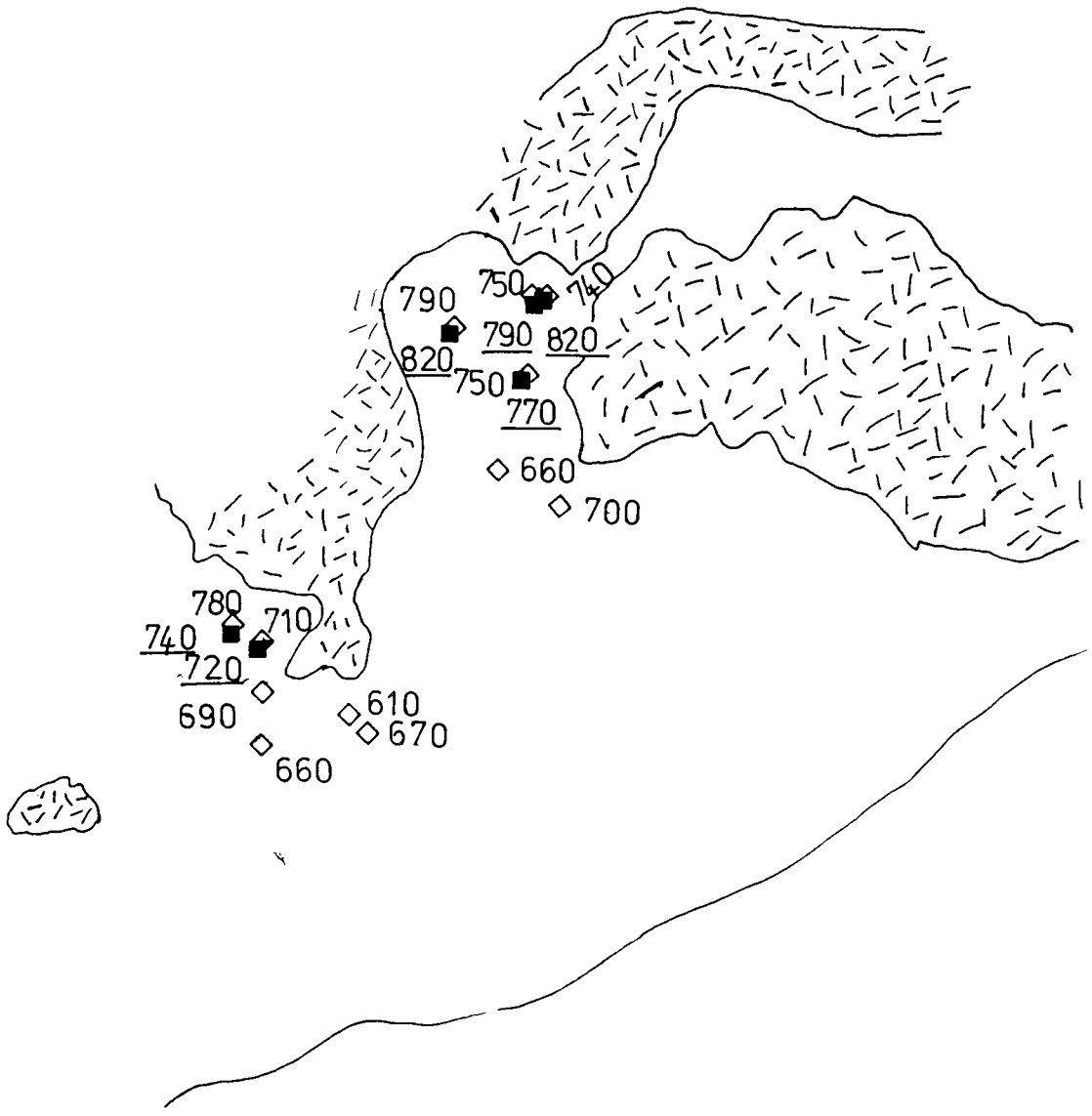

FIGURE 3.23

Temperature estimates from amphibolites in the Glen Muick area. Squares and underlined figures : garnet-cpx temperatures, diamonds : garnet amphibole temperatures.

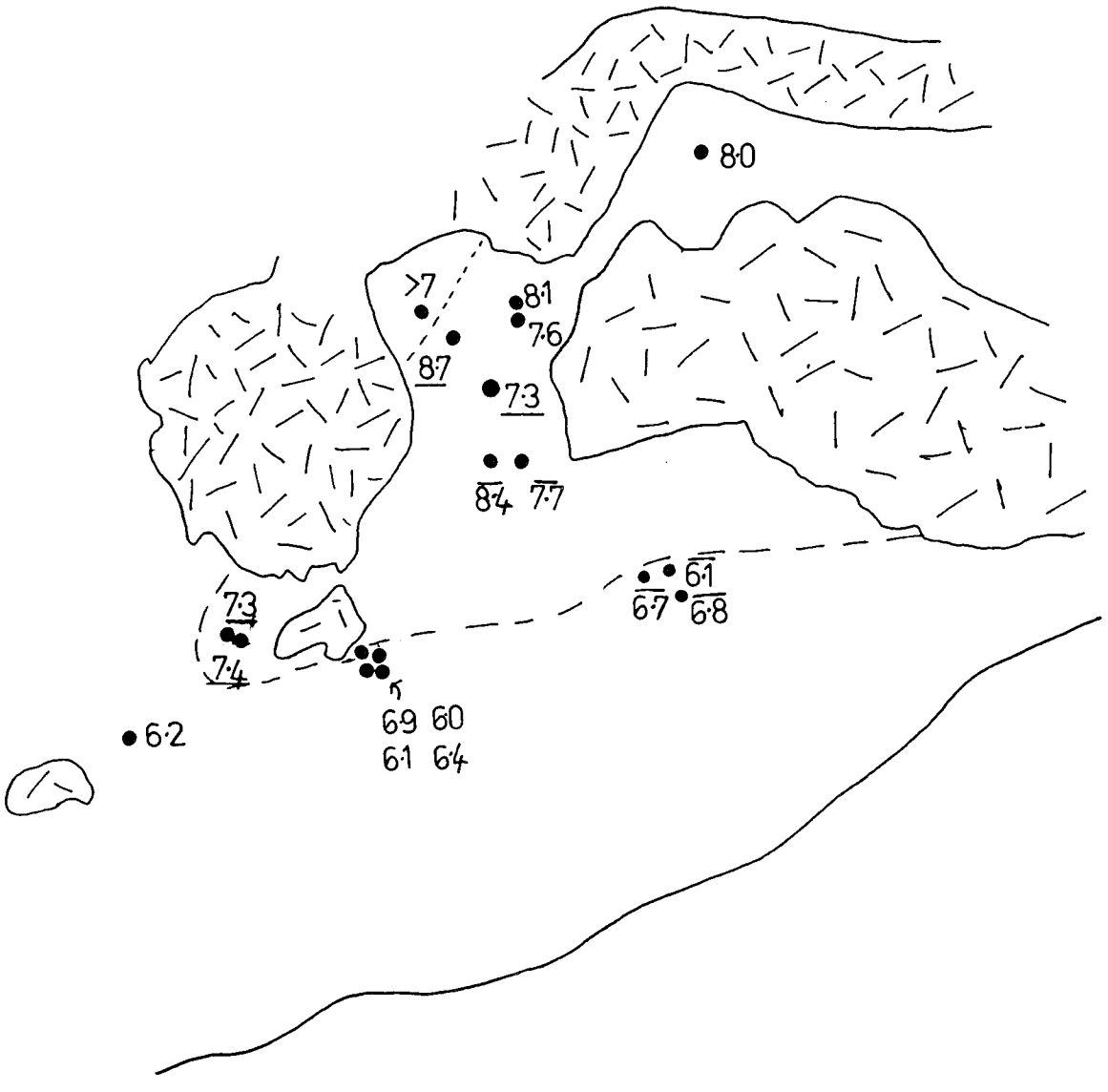

FIGURE 3.24

Pressures in the Glen Muick area. Estimated using the methods of chapter 6. Reactions used are ALSIL, CPX (underlined) and MGMICA (overlined).

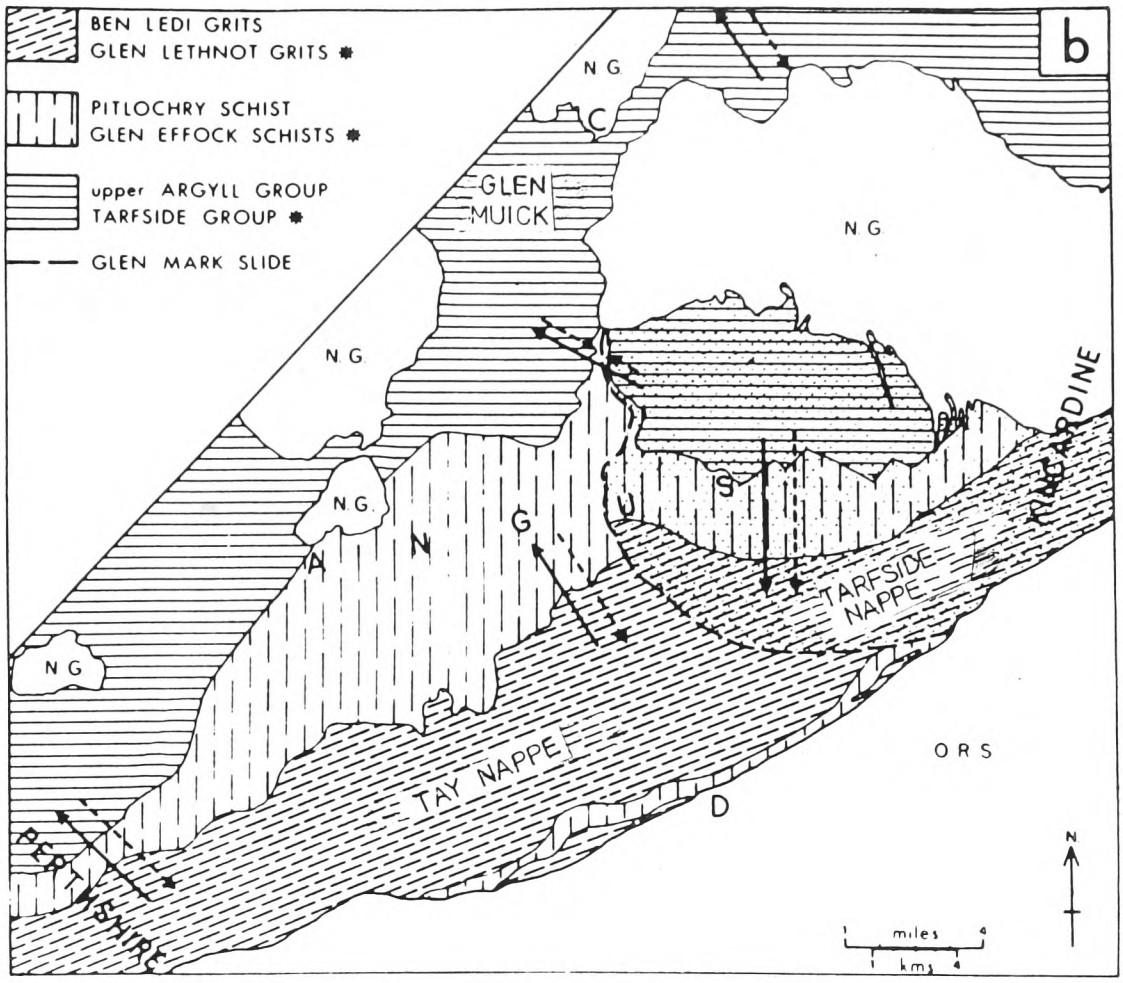

FIGURE 3.25

Structural relationships in the Glen Muick area, after Harte (1979). Starred formations are those within the Tarfside Nappe. Solid arrows show regional dips. Dashed arrows show younging directions.

FIGURE 3.26

D_3^m fold deforming D_2^m fold, E Glen Muick

(GR NO248889)

FIGURE 3.27

Sillimanite aggregates axial planar to D_2^m fold, E Glen Muick (GR NO348888)

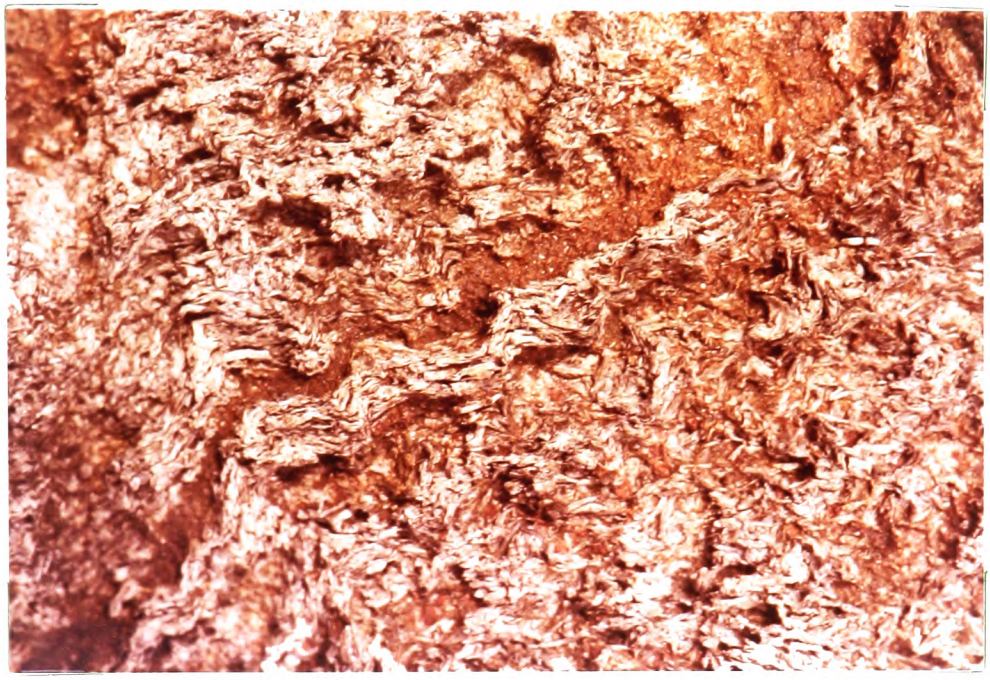

FIGURE 3.28

Crenulations of sillimanite aggregates by D_3^m folds, E. Glen Muick (GR NO348888)

FIGURE 4.1

Distribution of aluminosilicate zones following Chinner (1966) and Chinner (1980). Ticked line delimits the sillimanite zone, solid lines are kyanite isograds marked by the M/FM of biotite in the AFM assemblage kyanite-staurolite-biotite.

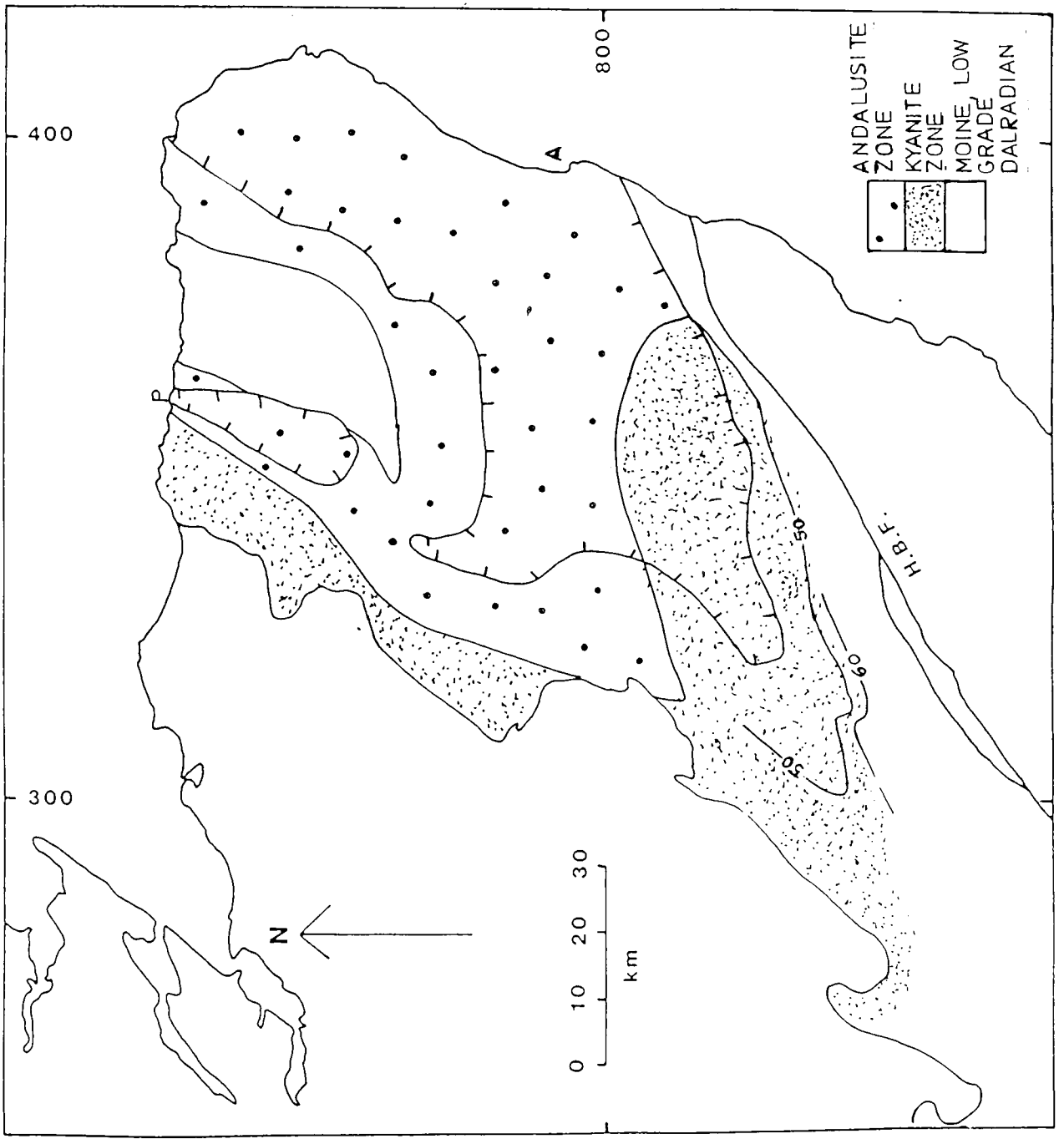

FIGURE 4.2

Locations mentioned in the text. Sketch map of the eastern Dalradian.

A : Aberdeen

B : Braemar

C : Cromar

D : Deeside

DO : Donside

E : Glen Ey

EL : Ellon Gneiss

GA : Glen Avon

GC : Glen Clova

GE : Glen Esk

GG : Glen Girnock

GM : Glen Muick

HH : Haddo House Gabbro

HP : Huntly Portsoy Gabbro

IH : Inzie Head Gneisses

M : Glen Mark

MC : Morven Cabrach Newer Gabbro

MA : Maryculter

P : Portsoy

S : Schichallion

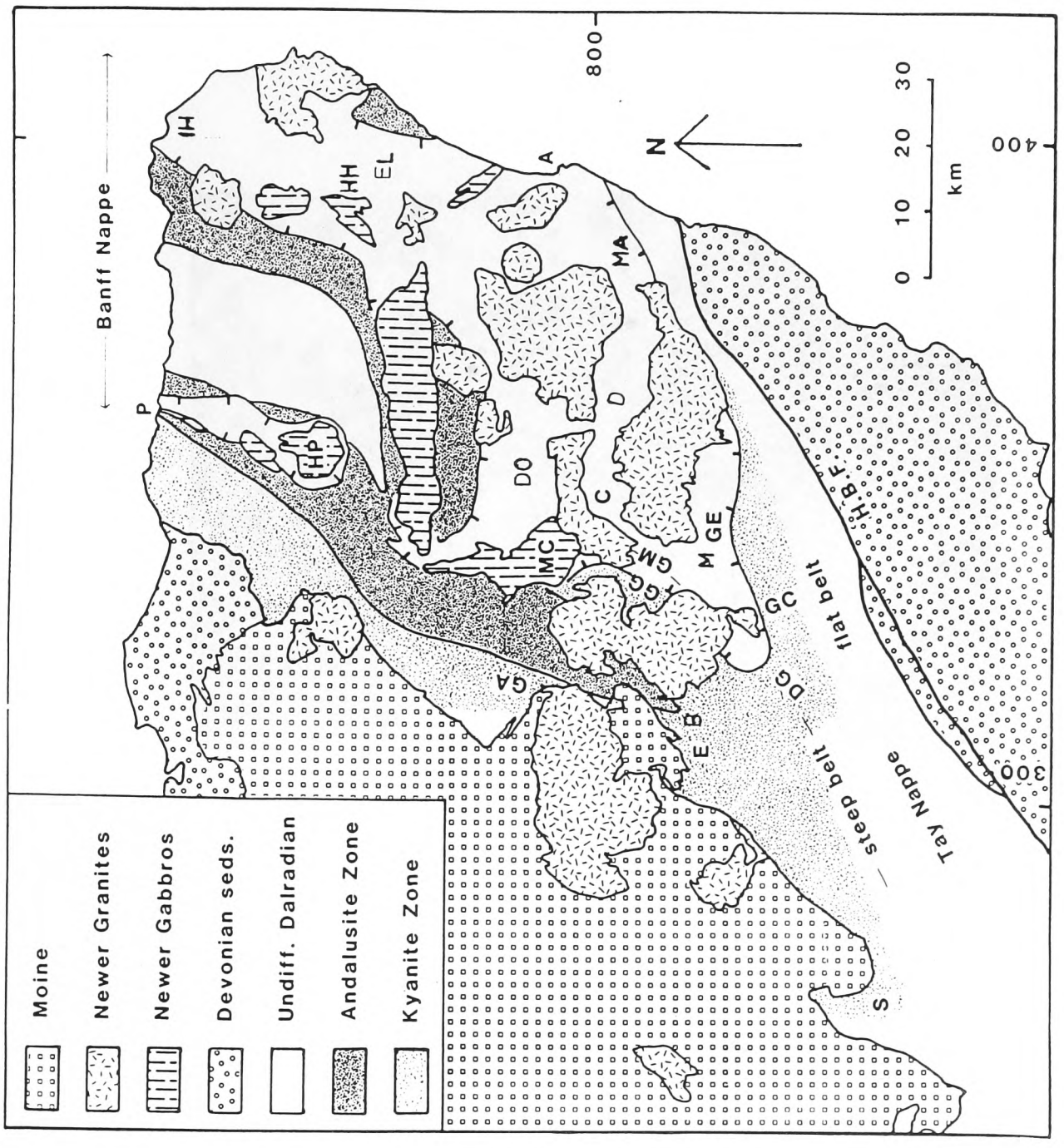
Moine
Newer Granites
Newer Gabbros
Devonian seds.
Undiff. Dalradian
Andalusite Zone
Kyanite Zone
Banff Nappe
800
400
300
N
0 10 20 30
km
IH
HH
EL
A
MA
D
C
DO
P
HP
MC
GM
GC
GE
GA
E B
DG
H.B.F.F.
steep belt
flat belt
Tay Nappe
S

FIGURE 4.2

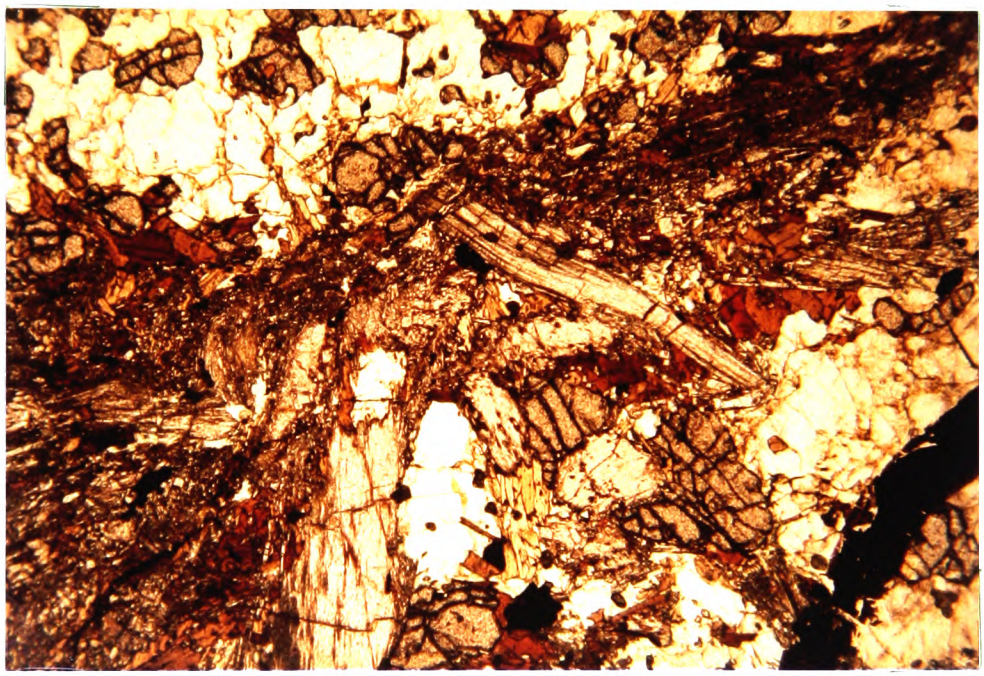

FIGURE 4.3

(x50) Aggregate of prismatic sillimanite,

Cairn Leuchan, Glen Muick.

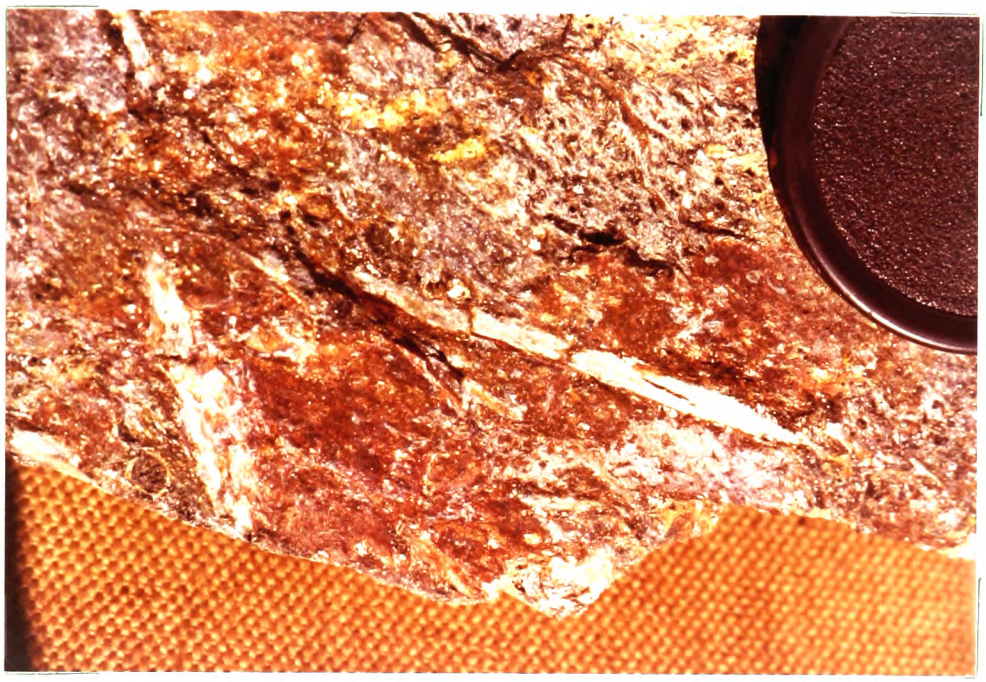

FIGURE 4.4

563A. Pseudomorph after kyanite from SE of Glen Muick (length~6cm), also figured in figure 4.7

FIGURE 4.5

DH5 (x50) Andalusite, including fragments of resorbed garnet (centre plate), surrounded by shimmer aggregate, Dinnet House, Cromar.

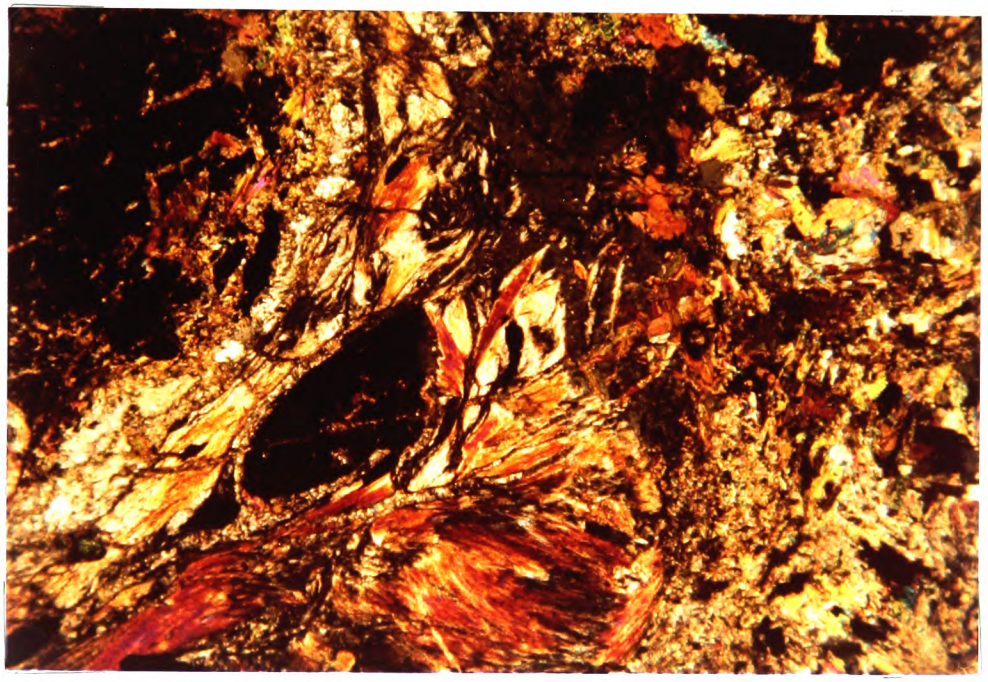

FIGURE 4.6

560A (x50). Garnet surrounded fibrolite mats overgrown by andalusite. East Glen Muick.

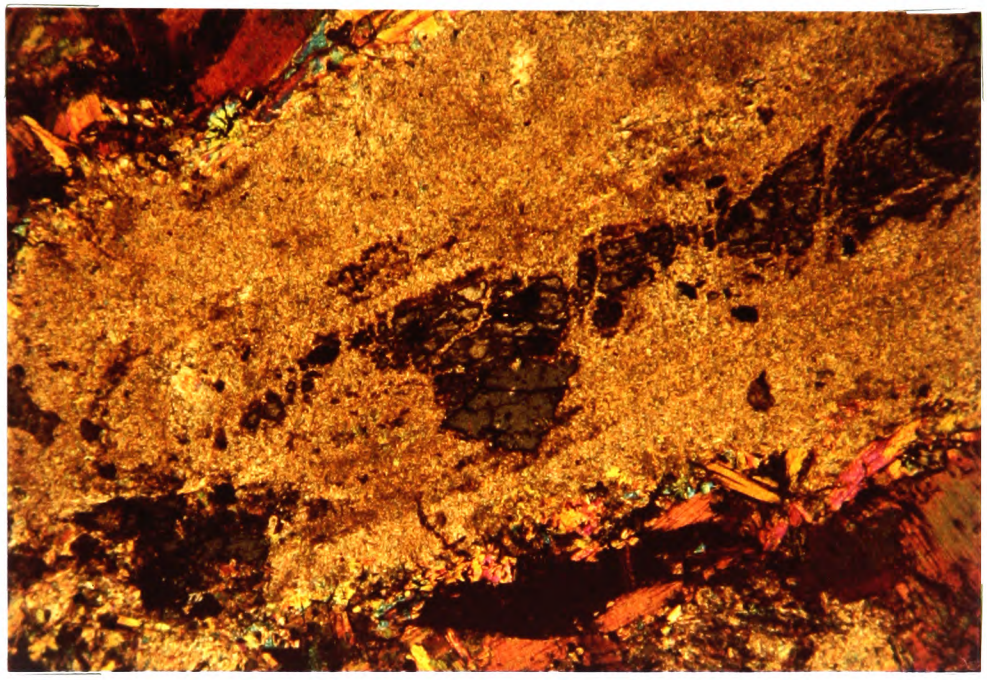

FIGURE 4.7

563A (x50). Aggregate of prismatic sillimanites probably pseudomorphing kyanite surrounded by shimmer aggregate and overgrown by andalusite (centre plate). Rest of the rock is predominantly shimmer aggregate and porphyroblastic muscovite and biotite. Upper Glen Tanar.

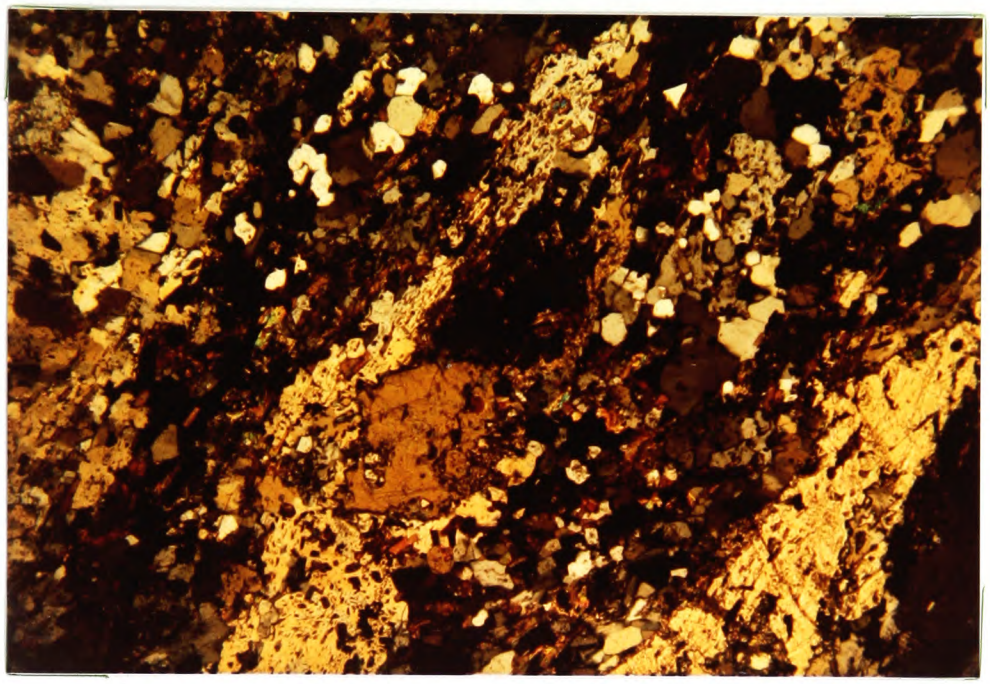

FIGURE 4.8

IN1 (x50). Andalusite-cordierite hornfels with aggregate of andalusite probably after kyanite. Lochnagar Aureole.

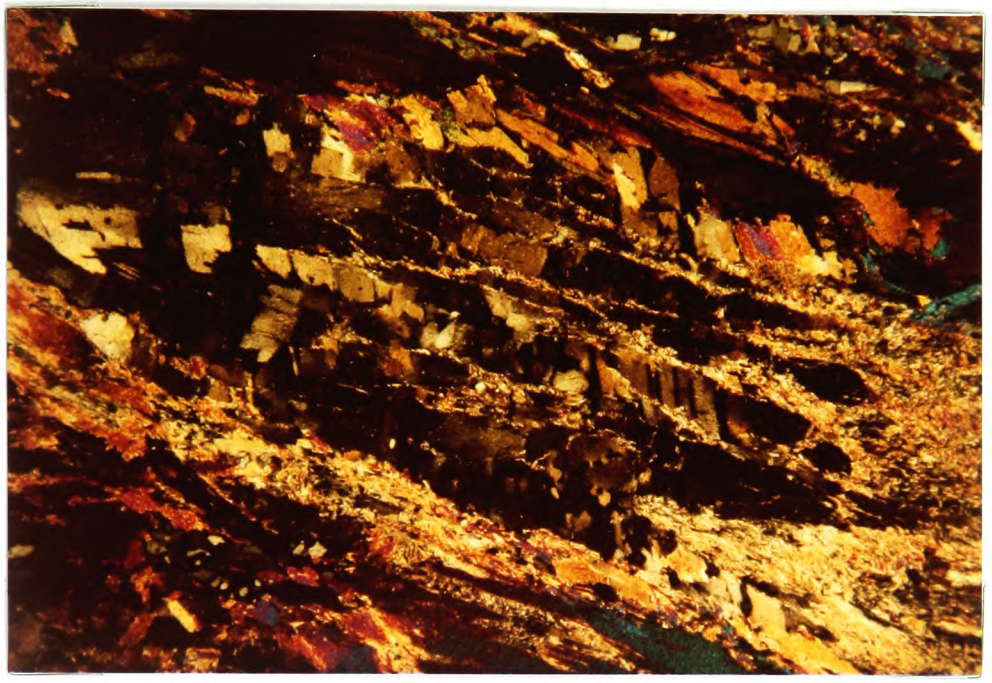

FIGURE 4.9

827A (x50) Pseudomorph probably after kyanite. Comprises large porphyroblastic muscovites now kinked. Glen Mark.

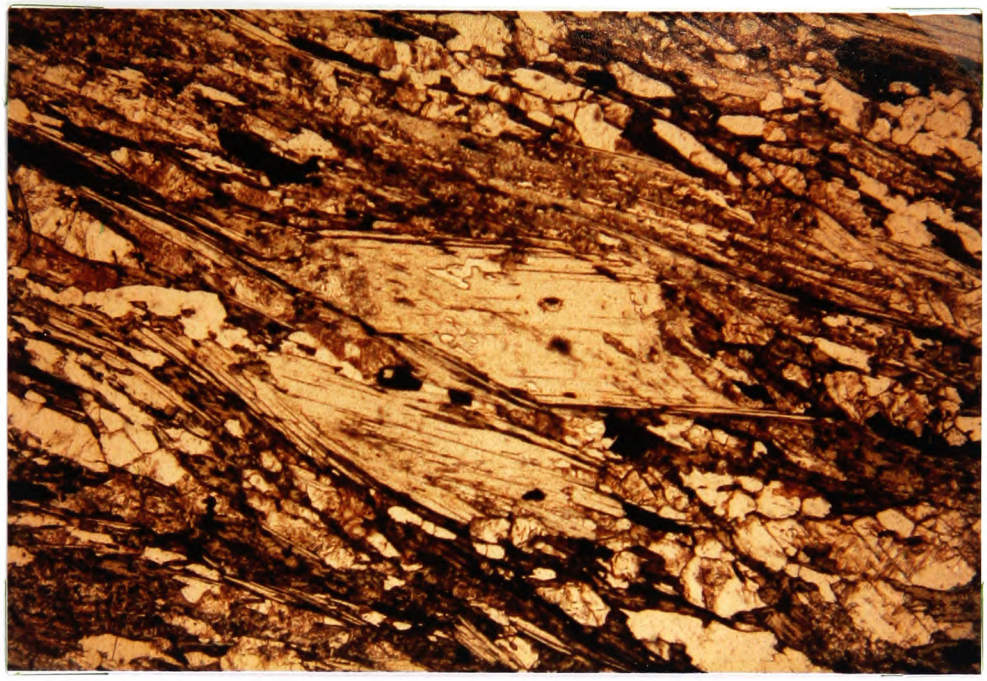

FIGURE 4.10 (a)

938A (x50) Fibrolite trails in muscovite aligned parallel to rock fabric. West Glen Muick.

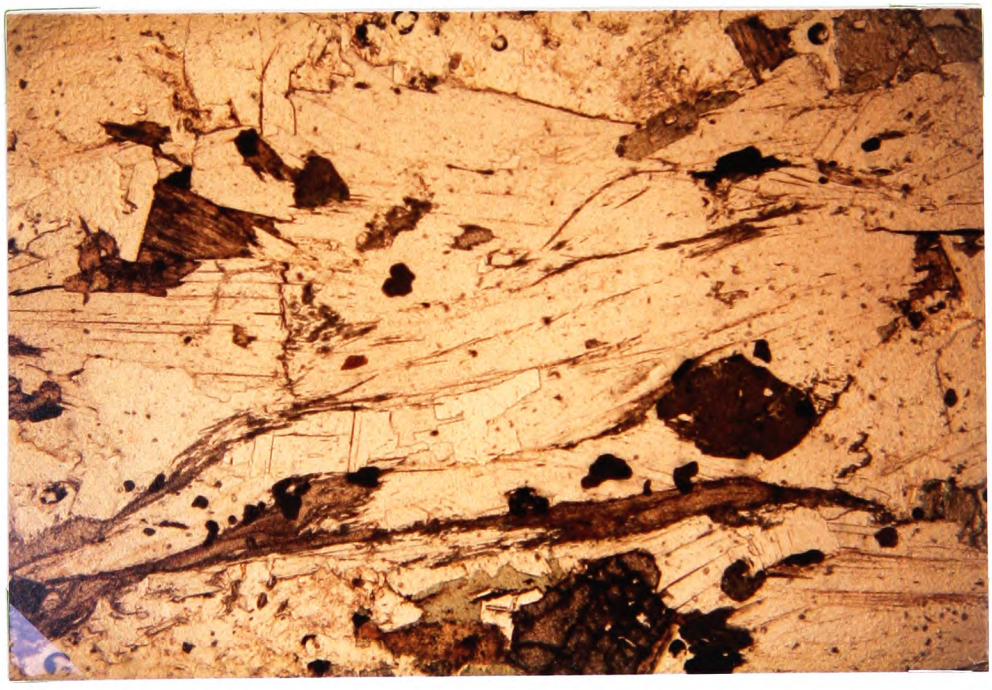

FIGURE 4.10 (b)

135B (x200) Aligned fibrolite trails Glen Clova.

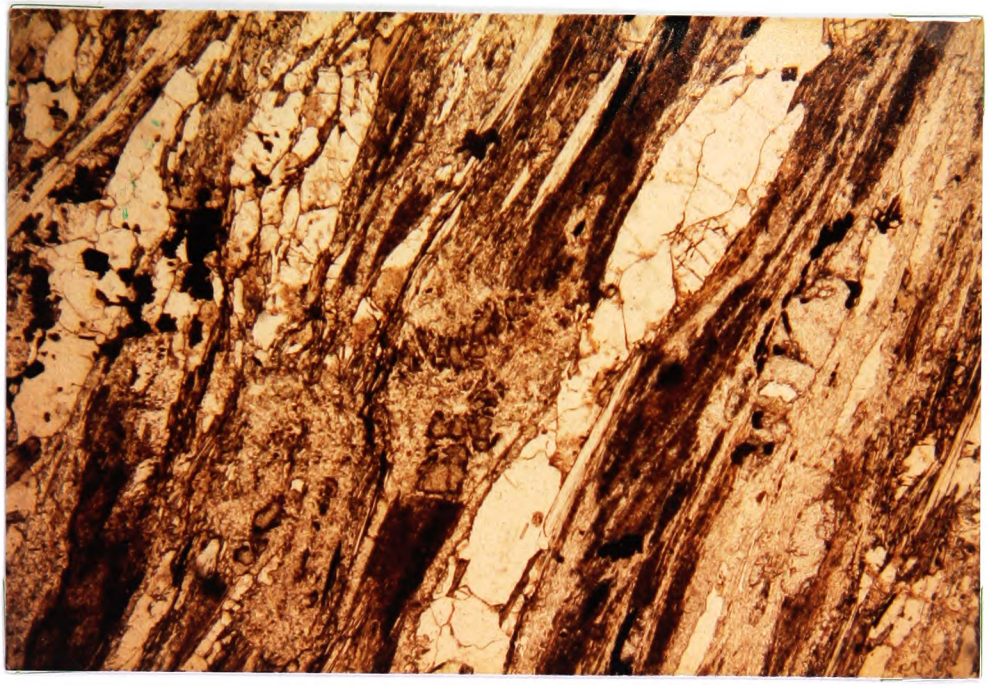

FIGURE 4.11 (a)

Staurolite surrounded by shimmer aggregate overgrowing a trail of very fine prismatic sillimanite. West Glen Muick. (x50)

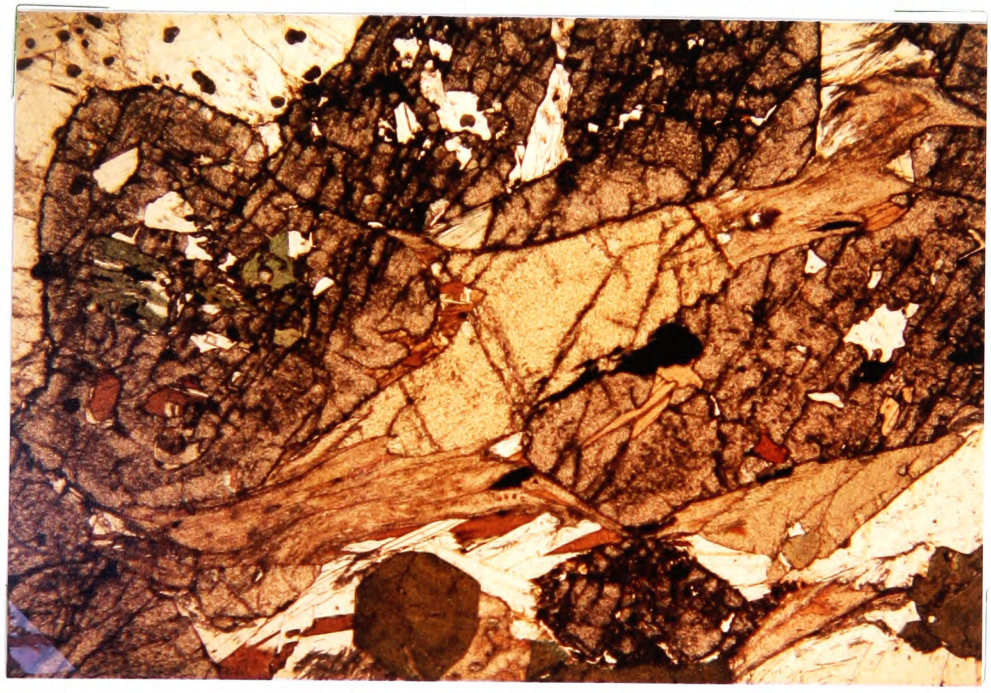

FIGURE 4.11 (b)

135B (x50) Late staurolite overgrowing fibrolite trail. Glen Clova.

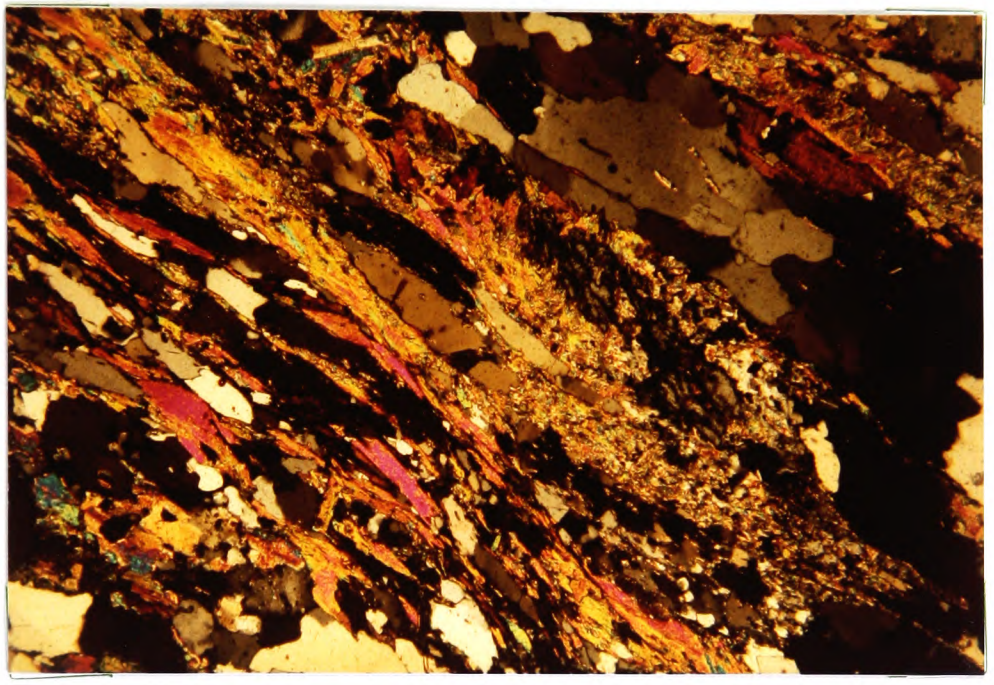

FIGURE 4.12

454A (x50). Andalusite surrounded by shimmer aggregate in a deformed gneiss. Muscovite parallel to fabric. Upper Glen Tanar

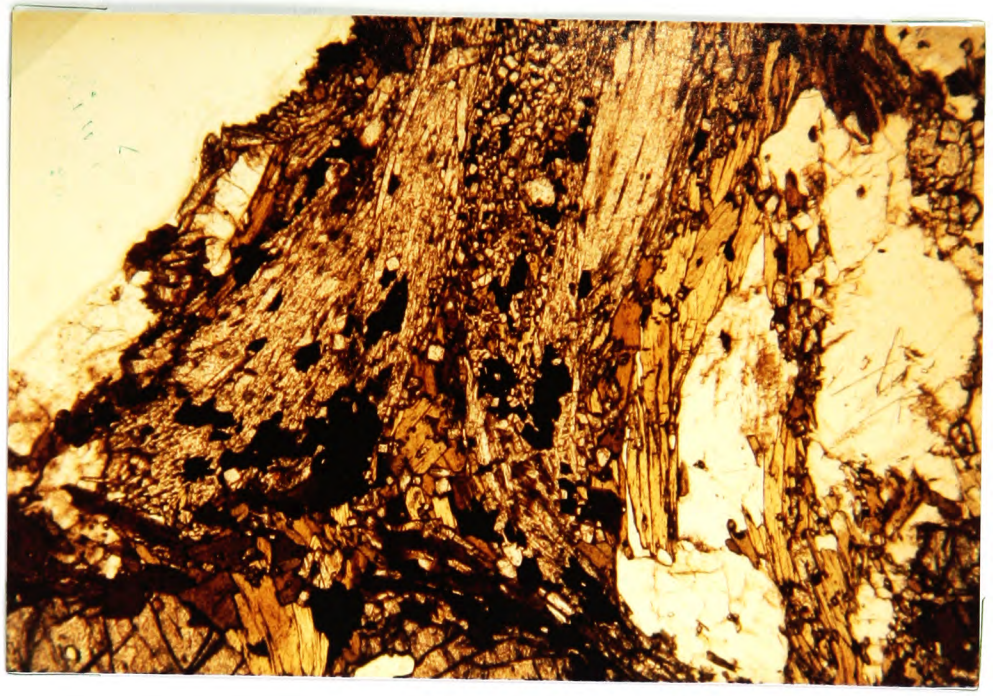

FIGURE 4.13 (a)

919B (x50) Fresh sillimanite-K feldspar gneiss. Aggregate of coarse prismatic sillimanite, biotite and ilmenite near garnet. Scar Hill, Cromar.

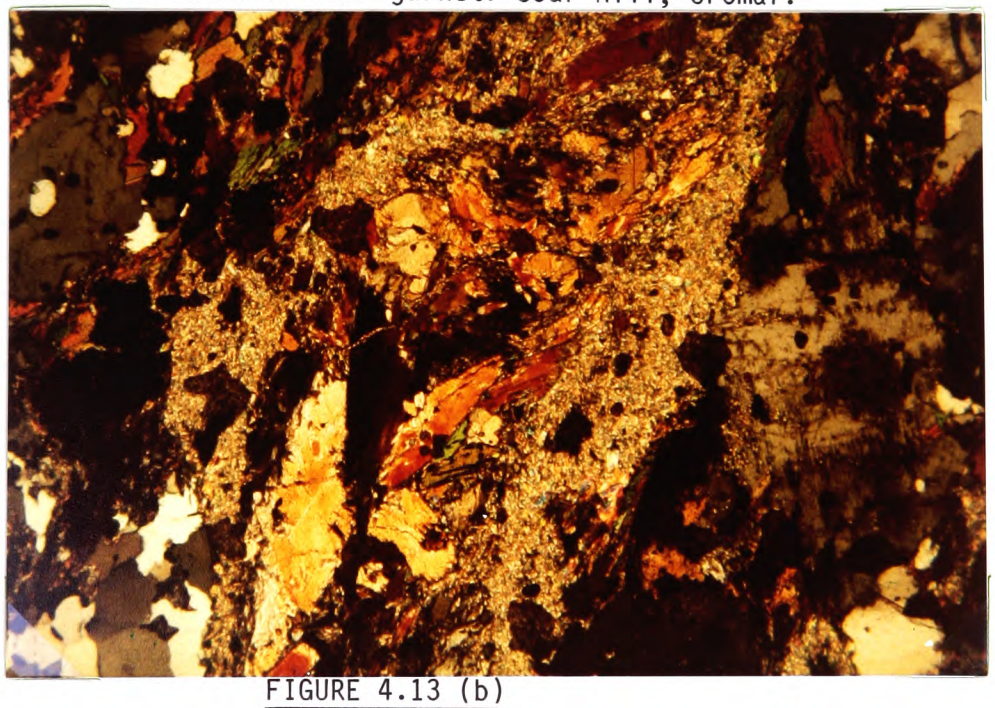

FIGURE 4.13 (b)

919A (x50) Sillimanite Gneiss with aggregate of prismatic sillimanite surrounded by shimmer aggregate Scar Hill, Cromar.

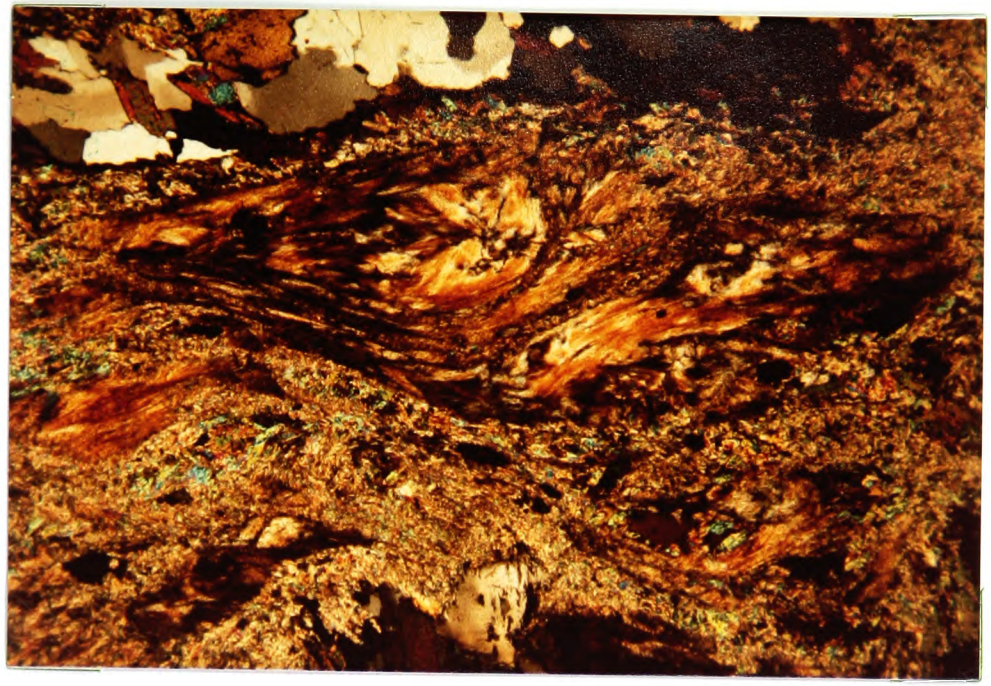

FIGURE 4.14 (a)

919E (x50) More retrogressed sillimanite gneiss. Mats of fibrolitic sillimanite surrounded by shimmer aggregate probably replacive of aggregate of coarse prismatic sillimanite. Near Scar Hill, Cromar.

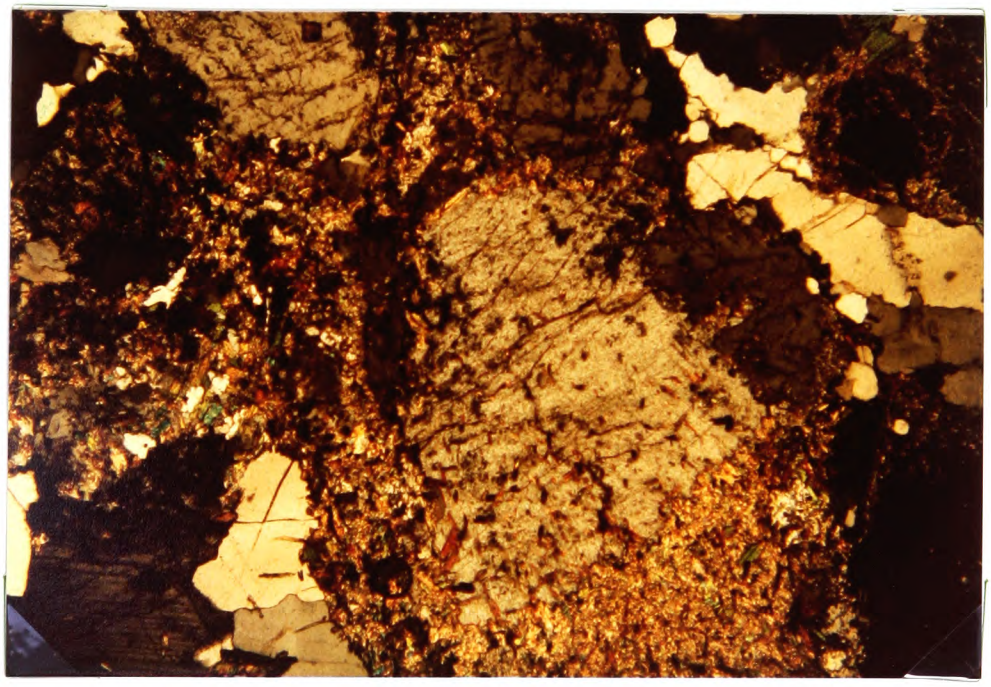

FIGURE 4.14 (b)

919F (x50). Andalusite replacing shimmer aggregate itself having replaced a sillimanite aggregate.

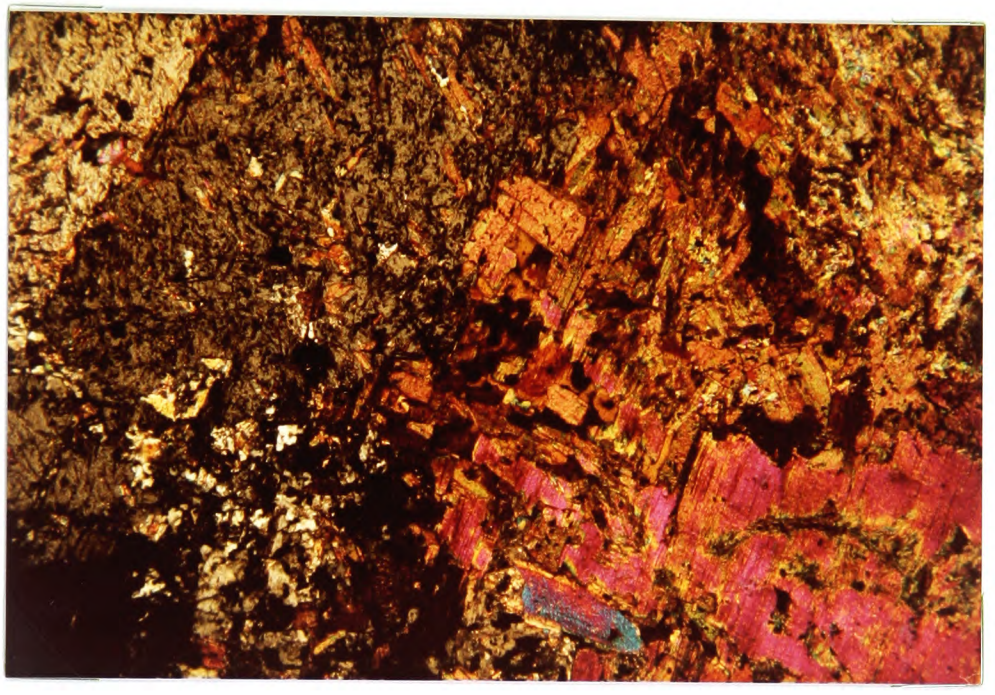

FIGURE 4.15

MC4 (x50). Large late andalusite surrounded by porphyroblastic micas. Fibrolite shreds in muscovite bottom right. Maryculter.

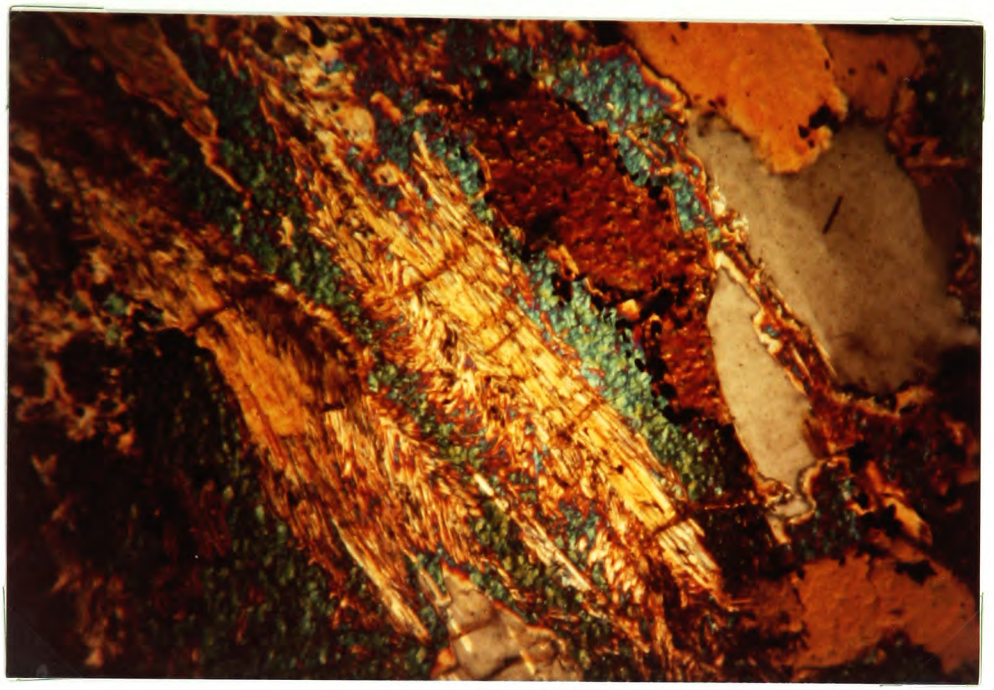

FIGURE 4.16

MC5 (x200) Very fine crenulated prismatic sillimanite enclosed in porphyroblastic mica. Sillimanites consistently aligned parallel to fabric. Maryculter.

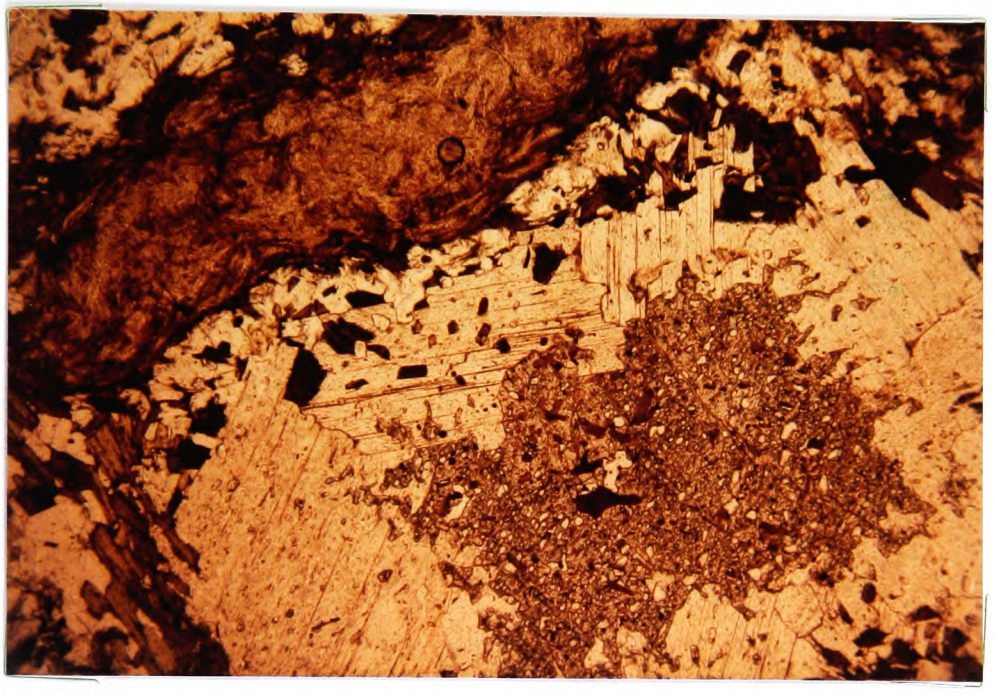

FIGURE 4.17

599A (x50). Andalusite replaced by large porphyroblastic muscovites surrounded by fibrolite mats.

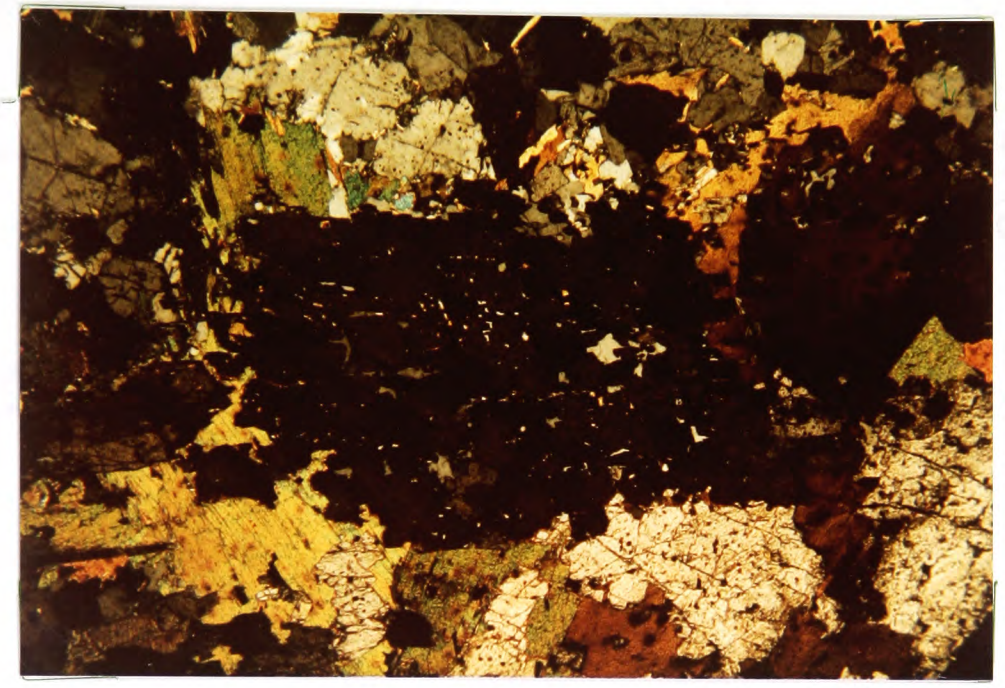

FIGURE 4.18

609B. (x50). Andalusite pseudomorphed by aggregate of prismatic sillimanites. Aureole of Haddo House Gabbro.

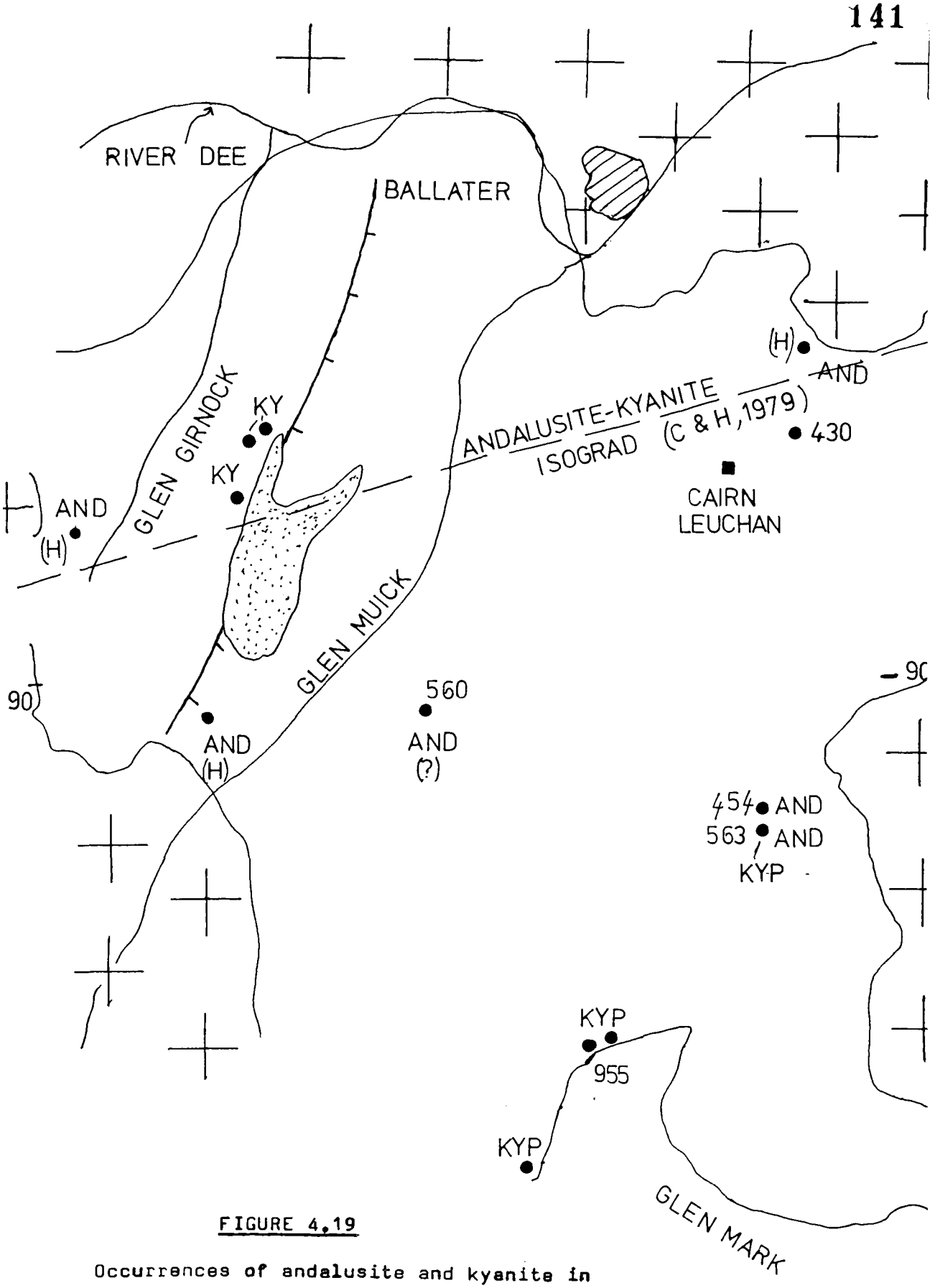

FIGURE 4,19

Occurrences of andalusite and kyanite in the Glen Muick area. AND: Andalusite, KY: Kyanite KYP: Kyanite pseudomorphs, (H) Hornfelsic andalusite, (?) Andalusite of uncertain status. Ticked line is kyanite sillimanite isograd, crosses: Newer Granite and stipple: serpentinite.

FIGURE 4.20

Revised zonal map of the aluminosilicates in the eastern Dalradian. Ticked line delimits the sillimanite zone. Numbered lines are isopleths of M/FM of biotite in the AFM assemblage kyanite-staurolite-biotite. The western segment of the andalusite kyanite isograd is from Chinner and Heseltine (1979). The dashed lines represent possible courses for the eastern segment.

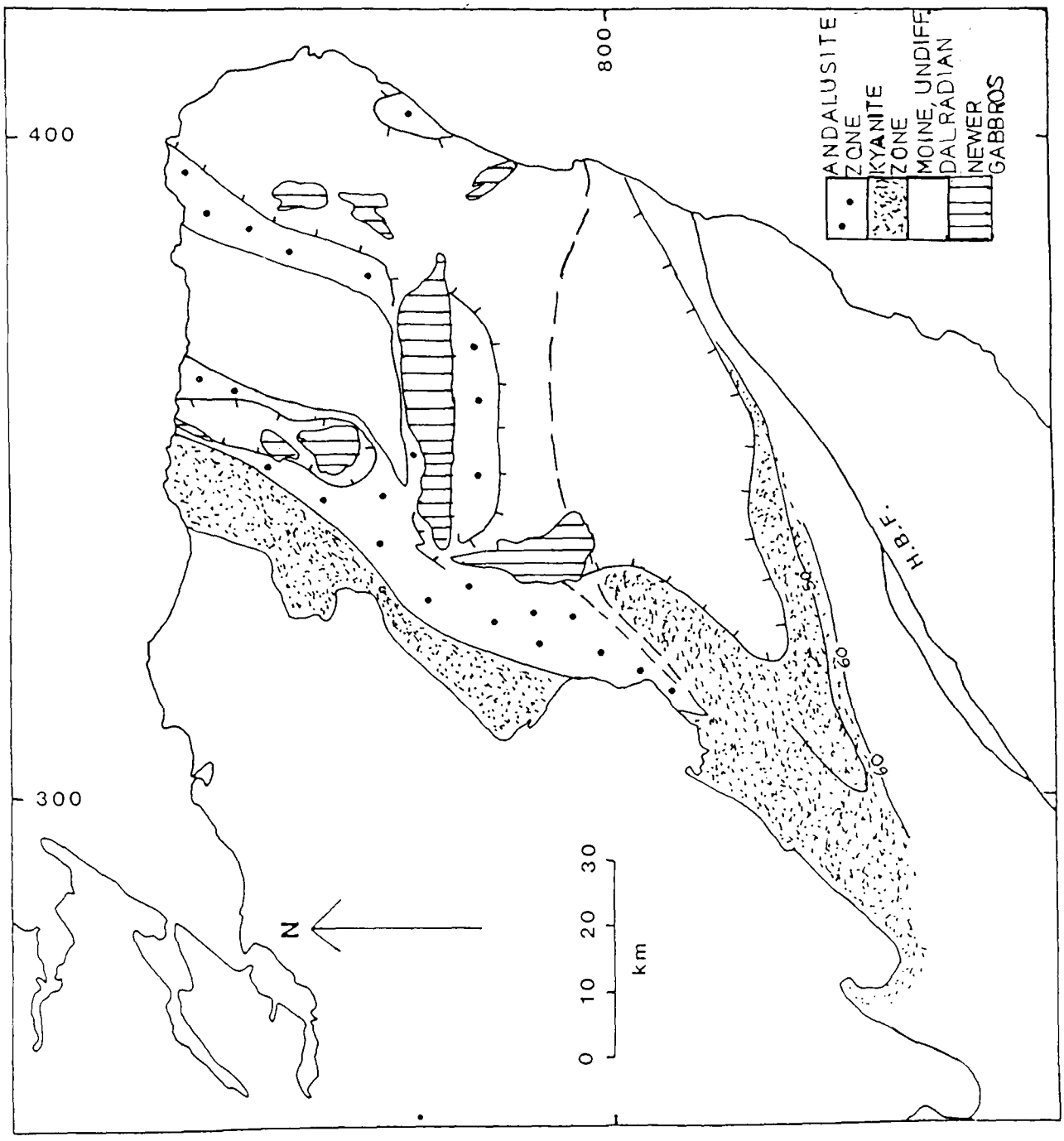

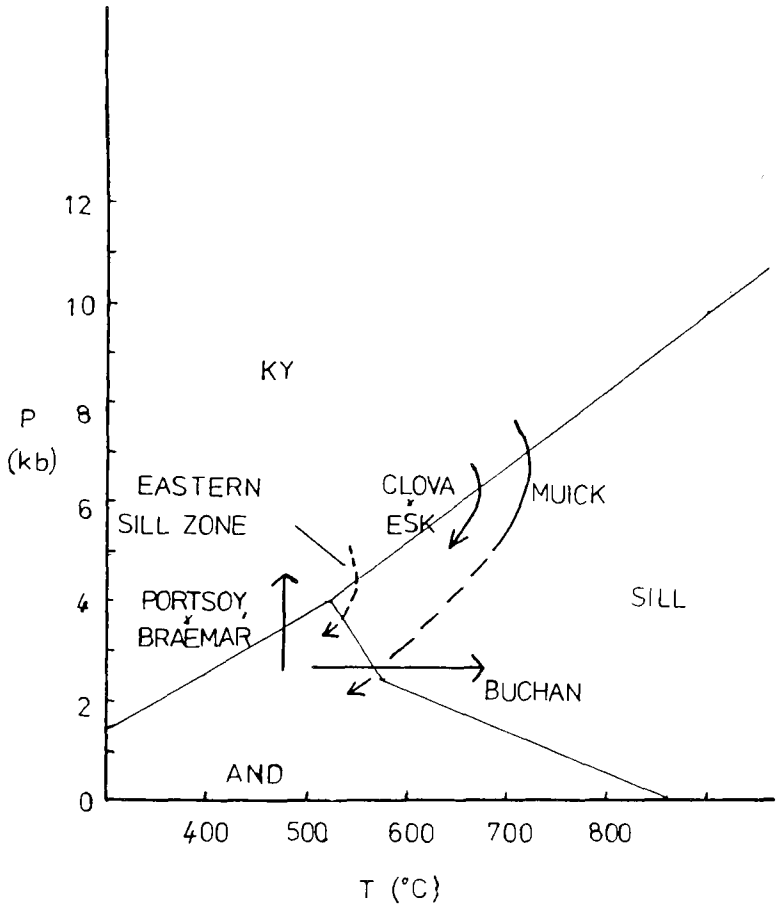

FIGURE 4.21

Hypothetical P-T paths in the Dalradian alsilicate zones

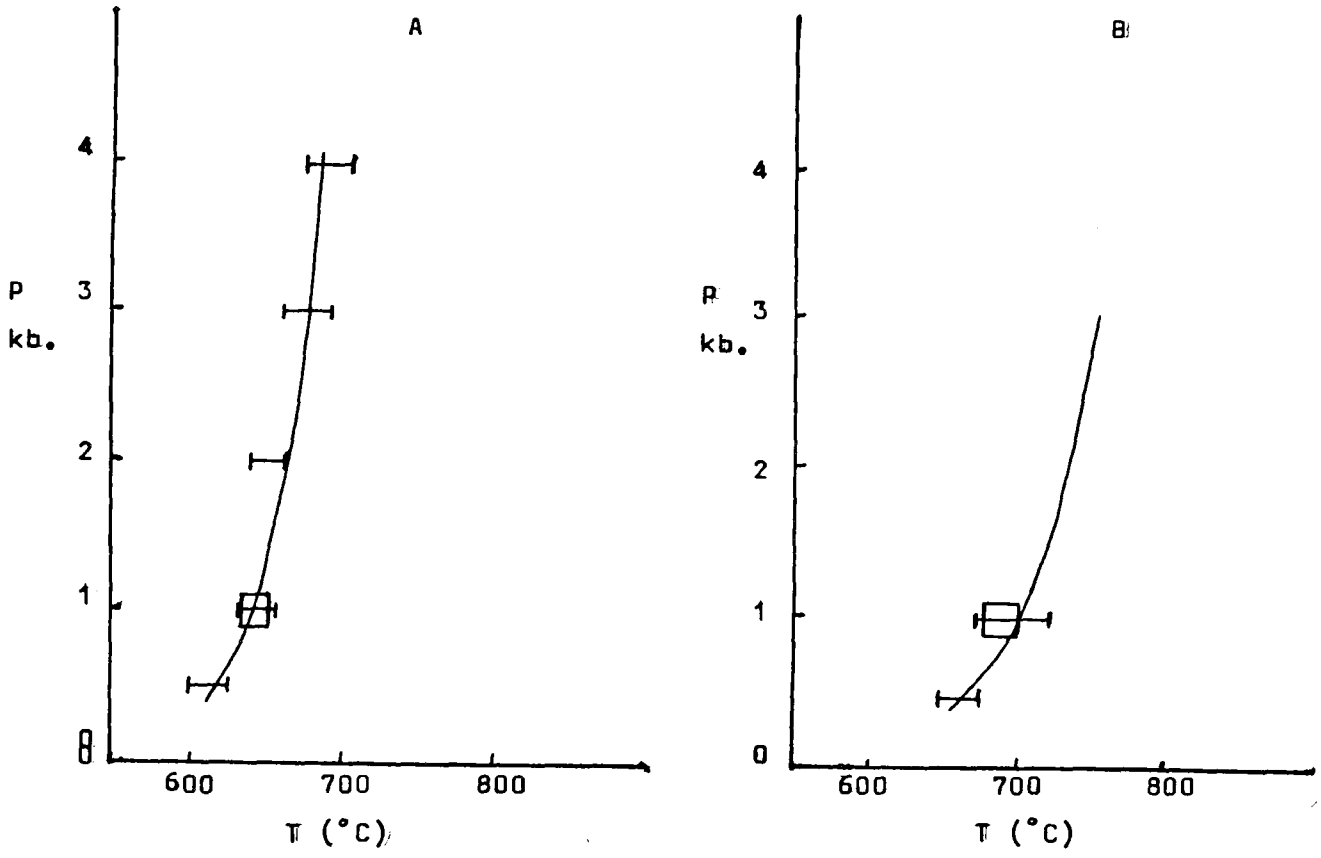

FIGURE 5.1

A : Forsterite + Talc $\rightarrow$ 5Enstatite + H_2O

□ Hemley et al. (1977)

⊢⊣ Chernosky (1976)

B : Talc $\rightarrow$ 3Enstatite + Quartz + H_2O

□ Hemley et al. (1977)

⊢⊣ Chernosky (1976)

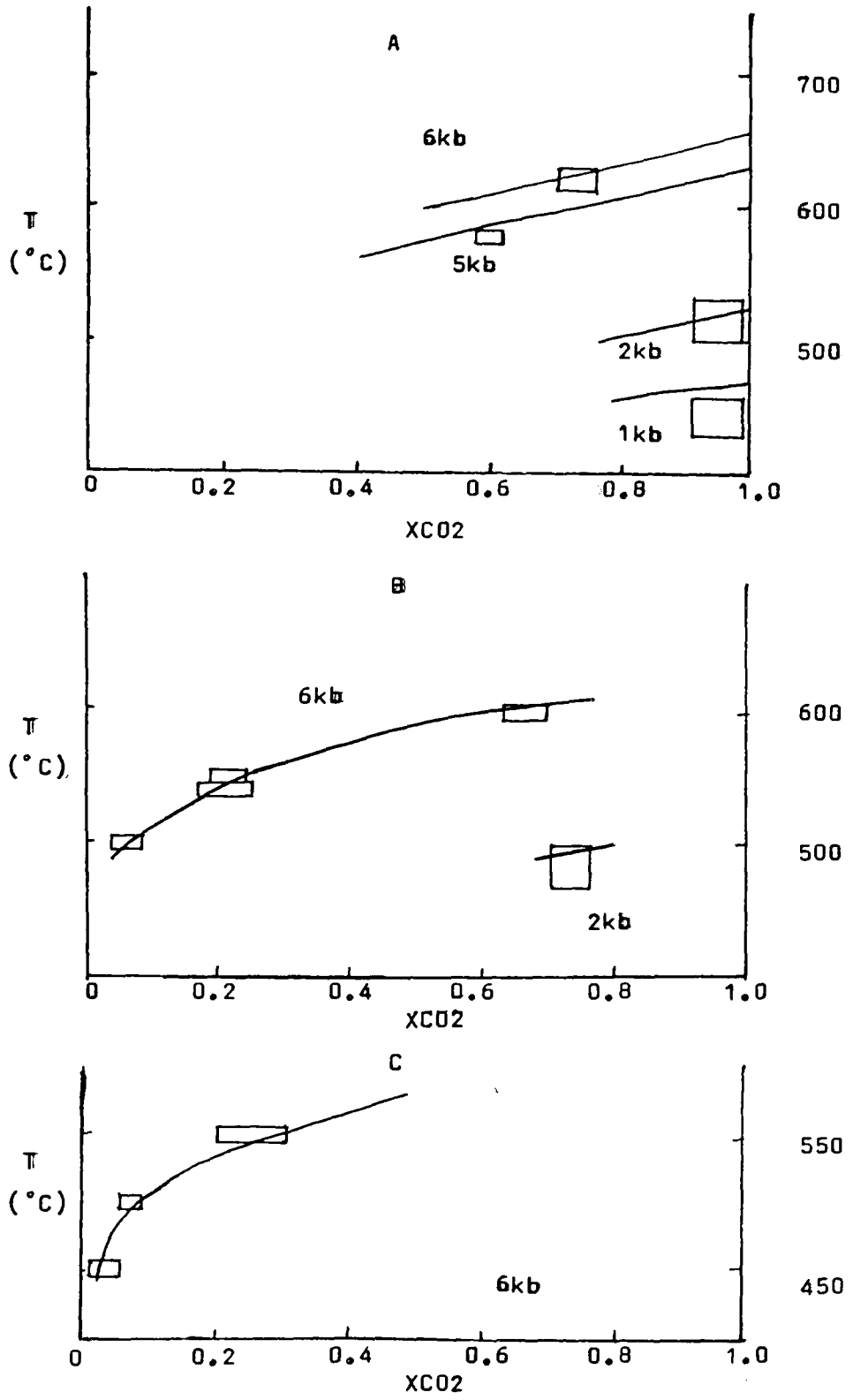

FIGURE 5.2

A : Dolomite + 2Quartz → Diopside + $2CO_2$

2kb Slaughter et al. (1975), 6kb Eggert and Kerrick (1981),
5kb Jacobs and Kerrick (1981).

B : 5Dolomite + 8Quartz + H_2O → Tremolite + 3Calcite + $7CO_2$

2kb Slaughter et al. (1975), 6kb Eggert and Kerrick (1981).

C : 3Dolomite + 4Quartz + H_2O → Talc + 3Calcite + $3CO_2$

Eggert and Kerrick (1981).

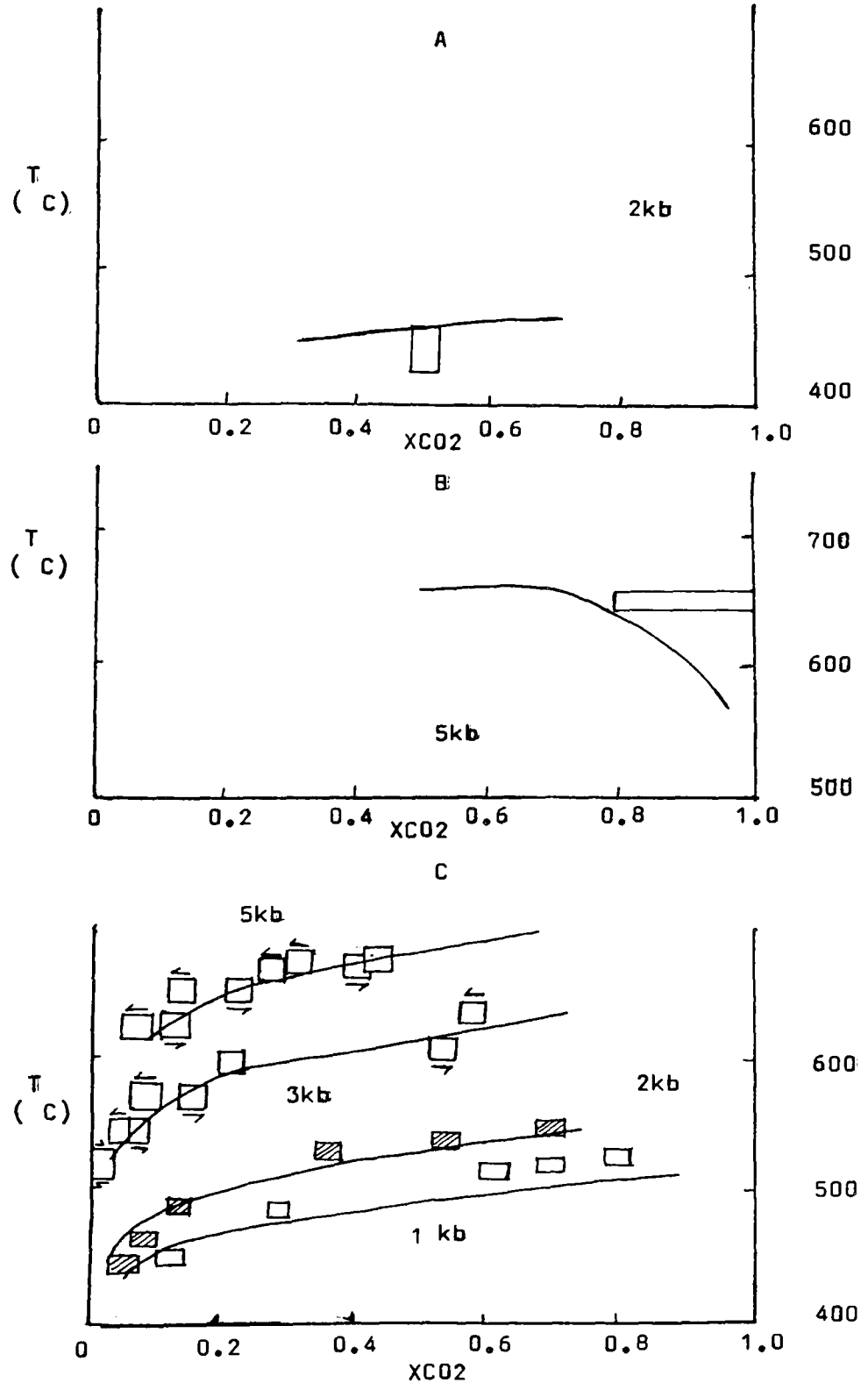

FIGURE 5.3

A : 5Talc + 6Calcite + 4Quartz → 3Tremolite + $6CO_2$ + $3H_2O$
Slaughter et al. (1975)

B : Tremolite + 3Calcite → Dolomite + 4Diopside + H_2O + CO_2
Slaughter et al. (1975).

C : Tremolite + 11Dolomite → 8Forsterite + 13Calcite + $9CO_2$ + H_2O Metz (1967, 1971, 1976).

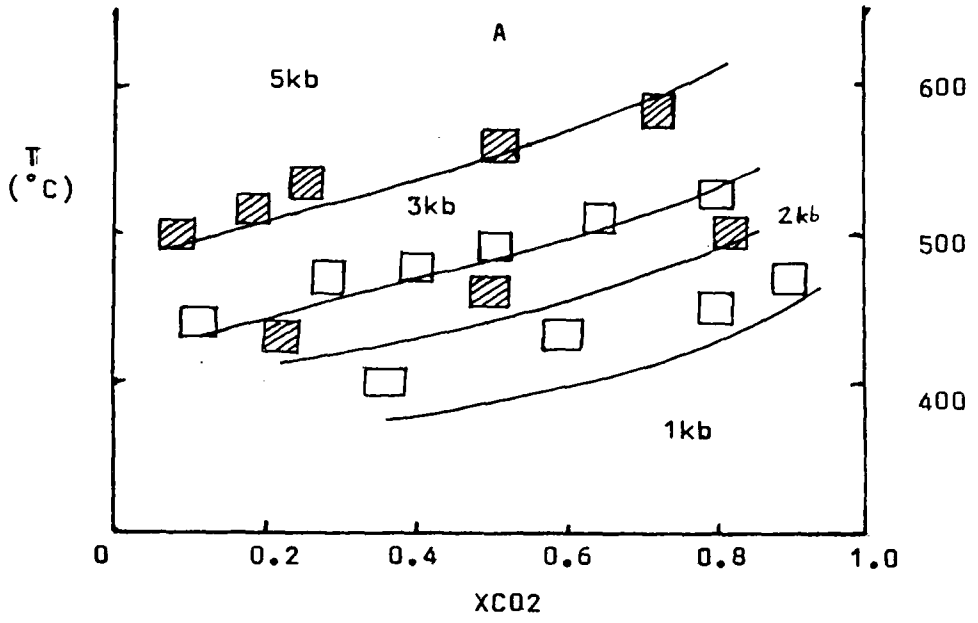

FIGURE 5.4

A : 3Dolomite + 4Quartz + H_2O → Talc + 3Calcite + $3CO_2$

Metz (1970, 1971).

FIGURE 5.5

A : Dolomite + 2Quartz $\rightarrow$ Diopside + $2CO_2$

Slaughter et al. (1975)

B : Diopside + 3Dolomite $\rightarrow$ 2Forsterite + 4Calcite + $2CO_2$

Kase and Metz (1980)

C : Tremolite $\rightarrow$ 2Diopside + 3Enstatite + Quartz + H_2O

An Yin and Greenwood (1983)

D : 5Phlogopite + 6Calcite + 24Quartz $\rightarrow$ 3Tremolite + 5K feldspar + $6CO_2 + 2H_2O$

Hewitt (1975)

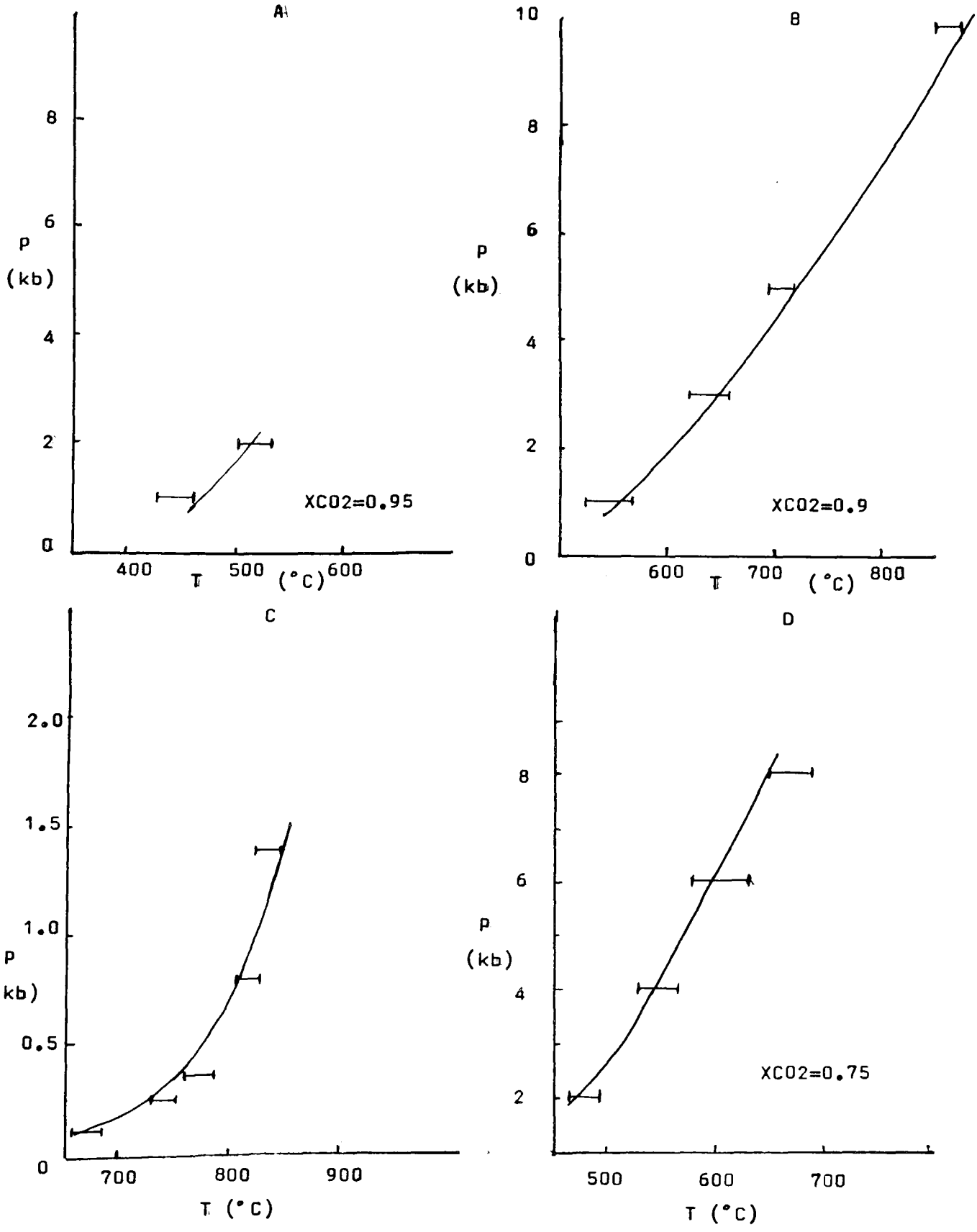
A
P
(kb)
8
6
4
2
0
400
500
600
T (°C)
XCO2=0.95
B
10
8
6
4
2
0
600
700
800
T (°C)
XCO2=0.9
C
2.0
1.5
1.0
0.5
0
700
800
900
T (°C)
D
8
6
4
2
500
600
700
T (°C)
XCO2=0.75

FIGURE 5.5

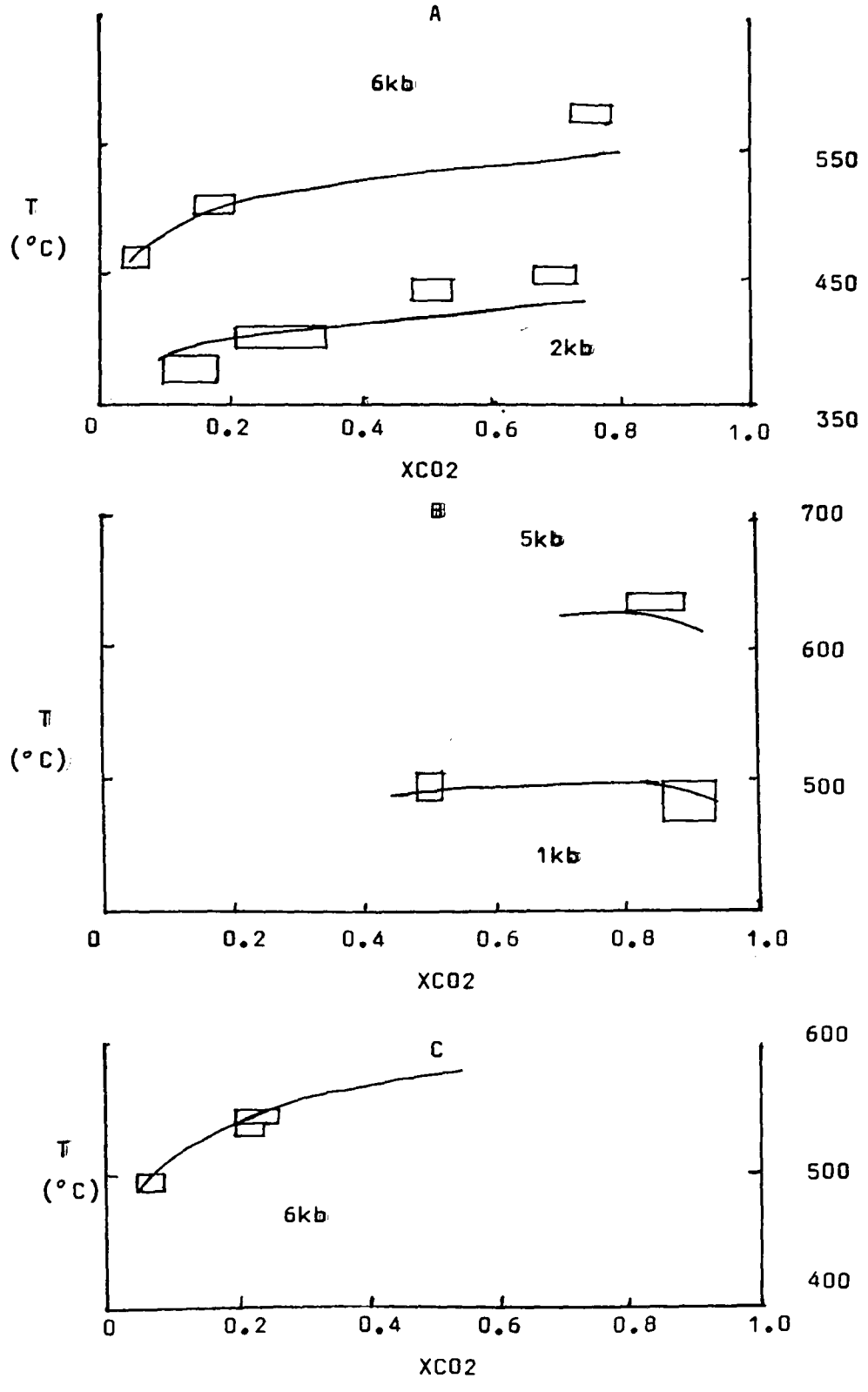

FIGURE 5.6

A : Calcite + Andalusite (2kb)/Kyanite (6kb)
$\rightarrow$ Anorthite + CO_2, Jacobs and Kerrick (1981

B : Tremolite + 3Calcite + 2Quartz $\rightarrow$ 5Diopside + $3CO_2$ + $2H_2O$
Slaughter et al. (1975)

C : 2Dolomite + Talc + 4Quartz $\rightarrow$ Tremolite + $4CO_2$
Eggert and Kerrick (1981)

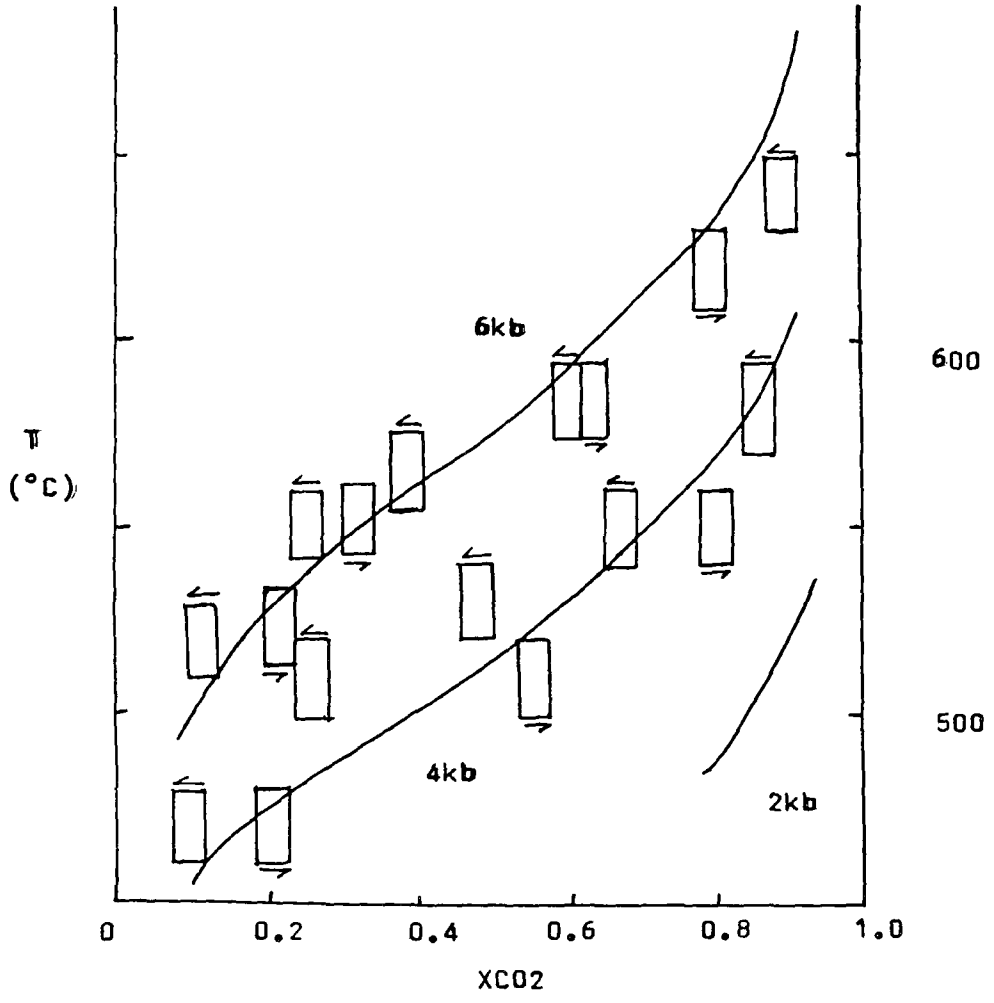

FIGURE 5.7

3Dolomite + K feldspar + H_2O $\longrightarrow$

Phlogopite + 3Calcite + $3CO_2$

Puhan and Johannes (1974)

Puhan (1978)

FIGURE 5.8

A : Muscovite + Quartz $\rightarrow$ K feldspar + Sillimanite + H_2O
Chatterjee and Johannes (1974)

B : Muscovite + Quartz $\rightarrow$ K feldspar + Andalusite + H_2O
Chatterjee and Johannes (1974)

C : Muscovite $\rightarrow$ K feldspar + Corundum + H_2O
Chatterjee and Johannes (1974)

D : Muscovite + Calcite + 2Quartz $\rightarrow$ Anorthite + K feldspar + H_2O + CO_2
Hewitt (1973)

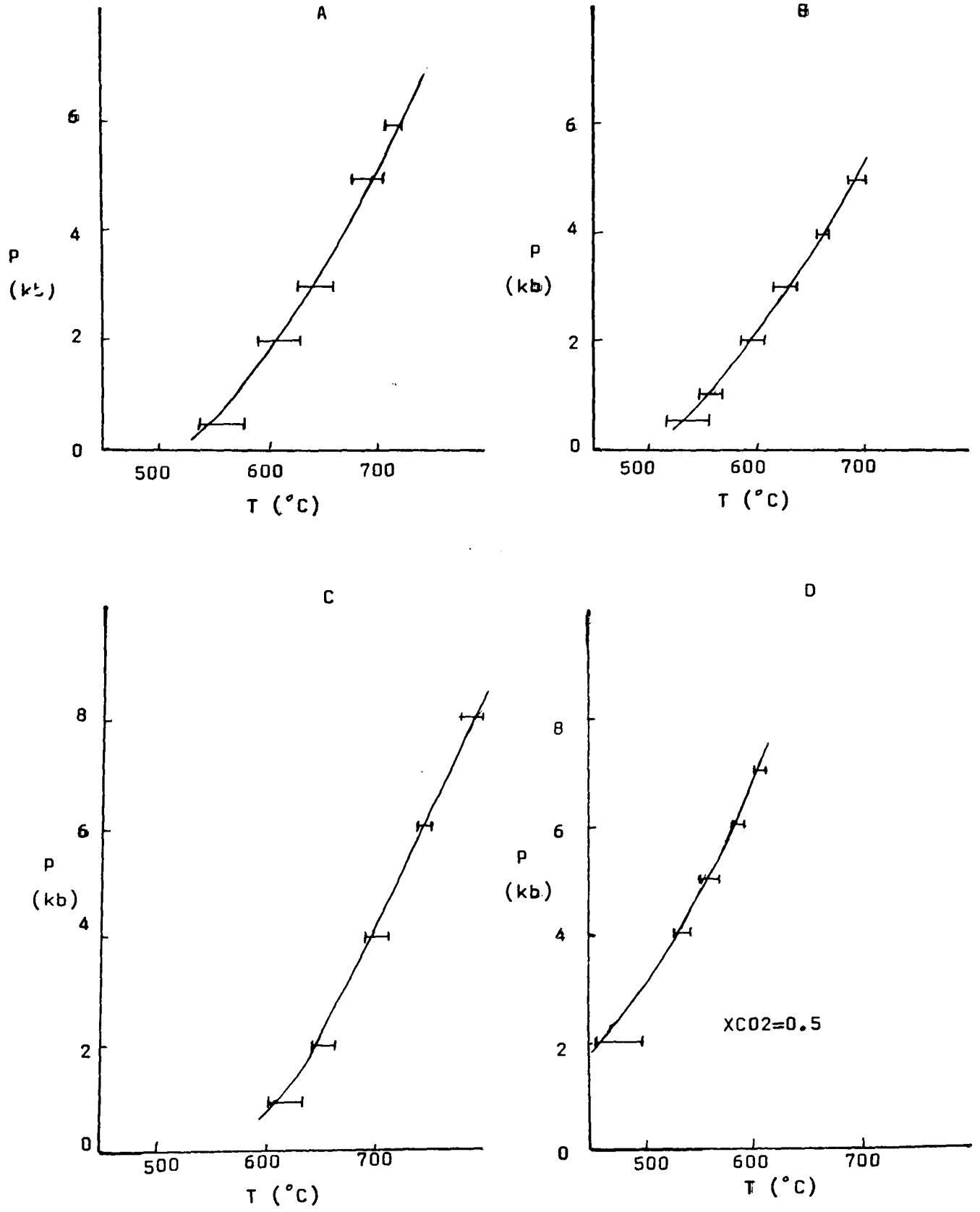

FIGURE 5.8

FIGURE 5.9

A : 4Zoisite + Quartz $\rightarrow$ 5Anorthite + Grossular + $2H_2O$

Newton (1966)

Boettcher (1970)

B : 6Zoisite $\rightarrow$ 6Anorthite + 2Grossular + Corundum + $3H_2O$

Newton (1965)

Boettcher (1970)

C : 2Zoisite + Quartz + Kyanite $\rightarrow$ 4Anorthite + H_2O

Goldsmith (1981)

D : 2Zoisite + Muscovite + 2Quartz $\rightarrow$ 4Anorthite + K feldspar + $2H_2O$

Johannes (1980)

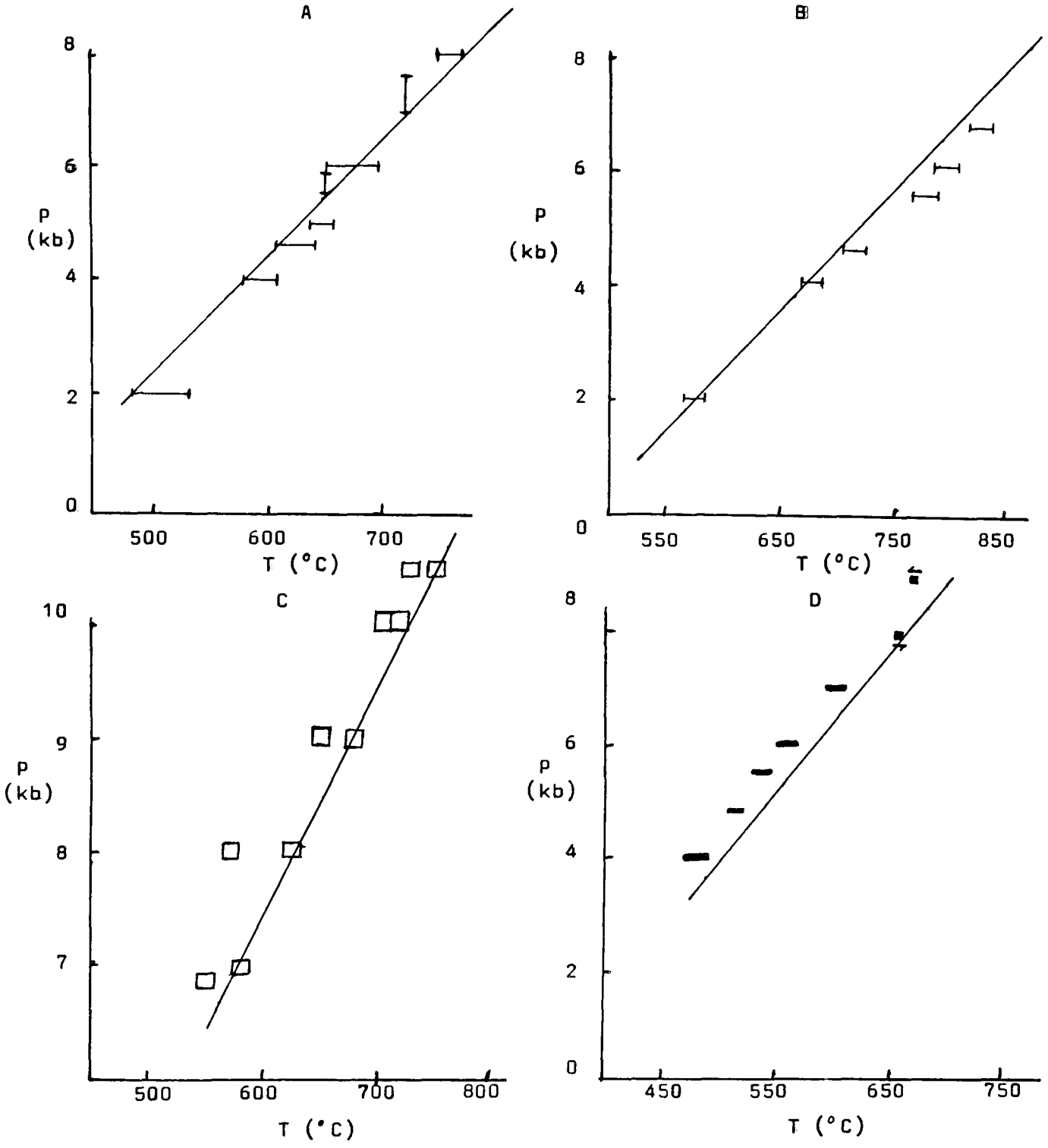

FIGURE 5.9

FIGURE 5.10

A : 3Anorthite → Grossular + 2Kyanite + Quartz

Goldsmith (1980)

B : Anorthite + 2Wollastonite → Grossular + Quartz

Newton (1966)

Hays (1967)

Boettcher (1970)

Windom and Boettcher (1976)

Huckenholz et al. (1975)

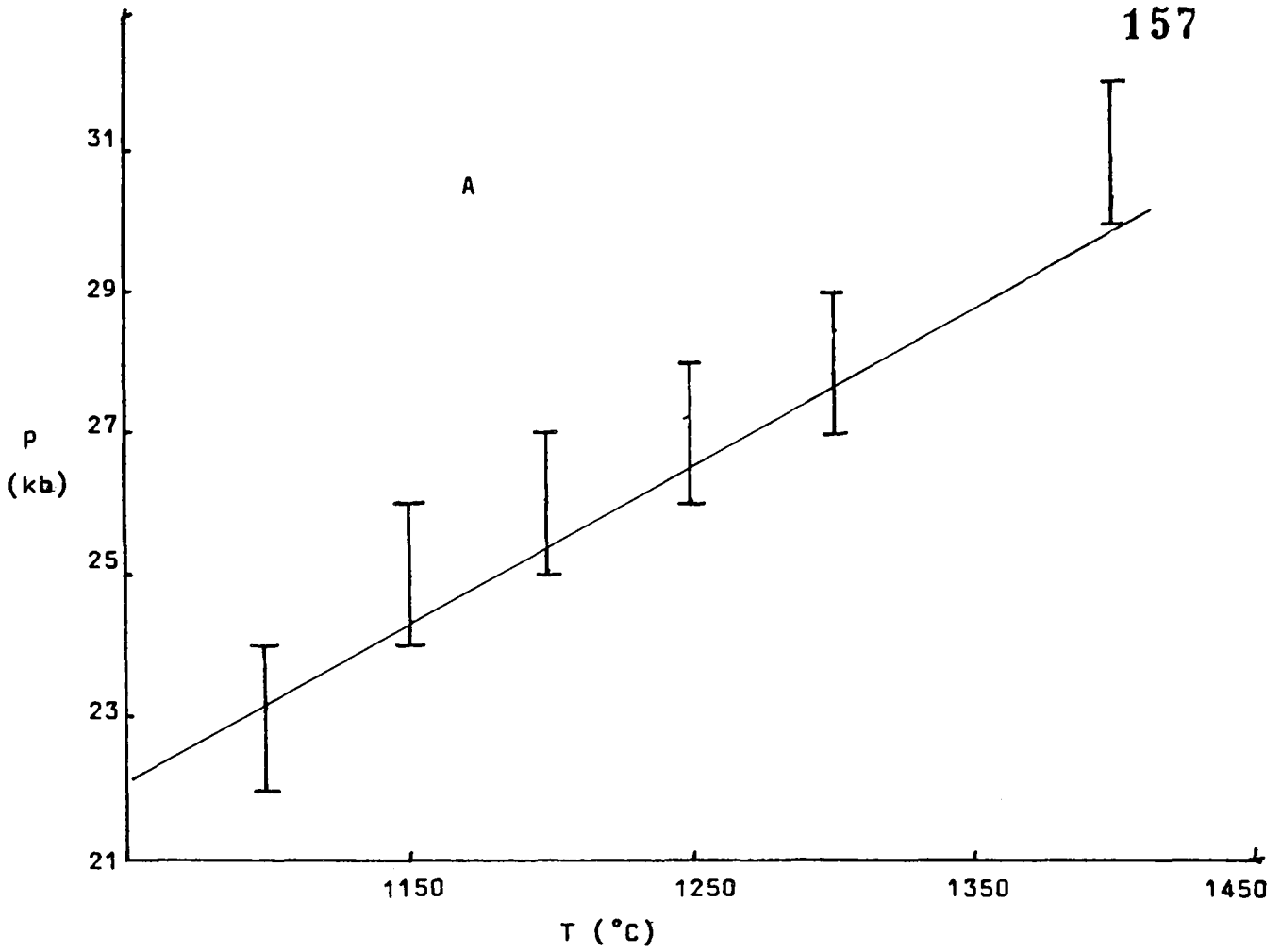
A
31
29
27
25
23
21
P
(kb)
1150
1250
1350
1450
T (°C)

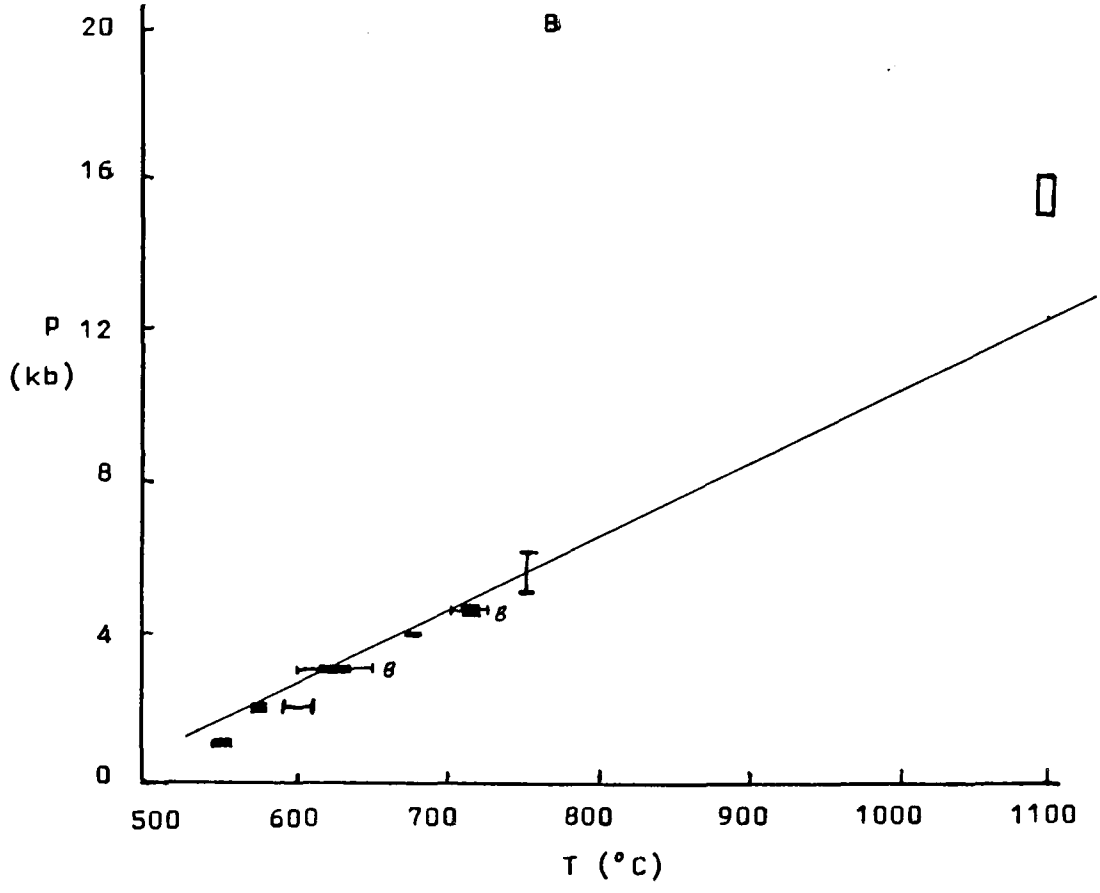
B
20
16
12
8
4
0
P
(kb)
500
600
700
800
900
1000
1100
T (°C)

FIGURE 5.10

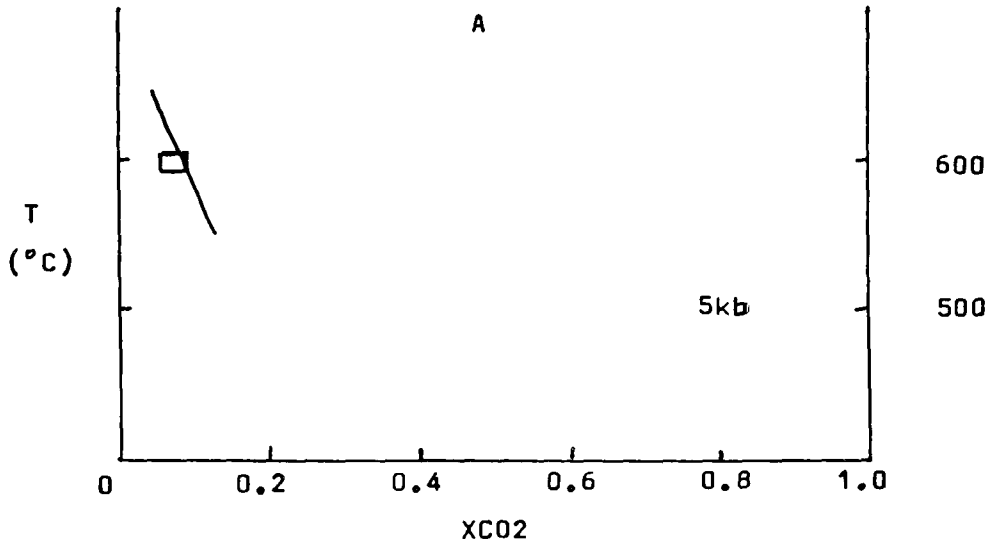

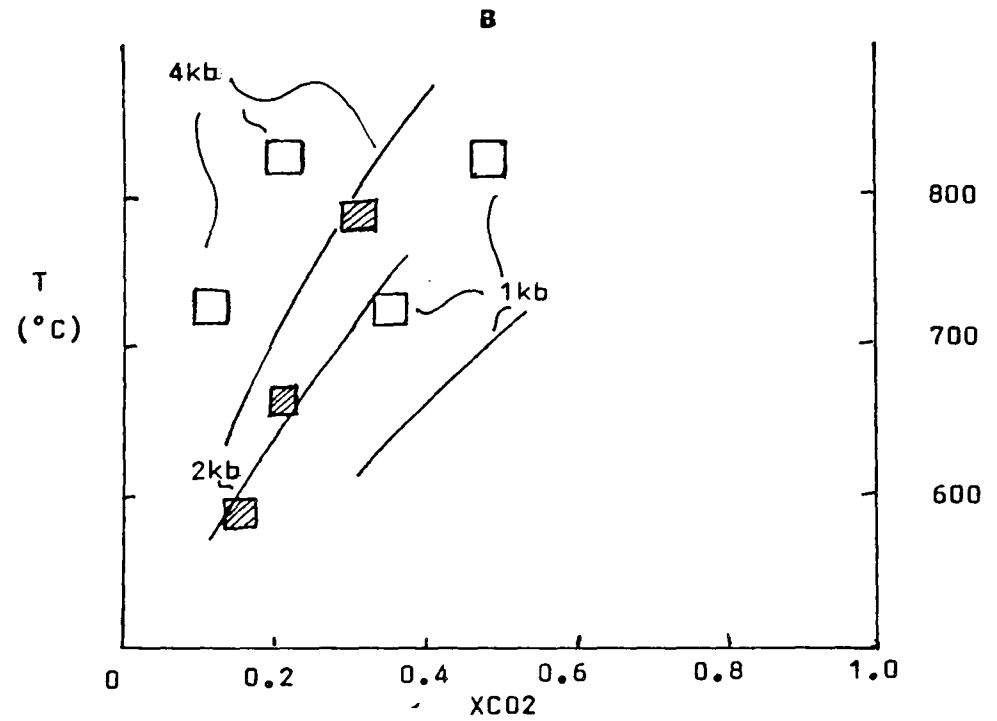

FIGURE 5.11

A : 2Zoisite + CO_2 → 3Anorthite + Calcite + H_2O

Allen and Fawcett (1982)

B : Anorthite + Calcite + Wollastonite

→ Grossular + CO_2

Gordon and Greenwood (1971)

Hoschek (1974)

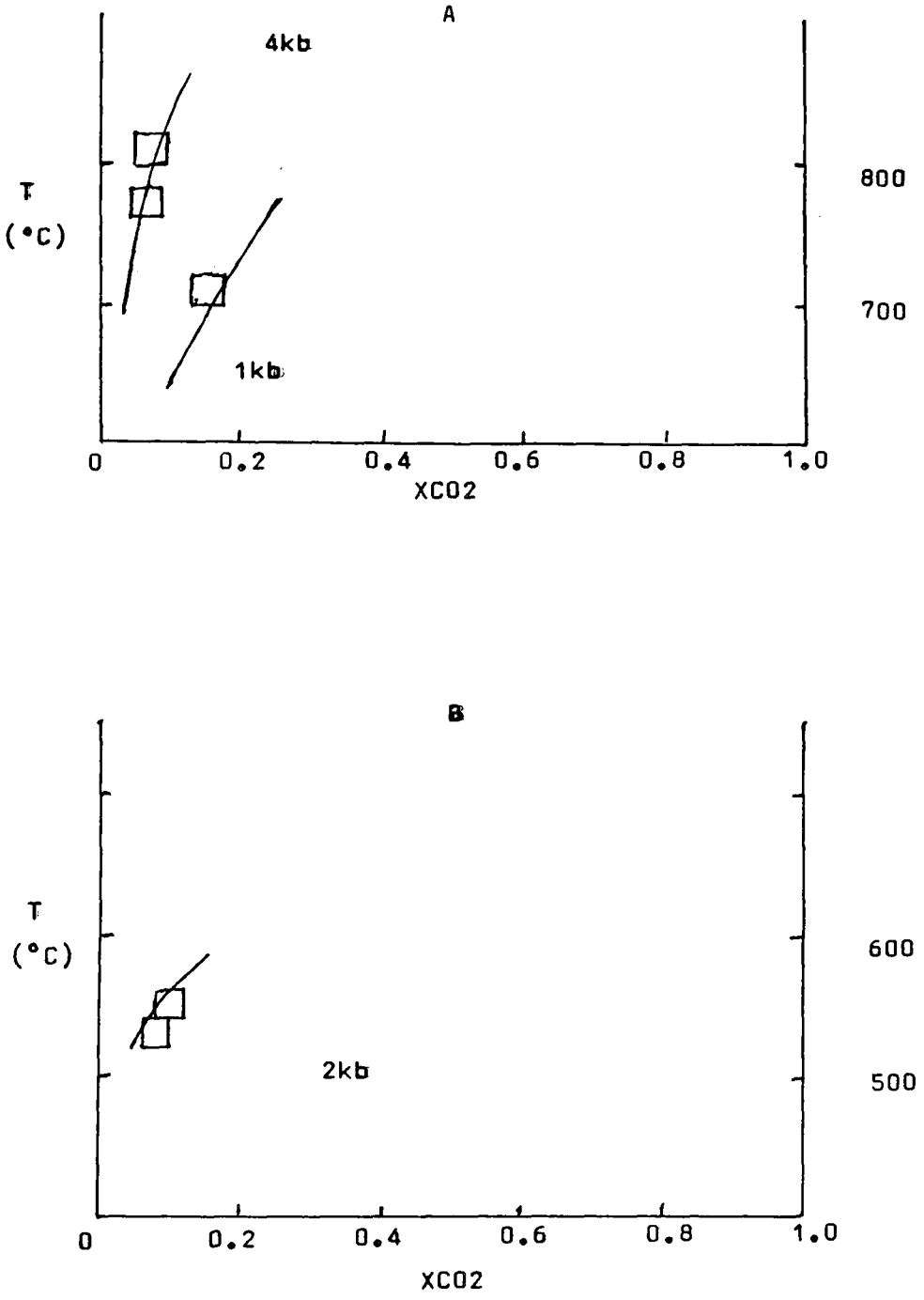

FIGURE 5.12

A : 3Anorthite + 3Calcite → 2Grossular + Corundum + $3CO_2$
Hoschek (1974)

B : 2Calcite + Anorthite + Quartz → Grossular + $2CO_2$
Hoschek (1974)

FIGURE 5.13

Calcite + Quartz $\longrightarrow$ Wollastonite + CO_2

A: 1 and 2kb data. Data at X_{CO_2} =1 from Harker and Tuttle (1956), other data from Greenwood (1967).

B: 2, 4 and 6kb data of Ziegenbein and Johannes (1974), circles; and of Jacobs and Kerrick (1981), box.

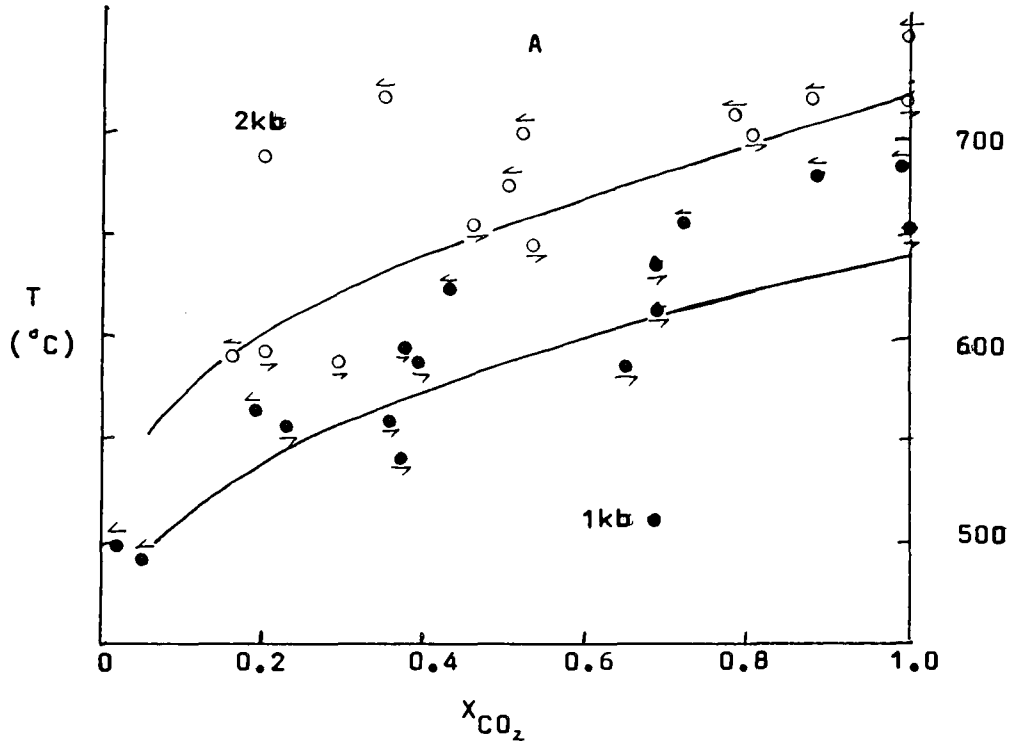
A
2kb
1kb
T
(°C)
700
600
500
0
0.2
0.4
0.6
0.8
1.0
X_{CO_2}

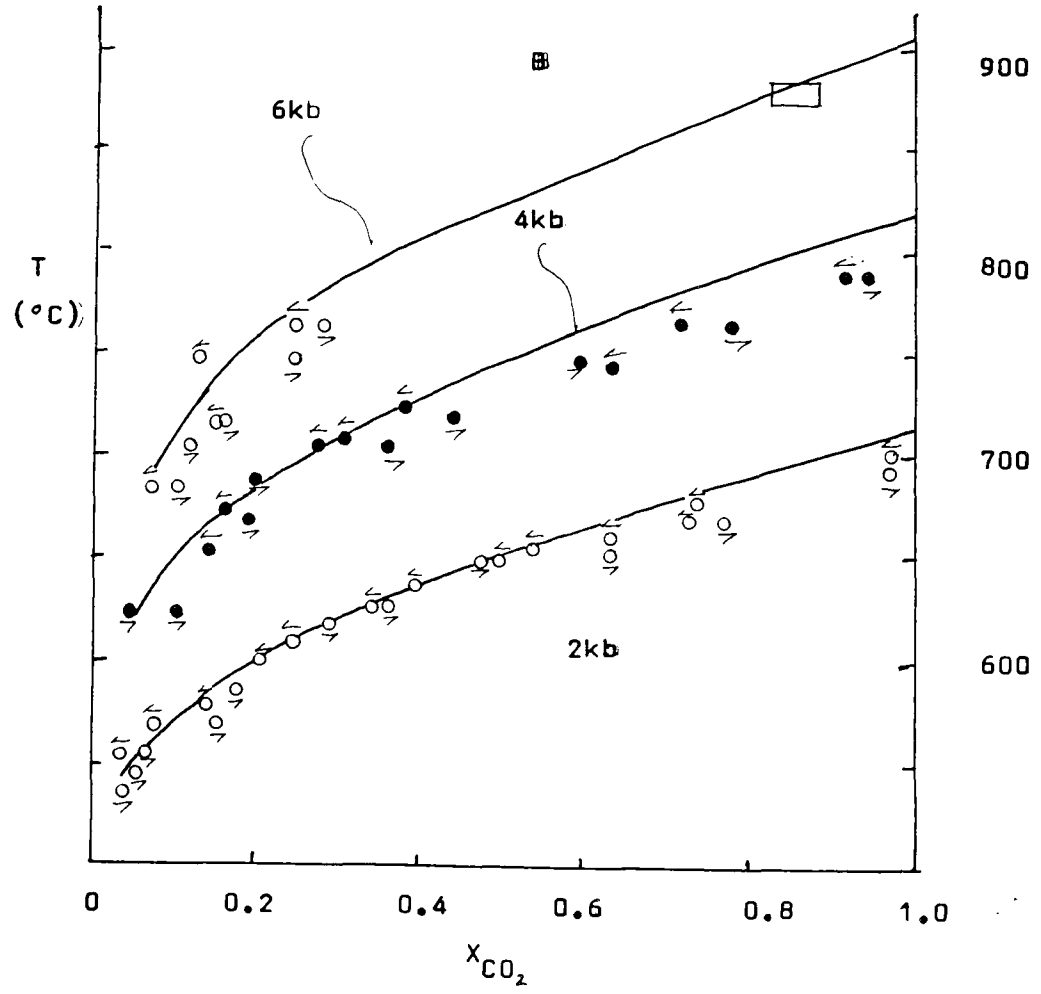
B
6kb
4kb
2kb
T
(°C)
900
800
700
600
0
0.2
0.4
0.6
0.8
1.0
X_{CO_2}

FIGURE 5.14

A: 4Enstatite + MgSpinel $\longrightarrow$ Pyrope + Forsterite
Danckwerth and Newton (1978) (<1200°C)
Perkins et al. (1981) (>1200°C)

B: 4Enstatite + Sillimanite $\longrightarrow$ Pyrope + Quartz
Perkins (1983) (circles)
Hensen and Essene (1971) (I bars)

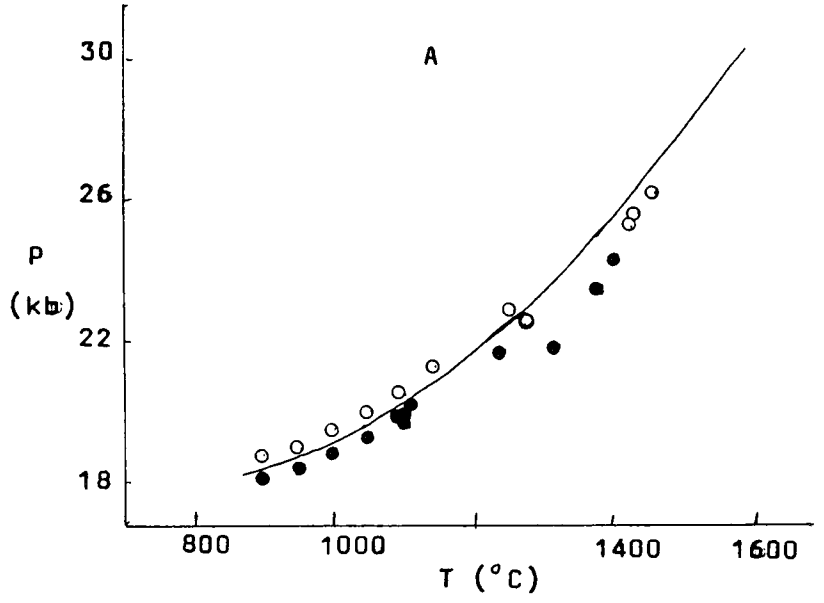
A
30
26
22
18
P
(kb)
800
1000
1400
1600
T (°C)

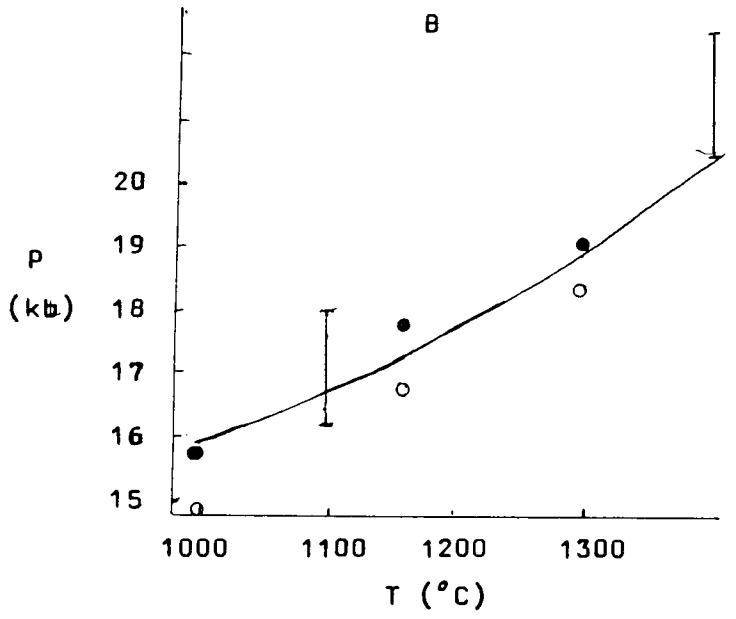
B
20
19
18
17
16
15
P
(kb)
1000
1100
1200
1300
T (°C)

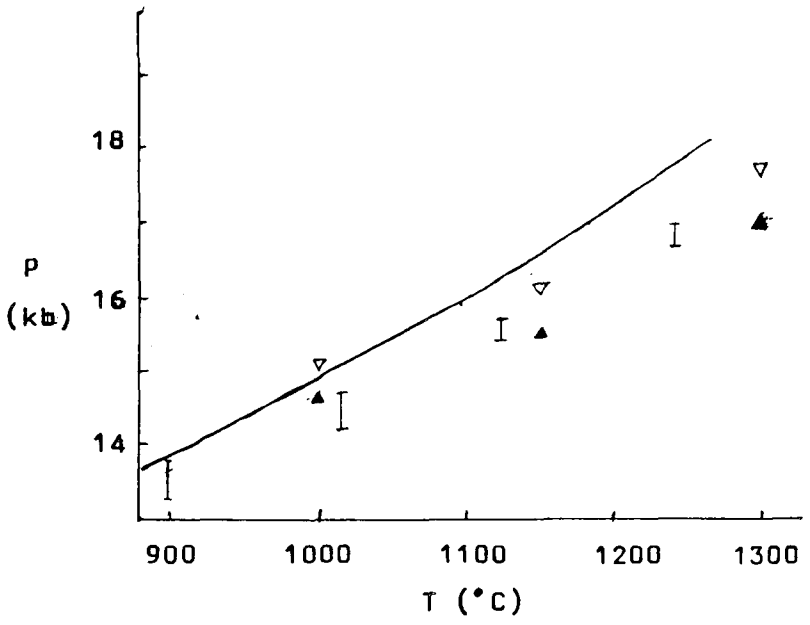

Anorthite + Orthopyroxene

⟶ Garnet + Clinopyroxene + Quartz

Perkins (1983) (triangles)

Hansen (1981) (I bars)

approximate position assuming stoichiometric clinopyroxene.

FIGURE 5.15

FIGURE 5.16

A : 3MgClinochlore + 14Quartz

$\longrightarrow$ 5Talc + 3Kyanite + $7H_2O$

Massone et al. (1983)

B : 3MgClinochlore + 5Muscovite

$\longrightarrow$ 8Kyanite + 5Phlogopite + Quartz + $12H_2O$

Bird and Fawcett (1973)

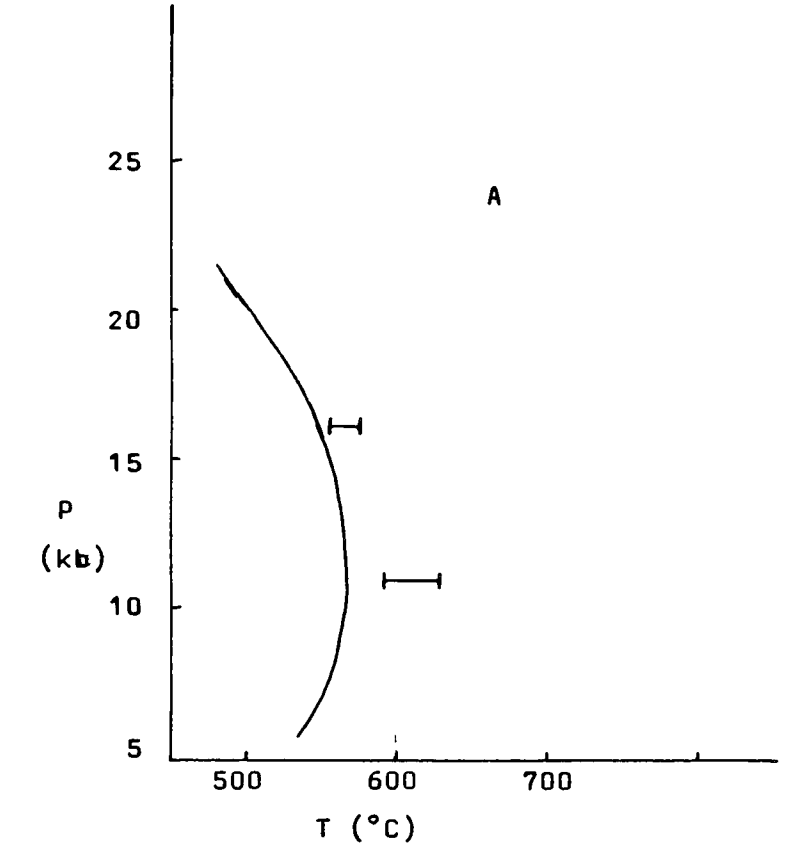
A
25
20
15
10
5
P
(kb)
500
600
700
T (°C)

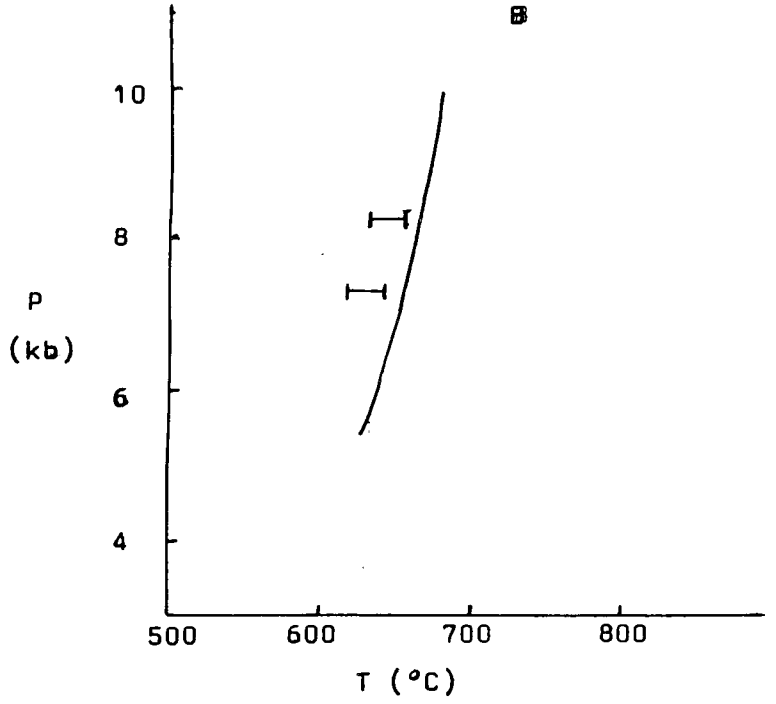
B
10
8
6
4
P
(kb)
500
600
700
800
T (°C)

FIGURE 5.17

A : MgClinochlore

$\longrightarrow$ Forsterite + Spinel + 2Enstatite + $4H_2O$

Fawcett and Yoder (1966)

B : 3MgClinochlore + 10Calcite + 21Quartz

$\longrightarrow$ 3Tremolite + 2Zoisite + $8H_2O$ + $10CO_2$

Best (1978)

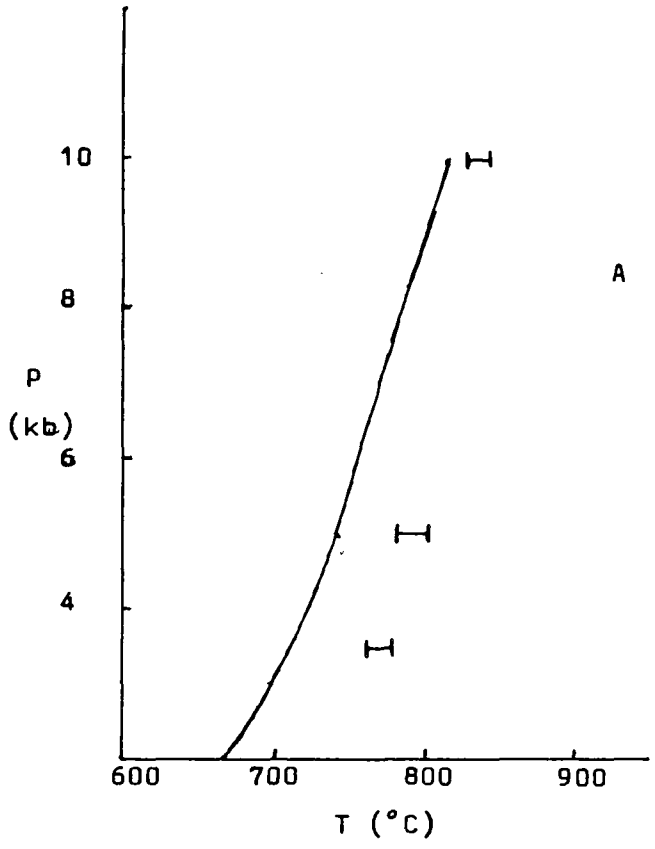
10
8
P
(kb)
6
4
A
600
700
800
900
T (°C)

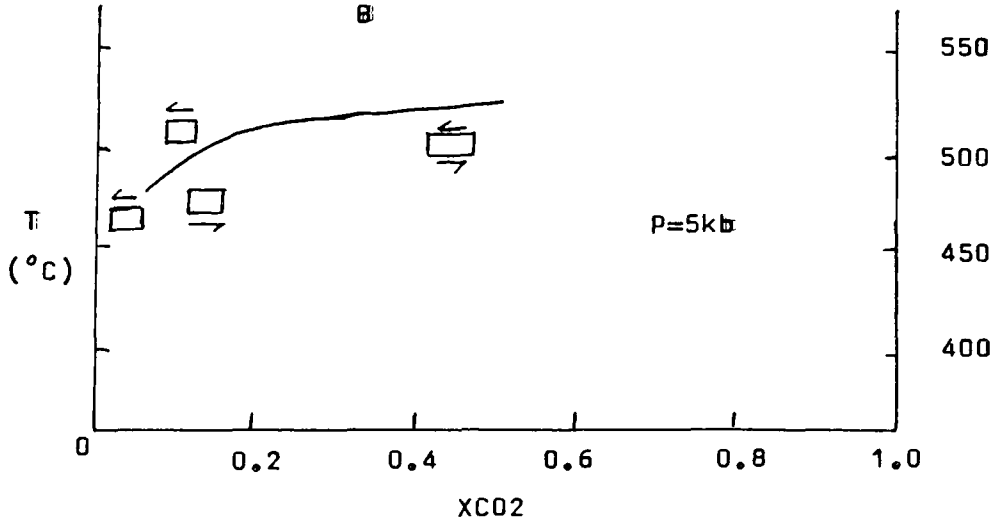
B
T
(°C)
P=5kb
550
500
450
400
0
0.2
0.4
0.6
0.8
1.0
XCO2

FIGURE 6.1

Geological sketch map of the Eastern Scottish Highlands showing locations mentioned in the text.

A Water of Ailnack
B Glen Brerachan
C Cowhythe Gneiss
CR Cromar
CL Glen Clunie
E Glen Ey
GA Glen Avon
GC Glen Clova
GE Glen Esk
GG Glen Girnock
GM Glen Muick
DG Duchray Hill Gneiss
M Glen Mark
S Schichallion
SH Glen Shee
ST Buchan Staurolite zone
P Portsoy

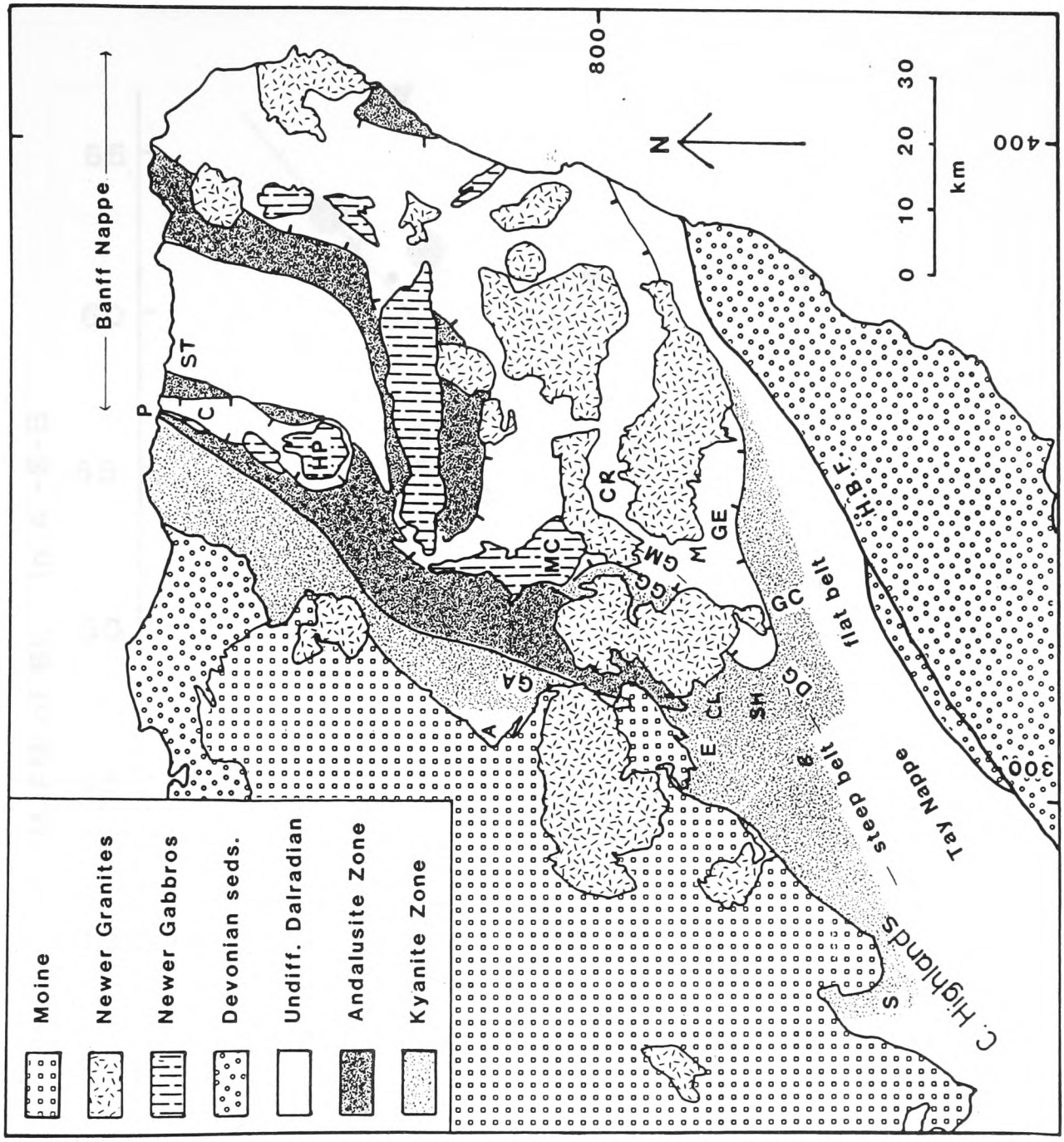
Moine
Newer Granites
Newer Gabbros
Devonian seds.
Undiff. Dalradian
Andalusite Zone
Kyanite Zone
Banff Nappe
P
C
ST
HP
MC
CR
GM
GE
GC
GA
A
E
CL
SH
DG
S
Tay Nappe
H.B.F.
flat belt
steep belt
C. Highlands
N
0 10 20 30
km
800
400
300

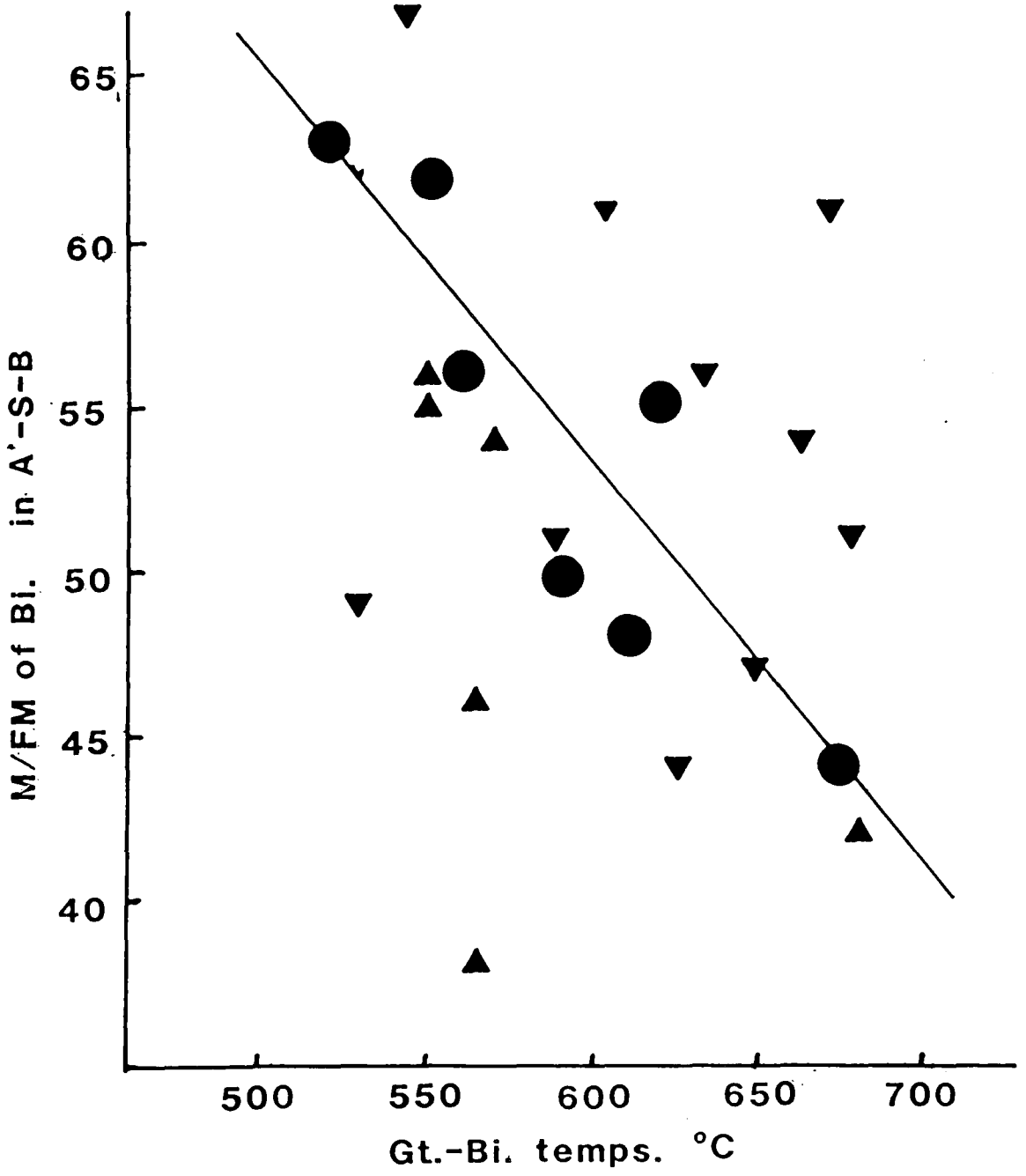

FIGURE 6.2

M/FM of biotite in the assemblage kyanite-staurolite-biotite muscovite-quartz plotted against garnet biotite temperatures calculated by the method of Hodges and Spear (1982). Data from table 6.5.

FIGURE 6.3

M/FM of biotite in the assemblage kyanite-staurolite-biotite. Some data from Harte and Hudson (1979) and Chinner (1980).

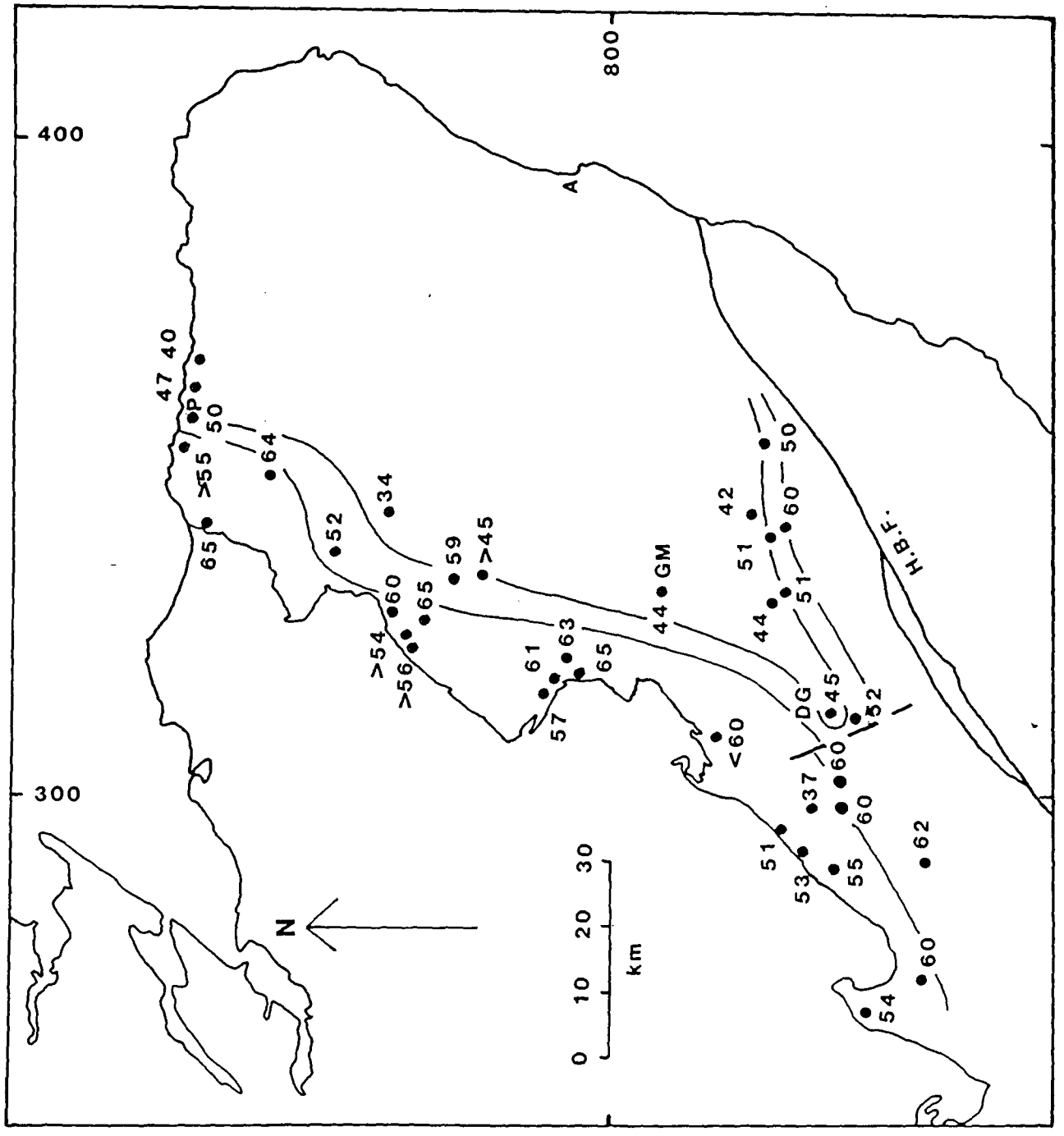

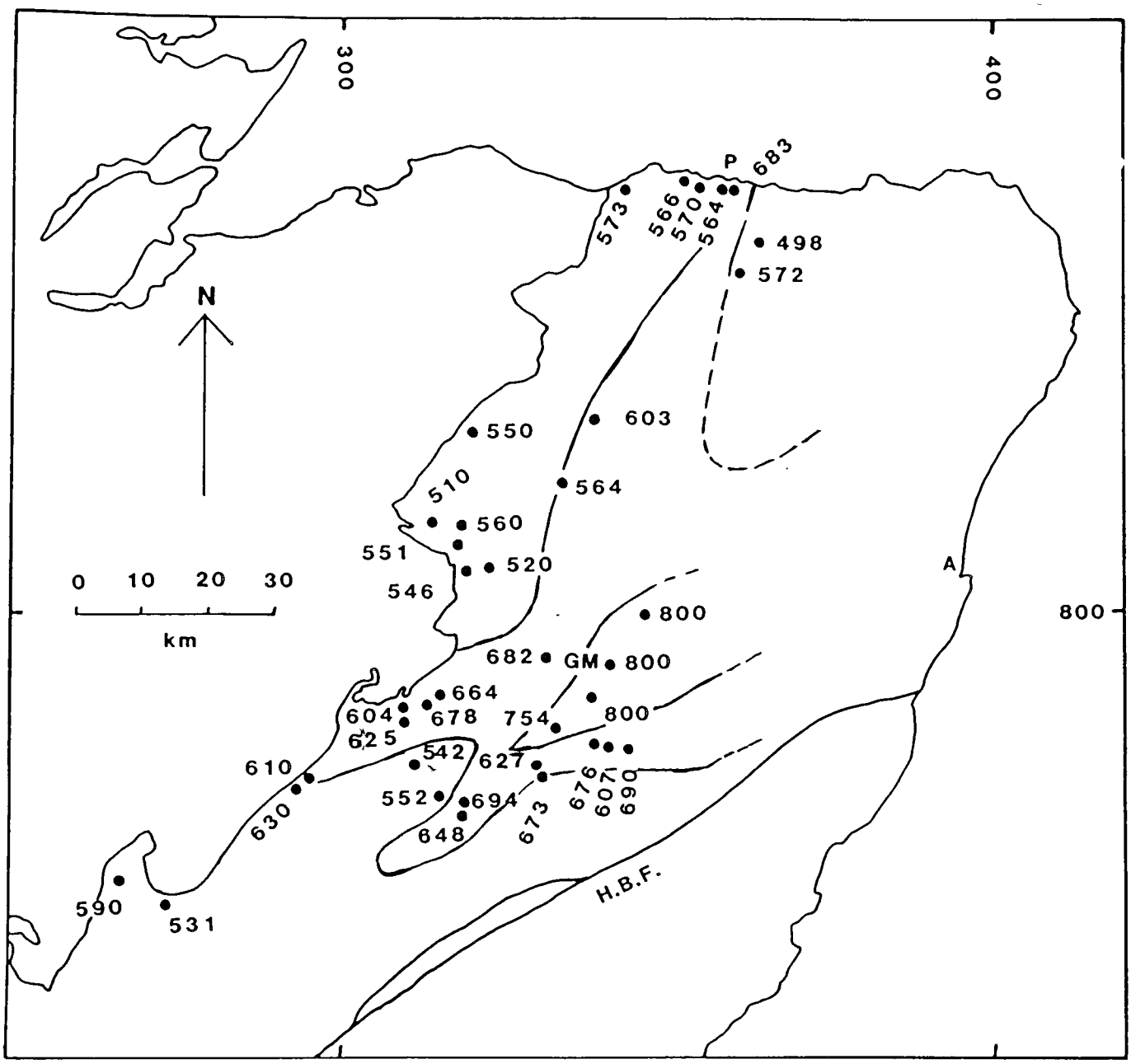

FIGURE 6.4

Sketch map of the eastern Dalradian showing estimated temperatures by garnet biotite thermometry (modified by Hodges and Spear (1982). Contoured at 600 °C and 700 °C.

FIGURE 6.5

Estimated pressures in the eastern part of the Dalradian.

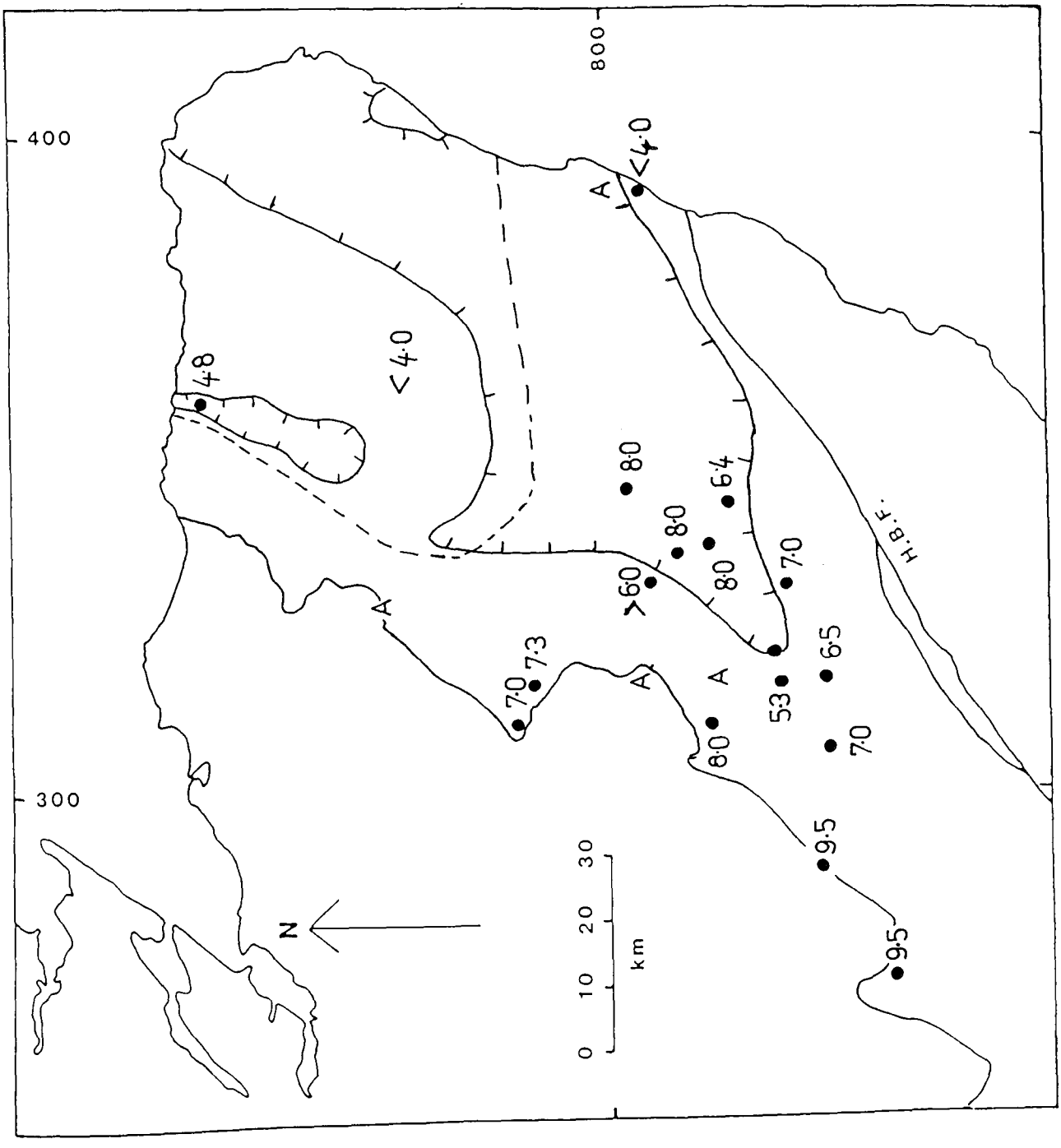

FIGURES 6.6 through 6.14

Plots of equilibria for various rocks in the aluminosilicate zones. Garnet biotite equilibria shown are both Ganguly and Saxena model (lower) and Hodges and Spear model (higher). (P in kb).

FIGURE 6.6

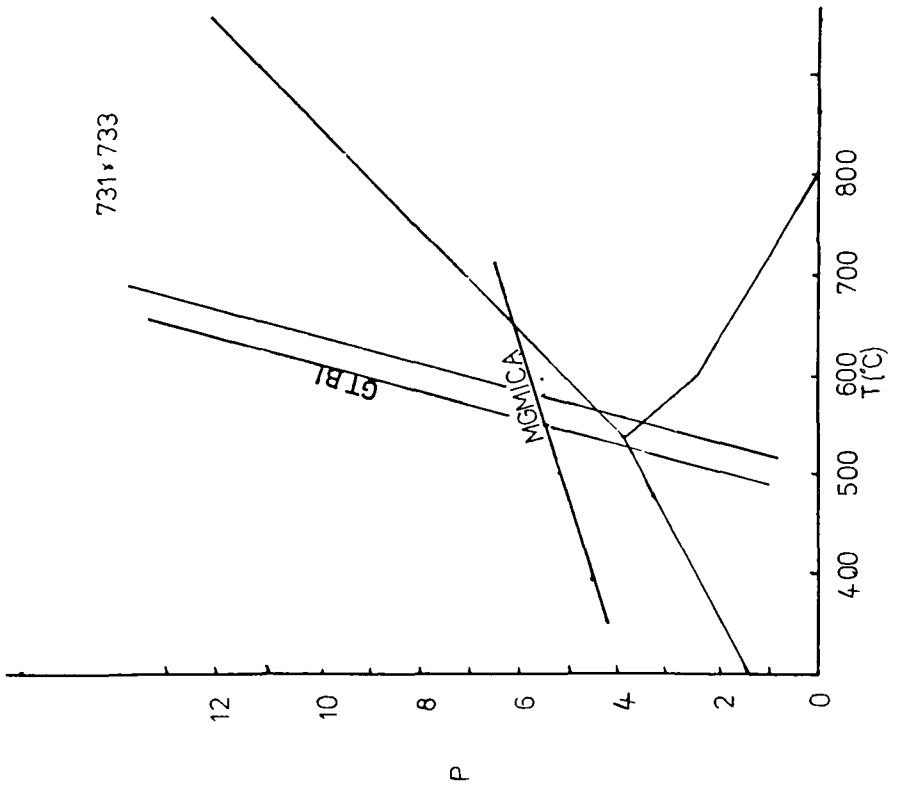

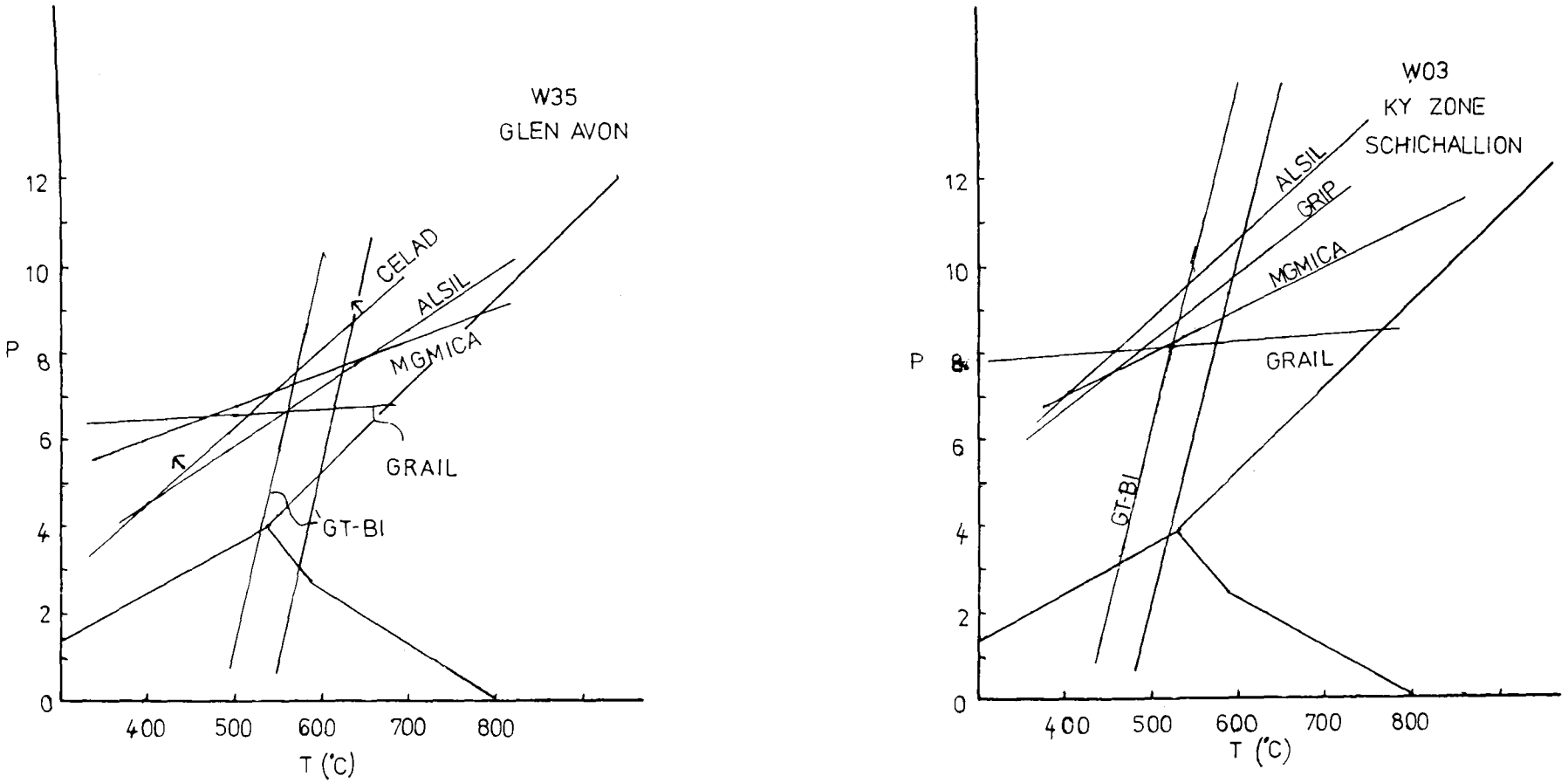
W35
GLEN AVON
CELAD
ALSIL
MGMICA
GRAIL
GT-BI
P
T (°C)
W03
KY ZONE
SCHICHALLION
ALSIL
GRIP
MGMICA
GRAIL
GT-BI
P
T (°C)

FIGURE 6.7

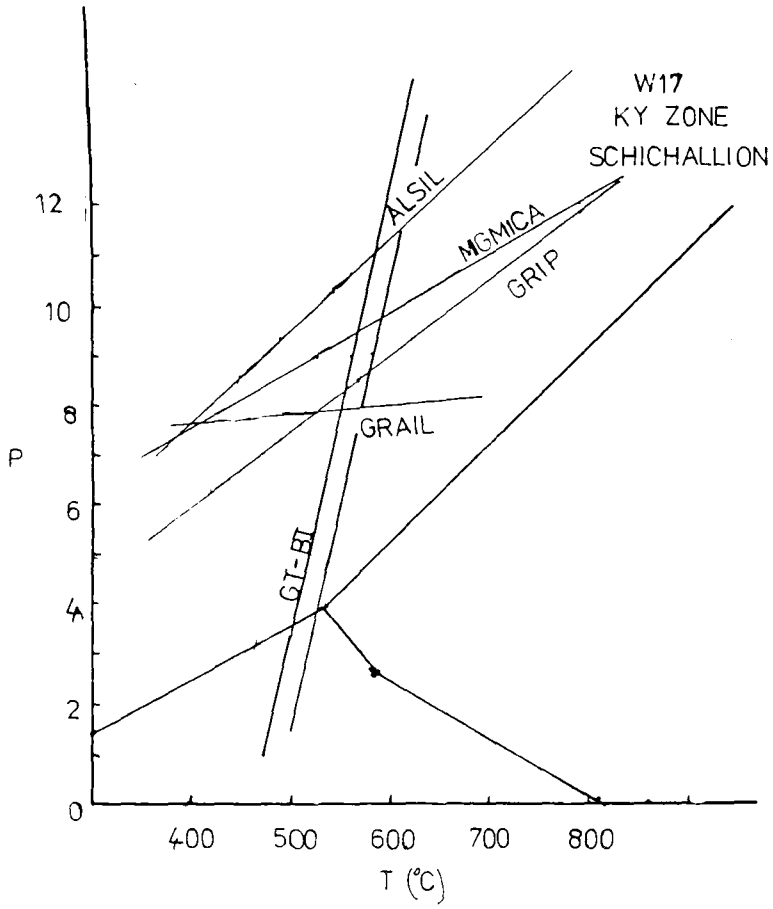
W17
KY ZONE
SCHICHALLION
ALSIL
MGMICA
GRIP
GRAIL
GT-BI
P
T (°C)
0
2
4
6
8
10
12
400
500
600
700
800

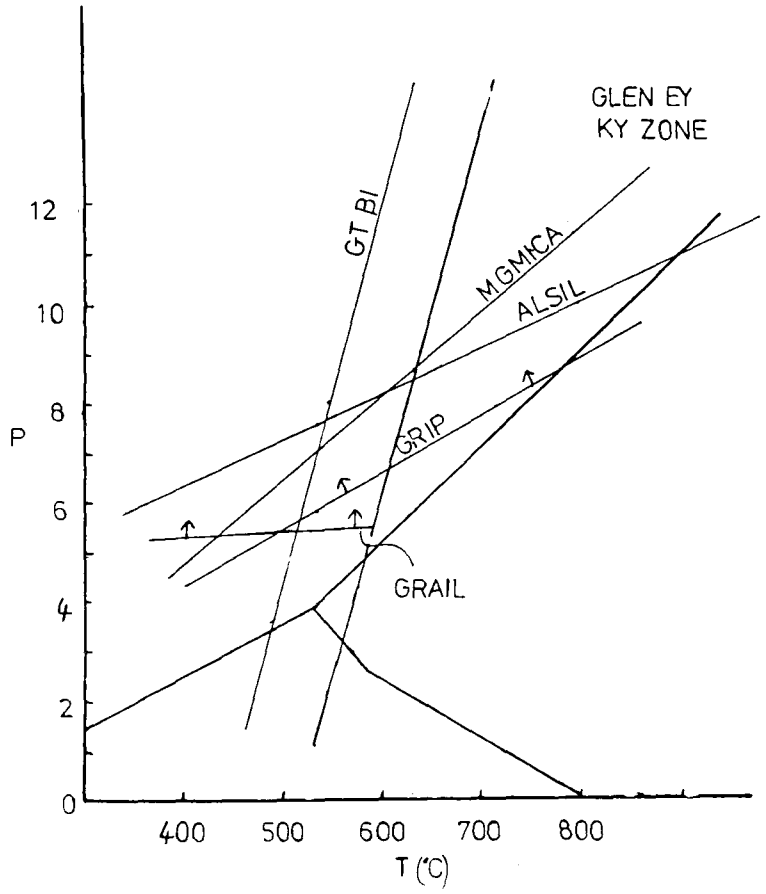
GLEN EY
KY ZONE
GT BI
MGMICA
ALSIL
GRIP
GRAIL
P
T (°C)
0
2
4
6
8
10
12
400
500
600
700
800

FIGURE 6.8

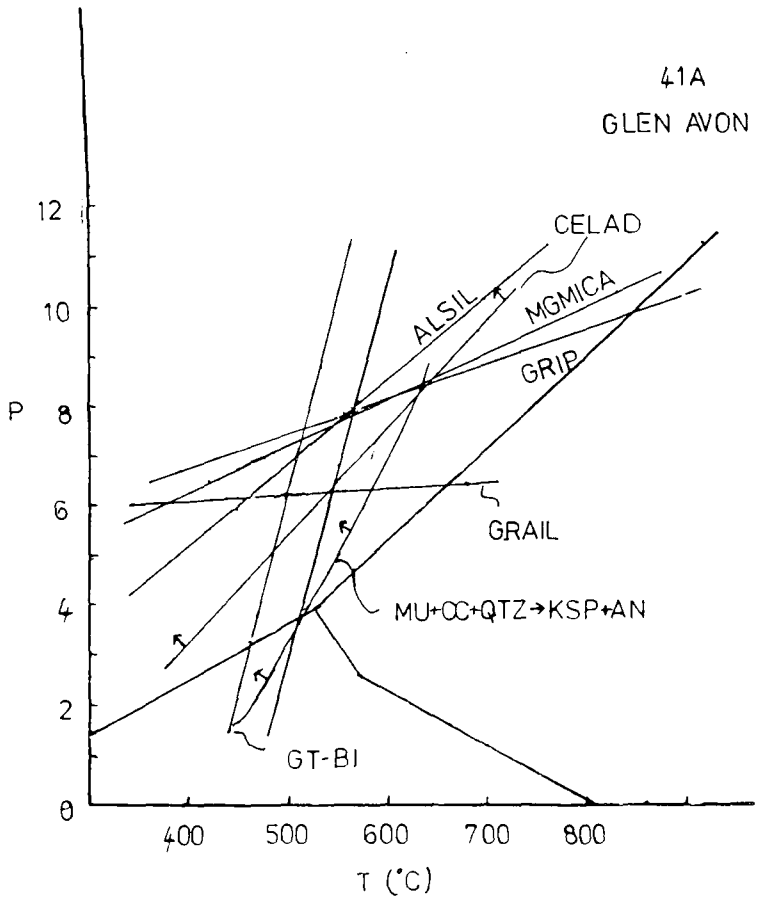
41A
GLEN AVON
CELAD
ALSIL
MGMICA
GRIP
GRAIL
MU+CC+QTZ→KSP+AN
GT-BI
P
T (°C)
0
2
4
6
8
10
12
400
500
600
700
800

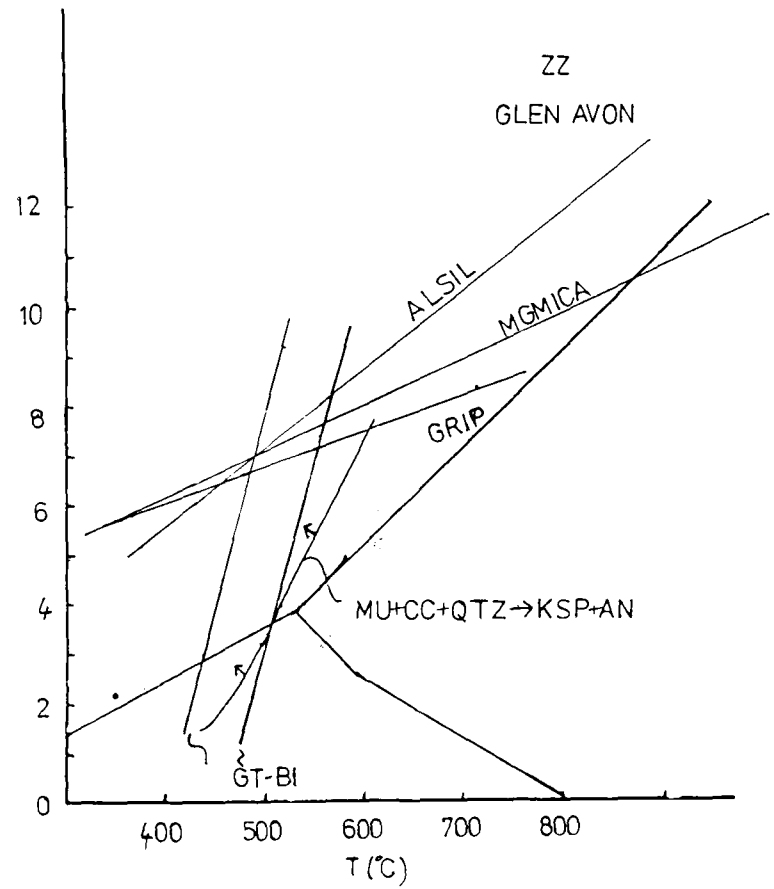
ZZ
GLEN AVON
ALSIL
MGMICA
GRIP
MU+CC+QTZ→KSP+AN
GT-BI
T (°C)
0
2
4
6
8
10
12
400
500
600
700
800

FIGURE 6.9

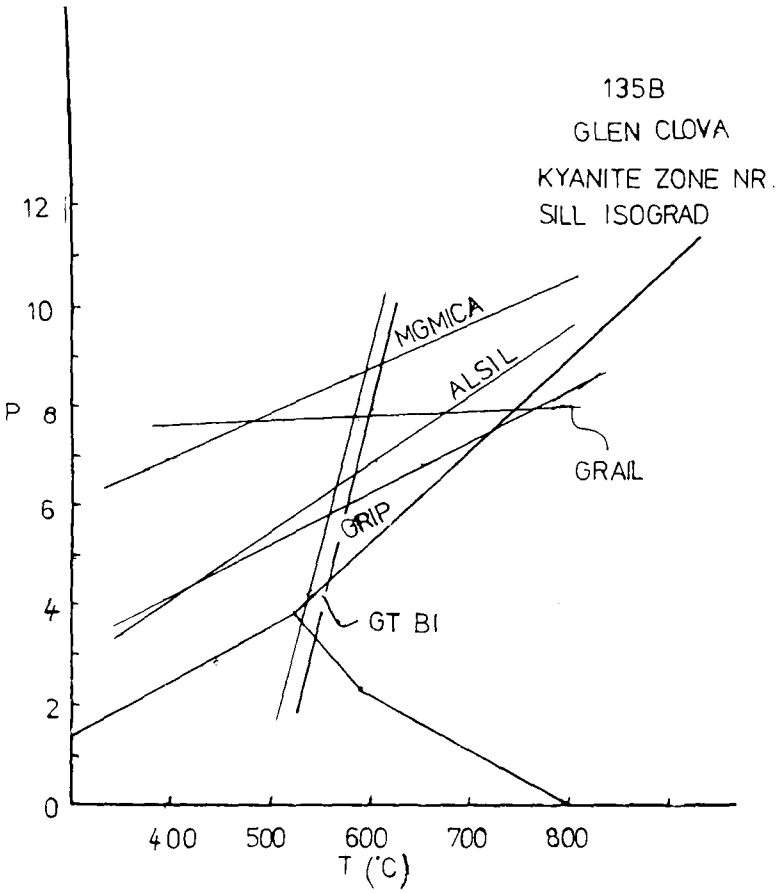
135B
GLEN CLOVA
KYANITE ZONE NR.
SILL ISOGRAD
MGMICA
ALSIL
GRAIL
GRIP
GT BI
P
T (°C)
0
2
4
6
8
10
12
400
500
600
700
800

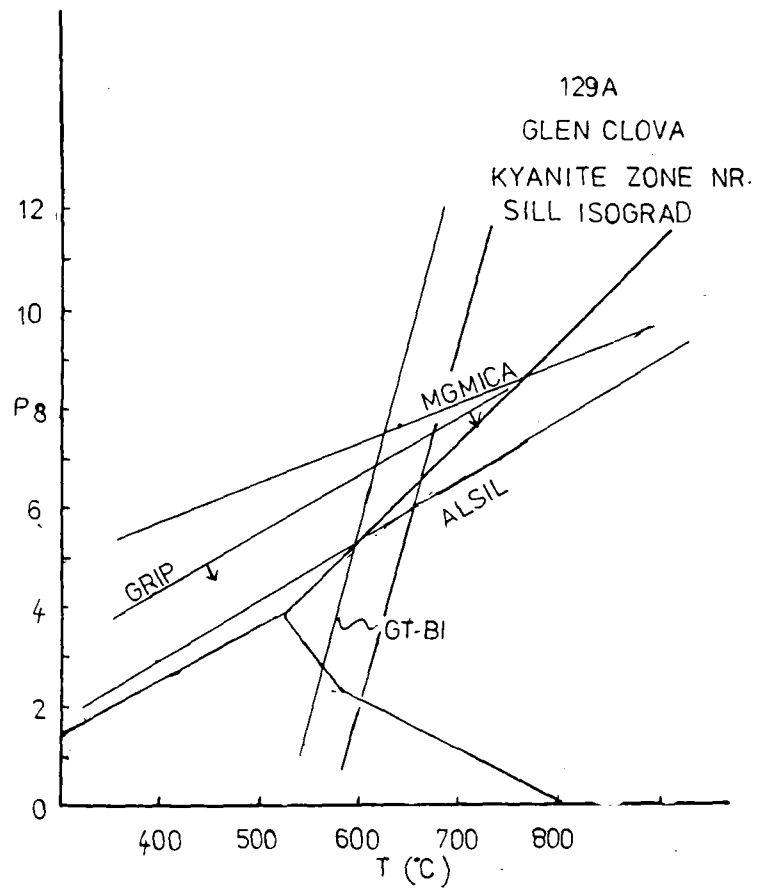
129A
GLEN CLOVA
KYANITE ZONE NR.
SILL ISOGRAD
MGMICA
ALSIL
GRIP
GT-BI
P
T (°C)
0
2
4
6
8
10
12
400
500
600
700
800

FIGURE 6.10

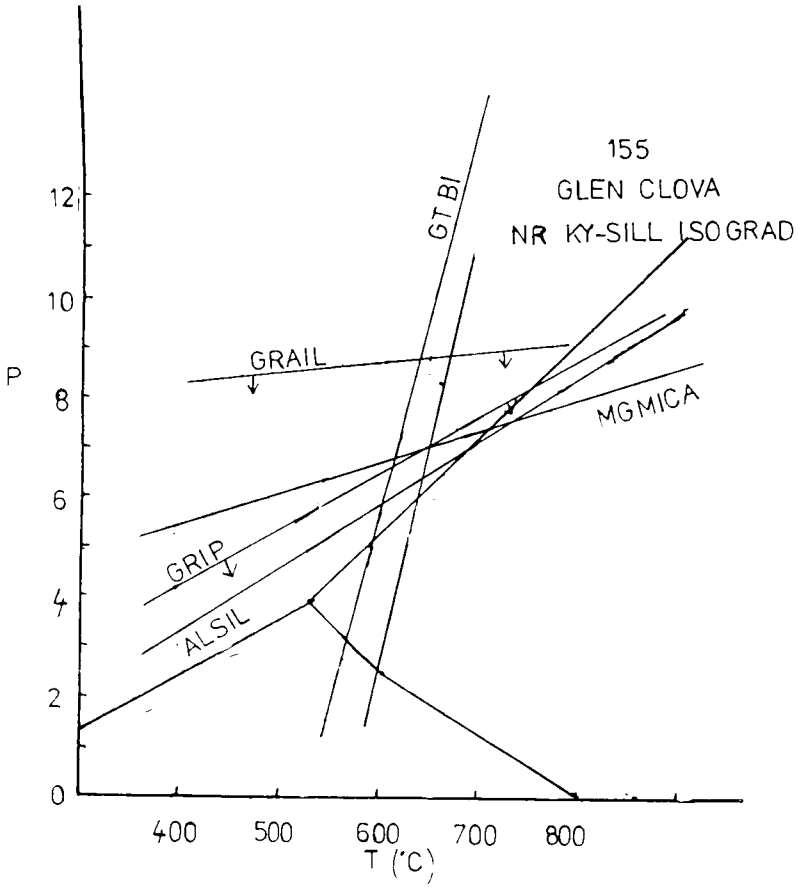
155
GLEN CLOVA
NR KY-SILL ISOGRAD
GT BI
GRAIL
MGMICA
GRIP
ALSIL
P
T (°C)
0
2
4
6
8
10
12
400
500
600
700
800

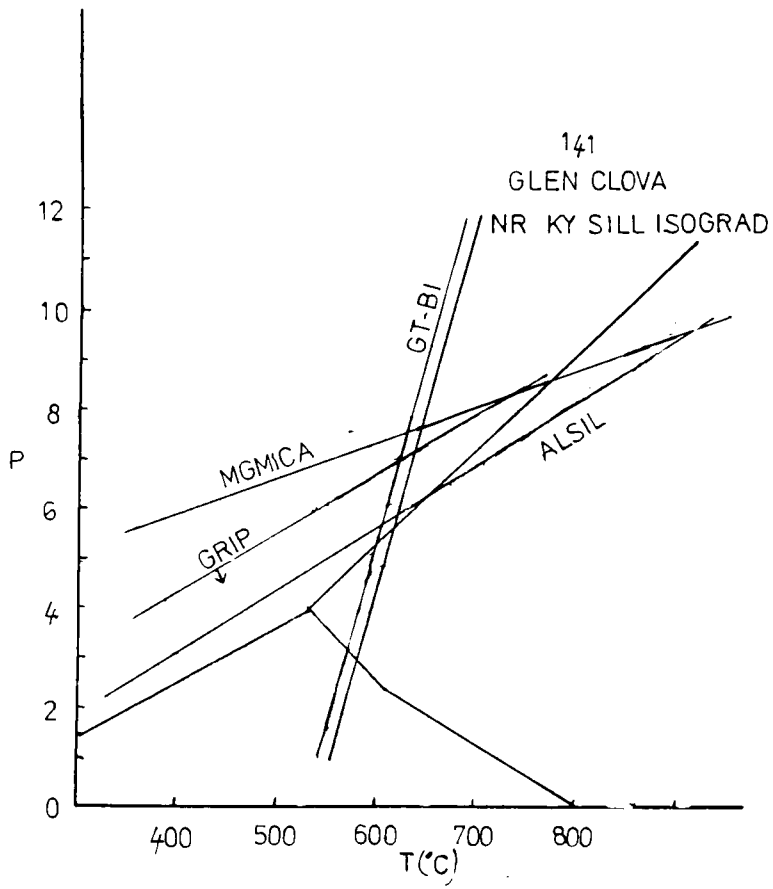
141
GLEN CLOVA
NR KY SILL ISOGRAD
GT-BI
MGMICA
GRIP
ALSIL
P
T(°C)
0
2
4
6
8
10
12
400
500
600
700
800

FIGURE 6.11

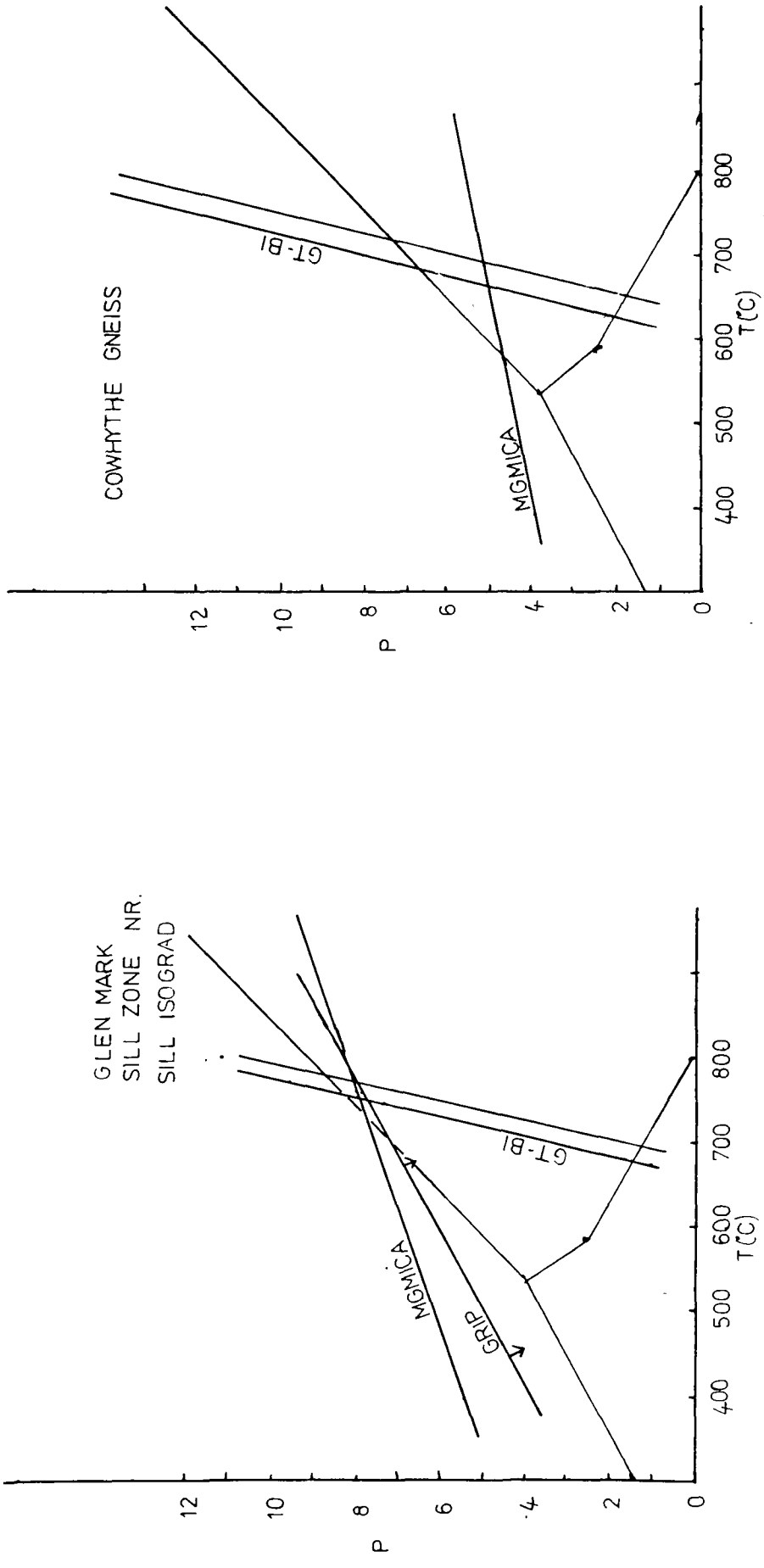
COWHYTHE GNEISS
GT-BI
MGMICA
P
T(°C)
0
2
4
6
8
10
12
400
500
600
700
800
GLEN MARK
SILL ZONE NR.
SILL ISOGRAD
GT-BI
MGMICA
GRIP
P
T(°C)

FIGURE 6.12

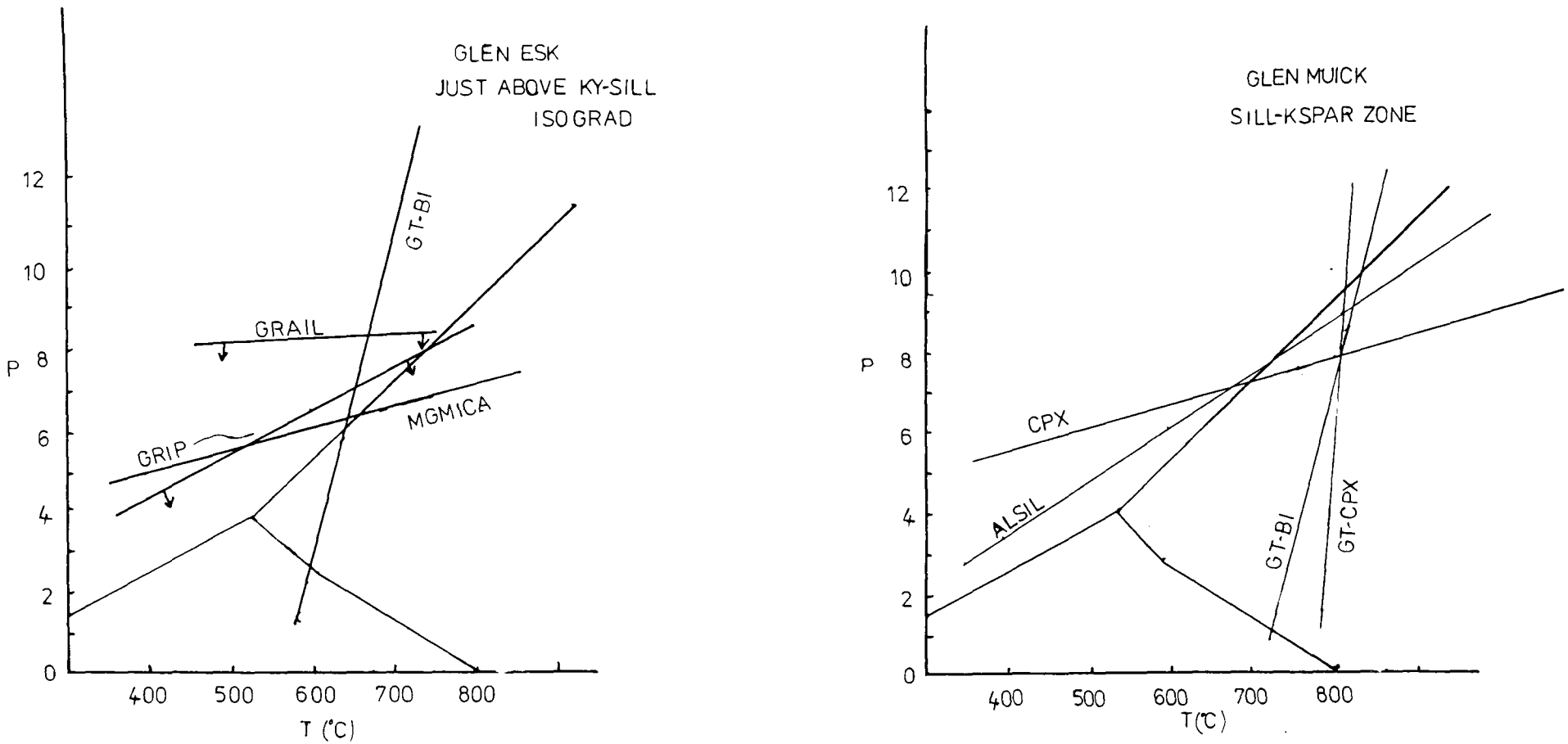
GLEN ESK
JUST ABOVE KY-SILL
ISOGRAD
GT-BI
GRAIL
GRIP
MGMICA
P
T (°C)
GLEN MUICK
SILL-KSPAR ZONE
CPX
ALSIL
GT-BI
GT-CPX
P
T(°C)

FIGURE 6.13

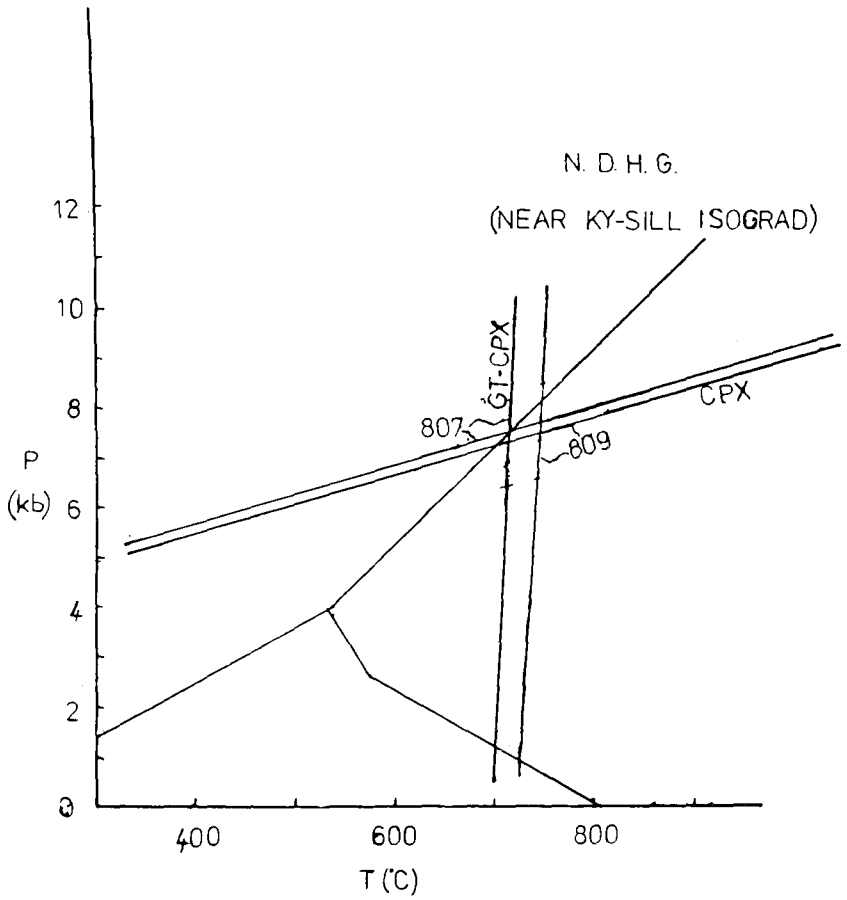
N. D. H. G.
(NEAR KY-SILL ISOGRAD)
GT-CPX
CPX
807
809
P
(kb)
T (°C)
0
2
4
6
8
10
12
400
600
800

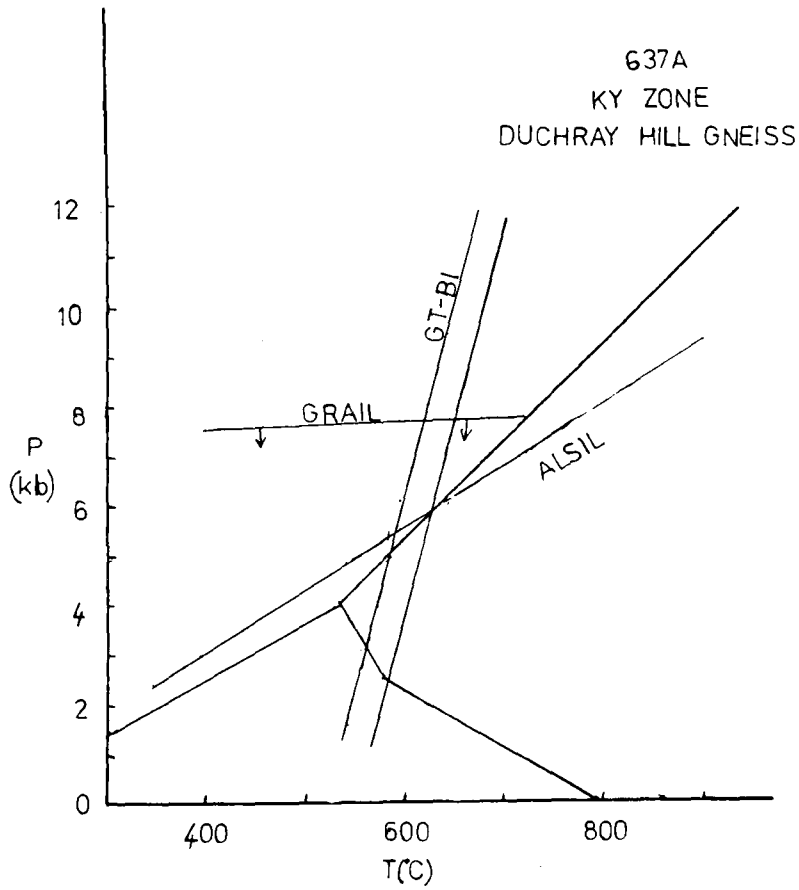
637A
KY ZONE
DUCHRAY HILL GNEISS
GT-BI
GRAIL
ALSIL
P
(kb)
T(°C)
0
2
4
6
8
10
12
400
600
800

FIGURE 6.14

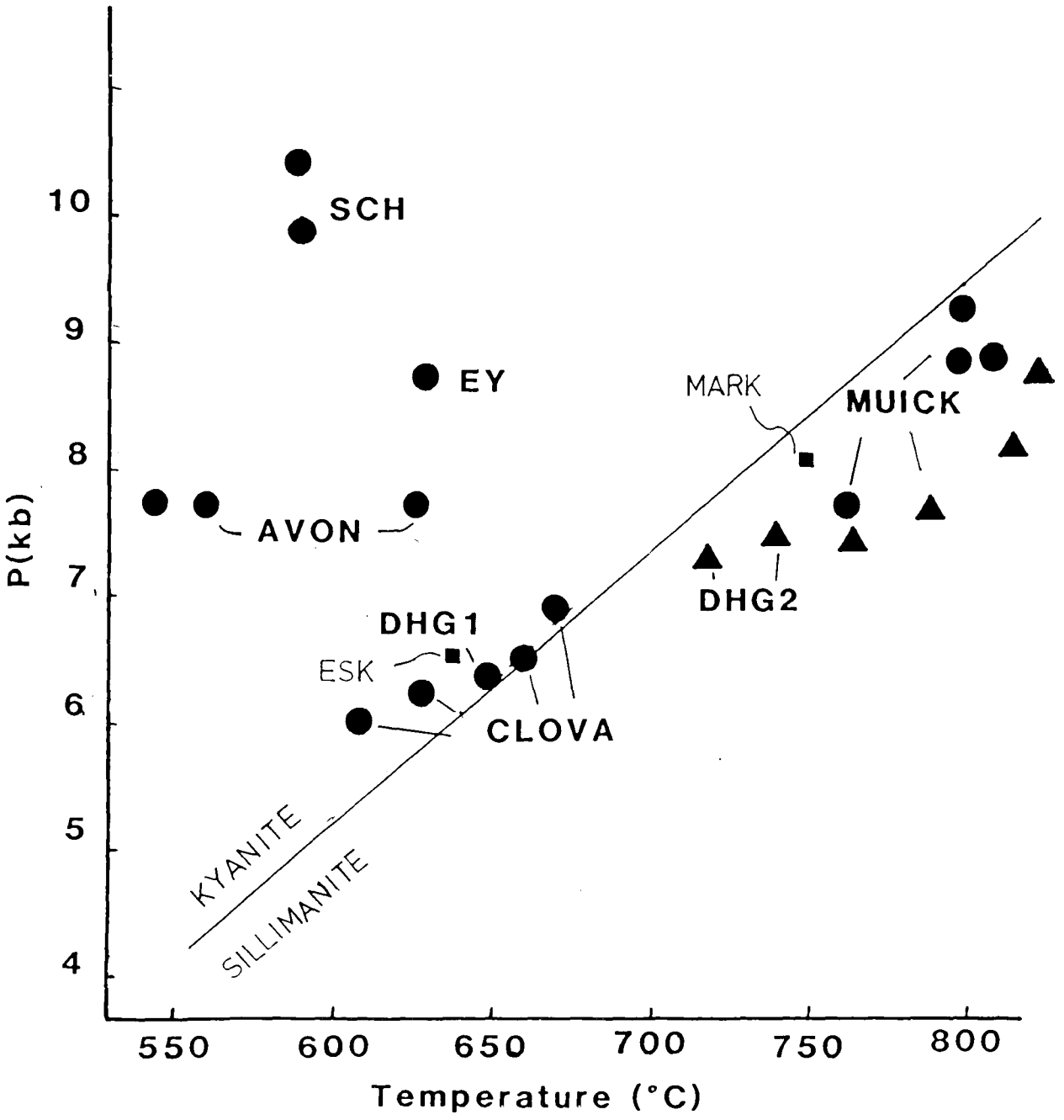

FIGURE 6.15

Estimated pressures and temperatures compared to the kyanite sillimanite equilibrium after Robie and Hemingway (1984). Circles : ALSIL, triangles : CPX, and squares MGMICA.

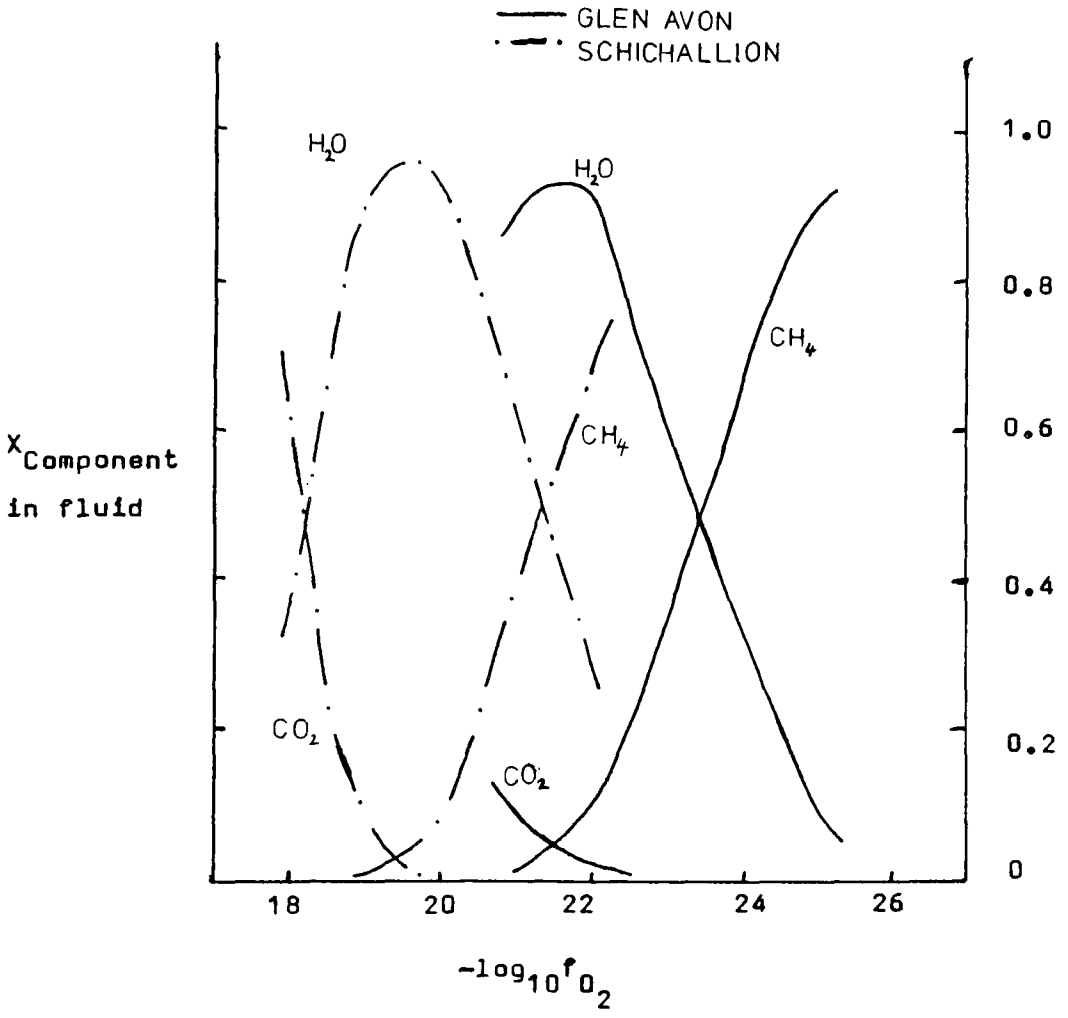

FIGURE 6.16

Composition of fluids in equilibrium with graphite as a function of log f_{O_2} for rocks in the Glen Avon area (550°C and 7kb) and in the Schichallion area (600°C and 10kb).

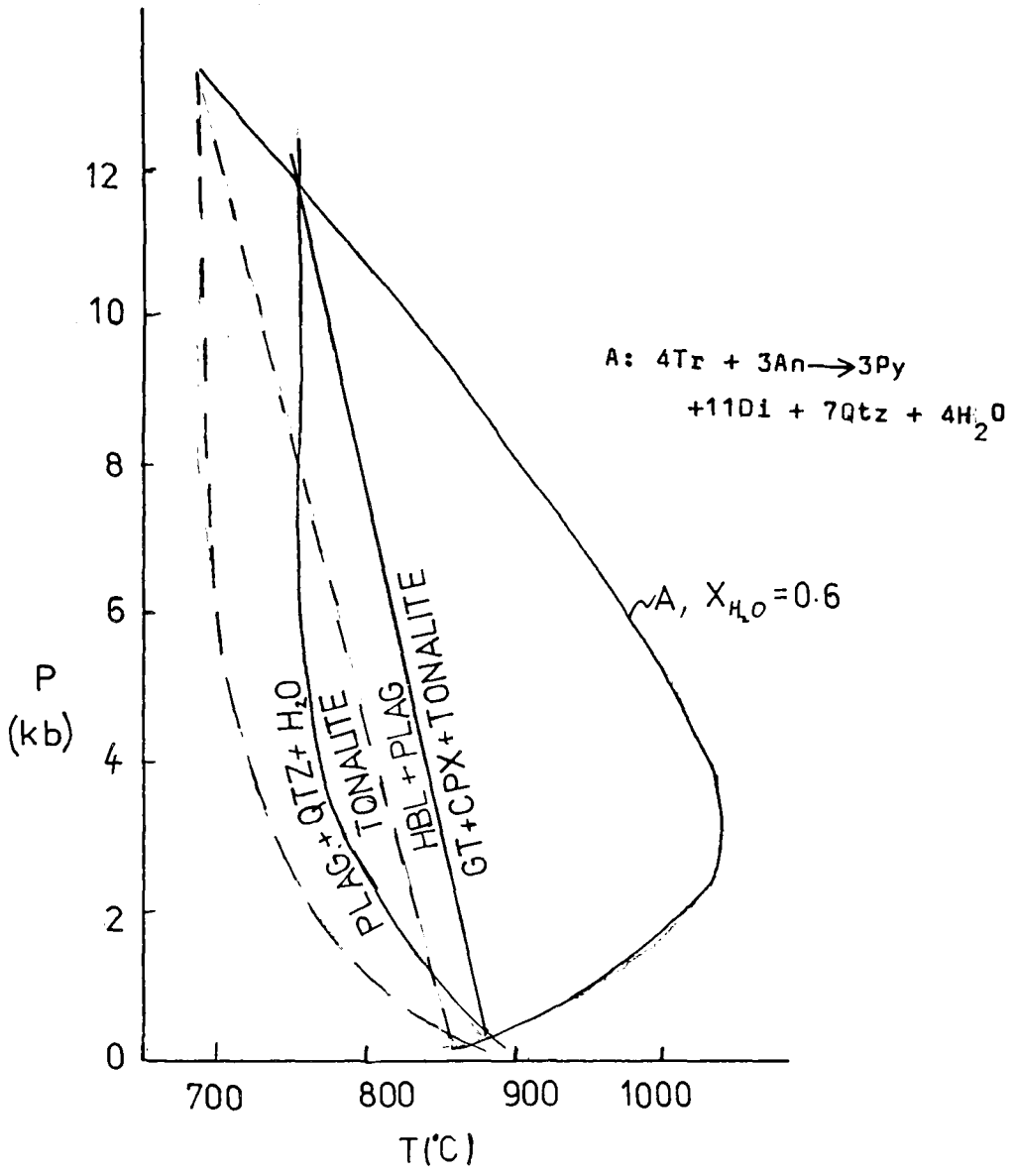

FIGURE 6.17

Melting reactions for rock CL2. Dotted lines are :
Plag + Qtz + H_2O → Tonalite for X_{H_2O}=1 and Hbl + Plag →
Gt + Cpx + Tonalite assuming reaction A is for X_{H_2O}=1

FIGURE 7.1

Map of the eastern Dalradian, showing locations mentioned in the text.

A: Aberdeen

AV: Glen Avon

B: Braemar

BS: Boyndie Syncline

C: Glen Clova

CR: Cromar

D: Deeside

D.H.G.: Duchray Hill Gneiss

E: Glen Esk

EY: Glen Ey

H.B.F.: Highland Boundary Fault

HP: Huntly Portsoy Newer Gabbro

IH: Inzie Head Gneisses

MC: Morven Cabrach Newer Gabbro

P: Portsoy

S: Glen Shee

WA: Water of Ailnack

GM: Glen Muick

GG: Glen Girnock

FIGURE 7.1

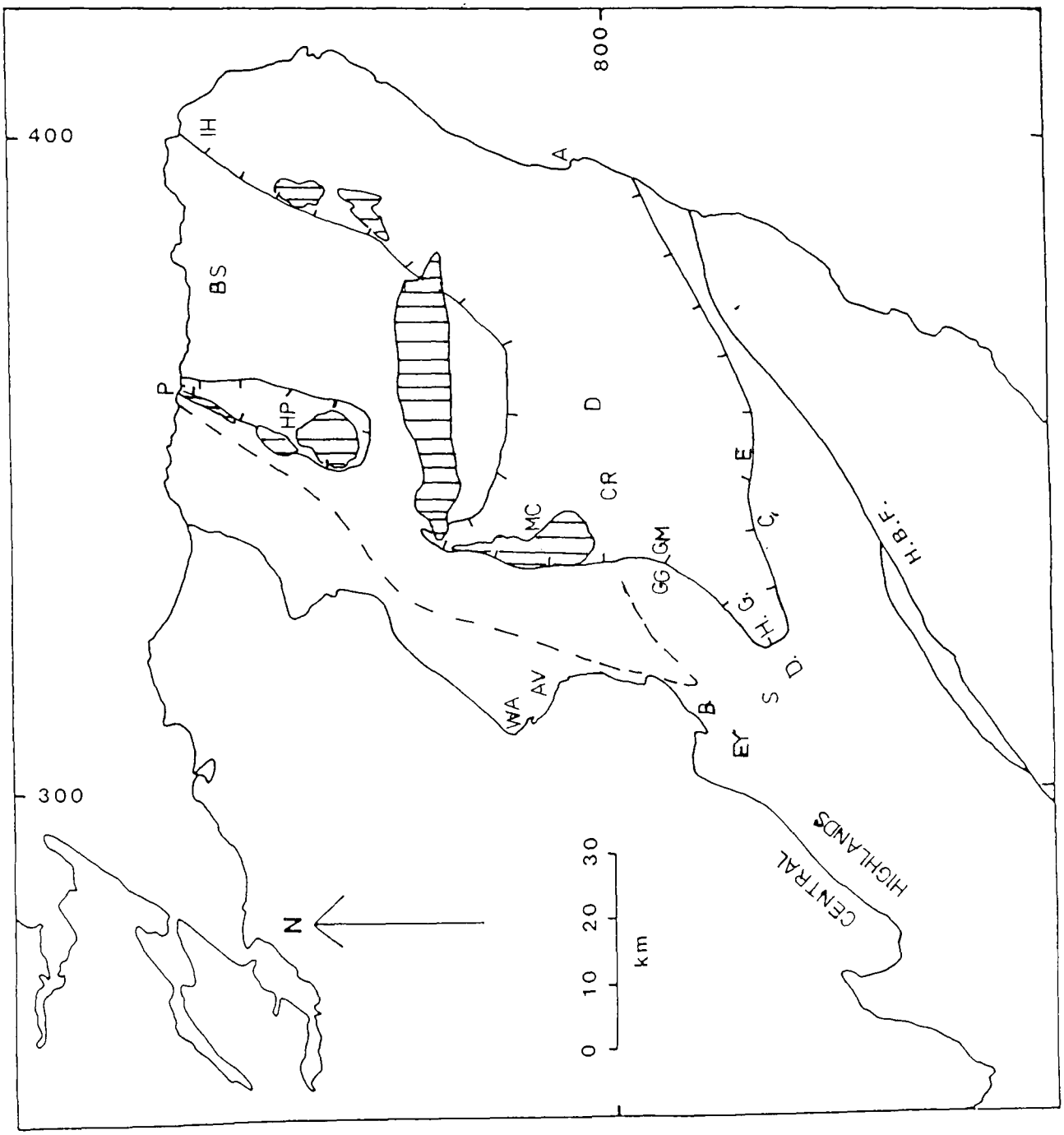
800
400
300
IH
A
BS
P
HP
D
CR
MC
E
G
GM
GG
H.B.F.
H.
G.
S.
D.
B
EY
AV
WA
CENTRAL
HIGHLANDS
N
0 10 20 30
km

FIGURE 7.2

Distribution of pressure and temperature in the eastern Dalradian. Dashed lines- isobars, dot-dash lines isotherms.

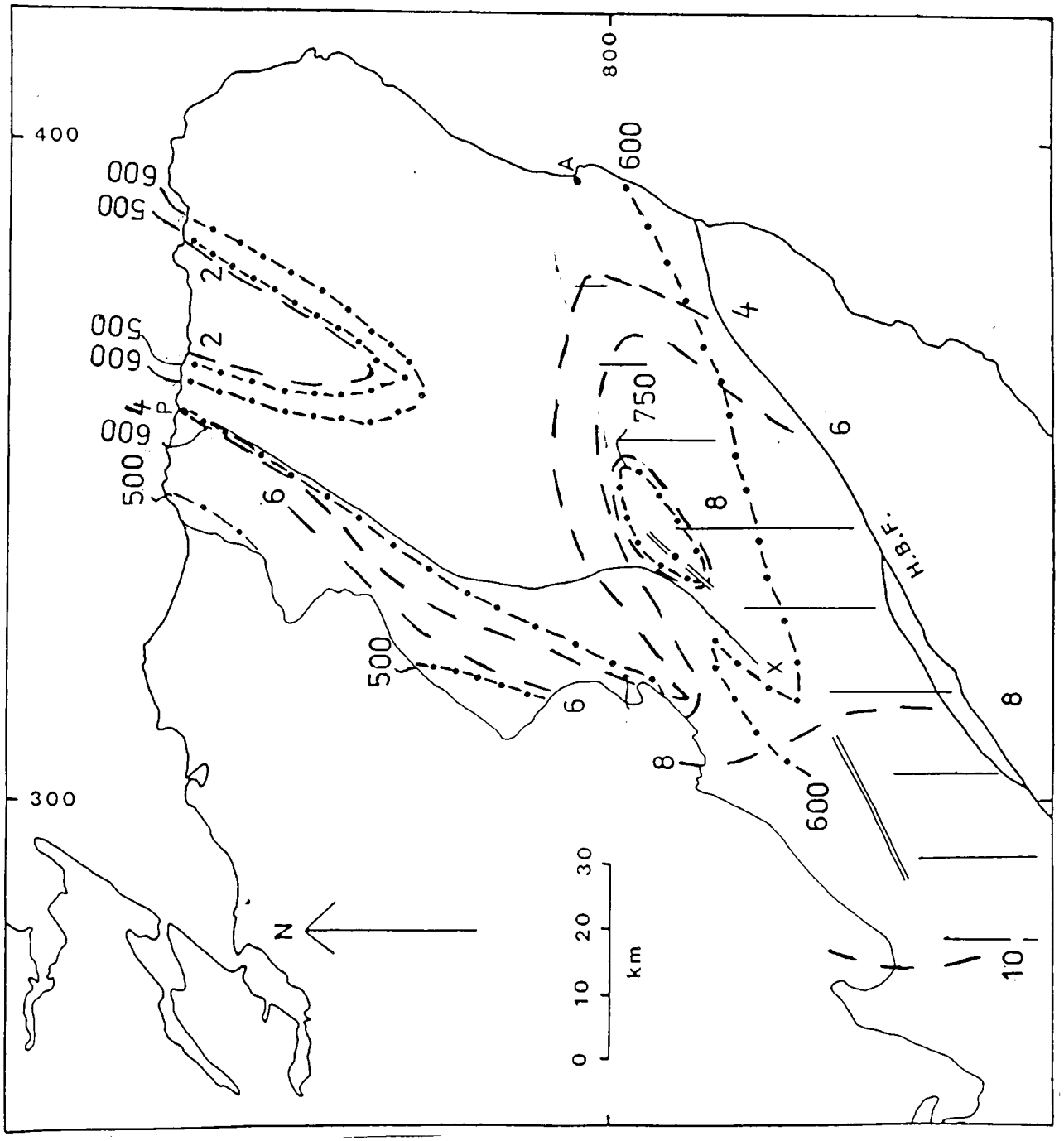

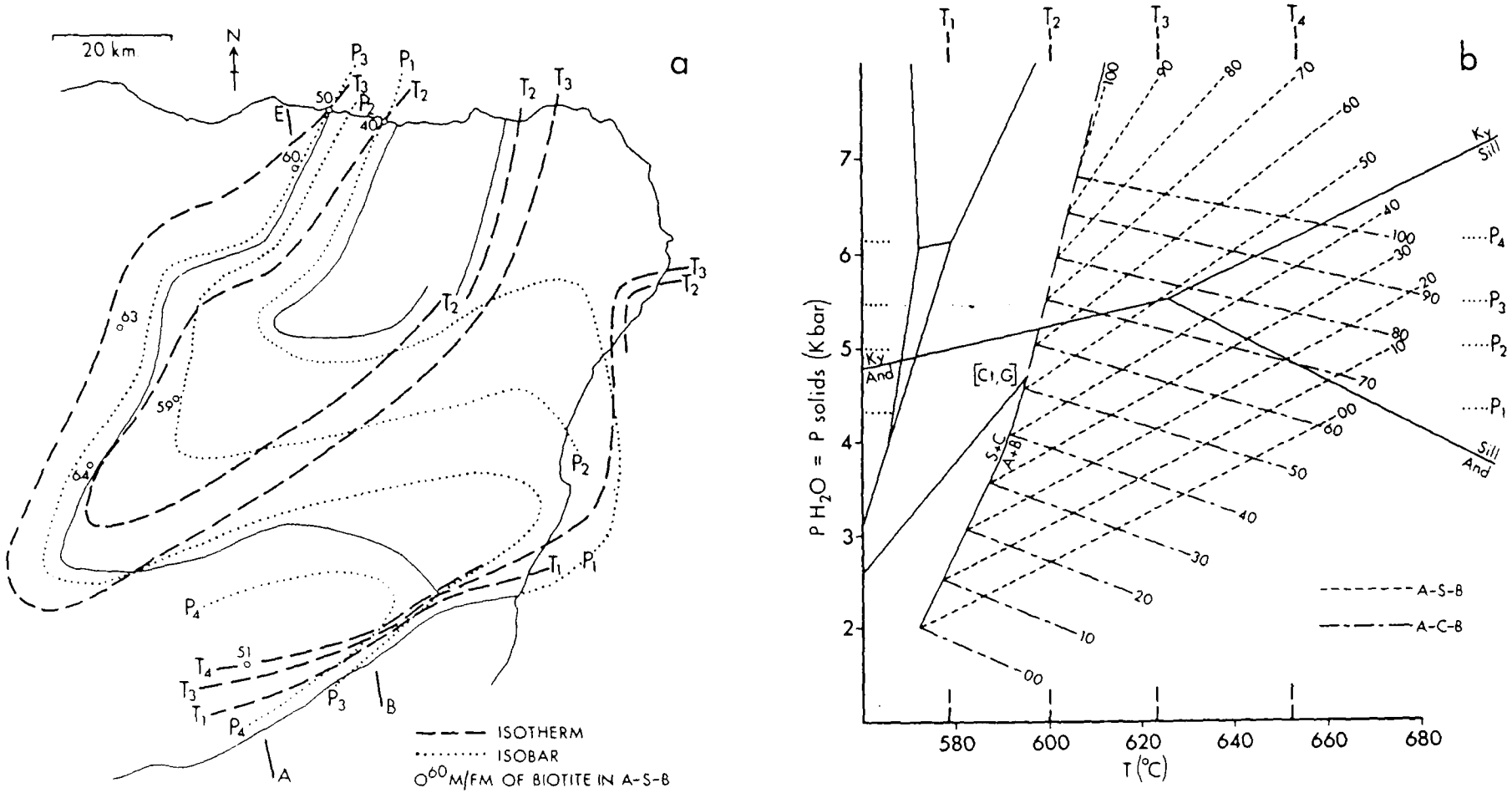

FIGURE 7.3

a. Synthesis of pressure and temperature in the Eastern Dalradian.

b. Isopleths of M/FM of biotite in AFM assemblages alsilicate-staurolite-(cordierite)-biotite, used in construction of a.

Both from Harte and Hudson (1979).

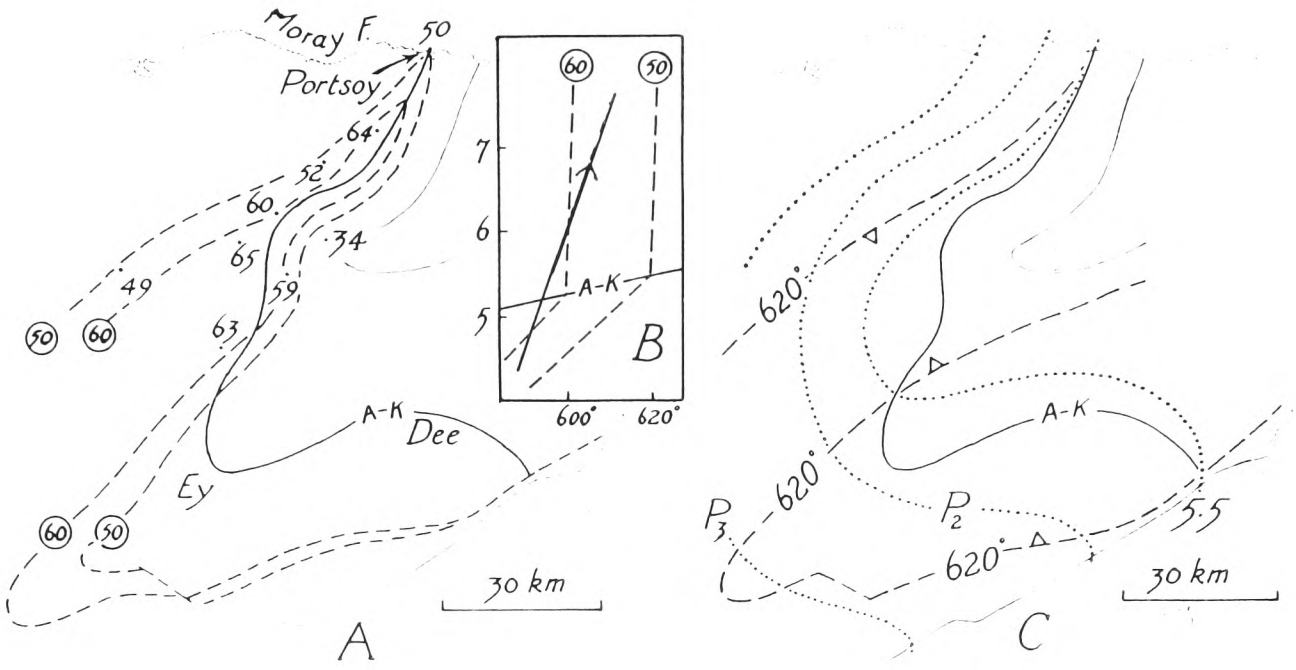

FIGURE 7.4

Distribution of temperature and pressure in the E. Dalradian following Chinner (1980).

A M/FM of biotite in the AFM assemblage alsilicate-staurolite-biotite.

B Refraction of isopleths of M/FM of biotite in this assemblage at the andalusite kyanite isograd. The arrowed line represents Chinner's proposed facies series from E to W through Portsoy.

C Distribution of pressure and temperature derived from calibration of the isopleths figured in A.

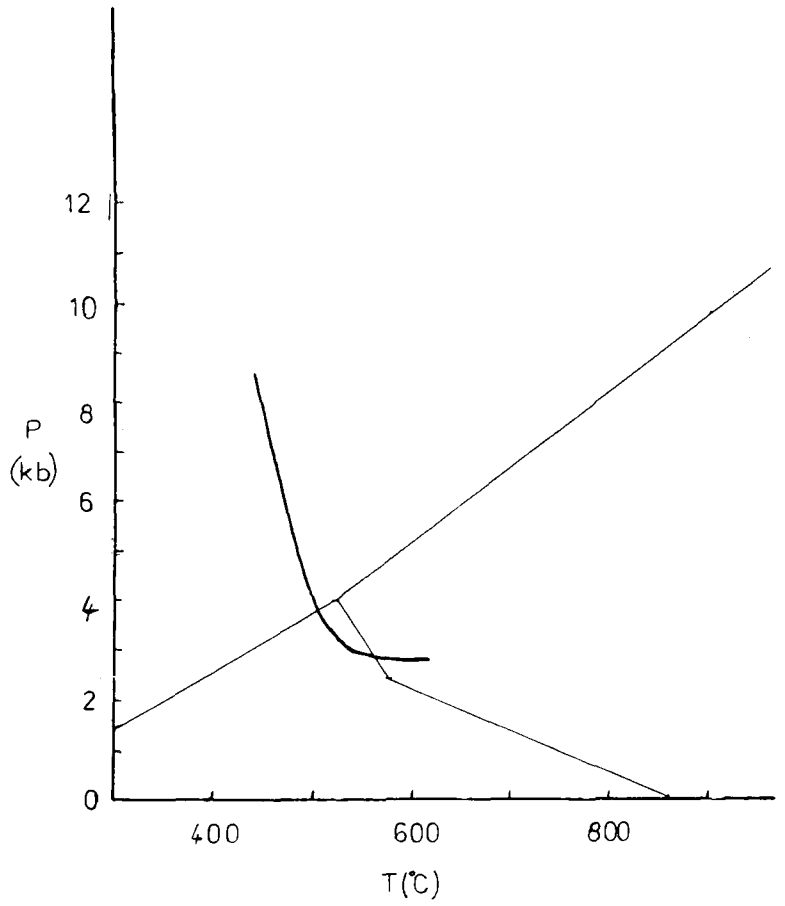

FIGURE 7.5

Preserved surface P-T trajectory along a transect E-W through Glen Avon (Glen Avon being at the high pressure end).

FIGURE 8.1

Plagioclase zoning profiles

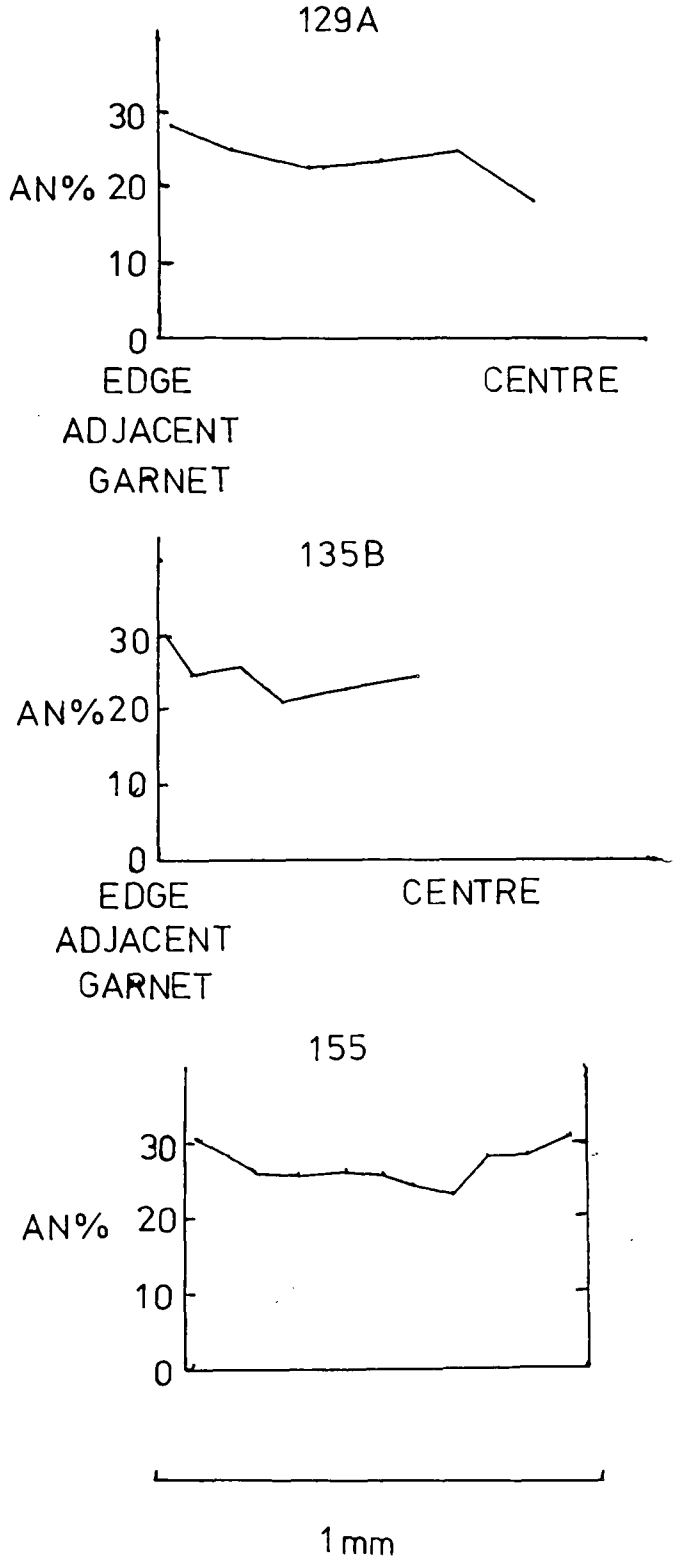

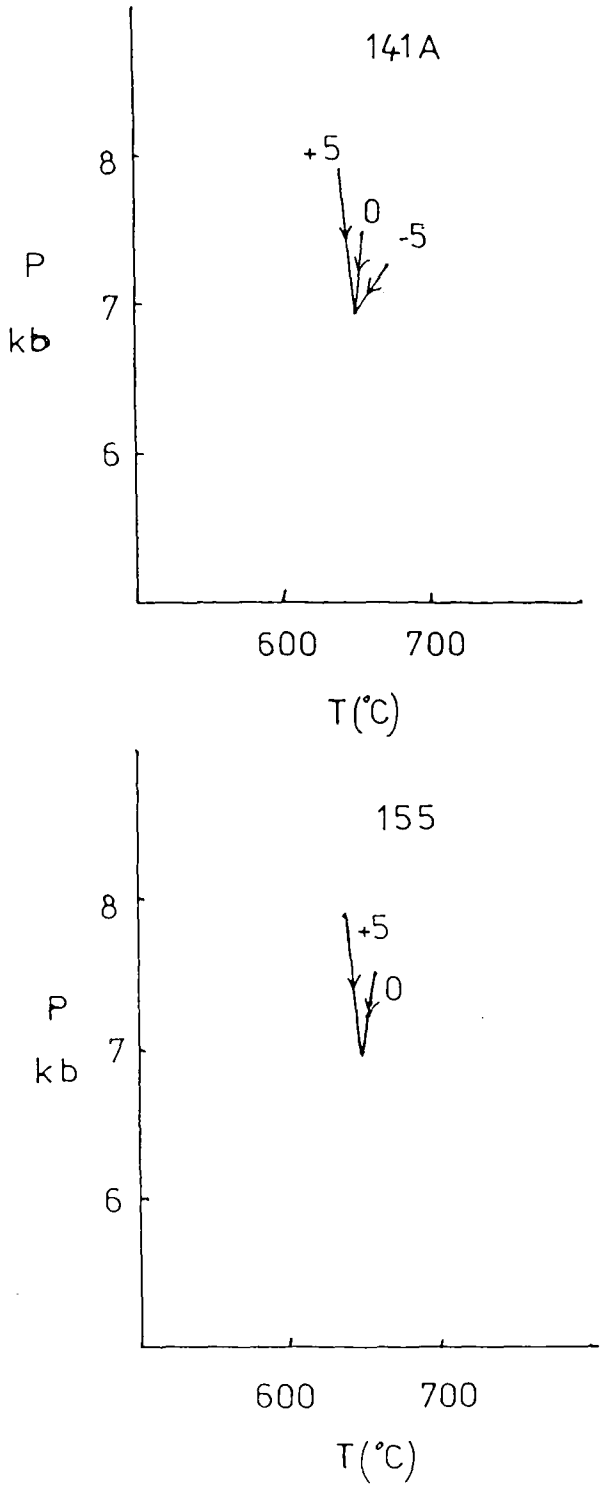

FIGURE 8.2 (a)

P-T paths, inferred from garnet zoning profiles for rocks from Glen Clova, near the kyanite-sillimanite isograd. Figures indicate the change in anorthite content of plagioclase from core to rim.

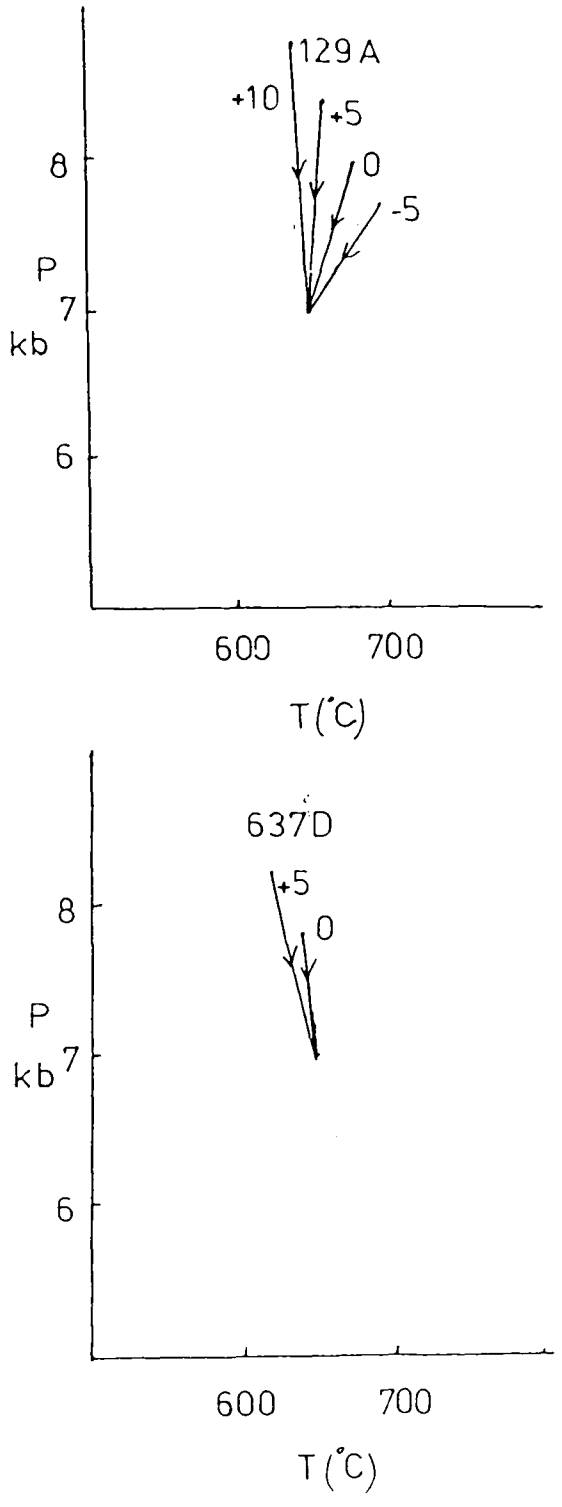

FIGURE 8.2 (b)

P-T paths, inferred from garnet zoning profiles for a rock from Glen Clova (129A) and from the Duchray Hill Gneiss (637D). Figures indicate the change in anorthite content of plagioclase from core to rim.

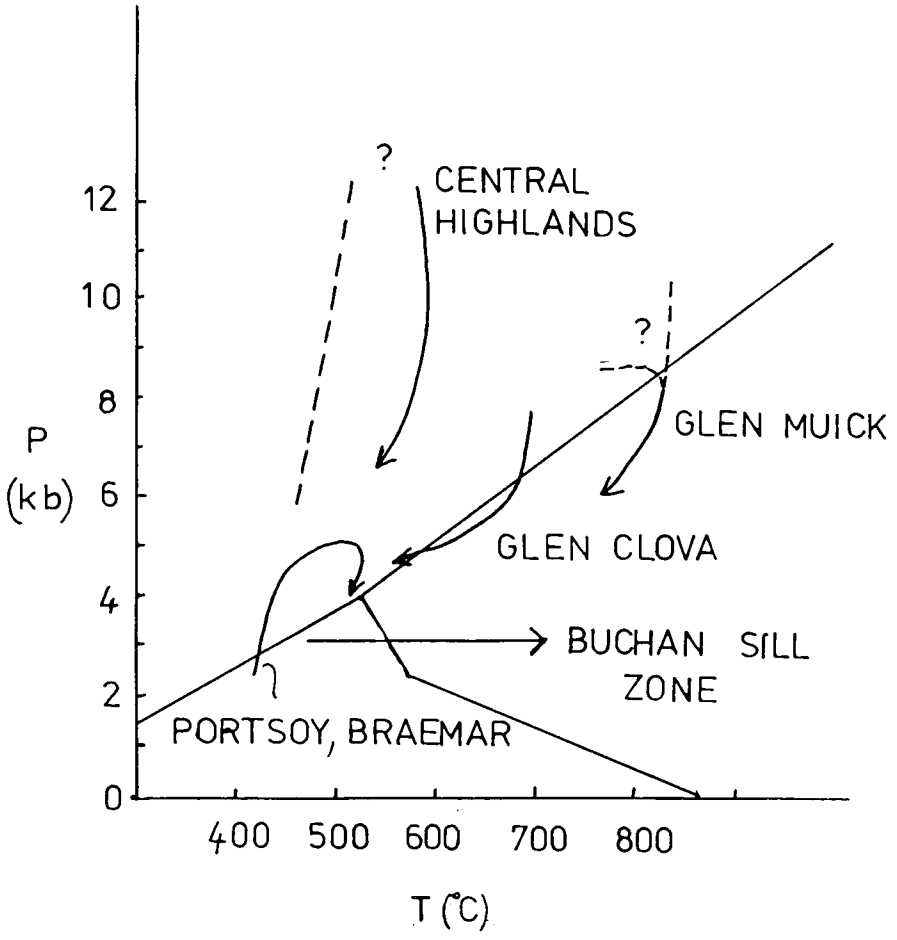

FIGURE 8.3

Proposed pressure-temperature paths, deduced for different parts of the Dalradian.

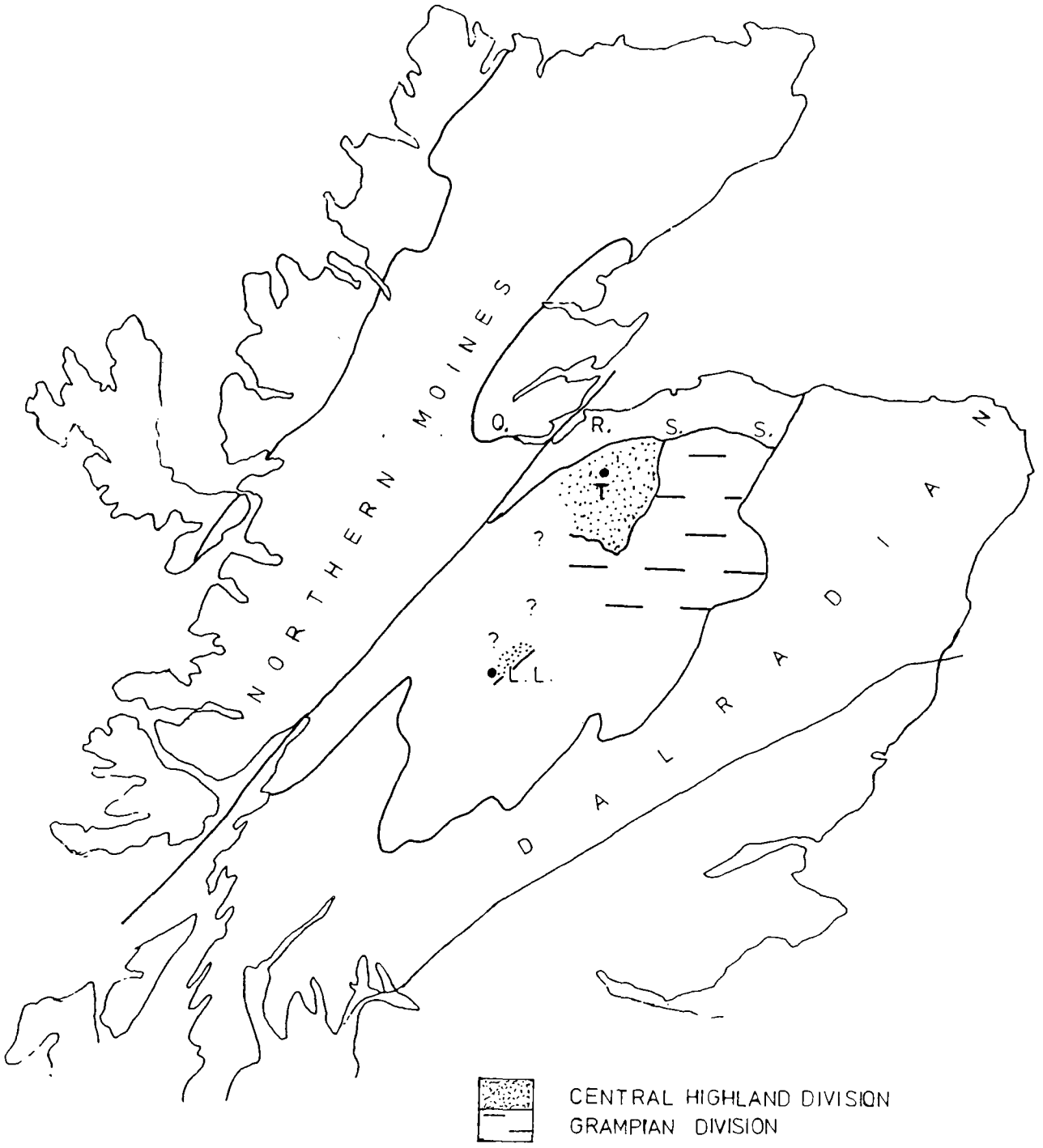

FIGURE 9.1

Sketch map of the Scottish Highlands showing the location of the Tomatin (T) and Loch Laggan (L.L.) metabasites.

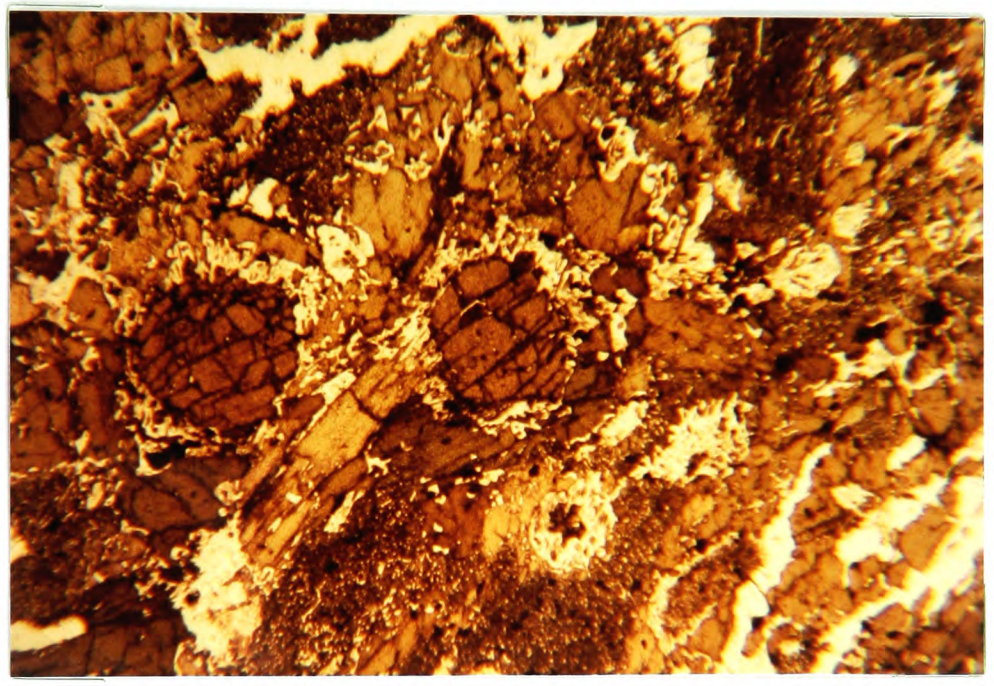

FIGURE 9.2

107B Resorbed garnets with plagioclase coronas and clinopyroxene-plagioclase symplectites. (x20)

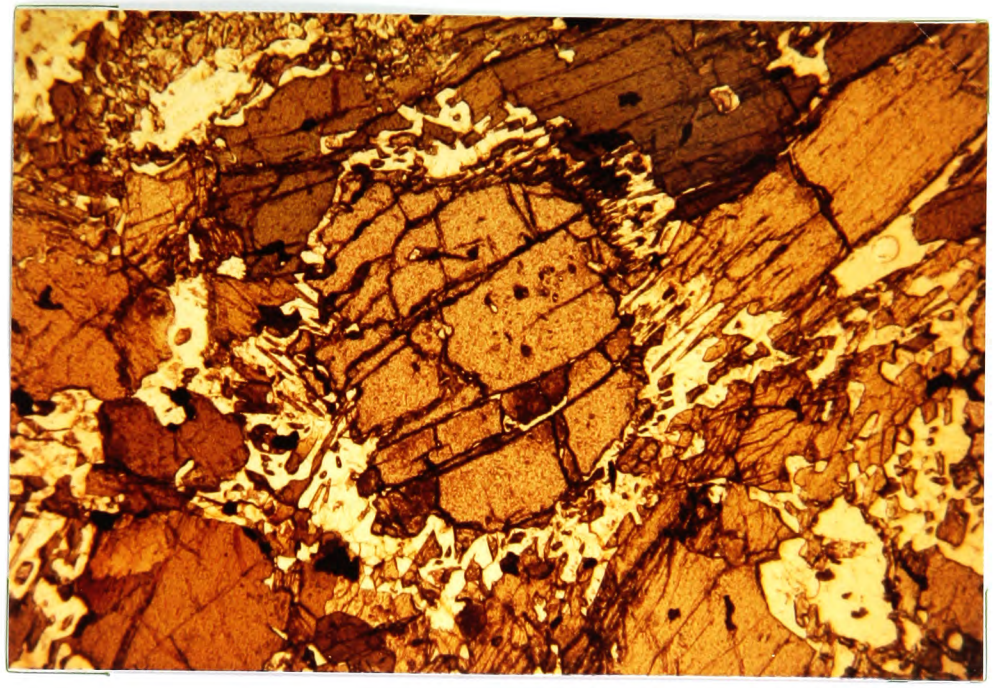

FIGURE 9.3 (a)

Retrogressed eclogite 107B. (x50).
Resorbed garnet surrounded by a plagioclase corona.

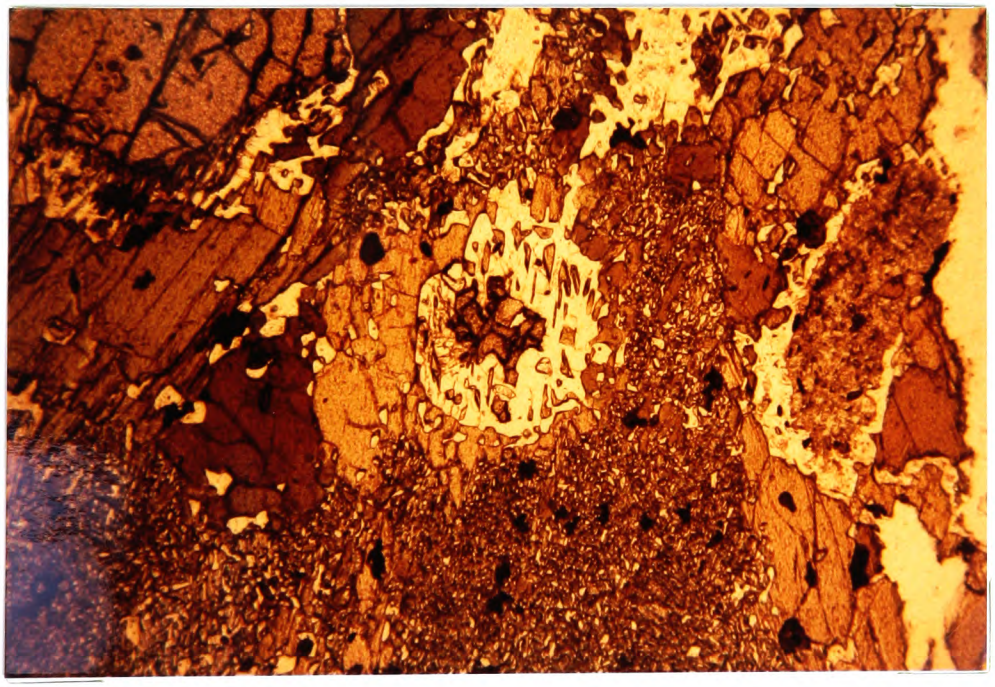

FIGURE 9.3 (b)

Garnet corona separated from symplectite by a reaction rim of hornblende. 107B (x50).

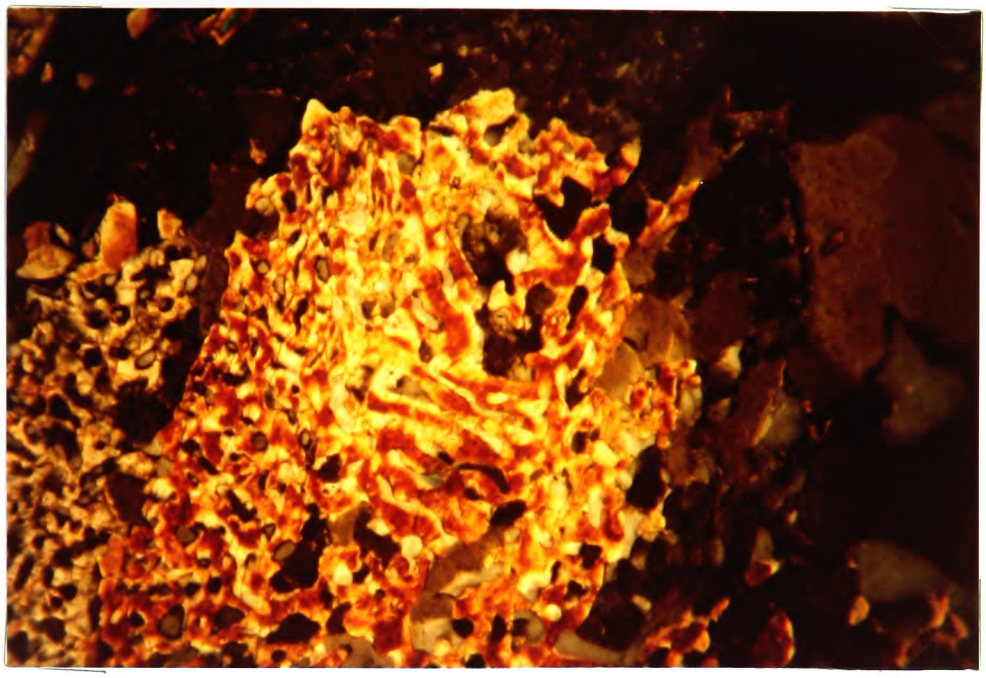

FIGURE 9.4(a)

107B (x200) Plagioclase-clinopyroxene symplectite, being replaced by hornblende.

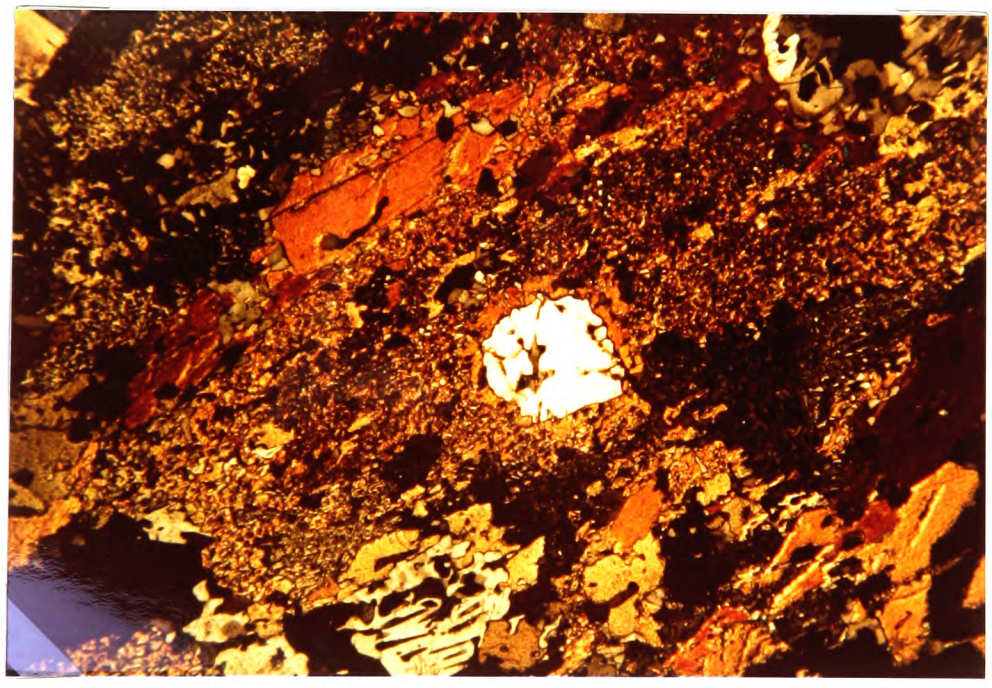

FIGURE 9.4 (b)

107B (x50). Area of symplectite. Qtz surrounded by a reaction rim of hornblende. Large hornblendes growing on margin of symplectite.

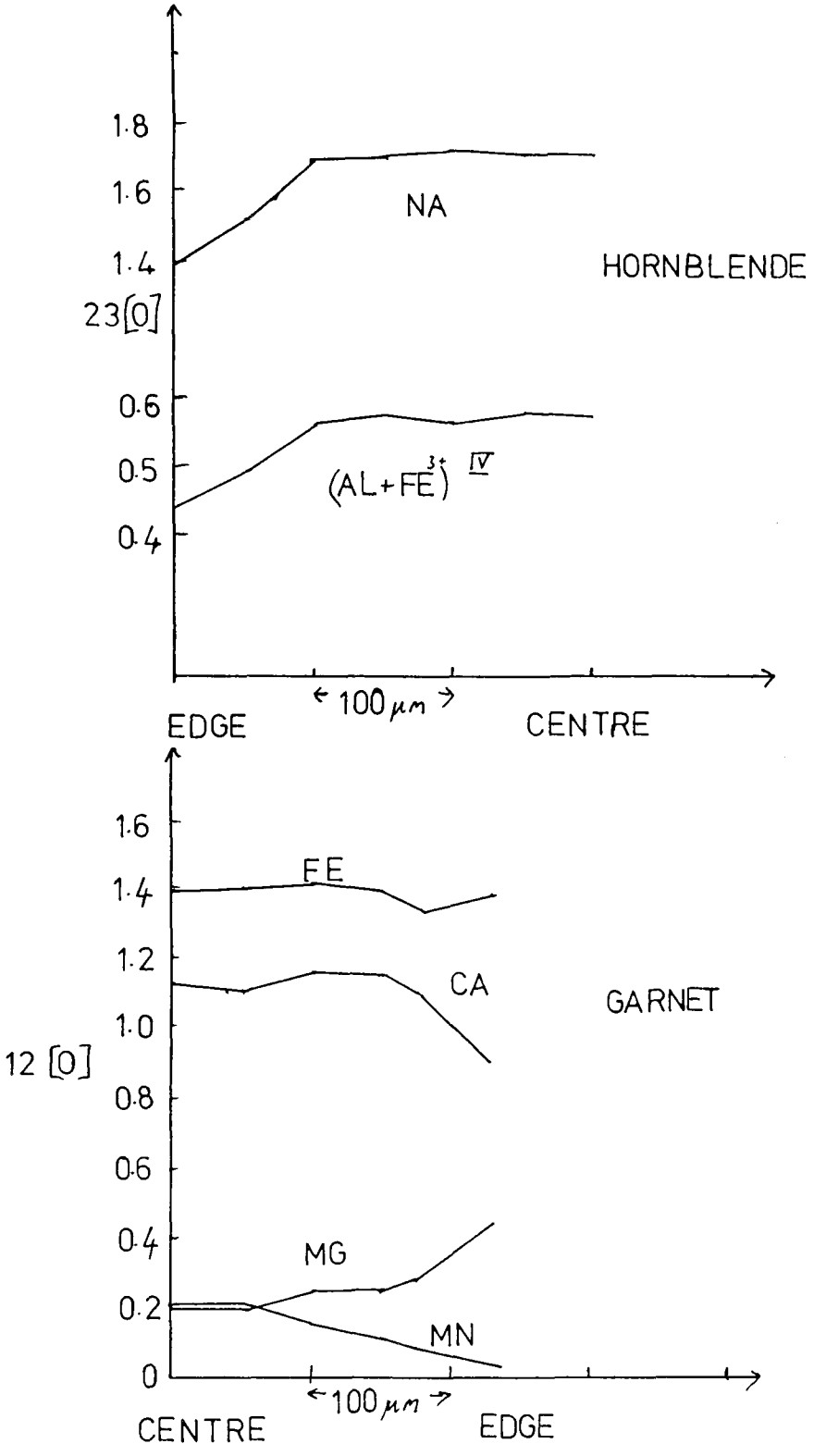

FIGURE 9.5

Zoning profiles of garnet and hornblende in 107A.

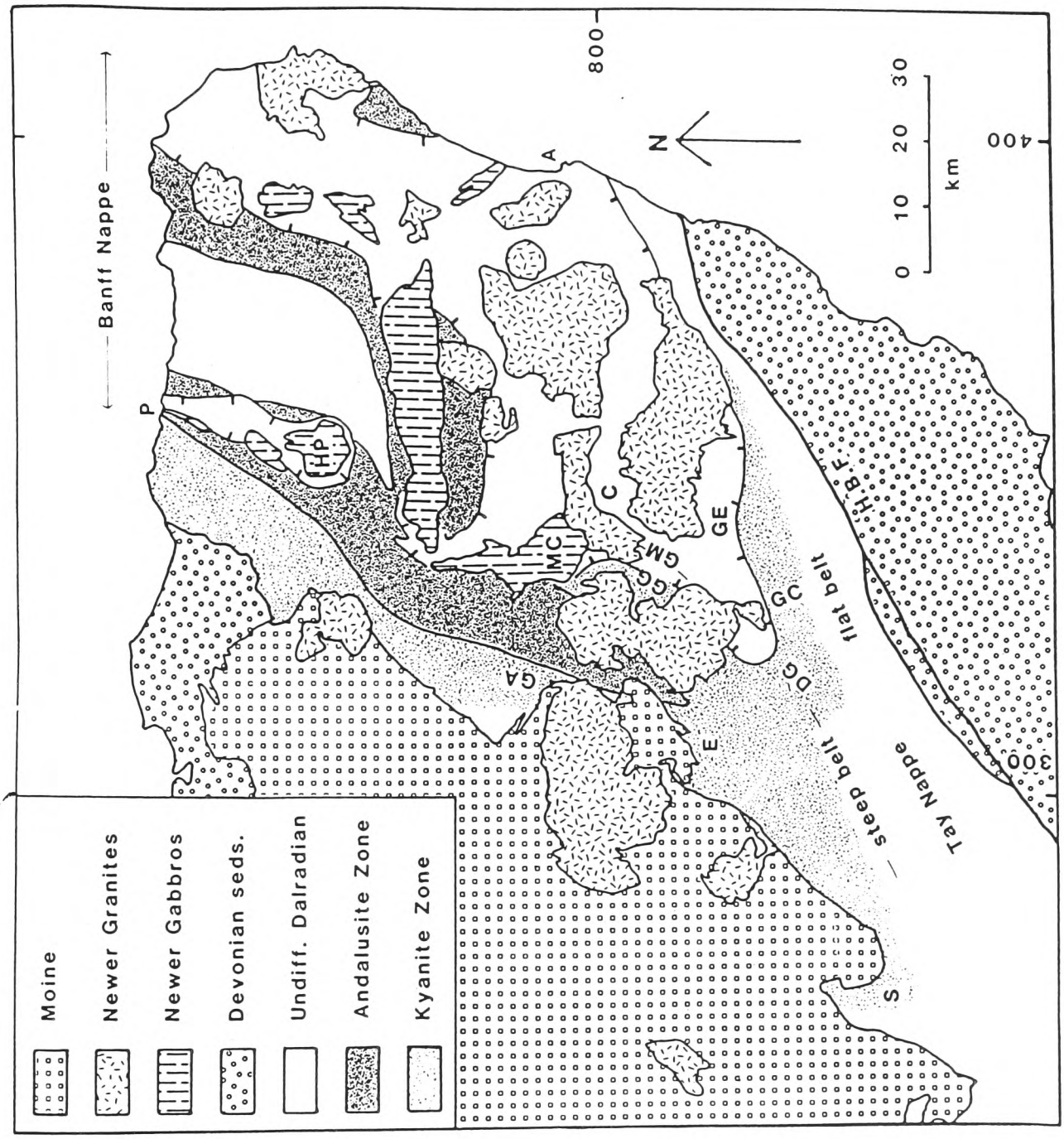

FIGURE 10.1

Geological Sketch Map of the eastern Dalradian.

A-Aberdeen, P-Portsoy, E-Glen Ey, C-Cromar, GM-Glen Muick, GG-Glen Girnock, GE-Glen Esk, GC-Glen Clova, DG-Duchray Hill Gneiss, S-Schichallion, GA Glen Avon, MC-Morven Cabrach, HuntlyPortsoy Newer Gabbros.

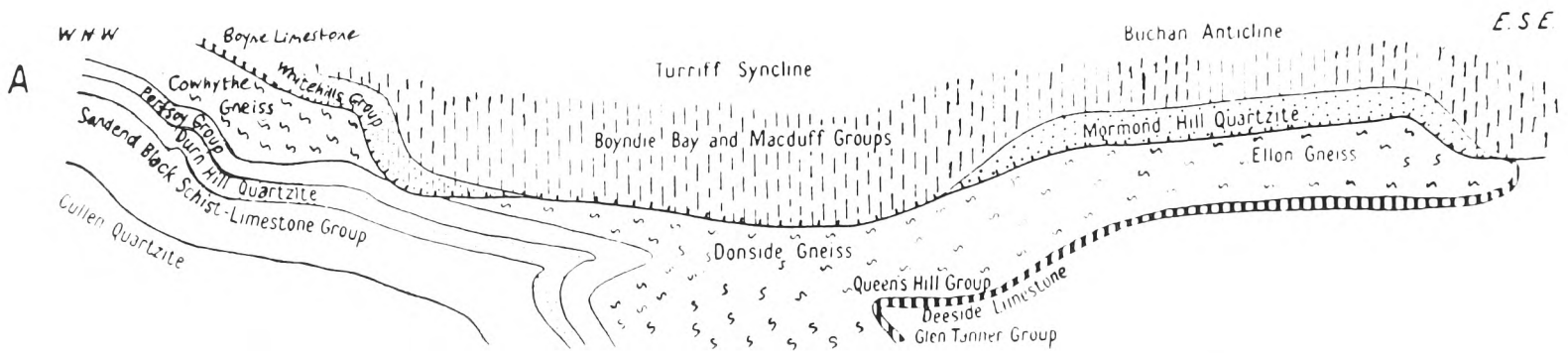

FIGURE 10.2

The Banff Nappe of Read (1955). The ticked line represents the Boyne Line. Length of section about 80km from west of Portsoy to Aberdeen.

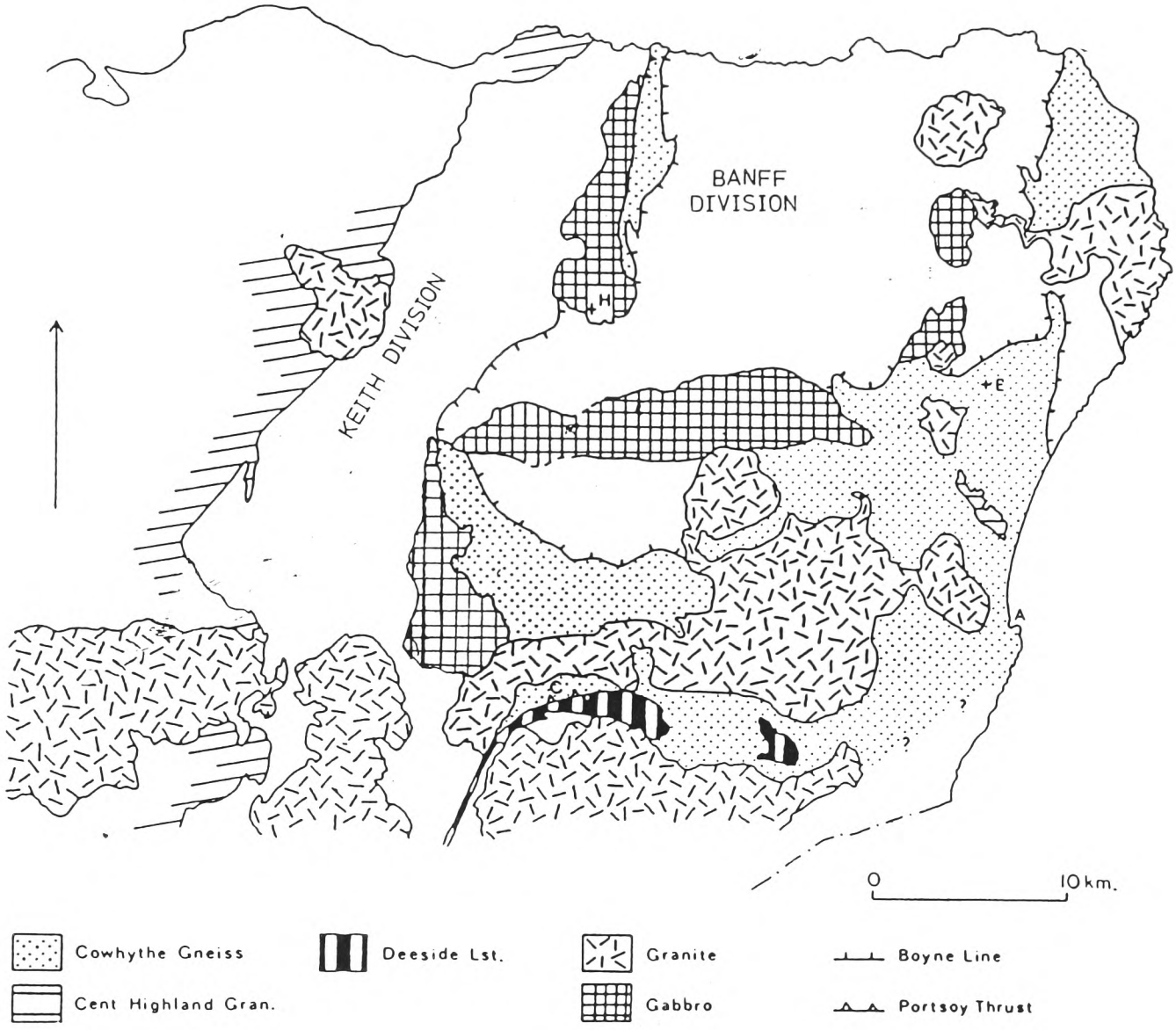

FIGURE 10.3

The Banff Nappe as envisaged by Ramsay and Sturt (1979). The Cowhythe Gneiss is a slice of Precambrian basement emplaced on the lower part of the Dalradian (Keith Division). The Boyne Line is interpreted as a thrust between the upper part of the Dalradian (Banff Division) and Precambrian basement.

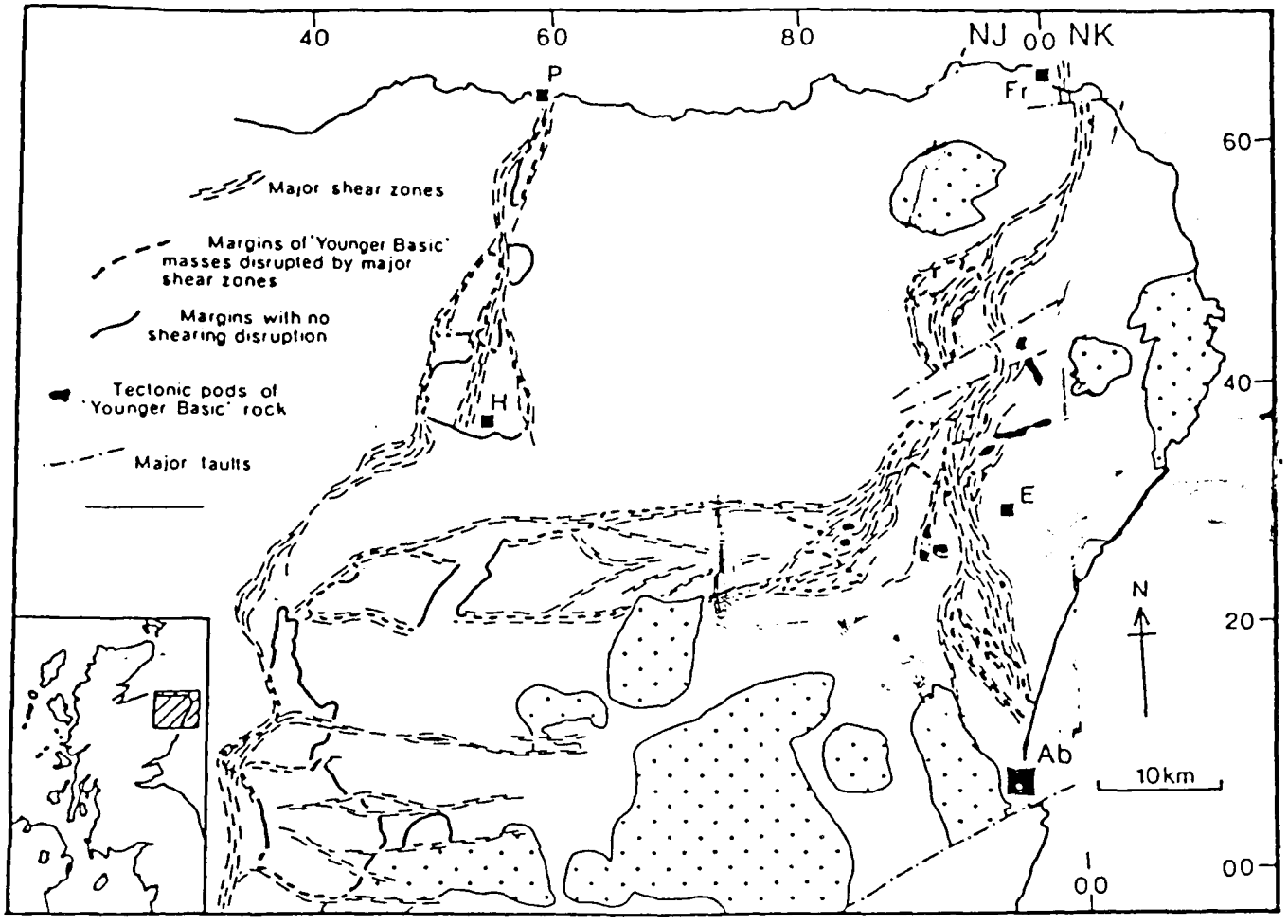

FIGURE 10.4

NE Scotland Sheer Zones (Kneller and Leslie ,1984).

FIGURE 10.5

Sketch map of the geological structure of the eastern Dalradian. Compiled from the following sources:

Roberts and Treagus (1979)
Harte (1979)
Bradbury et al. (1979)
Read and Farquhar (1956)
Treagus and Roberts (1981)
Coward (1983a)
Ashcroft et al. (1984)
Bailey (1925)

P: Portsoy
Ab: Aberdeen
H.B.F. Highland Boundary Fault
H.B.D. Highland Border Downbend
TN: Tay Nappe
TS: Tarfside Nappe
BA. Buchan Anticline
BS. Boyndie Syncline.

Vertical ruling indicates the Newer Gabbros, horizontal ruling indicates areas where the stratigraphy is dominantly inverted. Fine dashed lines are the shear zones of Ashcroft et al. (1984). The line A-B must represent either the trace of the axis of a fold nappe or a major slide.

FIGURE 10.5

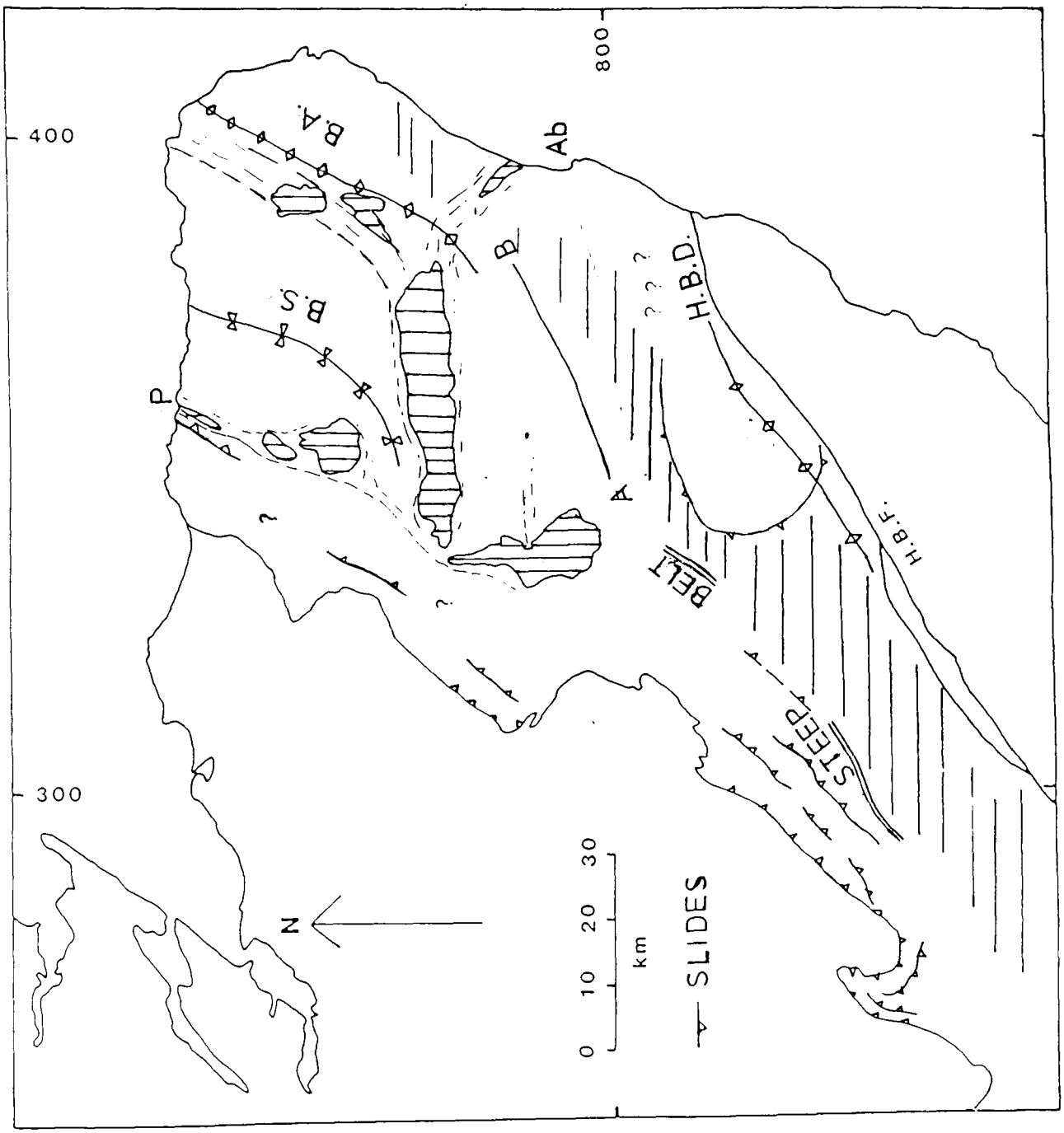

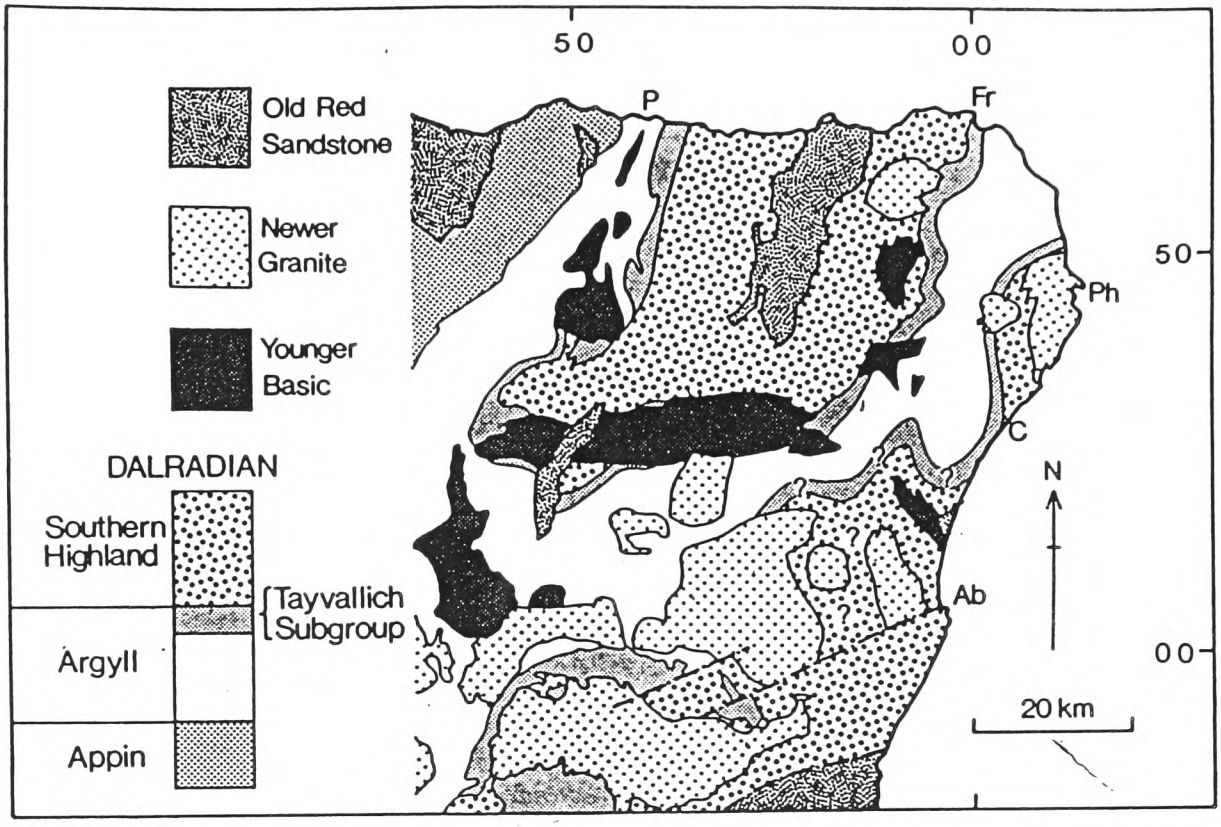

FIGURE 10.6

Sketch map of the northeast Dalradian showing the stratigraphy, from Ashcroft et al. (1984).

FIGURE 10. 7

The distribution of pressure and temperature in the eastern part of the Dalradian according to the interpretation of chapter 7. Dashed lines isobars, dash-dot lines are isotherms. Line P-X represents approximately the western limit of the Banff Nappe, parallel lines : steep belt.

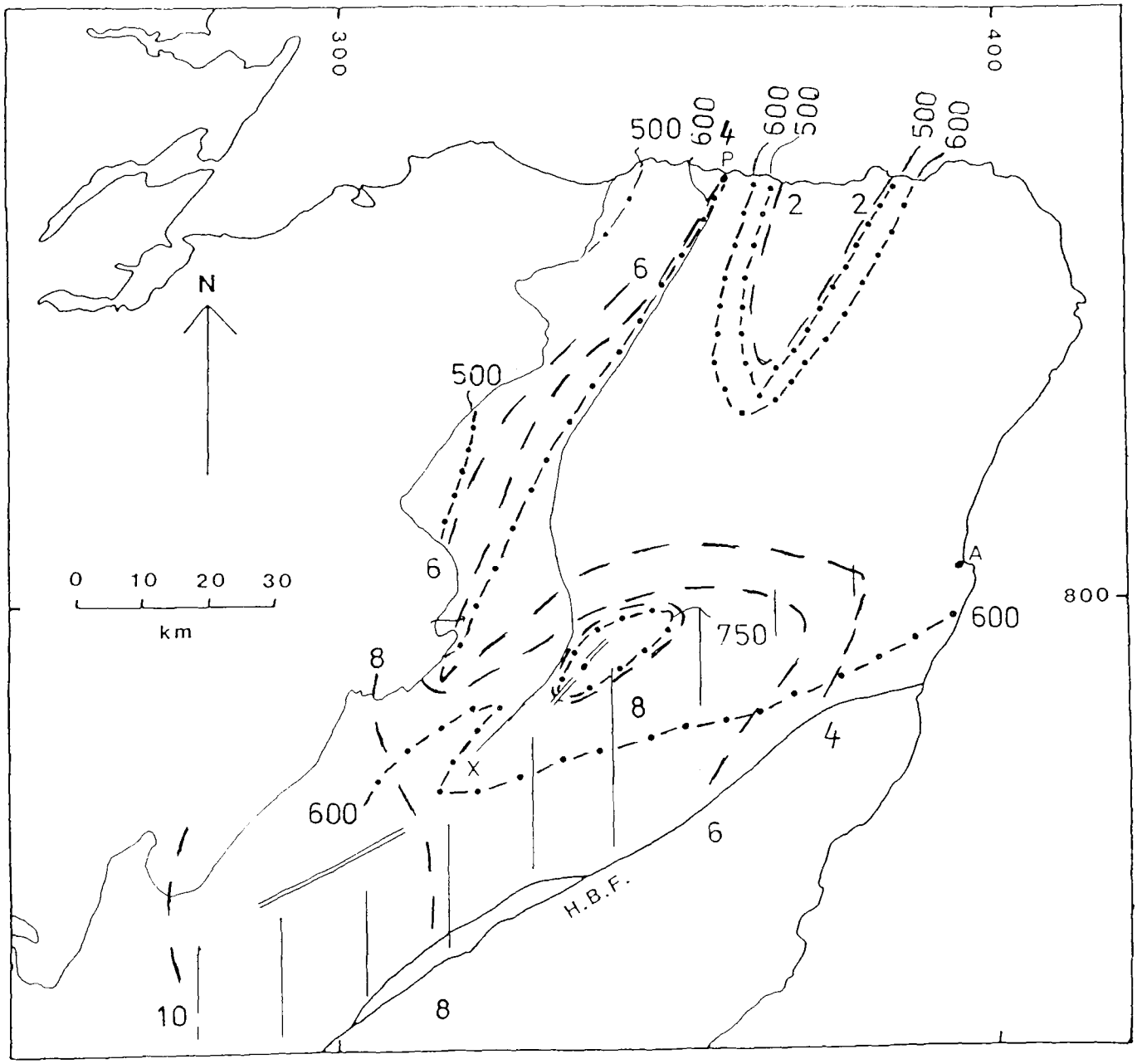

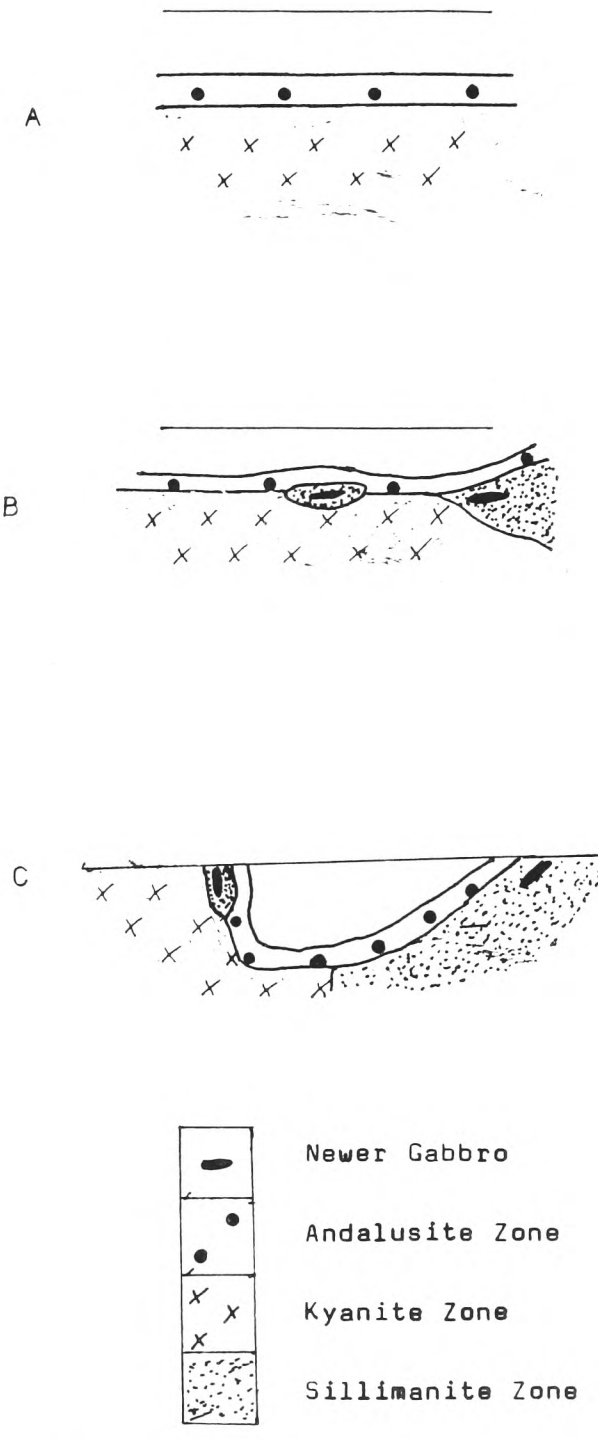

FIGURE 10.8

Diagrams illustrating the evolution of NE Scotland after the model of Harte and Hudson (1979).

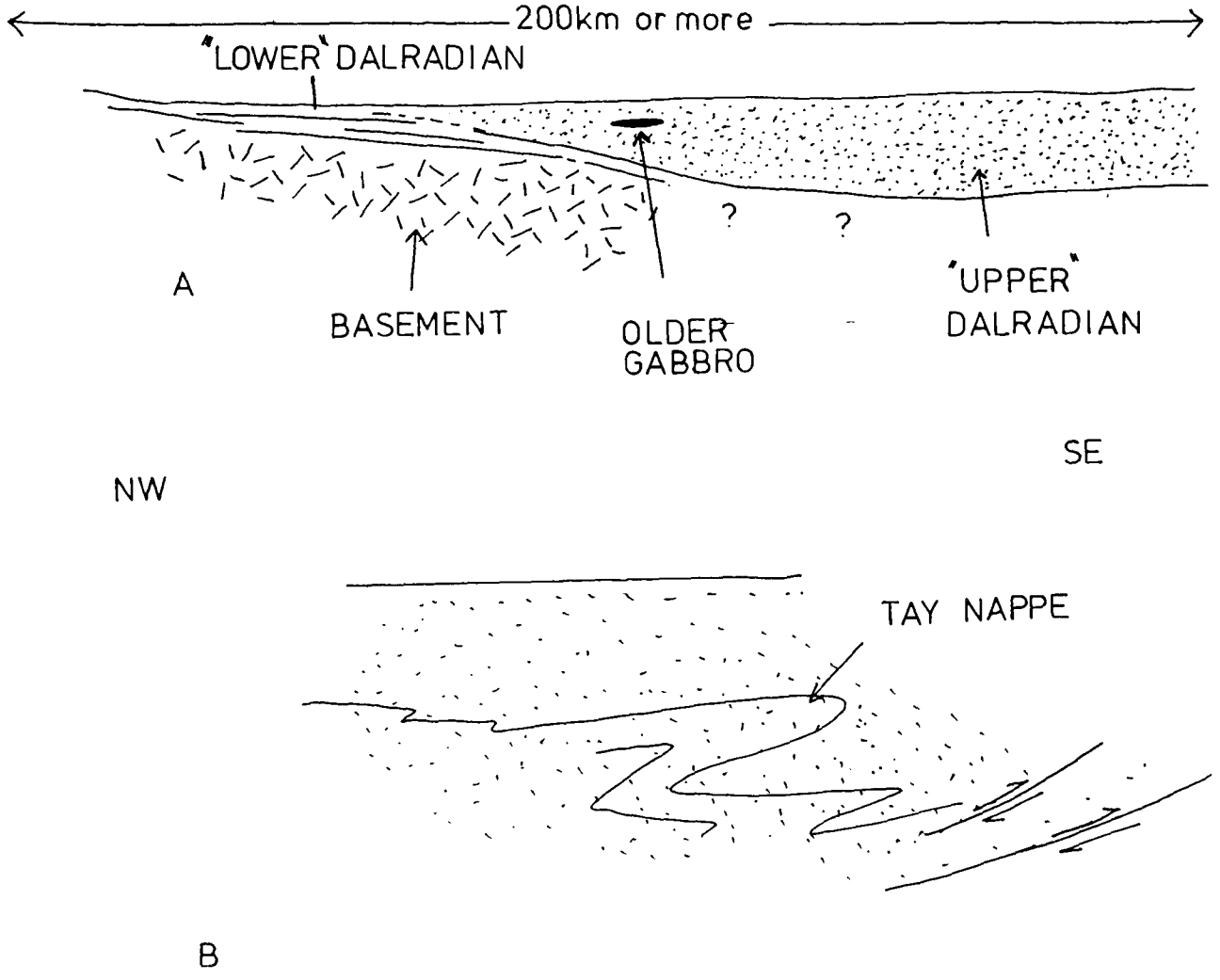

FIGURE 10.9 (a)

Suggested tectonic history for the eastern Dalradian

A Dalradian basin (upper-Crinan Subgroup and above)

B Formation of Tay Nappe in upper Dalradian rocks (SE part of section A)

FIGURE 10.9 (a) (Ctd.)

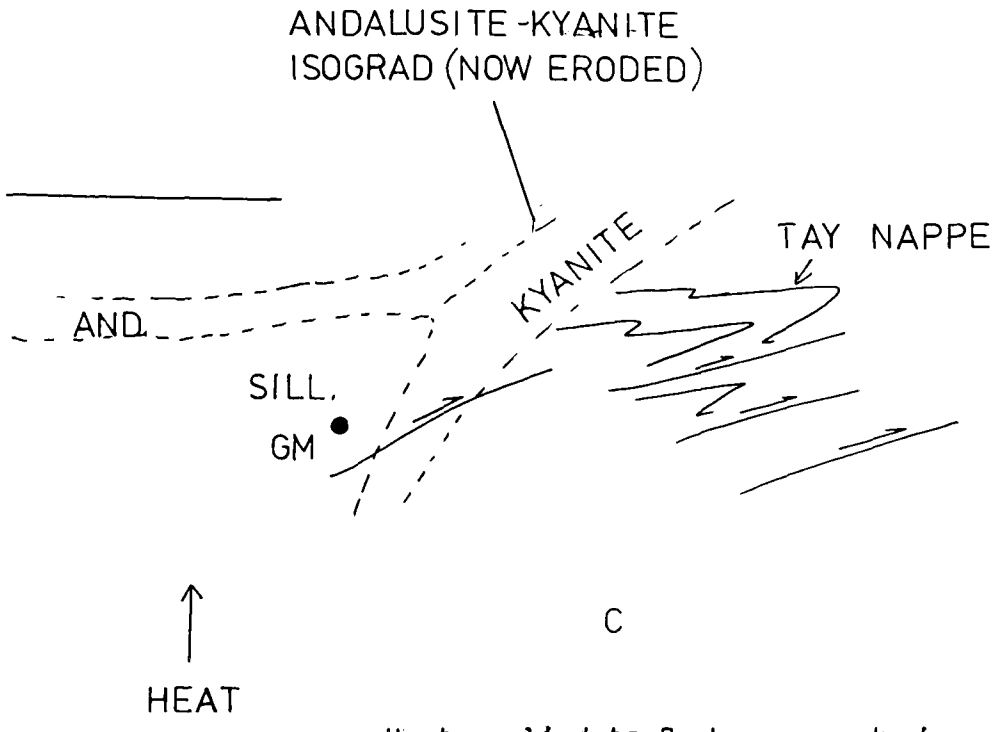

Heat applied to Buchan area during continued SE directed thrusting. (Dotted lines-isograds)

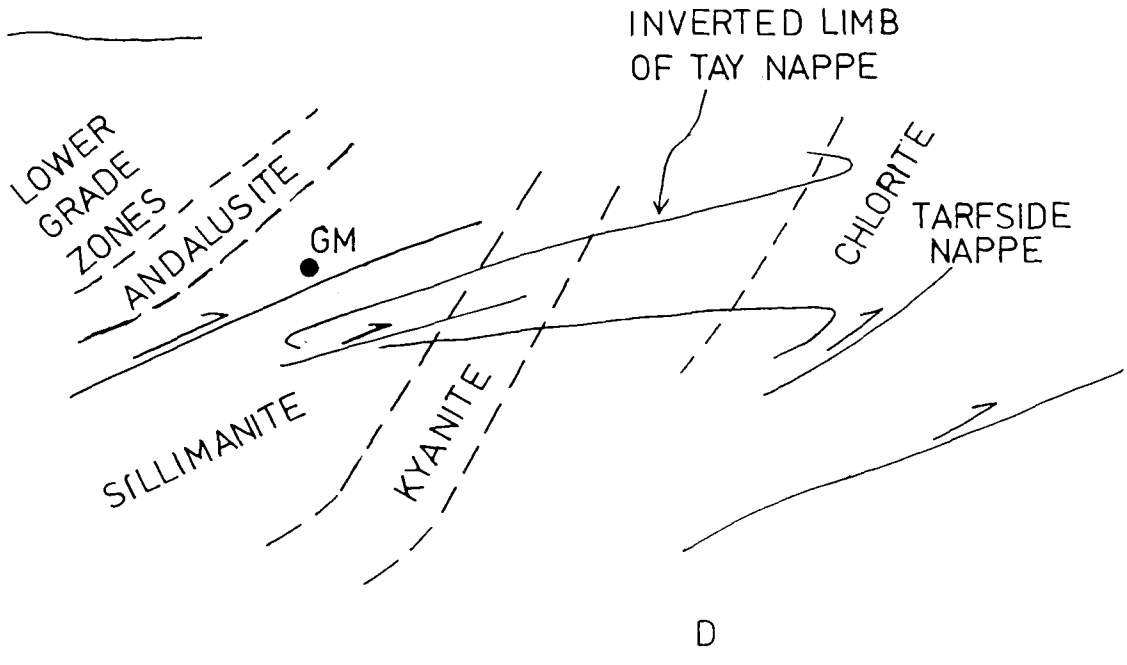

Final configuration of isograds results from interplay between SE directed overthrusting and supply of heat from below. Isograds may be inverted.

FIGURE 10.9 (a), (Ctd.)

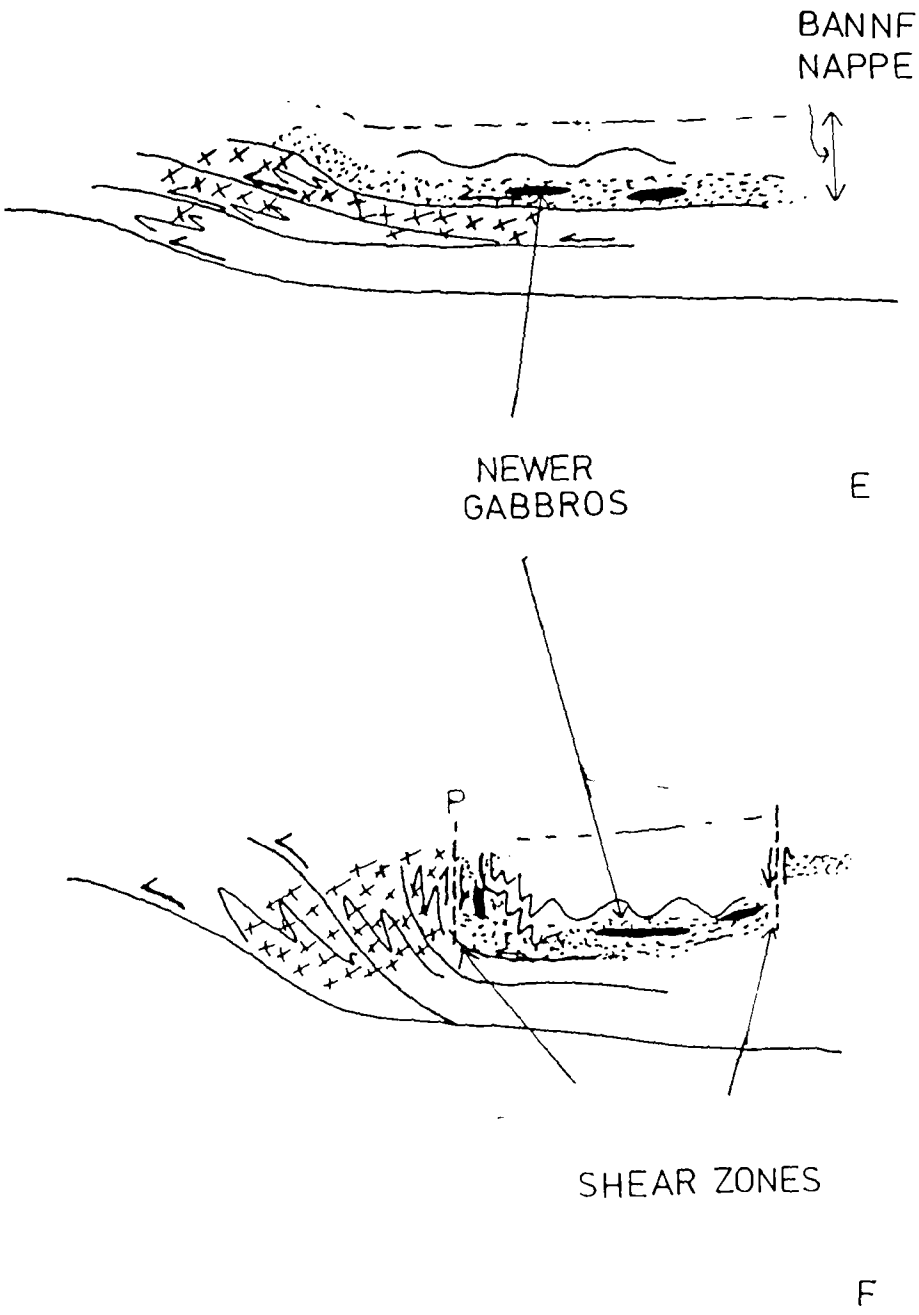

E NW thrusting of Buchan area over lower Dalradian rocks. (Sill. zone is dotted, kyanite zone-crosses).

F Structurally lower rocks to the west of Portsoy later uplifted relative to the Buchan area. Late differential uplift accomadated on shear zones.

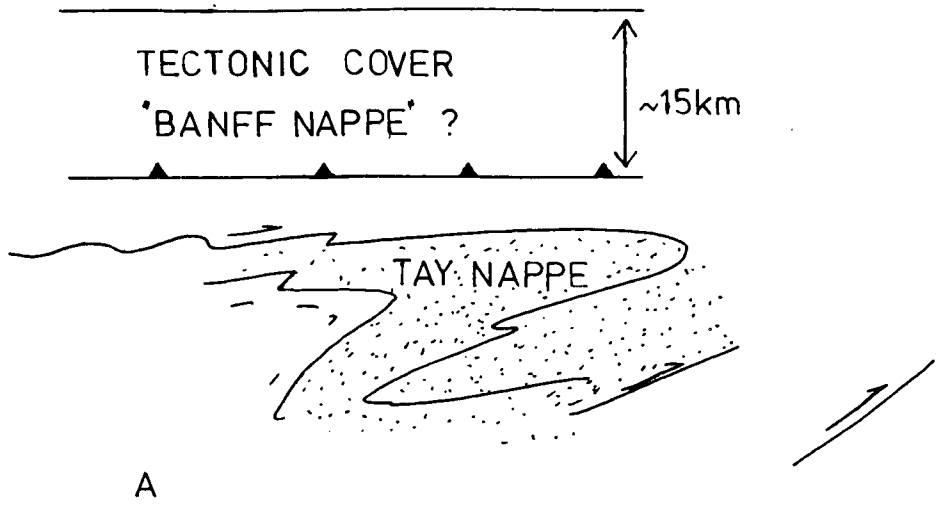

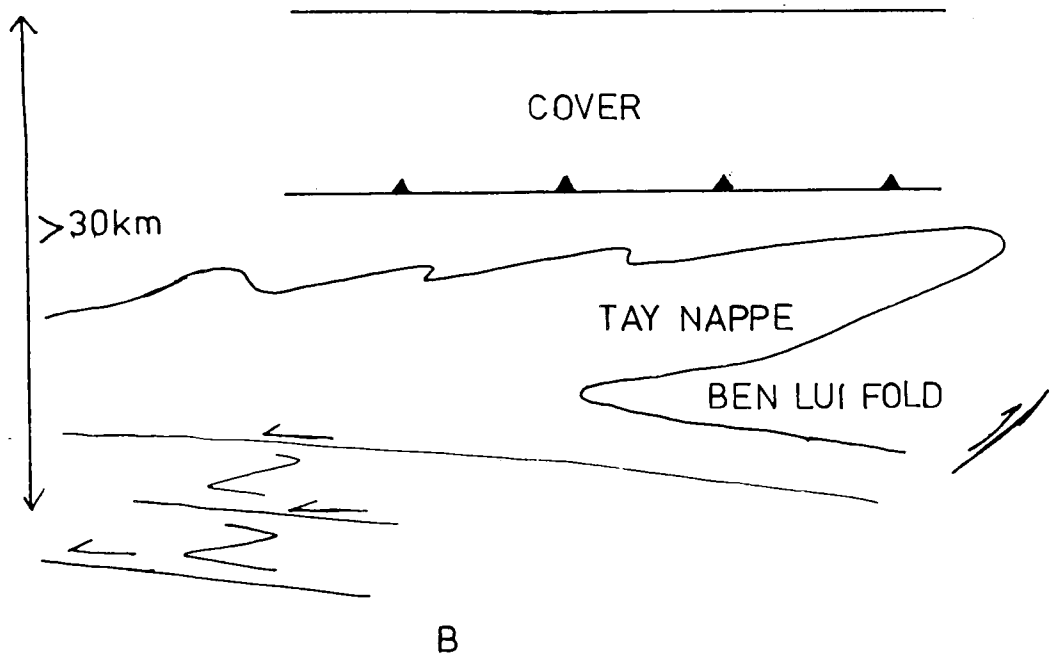

FIGURE 10.9 (b)

A: Tay Nappe formed, followed by overthrusting of tectonic cover, which may comprise a stratigraphic and metamorphic equivalent of the Banff Nappe.

B: NW thrusting results in the tectonic burial rocks to the NW.

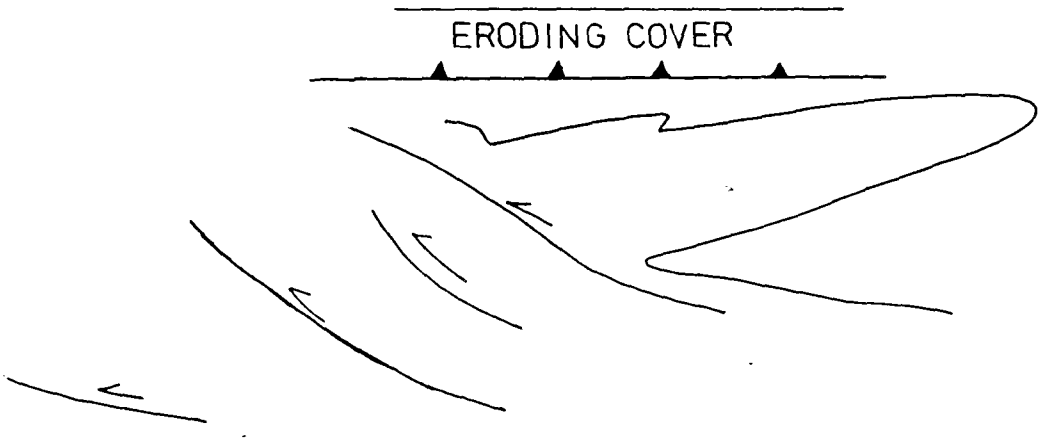

C

FIGURE 10.9 (b), (ctd.)

C:Later uplift of structurally lowest rocks as a result of further deformation and erosion of tectonic cover.

FIGURE 10.10

Geological Sketch Map of the Portsoy coast section, in part after Read (1923). The whole section is characterised by folds with axes plunging steeply towards the southeast.

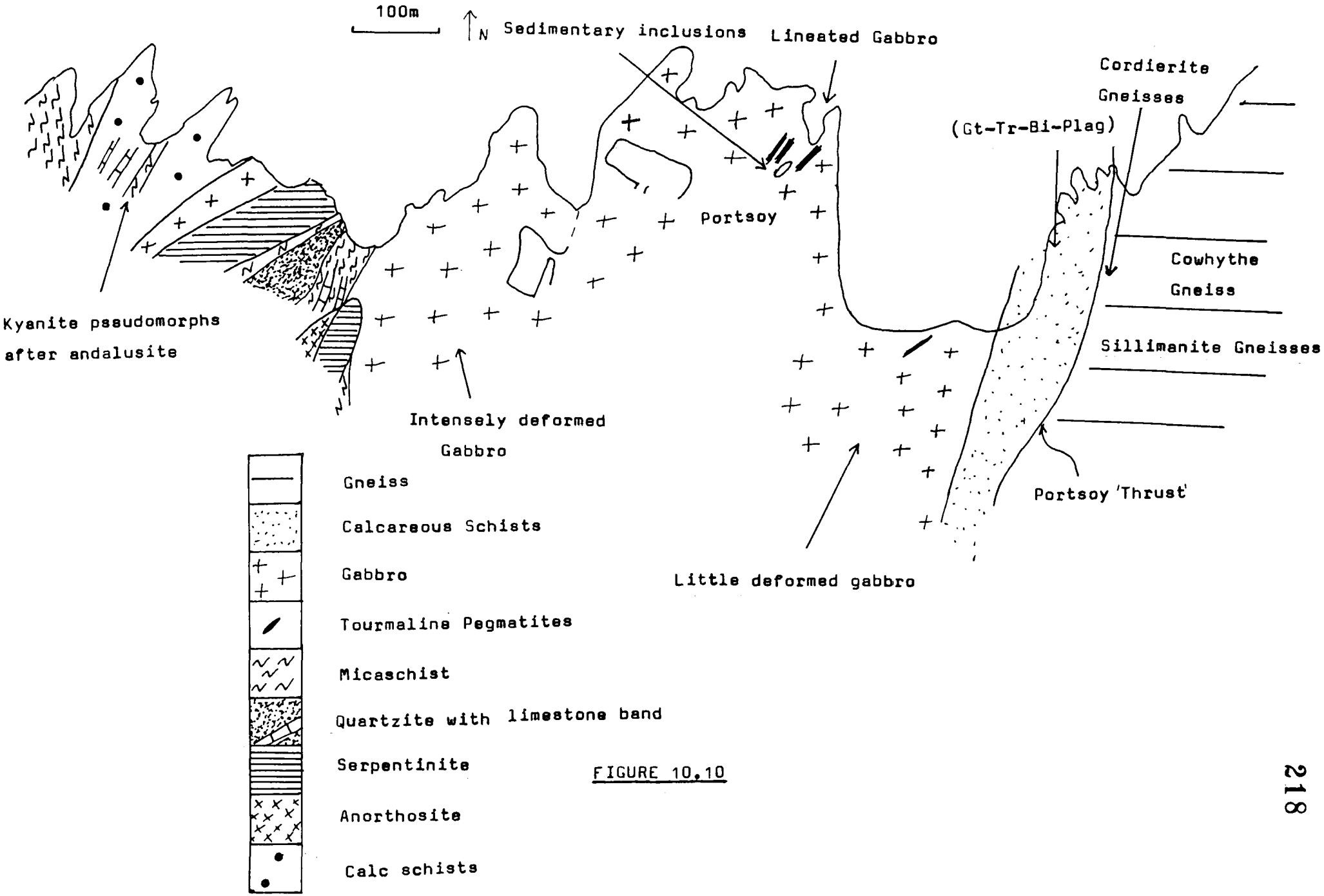
100m
N
Sedimentary inclusions
Lineated Gabbro
Cordierite
Gneisses
(Gt-Tr-Bi-Plag)
Portsoy
Cowhythe
Gneiss
Sillimanite Gneisses
Kyanite pseudomorphs
after andalusite
Intensely deformed
Gabbro
Portsoy 'Thrust'
Little deformed gabbro
Gneiss
Calcareous Schists
Gabbro
Tourmaline Pegmatites
Micaschist
Quartzite with limestone band
Serpentinite
Anorthosite
Calc schists

FIGURE 10.10

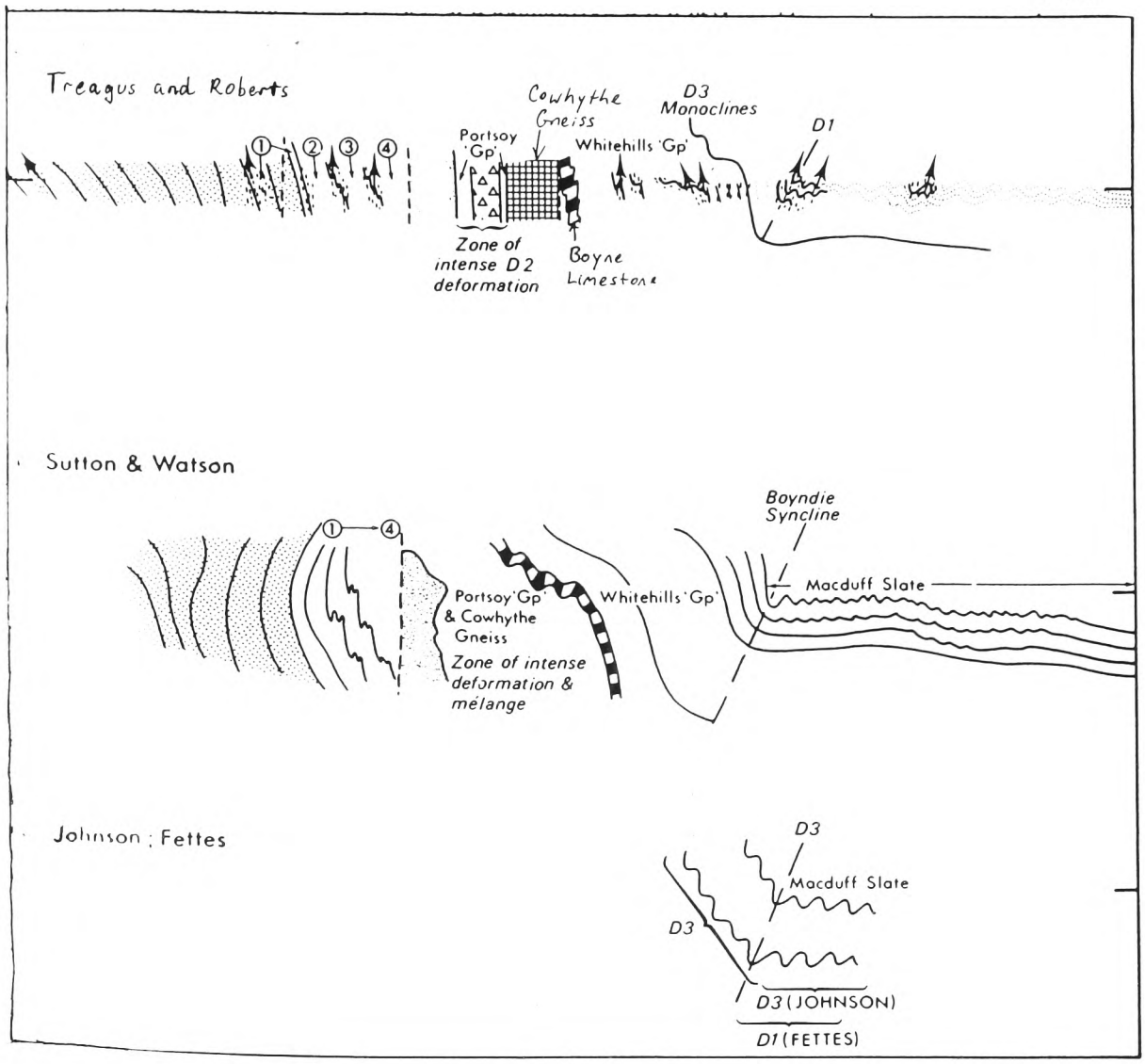

FIGURE 10.11

Structural interpretations of the Banff Coast Section through Portsoy. Interpretations by Treagus and Roberts (1981), Sutton and Watson (1956), Johnson (1963) and Fettes (1971).

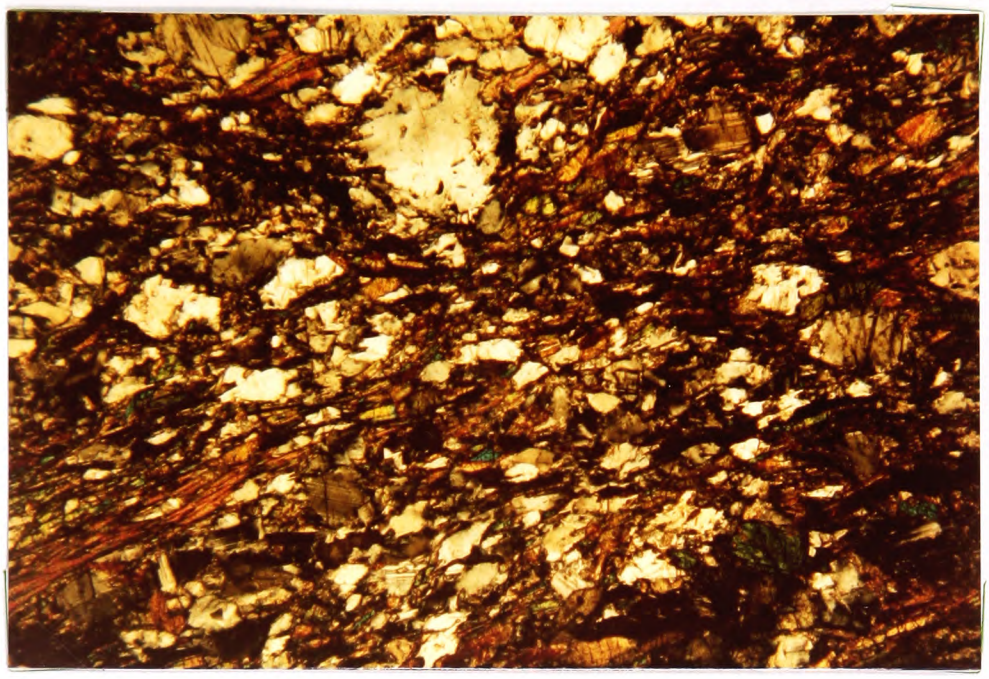

FIGURE 10.12 (a)

893A (x50) Deformed metagabbro, Portsoy.

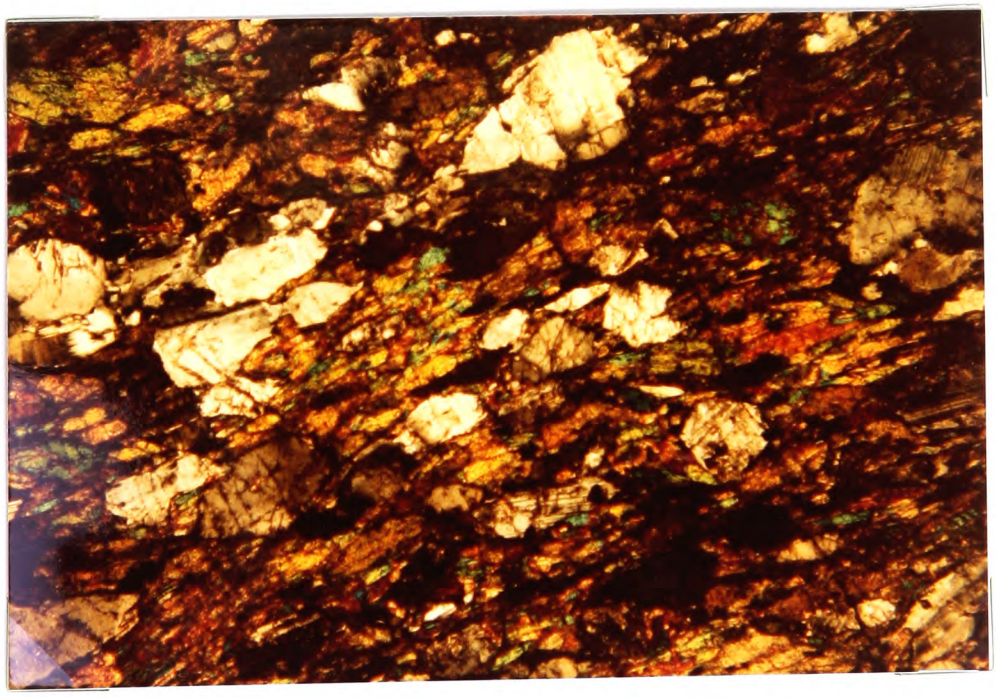

FIGURE 10.12 (b)

904A (x50) Deformed metagabbro, Portsoy.

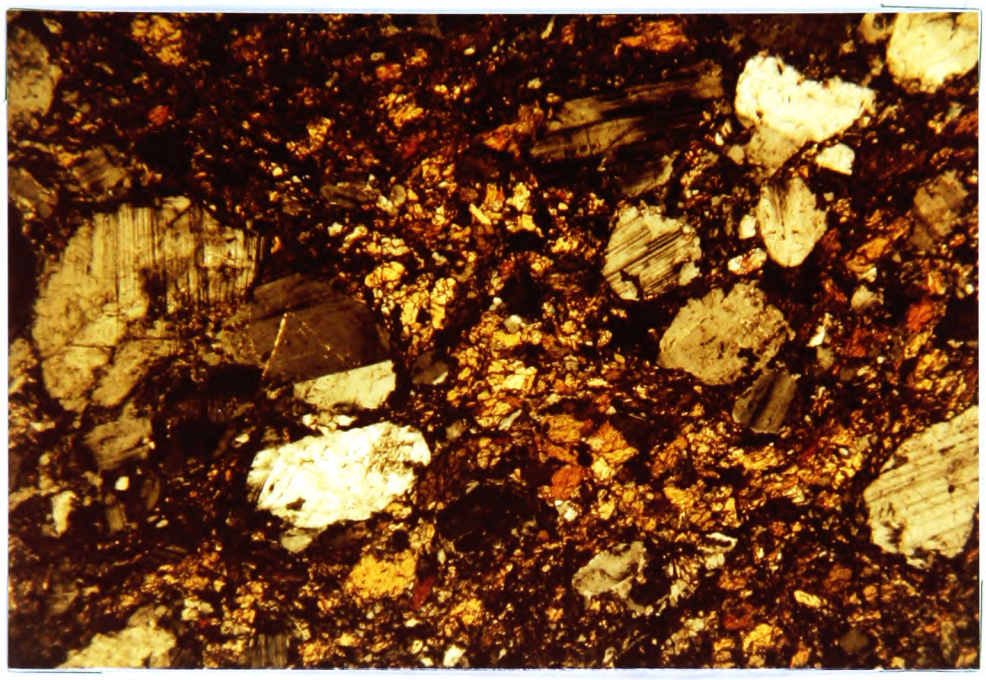

FIGURE 10.13 (a)

903A (x50) Deformed metagabbro, Portsoy.

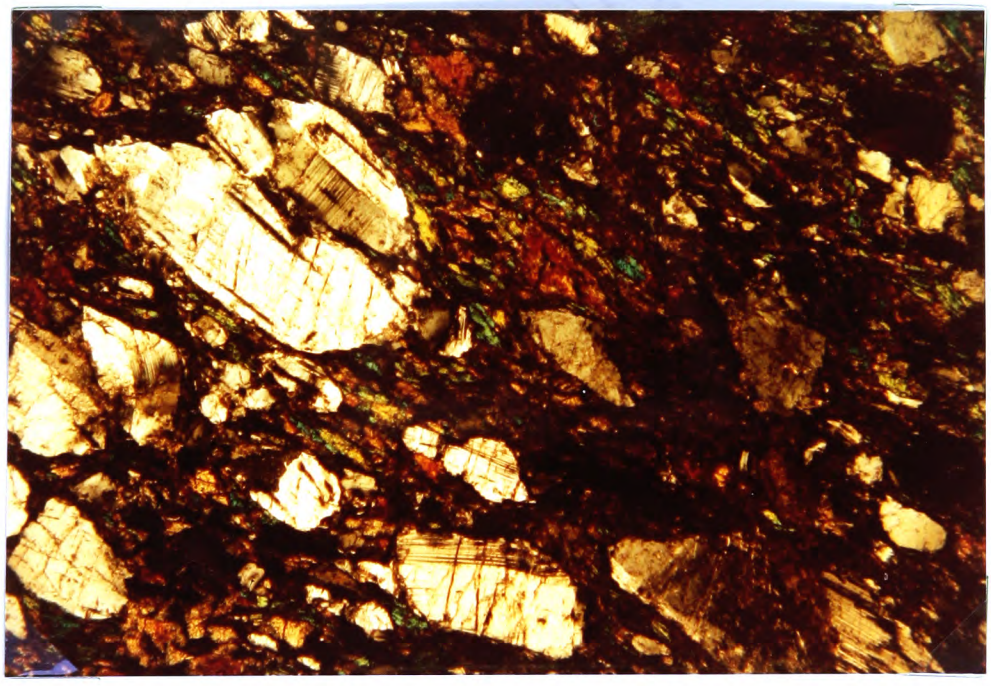

FIGURE 10.13(b)

903A (x50) Deformed metagabbro, Portsoy.

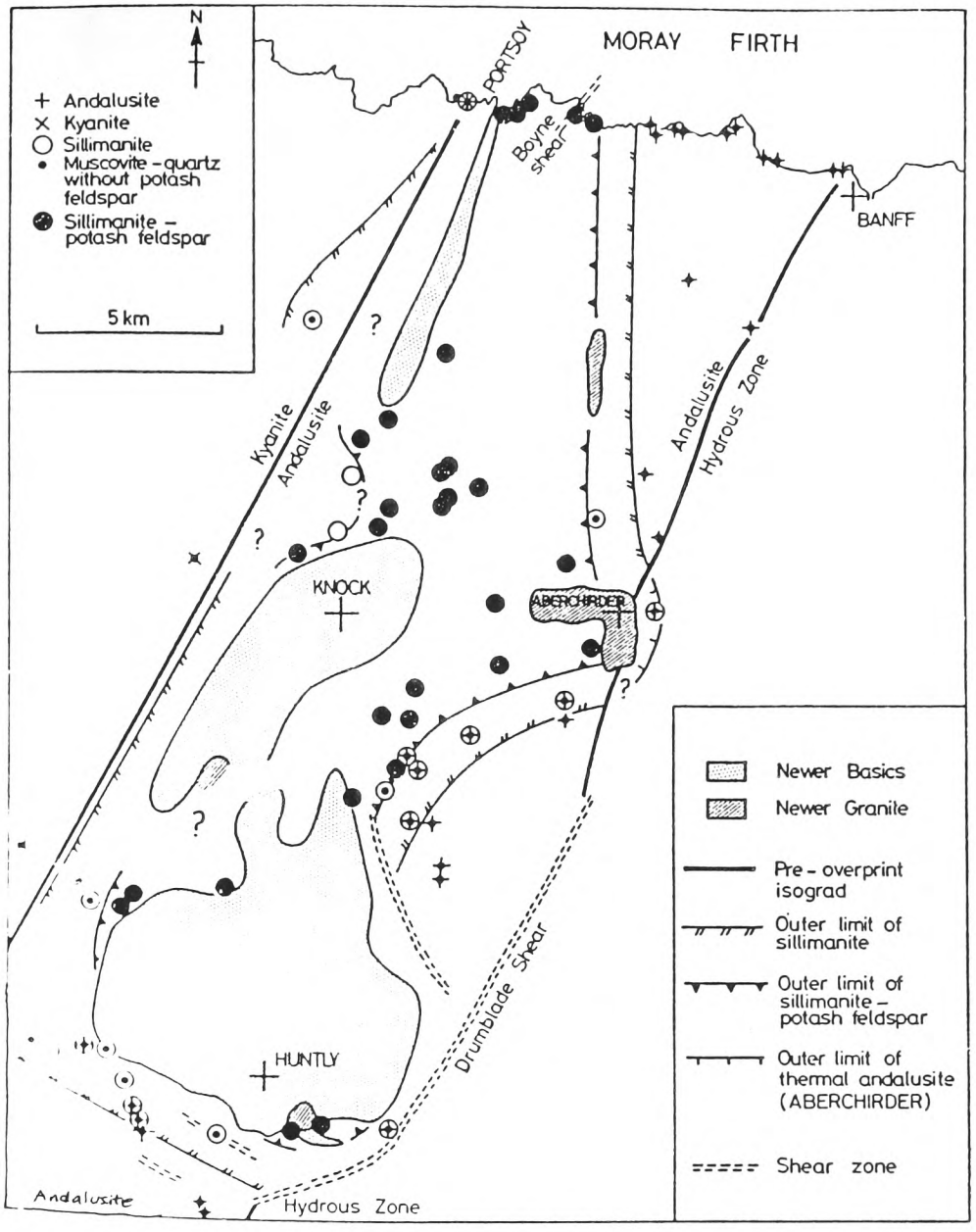

FIGURE 10.14

Metamorphic Zones around the Huntly Portsoy Gabbro, from Ashworth (1975).

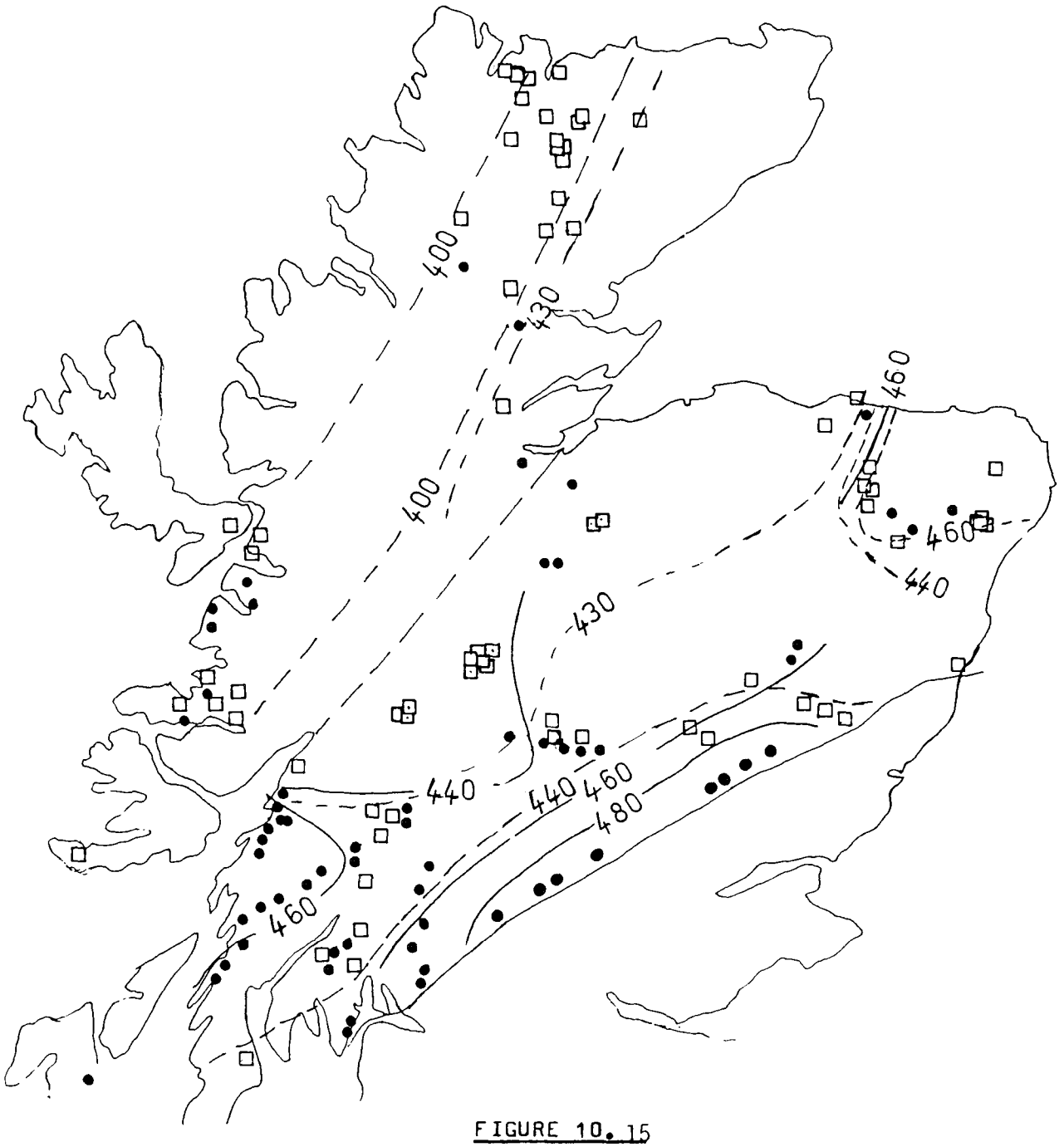

FIGURE 10.15

K-Ar mica cooling dates in the Dalradian squares : biotites, circles : muscovites and whole rocks. Data from compilation of Dewey and Pankhurst (1970). Dotted lines are for biotite, solid for muscovite.